200 copies

TECHNICAL REPORT STANDARD TITLE PAGE

1. Report No.	2. Government Accession No.	3. Recipient's Catalog No.
FHWA/TX-89+381-3		

4. Title and Subtitle	5. Report Date
A STUDY OF PRETENSIONED HIGH STRENGTH CONCRETE GIRDERS IN COMPOSITE HIGHWAY BRIDGES—LABORATORY TESTS	January 1988
	6. Performing Organization Code
7. Author(s)	8. Performing Organization Report No.
Reid W. Castrodale, Ned H. Burns, and Michael E. Kreger	Research Report 381-3
9. Performing Organization Name and Address	10. Work Unit No.
Center for Transportation Research The University of Texas at Austin Austin, Texas 78712-1075	11. Contract or Grant No. Research Study 3-5-84-381
12. Sponsoring Agency Name and Address	13. Type of Report and Period Covered
Texas State Department of Highways and Public Transportation; Transportation Planning Division P. O. Box 5051 Austin, Texas 78763-5051	Interim
	14. Sponsoring Agency Code

15. Supplementary Notes

Study conducted in cooperation with the U. S. Department of Transportation, Federal Highway Administration. Research Study Title: "Optimum Design of Bridge Girders Made Using High Strength Concrete and Deflection of Long-Span Prestressed Concrete Beams"

16. Abstract

Recent studies have shown that it is commercially feasible to produce prestressed concrete girders utilizing concrete strengths in the 12,000 psi range. However, current codes and specification provisions for flexural strength are based on tests using concrete strengths less than 6000 psi. This program was undertaken to evaluate the adequacy of current design provisions for flexural capacity when applied to high strength concrete girders.

Due to the lack of data in the literature on composite bridge construction with high strength concrete pretensioned girders, two test programs were developed to provide data that would allow evaluation of the use of high strength concrete in the design of pretensioned bridge girders. The first series was a limited comparison of transfer characteristics of 0.5-in.-diameter strand in normal and high strength concrete. These tests provided data to evaluate whether current transfer length provisions found in the codes could be applied to high strength concrete members. The second series involved testing of scale-model high strength concrete pretensioned girders with a normal strength composite deck, representative of actual long-span bridge designs. Tests of two one-third scale girder specimens provided data for the evaluation of current design provisions, for verification of analysis techniques, and permitted development of recommendations where revision of the codes was necessary as covered in a subsequent report.

17. Key Words	18. Distribution Statement
pretensioned, prestressed, high strength concrete, concrete girders, flexural strength, capacity, transfer characteristics, length, specimens	No restrictions. This document is available to the public through the National Technical Information Service, Springfield, Virginia 22161.

19. Security Classif. (of this report)	20. Security Classif. (of this page)	21. No. of Pages	22. Price
Unclassified	Unclassified	234	

Form DOT F 1700.7 (8-69)

A STUDY OF PRETENSIONED HIGH STRENGTH CONCRETE GIRDERS IN COMPOSITE HIGHWAY BRIDGES - LABORATORY TESTS

by

Reid W. Castrodale
Ned H. Burns
Michael E. Kreger

Research Report 3-5-84-381-3

Research Project 3-5-84-381

"Optimum Design of Bridge Girders Made Using High Strength Concrete and Deflection of Long-Span Prestressed Concrete Beams"

Conducted for

Texas
State Department of Highways and Public Transportation

In Cooperation with the
U.S. Department of Transportation
Federal Highway Administration

by

CENTER FOR TRANSPORTATION RESEARCH
BUREAU OF ENGINEERING RESEARCH
THE UNIVERSITY OF TEXAS AT AUSTIN

January 1988

PREFACE

This report is the third report in a series which summarizes an investigation of the feasibility of utilizing high strength concrete and improved low relaxation steels in pretensioned bridge girders. The first report summarized results of a field measurement program concerned primarily with the deformation history of long span pretensioned girders throughout their construction history. The second report summarizes a laboratory investigation of the shear capacity of large-scale pretensioned girders fabricated with very high strength concretes. This report gives test results for flexural tests of two one-third scale high strength concrete pretensioned girders with normal strength concrete composite deck. A limited test program comparing transfer characteristics of 0.5 in. diameter strand in normal and high strength concrete is also presented.

This work is part of Research Project 3-5-84-381 entitled, "Optimum Design of Bridge Girders Made Using High-Strength Concrete and deflections of Long-Span Prestressed Concrete Beams." This report is specifically addressed to verifying the adequacy of current design specification provisions for the flexural strength of prestressed concrete girders made with high strength concrete to ensure that they are applicable and safe at the higher ranges of concrete strengths which may be used in the future. The research was conducted by the Phil M. Ferguson Structural Engineering Laboratory as part of the overall research program of the Center for Transportation Research of the University of Texas at Austin. The work was sponsored jointly by the Texas State Department of Highways and Public Transportation and the Federal Highway Administration under an agreement with the University of Texas at Austin and the State Department of Highways and Public Transportation.

Liaison with the State Department of Highways and Public Transportation was maintained through the contact representative, Mr. David P. Hohmann. Mr. R.E. Stanford was the contact representative for the Federal Highway Administration.

This portion of the overall study was directed by Ned H. Burns, who holds the Barrow Centennial Professorship in Civil Engineering in cooperation with Michael E. Kreger, Assistant Professor of Civil Engineering. Co-director supervising other portions of Project 381 was John E. Breen. The design, fabrication and testing of the girders were under the direction of Reid W. Castrodale, Research Engineer.

SUMMARY

Recent studies have shown that it is commercially feasible to produce prestressed concrete girders utilizing concrete strengths in the 12,000 psi range. However current codes and specification provisions for flexural strength are based on tests using concrete strengths less than 6000 psi. This program was undertaken to evaluate the adequacy of current design provisions for flexural capacity when applied to high strength concrete girders.

Due to the lack of data in the literature on composite bridge construction with high strength concrete pretensioned girders, two test programs were developed to provide data that would allow evaluation of the use of high strength concrete in the design of pretensioned bridge girders.

The first series was a limited comparison of transfer characteristics of 0.5-in. diameter strand in normal and high strength concrete. These tests provided data to evaluate whether current transfer length provisions found in the codes could be applied to high strength concrete members.

The second series involved testing of scale-model high strength concrete pretensioned girders with a normal strength composite deck, representative of actual long- span bridge designs. Tests of two one-third scale girder specimens provided data for the evaluation of current design provisions, for verification of analysis techniques, and permitted development of recommendations where revision of the codes was necessary as covered in a subsequent report.

Shear strength tests were made on the ends of the test specimens of the second series (girders) and these results are included in a separate report (Ref. 138) along with results from other shear strength specimens.

IMPLEMENTATION

This report summarizes the results of test programs involving high-strength concrete with f'_c values up to 13,000 psi. The demonstration in the laboratory that concrete with almost twice the usual strength could be made and placed in thin-web cross section is significant in itself. The use of high strength concrete for use in pretensioned highway bridge girders is indicated as a real possibility on the basis of these tests of two one-third scale specimens.

The data in this report is used in the following report, a study which reviews assumptions contained in present codes and specifications. Physical data from these tests validate the extension of previously used assumptions into the range of high strength concrete. Actual behavior is most important in carrying the review of analysis into the actual design of real members, and these data are essential in formulating subsequent design recommendations.

Use of high strength concrete in pretensioned girders with normal strength deck concrete is shown by these tests to be realistic on the basis of flexural performance. The following report, using these data, formulates specific limitations on some design assumptions which suggest that high strength concrete plays a significant role in planning for future development of use of prestressed concrete girders in highway bridges.

TABLE OF CONTENTS

TABLE OF CONTENTS (continued)

LIST OF FIGURES

LIST OF FIGURES

LIST OF FIGURES

LIST OF FIGURES

LIST OF FIGURES

LIST OF FIGURES

LIST OF FIGURES

LIST OF FIGURES

LIST OF FIGURES

LIST OF TABLES

LIST OF TABLES

CHAPTER 1

INTRODUCTION

1.1 Background

The use of high strength concrete as a building material has been a topic of discussion for many years. In an article published in 1932, Thomas T. Towles [129] speculated on the benefits of using concrete with a design compressive strength of 7,000 psi compared with a 5,000 psi mix, which was considered to be near the maximum practical concrete strength at the time. It was clear to him that the use of higher strength concrete would lead to significant cost benefits, especially in long span construction and where many spans are required.

Since that time, it has become possible to produce concrete with a design strength much higher than even the expectations of Towles in 1932. Peterman and Carrasquillo [104] have demonstrated that concrete with a compressive strength between 9,000 and 12,000 psi can be readily obtained on a commercial basis by careful mix proportioning using standard portland cements, selected common aggregates, and chemical admixtures. The use of high range water reducers (HRWR), which are also referred to as "super-plasticizers", have made it possible to produce workable mixtures with the extremely low water/cement ratios that are required to attain high strengths.

The same observations that Towles made in 1932 are being made today, but with even greater expectations for cost benefits because of the higher strengths that are now possible. One way in which the use of high strength concrete has been demonstrated to provide greater efficiency is illustrated by the two bridge cross sections shown in Fig. 1.1, which illustrates the results of a study performed in Sec. 2.4.1. This figure shows that, for a span length of 115 ft and a bridge width of 36 ft, the required number of AASHTO-PCI Type IV girders can be reduced from nine using 6,000 psi concrete, which is the standard concrete strength for pretensioned girders in Texas, to four when 10,000 psi concrete is used. As indicated on the figure, the use of high strength concrete also results in a reduction in the total number of strands required for the bridge, which is a result of the reduced dead load. A normal strength concrete (4,000 psi) deck was used in both cases. The deck thickness was 1 in. greater for the design using high strength concrete girders because of the increased deck span. The use of fewer girders for a given span leads to savings in material, shipping, and erection costs and also reduces the time required for fabrication and erection.

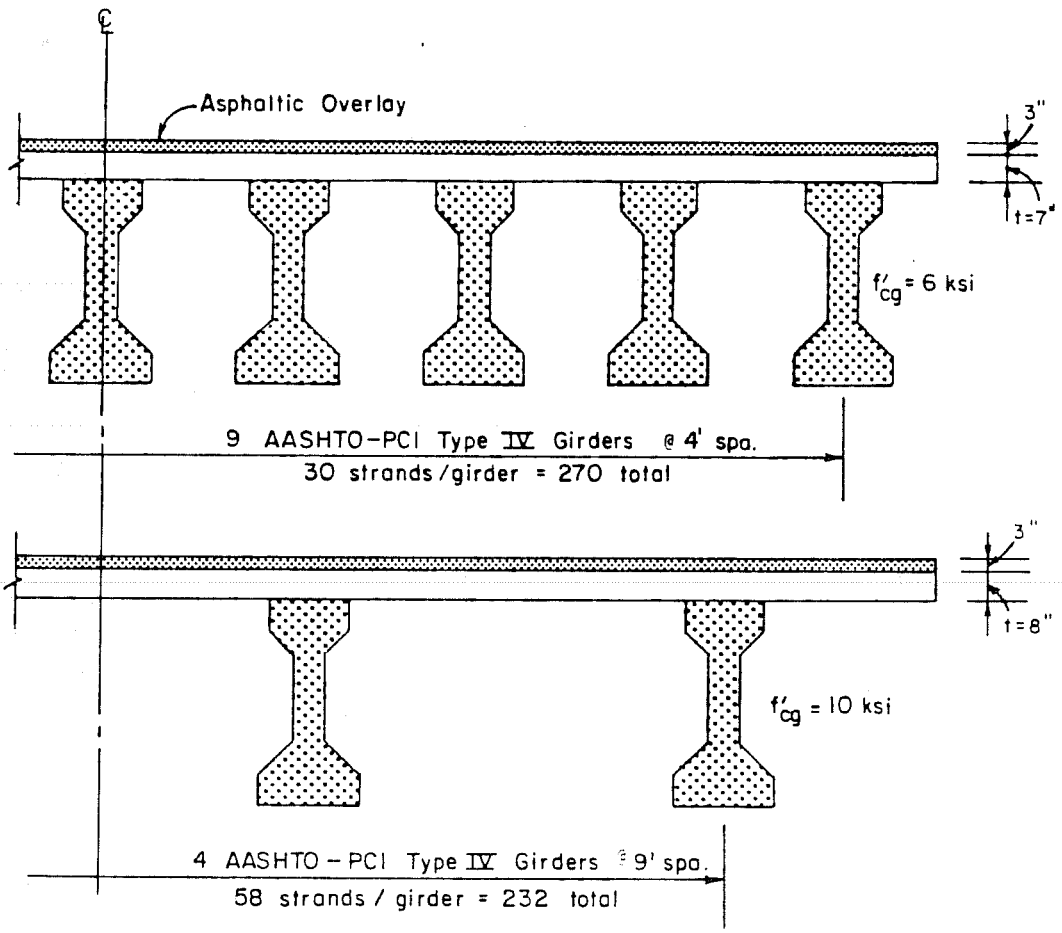

Fig. 1.1 Comparison of bridge designs for same span using normal and high strength concrete

Another benefit of the use of high strength concrete in highway bridge design is illustrated in Fig. 1.2, where an increase in girder concrete strength is shown to result in significantly greater maximum spans for a given cross-section, girder spacing (GS), and deck thickness. The dashed line indicates spans which exceed a limiting span length based on stability considerations. While means are available to increase the limiting span for a section, the extent of the line emphasizes the importance of considering stability in the design of long-span girders.

Where multiple spans are required, an increase in possible span lengths leads to a reduced number of piers and lower shipping costs. Increased span lengths can also allow elimination of supports, which can improve traffic safety at highway crossings. Another possible benefit from increased maximum span lengths is the use of shallower members for the same span length, which would improve clearances or result in reduction of embankment costs.

There are uncertainties, however, regarding the adequacy of current design codes for high strength concrete. Research on material properties of high strength concrete has shown that some properties differ significantly from those of normal strength concrete. A major area of difference is in the stress-strain behavior as illustrated in Fig. 1.3 [81], where typical stress-strain curves are shown for a range of concrete strengths. High strength concrete has a greater stiffness (or modulus) than other concrete and is more brittle, which is demonstrated by the short and steep descending branch of the stress-strain curve. The more brittle nature of high strength concrete has led to concern regarding the ductility of members constructed using high strength concrete. It has also been speculated [22] that the brittle nature of high strength concrete will lead to smooth shear cracks which would reduce the contribution of aggregate interlock to the ultimate shear strength. Furthermore, many of the present code design provisions are based on test data for which the concrete strengths rarely exceed 6,000 psi. Since little data is available on the behavior of high strength concrete pretensioned bridge members, it is not possible to establish whether current codes are adequate for the design of such members.

The realization of the full potential of high strength concrete in pretensioned bridge girders may also be limited by traditional techniques and methods of design and construction which were developed for use with normal strength concrete. This may be especially true where standardization has taken place such as for pretensioned girders, where most cross sections in use today were developed in the late 1950's and early 1960's for use with normal strength concrete.

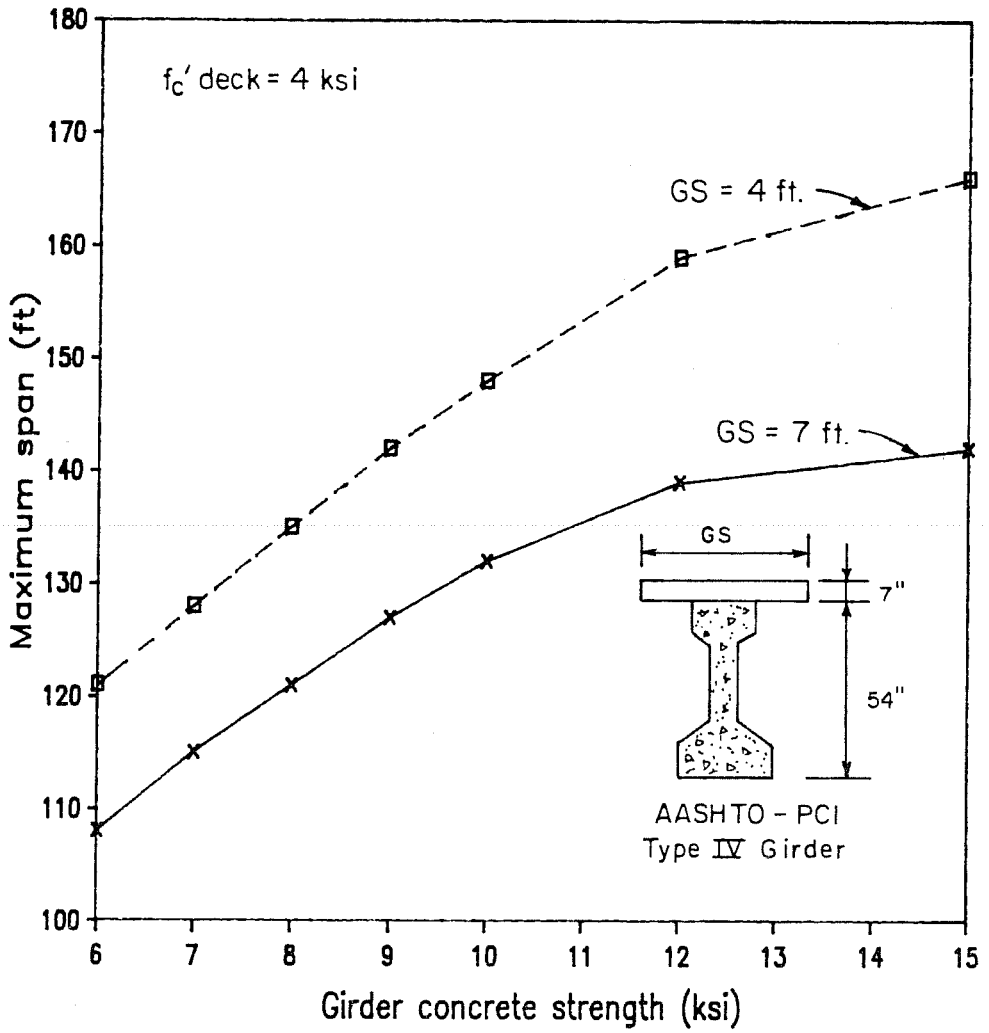

Fig. 1.2 Maximum span versus girder concrete strength

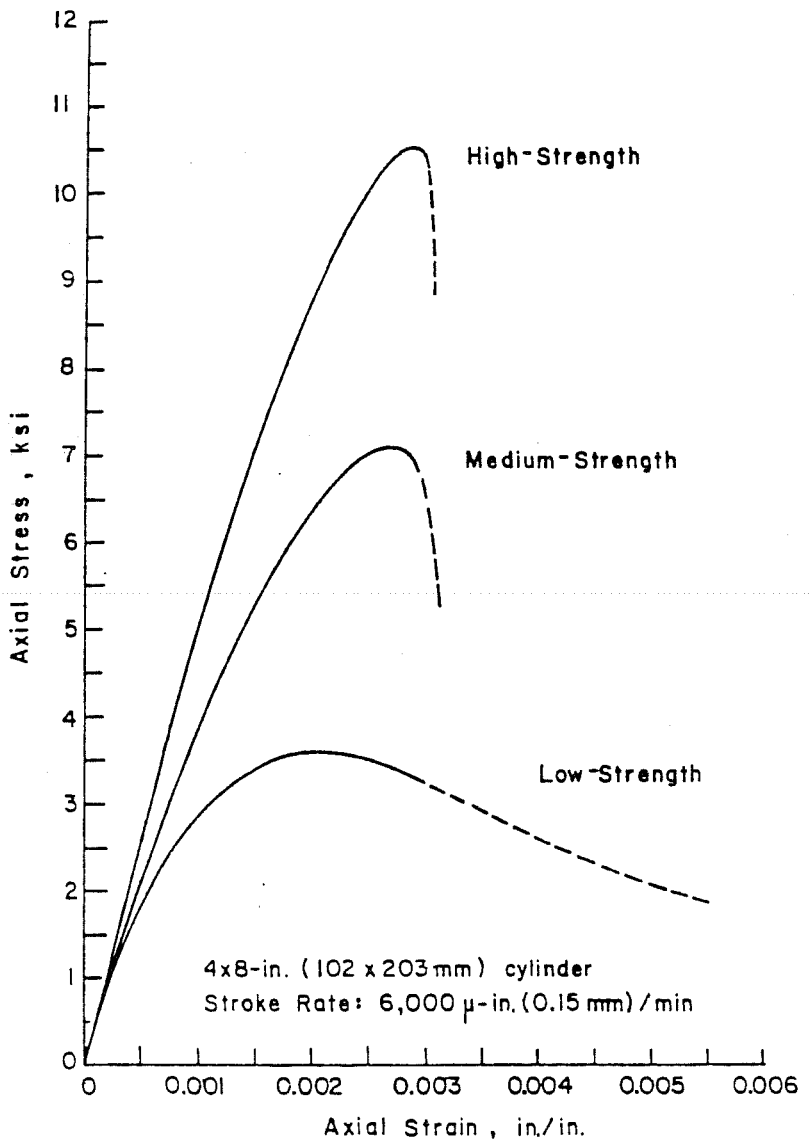

Fig. 1.3 Typical stress-strain curves

Because of these concerns regarding the use of high strength concrete and the applicability of current bridge codes to its use, it is essential that the material and structural behavior be clearly understood and incorporated into design codes before high strength concrete comes into general use. Current design and construction techniques should also be reviewed to determine where changes could be made for more efficient use of the material.

1.2 Objectives and Scope of the Study

1.2.1 General. This study was begun to investigate the feasibility and criteria for use of high strength concrete in the design of pretensioned highway bridge girders.

While the definition of high strength concrete varies for different regions of the country, for this study it is considered to be concrete with a design compressive strength between 6,000 and 12,000 psi. The lower limit corresponds to the standard concrete strength for pretensioned girders in Texas which is 6,000 psi and the upper limit represents a practical maximum strength that can be produced commercially. Since the upper limit is not intended to be restrictive, strengths higher than 12,000 psi are considered in some analyses that follow in order to better define trends. Only concrete made using common materials and admixtures will be considered.

The study is limited to the consideration of high strength concrete pretensioned bridge girders which become part of a highway bridge with a normal strength composite deck. Only simple span, non-skew bridges are considered. The deck is assumed to be applied with the girder unshored. Low relaxation strands are the only type considered in the study since this type of strand has virtually become the industry standard. Draping is used to control stresses at the ends of members.

The 13th edition of the American Association of State Highway and Transportation Officials (AASHTO) Standard Specifications for Highway Bridges [10] is used as the main source for design practice for the girders and bridge structures considered. Where helpful, the American Concrete Institute (ACI) Building Code Requirements for Reinforced Concrete (ACI 318-83) [15] and the Commentary on Building Code Requirements for Reinforced Concrete (ACI 318-83) [17] are also consulted for design practice.

1.2.2 Test Programs. Due to the lack of data in the literature on composite bridge construction with high strength concrete pretensioned girders, two test programs were developed to

provide data that would allow evaluation of the use of high strength concrete in the design of pretensioned bridge girders.

Tests were conducted at the Phil M. Ferguson Structural Engineering Laboratory at the University of Texas Balcones Research Center.

1.3 Organization of the Study

The second chapter of this report describes and evaluates the transfer specimen tests. Chapter Three describes construction and testing procedures for the scale-model girder tests while Chapter Four provides comments on behavior, and reports the data collected during construction and testing of the girder specimens.

Chapter Five contains an evaluation of the current philosophy of design for highway bridges. A review of the basic properties of high strength concrete is presented. Test data gathered in these tests of high strength concrete girders are summarized in plots of data including results from several other test program. The study concludes in Chapter Six with a summary of the investigation, and presentation of conclusions and recommendations.

Appendix A contains mix and strength design data for the high strength concrete used i the scale-model girders, and Appendix B details the history of the girder specimens.

A separate report (Ref. 139) consists of the comparison and evaluation of bridge designs using selected pretensioned girder cross-sections. Three proposed cross-sections, developed for use with high strength concrete, are included in the comparisons. Also included in that report is a literature review of the topics of interest in the study.

CHAPTER 2

TRANSFER LENGTH TEST PROGRAM AND RESULTS

2.1 Introduction

"Transfer length" is the distance required to transfer prestressing force from a strand to concrete at release. The concept is illustrated by the two plots of Fig. 2.1 which show the variation in strand and concrete stresses after release. Prior to release the strand is at a constant stress along its entire length (f_{so}). The transfer length is important because it defines the location at which the full effect of the prestress is available which is especially critical for shear design. Both the ACI and AASHTO codes provide an expression to estimate the transfer length.

A limited series of transfer tests was performed to determine how the transfer length for strand in high strength concrete compares to that for normal strength concrete, because data for high strength concrete is very limited. The goal of the test program was to determine whether the current code expression for computing transfer lengths may be applied to high strength concrete. It was not the intent of the program to provide sufficient data to permit development of a new expression for estimating transfer length.

The primary variable considered in the study was the strength of the concrete, with secondary variables being the effect of gradual or sudden release of the prestress force and the level of concrete stress after release. Specimens had a square cross section with a 0.5-in. diameter strand placed in the center of the section. The specimens were otherwise unreinforced. Twelve specimens were cast, eight from a normal strength mix and four from a high strength mix, providing measurements for determining the transfer length at 24 locations, since data was taken at both ends of each specimen. The transfer lengths were determined by concrete strain measurements taken by mechanical means.

2.2 Specimen Description

Previous studies on transfer length [64,65,67,70,100,112] were consulted to determine the specimen type and dimensions. The two square cross-sections shown in Fig. 2.2 were selected to approximate the concrete stresses present in the transfer regions of a

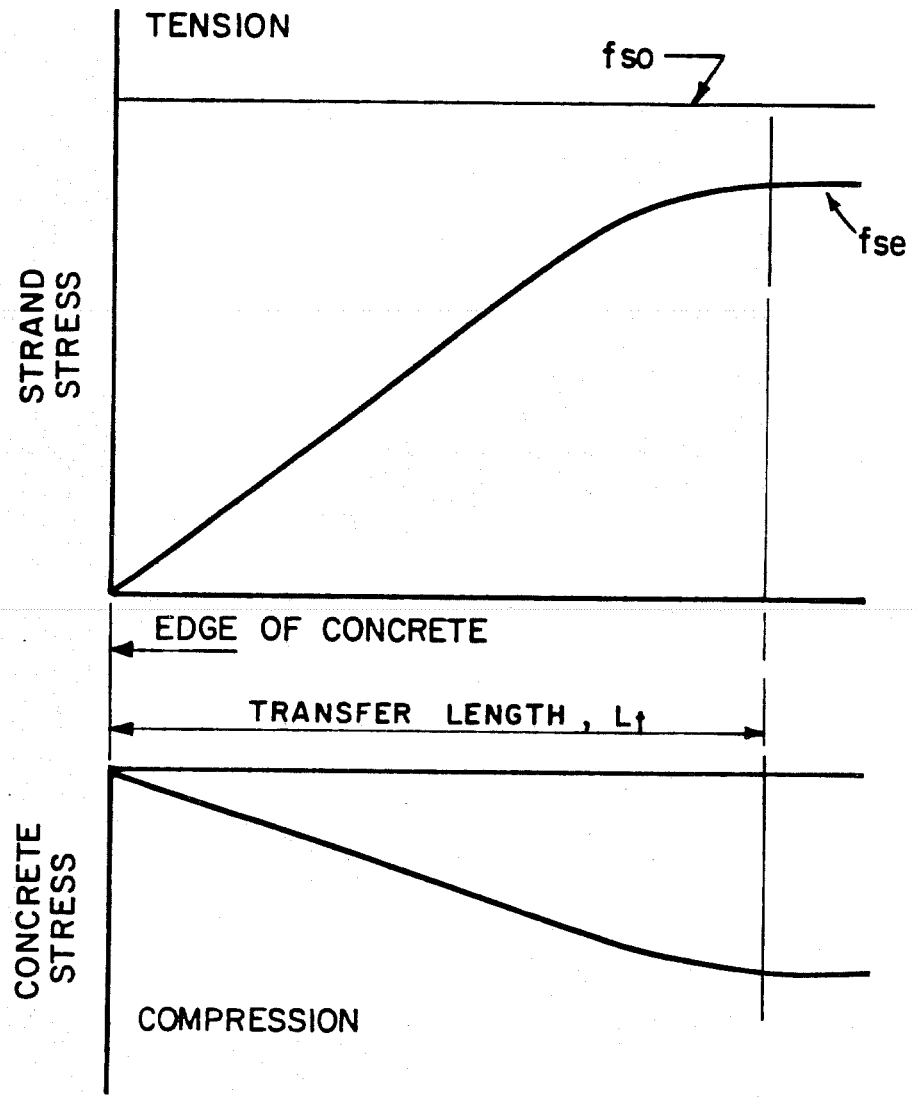

Fig. 2.1 Conceptual sketch of conditions defining the transfer length

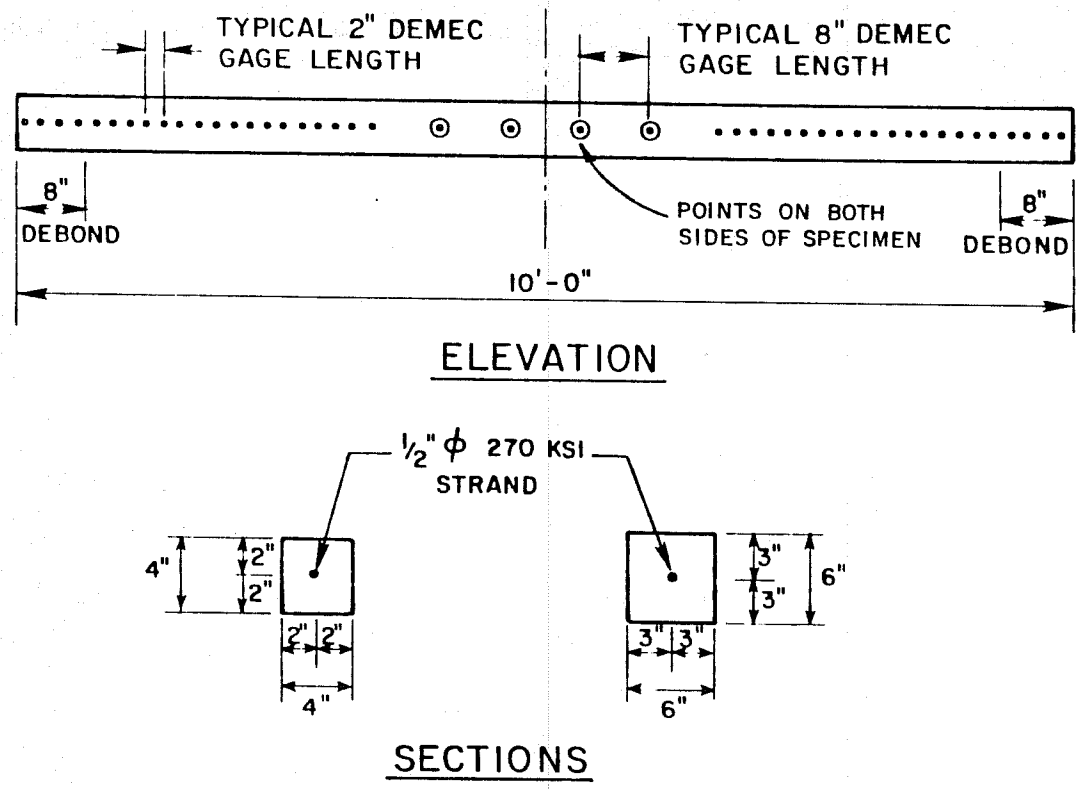

Fig. 2.2 Transfer length specimens

pretensioned girder and to provide a comparison of transfer lengths for concrete stressed to different levels. Specimens were 10 ft long with 8 in. of strand debonded at each end. The concrete surrounding the debonded strand remained unstressed after release. Therefore, the measured change in strain following release in the first gage length contained only the change in strain occurring between the end of the debond and the first gage point. In this way, the strain from the end of the bonded strand could be determined for each 2-in. interval along the specimen using an 8-in. long mechanical strain measuring device (demec gage). A steel extension has been provided by other investigators for the same purpose [70].

Two concrete mixes, with design strengths of 5,000 psi and 10,000 psi, were used in the specimens. Layout of the specimens in the prestressing bed for each cast is shown in Fig. 2.3. The use of two lines of specimens permitted the investigation of both sudden and gradual release of the prestress force.

In Fig. 2.3 each specimen is given a unique label. The number and letter appearing first indicate the nominal concrete strength and whether release of the prestress force was sudden (S) or gradual (G). The second number indicates the size of the cross section (4 or 6 in.), and the final number distinguishes between pairs of otherwise identical specimens. Ends of the specimens will be distinguished by reference to the north or south end as shown on the figure. The figure also indicates the location where the strand was flame cut to produce the sudden release.

The normal strength specimens were cast first and included specimens of both size cross sections, while only the smaller cross section was used for the high strength specimens. The larger section specimens were omitted from the high strength series due to the difficulty in taking the large number of strain readings associated with eight specimens.

2.3 Materials

2.3.1 Concrete. As mentioned earlier, two strengths of concrete were used. The first cast used a mix with a design strength of 5,000 psi at 28 days and the second was designed for a strength of 10,000 psi at 28 days. Mix proportions for the two batches are given in Table 2.1. Cylinder strengths were determined the day of release or the following day and at 28 days. The results of the cylinders tests are given in Table 2.2.

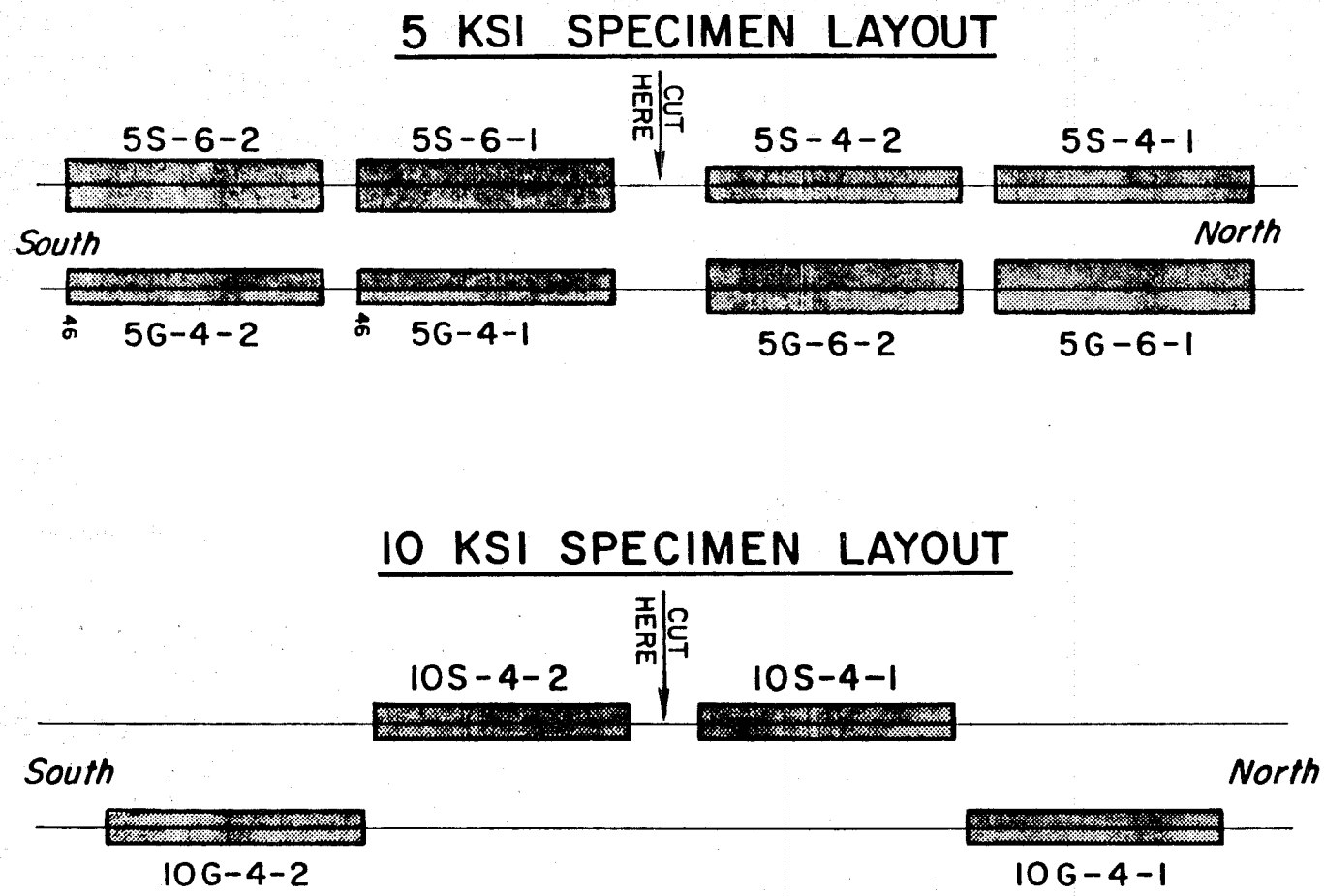

Fig. 2.3 Layout of transfer specimens in prestressing bed

Table 2.1 Mix designs and properties

	Normal Strength	High Strength
Design Strength (psi)	5,000	10,000
Mix Design (Quantities in lbs. per cu. yard)		
Type I Cement	564	814
Sand	1,340	1,279
3/8 in. Crushed Limestone	2,000	1,740
Water (gallons)	25	31.5
Water Reducing Admixture (Note 1)	---	16 oz.
Super-plasticizer (Note 2)	---	48 oz.
Quantity Delivered (c.y.)	1.5	4
Cost per Yard Delivered	$47	$56
Mix Properties		
Slump (in.)	5	1 and 10 (Note 3)
Water / Cement Ratio	0.59	0.29
Cement Content (sacks/cy)	6	10.5

Note 1 - 300 R - Master Builders
Note 2 - 400 N - Master Builders - 32 oz. at plant after batching was complete, 16 oz. upon arrival of truck at laboratory.
Note 3 - 1 in. slump at batch plant prior to addition of super-plasticizer; 10 in. slump at laboratory after second dose.

Table 2.2 Concrete strength data

		Normal Strength	High Strength
Concrete Strength Data			
Age	(days)	7	8
Mean Strength	(ksi)	5.1	9.5
No. of Cylinders		3	3
Age	(days)	28	28
Mean Strength	(ksi)	5.9	10.2
No. of Cylinders		4	4

2.3.2 Prestressing Strand. The prestressing strand used met the specifications for 0.5-in. diameter seven wire stress- relieved Grade 270 ksi strand. The elastic modulus was taken to be 27,500 ksi. The surface condition of the strand was good with only very light rust (no pitting). The strand was wiped clean before use to remove accumulated dust.

2.4 Fabrication

Strands were tensioned in the pretensioning bed at the laboratory the day before the specimens were cast. An initial load of 1,000 lb was applied to each strand using a system of pulleys and dead weights. The remainder of the force required to tension the strand to approximately 189 ksi was applied by a 200 ton hydraulic ram that tensioned both strands simultaneously. Load was monitored by pressure in the ram, strand elongation, and load in each strand as measured by a load cell. The elongation was locked off using retaining nuts then the ram was depressurized.

Formwork consisted of a base section to which side forms were attached. Each specimen was cast in an independent form. Forms were lacquered and oiled before each use.

At ends of each specimen, the strand was debonded by covering the strand with an 8-in. piece of vinyl tubing that had been slit and filled with grease. The tubing was then wrapped with duct tape as shown in Fig. 2.4.

Concrete was batched in a commercial plant and brought to the laboratory in a mixer truck. The batching process was monitored by laboratory personnel. Concrete was placed in the forms and vibrated using internal vibrators. Figure 2.5 shows the forms after casting and prior to covering with plastic sheeting for curing. Side forms on Specimen 5S-6-1 deflected outward during casting. The specimen was not used because of the varying cross section. Cylinders were cast and cured with the specimens at ambient conditions for use in determining concrete strength of the specimens.

After the concrete had cured for four days, the plastic and side forms were removed. Demec gage measurement points were applied at midheight of one side of each specimen as shown in Figs. 2.2 and 2.6 using "5 minute" industrial type epoxy. Measurement points for three additional gage lengths were placed on the other side to allow determination of bending effects. A total of 50 points were applied

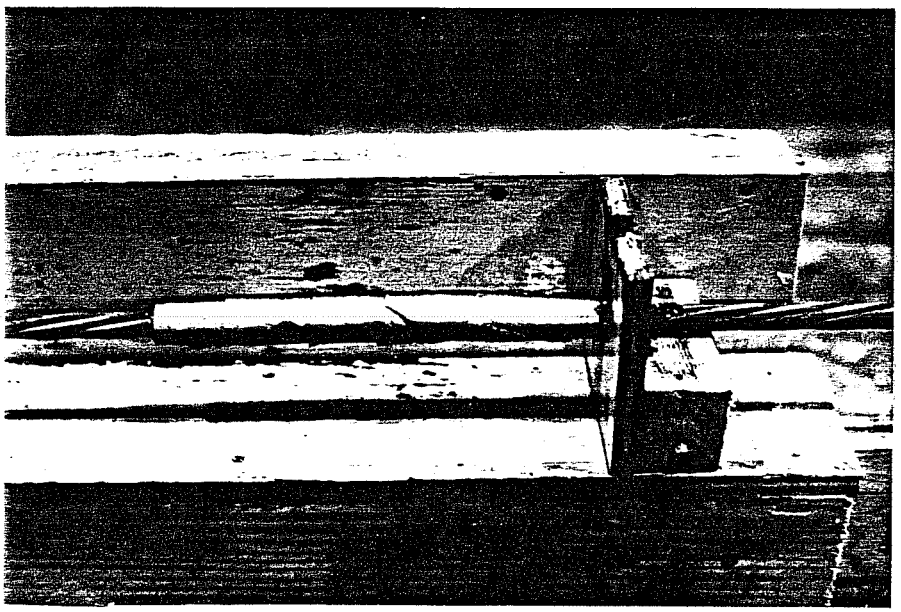

Fig. 2.4 Photograph of stand debond

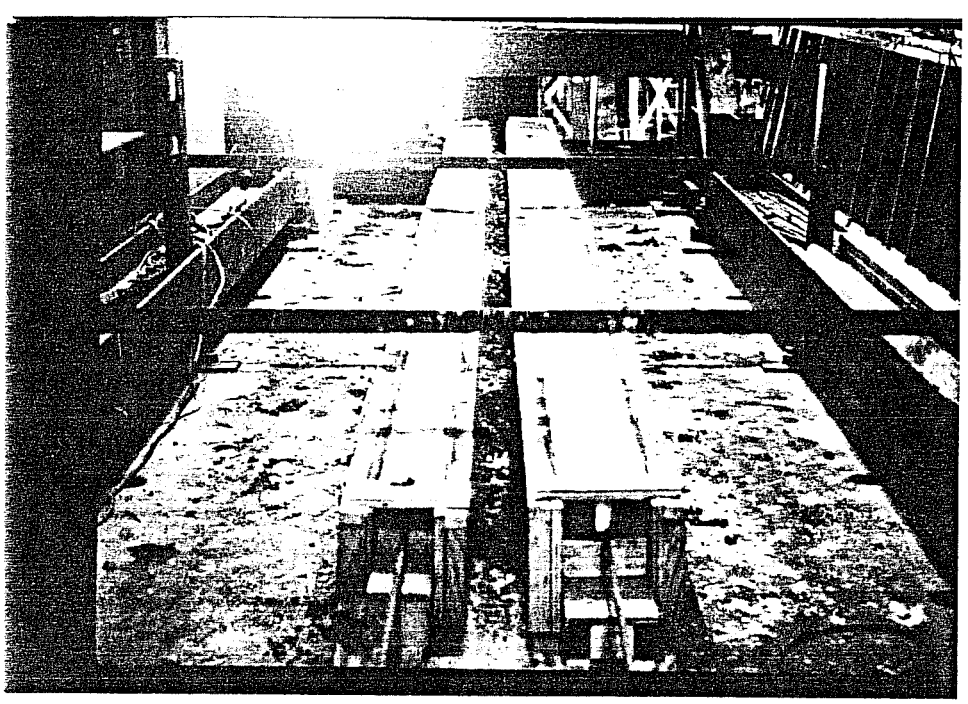

Fig. 2.5 Photograph of specimens in prestressing bed after placement of concrete

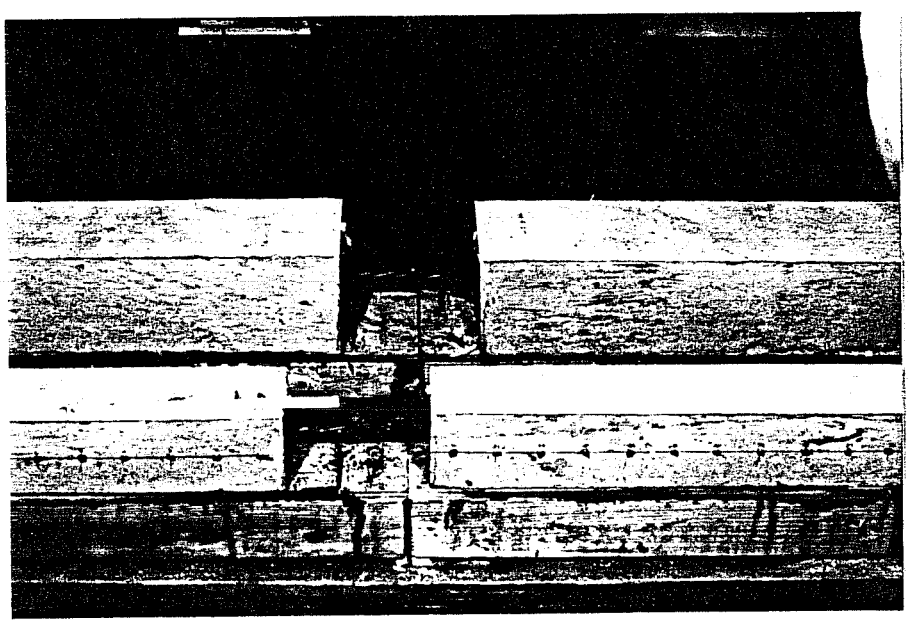

Fig 2.6 Photograph of specimens after release

to each specimen. Demec measurement points were placed on a cylinder from the high strength batch to provide a temperature correction for the readings.

2.5 Test Procedure

Release occurred seven days after the specimens were cast. An initial set of demec readings was taken for each interval. The first three gage lengths at the ends of each specimen were taken using a 2-in. demec gage while all others were taken using an 8-in. gage. Shortly after completion of the initial readings, one of the strands was flame cut to create a sudden release of the prestress force. Then the tensioning ram was repressurized, the retaining nuts loosened, and the pressure allowed to bleed off slowly to produce a gradual release of the prestress force in the other strand. A second set of readings was then taken. Readings were taken on the instrumented cylinder before and after taking readings for each specimen.

2.6 Test Results

The change in concrete strains at release was determined from initial and final demec gage readings. A plot was made for each specimen showing the variation of strains along the length of the specimen, excluding the debond length. The transfer length was then determined as the distance from the end of the bonded strand to the point at which the strain in the concrete becomes constant, as shown in Fig. 2.7 for a typical specimen from each concrete batch.

Distances from the end of the bonded strand to the point where the full prestress and 80 percent of the prestress have been developed are shown for both ends of each specimen in Table 2.3. The distance required for transfer of 80 percent of the prestress is included because it is viewed by some investigators as a more reliable measure of the transfer length. It should be noted that, because the 8-in. demec gage lengths did not overlap in the center of the specimens, transfer lengths could only be determined to the nearest 8-in. increment when greater than 25 in. A statistical summary of the full transfer data and comparison with transfer lengths computed by the AASHTO expression appear in Table 2.4. Frequency plots of distances required for transfer of the full prestress force are shown in Fig. 2.8 for the three categories of specimens.

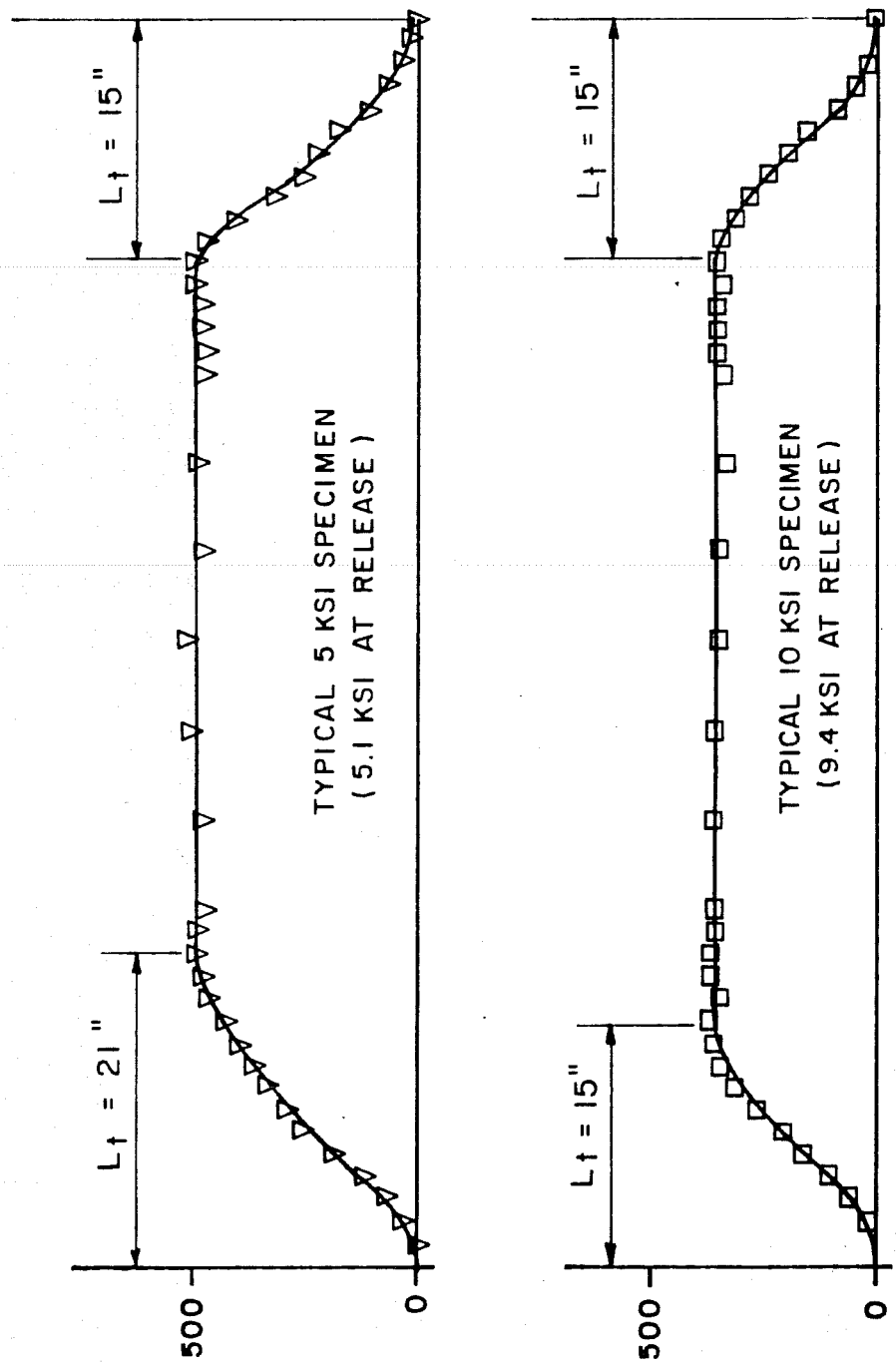

Fig. 2.7 Typical variation of strain with distance along specimens

Table 2.3 Results of transfer tests

Specimen Designation	Measured Transfer Lengths* (in.) Full Transfer North	Full Transfer South	80% Transfer North	80% Transfer South
5G-4-1	41	25	15	17
5G-4-2	21	15	13	11
5S-4-1	23	13	15	9
5S-4-2	15	23	11	17
10G-4-1	13	17	7	9
10G-4-2	15	15	9	9
10S-4-1	13	17	7	13
10S-4-2	19	11	17	9
5G-6-1	21	33	19	25
5G-6-2	25	33	19	27 (Estim.)
5S-6-2	23	19	17	11

* - Values shown for transfer lengths are distances (in inches) from end of bonded strand to point at which full prestress or 80 percent of the prestress was developed.

Note: Because 8-in. gage lengths in the center region of the specimens did not overlap, transfer lengths > 25 in. could only be determined in 8-in. increments.

Table 2.4 Summary of transfer test results

Specimen Type (in. x in.)	Concrete Strength (ksi)	Measured Mean (in.)	Measured Maximum (in.)	AASHTO Value (in.)
4 x 4	5.1	22	41	30
4 x 4	9.4	15	19	29
6 x 6	5.1	26	33	31

AASHTO Value: $L_t = f_{se}/3\ D$ (from Ref. [10], Sec. 9.27.1)

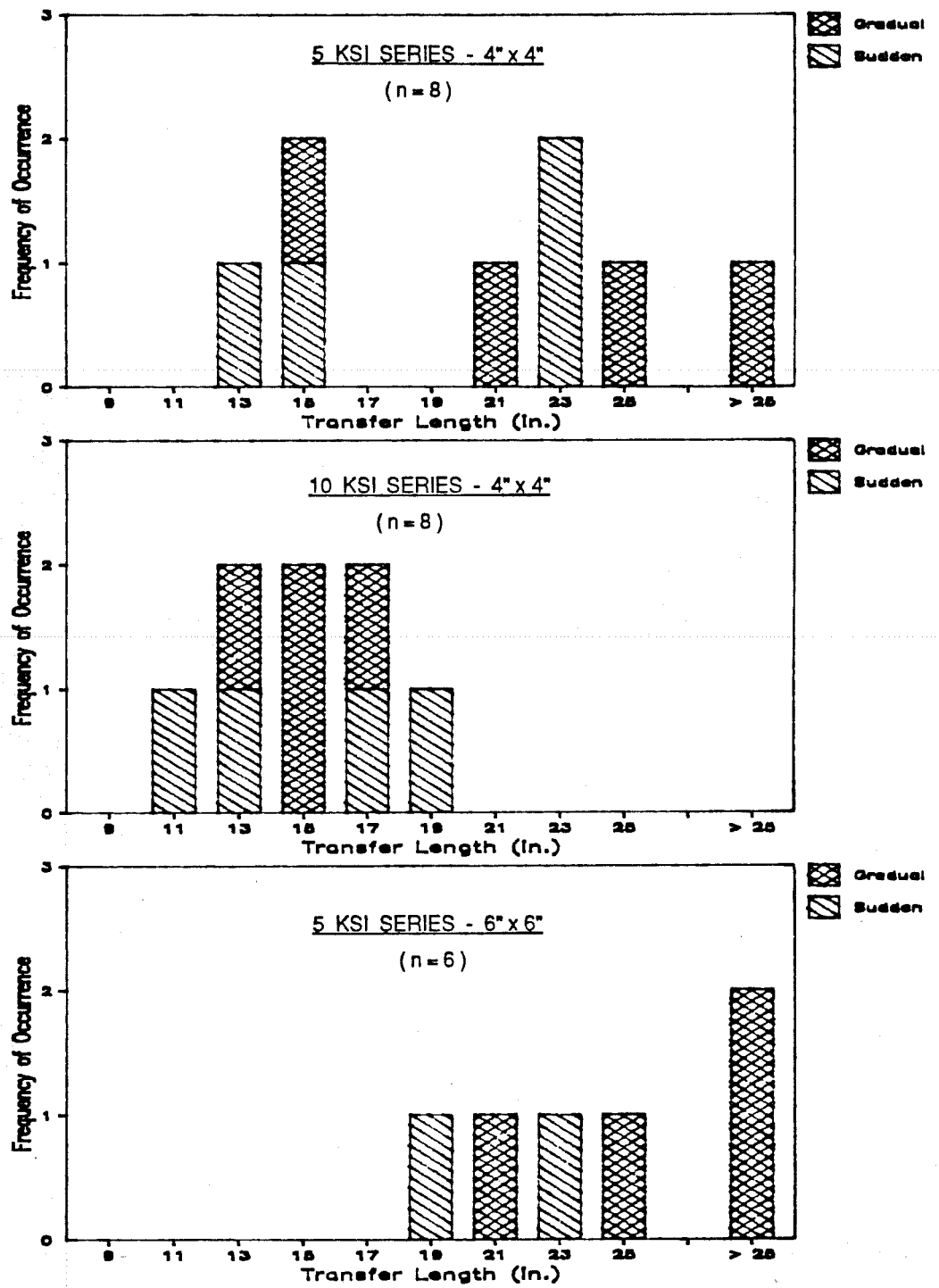

Fig. 2.8 Frequency plots of transfer length data

Concrete strains measured in the central portions of the specimens after release and effective strand stresses before and after release appear in Table 2.5. Strand stresses after release were determined by deducting the change in strand stress corresponding to the average concrete strain in the center of the specimen from the effective stress prior to release.

2.7 Observations and Conclusions

The following observations can be made from data obtained from this limited test series:

1. Transfer lengths for 0.5-in. diameter strand in high strength concrete were approximately 30 percent shorter than in normal strength concrete.

2. The gradual or sudden release of the prestress force had no significant effect on the transfer lengths measured in the 10 ksi series of tests, which was of primary interest in this study.

3. An increase in cross section size resulted in increased mean values for measured transfer lengths.

4. Measured transfer lengths for both high and normal strength concrete specimens were typically less than values computed using the AASHTO expression. Only one test in the entire series (22 tests) exceeded the computed value for transfer length.

While this was a limited series of tests, the following conclusions may be drawn from the above observations:

1. Transfer lengths for high strength concrete are shorter than for normal strength concrete.

2. The current AASHTO expression provides a conservative yet reasonable estimate for the transfer length of strand in high strength concrete.

Reference 141 reports transfer length test results on epoxy coated strand in normal strength concrete, with a very limited number of tests on uncoated strands. Their conclusion was that the experimental transfer length results for uncoated strands were longer than those calculated. This opposite conclusion from Ref. 141 compared to that given above for this test program indicates the need for more research in this area of transfer and development length.

Table 2.5 Concrete strain and effective strand stress data

	Normal Strength	High Strength
Concrete Strains after Release (microstrain)		
4 in. specimens		
Gradual	483	341
Sudden	449	355
6 in. specimens		
Gradual	204	
Sudden	210	
Effective Strand Stress Data (ksi)		
Before Release - 4 and 6 in. specimens		
Gradual	182.6	188.0
Sudden	185.3	191.2
After Release - 4 in. specimens		
Gradual	169.3	178.6
Sudden	172.9	181.4
After Release - 6 in. specimens		
Gradual	177.0	
Sudden	179.5	

Notes: Concrete strains are for central portion of specimen where strain is constant. Values shown represent an average for the type of specimen indicated.

Effective strand strains are determined by subtracting change in strand stress corresponding to concrete strains from effective strand stress before release.

Strand modulus = 27,500 ksi; area = 0.153 in).

CHAPTER 3

ONE-THIRD SCALE GIRDER TEST PROGRAM

3.1 Introduction

The purpose of this series of tests was to observe the behavior of pretensioned bridges constructed using high strength concrete girders and a normal strength concrete deck. Testing of such a structure was necessary because data on behavior of high strength concrete members is very limited and also because data related to composite bridge structures are not available in the literature. Analytical models used to predict service load and ultimate behavior have not been confirmed for use with high strength concrete because of this lack of data. There is also little data to demonstrate that structures employing high strength concrete, which is a brittle material, will have sufficient ductility.

Therefore, the purpose of this testing program was to gather data on the service-load and ultimate behavior of a composite bridge structure with a high strength concrete girder and low strength deck. Tests included specimens with both moderate and heavy reinforcement so that ductility of the structure could be studied.

Aspects of behavior that were of particular interest included ultimate capacity in flexure, load-deflection behavior (which gives an indication of member ductility), strains in the concrete and prestressing steel under load and at failure, and long-term deflections. Ultimate shear capacity was also of interest as preliminary data for a more complete series of shear tests that followed.

Test specimens were one-third scale models of a long-span modified AASHTO-PCI standard pretensioned bridge girder with a composite deck that was placed with the girder unshored. Specimens had identical external dimensions, and all strands were tensioned to the same force. Nominal concrete strength for the specimens was 12,000 psi in girders and 3,600 psi in slabs.

The principal variable in the investigation was the quantity of prestressing steel. Specimen 1 contained 13 3/8-in. diameter strands while nine strands were used for Specimen 2.

The second variable was the quantity of shear reinforcement. Stirrups in Specimen 1 provided the maximum stirrup contribution to shear strength permitted by the codes ($V_s=8\sqrt{f'_c}b_wd$). Specimen 2 had half the number of stirrups of Specimen 1, or ($V_s=4\sqrt{f'_c}b_wd$). The effect of stirrup details on shear capacity was investigated in Specimen 1 by using standard and modified stirrup details for the two ends of the girder. In Specimen 2, the effect of strand bond on shear capacity was studied by providing an overhang at one end of the girder but using standard details at the other end.

3.2 Specimen Description and Design

3.2.1 Flexural Design. Specimens were intended to be representative of members that are in wide use, yet make efficient use of high strength concrete. Therefore, a modified AASHTO-PCI Type IV girder was used for the prototype. The section was modified by reducing the distance between side forms by 2 in., as suggested in Ref. [109]. The nominal girder concrete strength of 12,000 psi is near the practical upper limit of field-produced concrete at this time. A concrete strength at release of 9,000 psi was assumed, although this did not control designs. A 3,600 psi composite cast-in-place deck was added to the unshored girder to complete the structure. Girders were pretensioned with 0.5-in. diameter Grade 270 low relaxation seven wire strands placed on a 2 by 2 in. grid. Rows were filled from the bottom and strands were draped to produce stresses within the allowable limits at the ends of the girder at release. A single typical interior girder and deck were used in the design. The presence of diaphragms was neglected. Composite section dimensions and properties are shown in Fig. 3.1.

The goal of the design of Specimen 1 was to obtain crushing of either the deck or girder concrete near the load at which strands yield (produce the balanced reinforcement condition). A series of preliminary designs were conducted for the prototype using AASHTO loadings and allowable stresses, with losses computed using the procedure given in Ref. [137]. This was supplemented by moment-curvature analyses to give an improved prediction of strand and concrete stresses at failure. The thickness of the slab was obtained from information found in Ref. [109] (see Table C.1).

It was found that a long span with close girder spacing would produce the desired balanced failure if strands were provided in addition to the minimum required for allowable stress design. A span

	PROTOTYPE
GIRDER	
I ($in.^4$)	233,854
A ($in.^2$)	681
y_t (in.)	29.63
y_b (in.)	24.37
STRAND PATTERN	
SPECIMEN 1	
No. of Strands	64
g at Midspan	8.063"
g at End	18.063"
SPECIMEN 2	
No. of Strands	44
g at Midspan	5.455"
g at End	8.636"

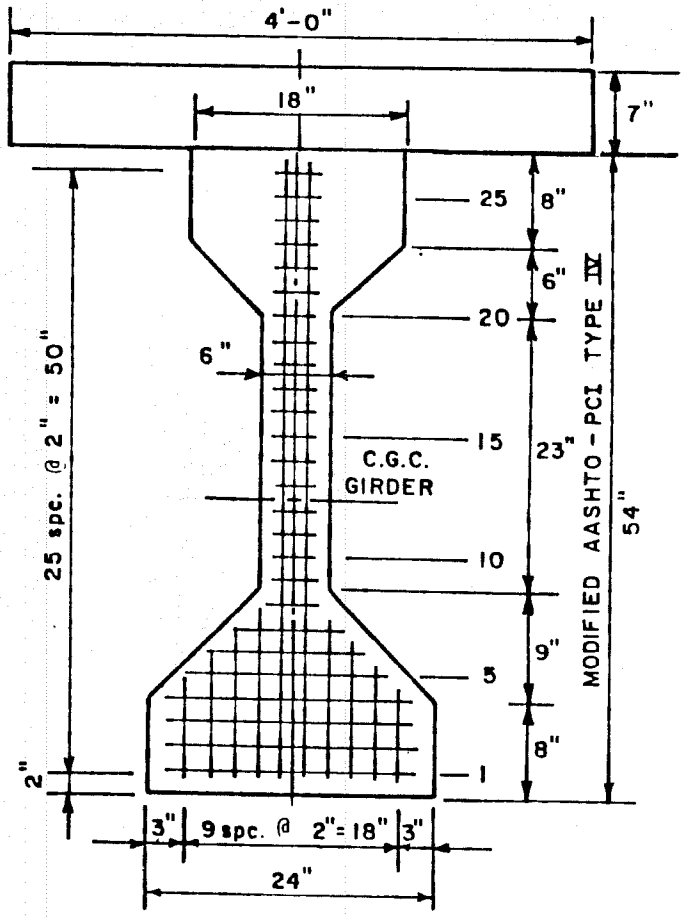

Fig. 3.1 Prototype dimensions and section properties

of 146 ft with girders spaced 4 ft apart was selected. This span is close to the maximum span for the section at this spacing. The prototype design required 64 strands to obtain a failure near the balanced reinforcement condition. While allowable stress design criteria could be satisfied with as few as 40 strands, it was felt that the additional strands could possibly be required to control long-term deflections.

In order to permit testing of a specimen in the laboratory, the prototype was reduced to a scale model. A scale factor of one-third was selected which reduced the span to 48 ft 8 in. with a girder spacing of 16 in. Dimensions and loads were scaled so that the same stresses would be present in the scale-model specimen as in the prototype. Because stresses were the same but the depth was reduced by one-third in the test specimens, the strain gradient across the depth of the section was not the same for specimen and prototype, with the strain gradient in the specimen being three times greater. Because strands could not be scaled directly, 3/8-in. diameter Grade 270 low relaxation seven-wire strand was used. Thirteen strands were required in the model, positioned on a 1 1/4 by 1 1/4 in. grid which provided a strand layout that closely resembled the prototype layout. However, the 3/8-in. strand could not properly model the bond of the 1/2-in. strands used in the prototype. This was unavoidable, but had a significant effect only in the shear tests. Dimensions and properties for the scale-model are shown in Fig. 3.2. Strand patterns at midspan and at ends of the girders are shown for both specimens in Fig. 3.3.

Design of Specimen 2 was postponed until testing of Specimen 1 was completed. Since a near-balanced flexure failure was obtained with Specimen 1, Specimen 2 was designed to produce a more ductile failure. It was also desired that both the girder and deck concrete be near crushing at ultimate, with the girder still making a significant contribution to the compression zone. A moment-curvature analysis was again used to determine the expected strains in concrete and steel at failure and the load- deflection response of the structure. These criteria were best satisfied for the model by a 9 strand pattern which corresponds to approximately 44 strands in the prototype. This design, which uses the fewest strands possible to satisy allowable stresses for the given span and spacing, is typical of current highway bridge designs.

As is the case whenever scale models are used, the dead weight of the scale model itself was insufficient to correctly model stresses. Therefore, concrete masses (dead load blocks) were suspended

	SCALE MODEL
GIRDER	
I ($in.^4$)	2876
A ($in.^2$)	75.25
y_t (in.)	9.876
y_b (in.)	8.124
STRAND PATTERN	
SPECIMEN 1	
No. of Strands	13
g at Midspan	2.788"
g at End	5.865"
SPECIMEN 2	
No. of Strands	9
g at Midspan	1.944"
g at End	3.083"

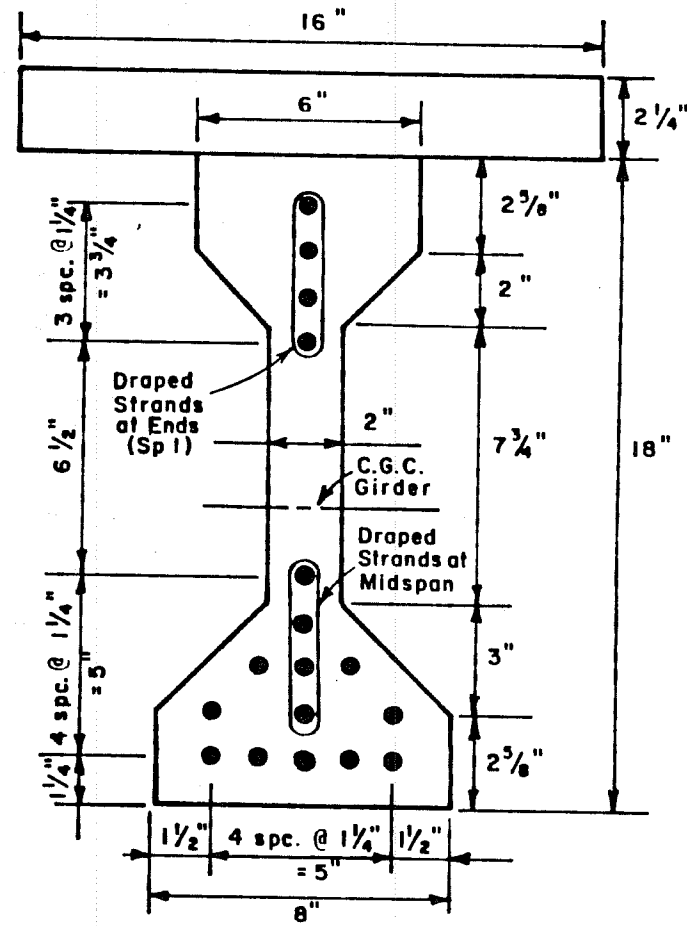

Fig. 3.2 Scale model dimensions and section properties

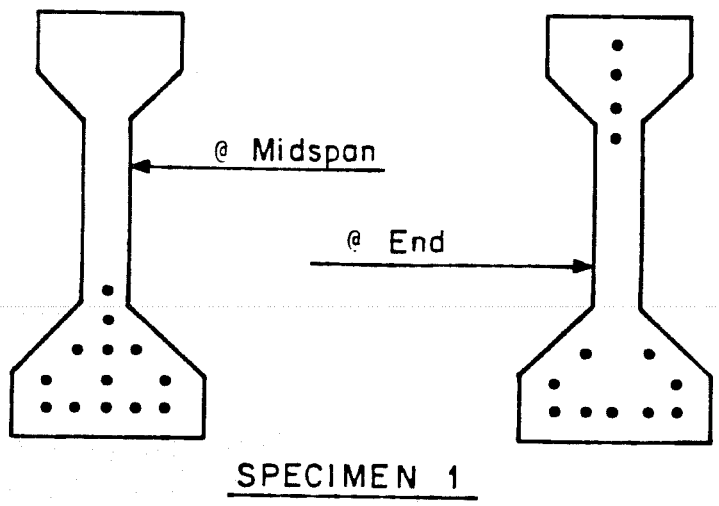

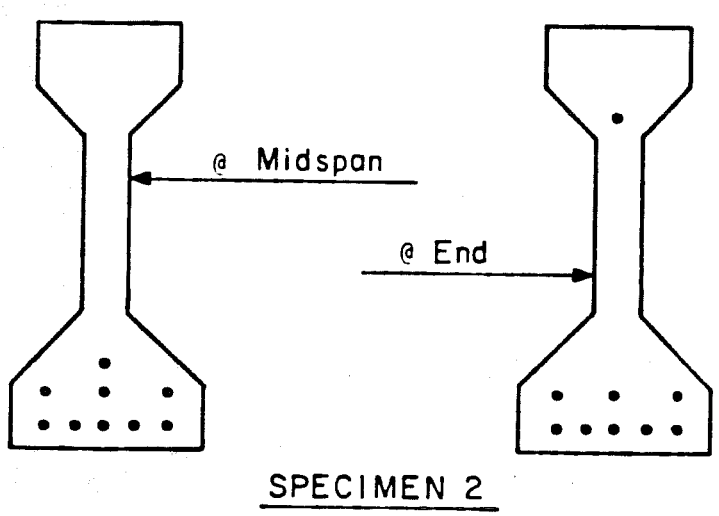

Fig. 3.3 Strand patterns for specimens

from the test specimens to compensate for the lack of dead load. The compensating load was equal to two times the actual weight of the specimen. The application and distribution of these loads are described elsewhere in this chapter.

The slab was designed to resist forces applied by dead load blocks. Stirrups extended into the slab provided sufficient reinforcement for these loads. Two No. 2 deformed reinforcing bars were placed longitudinally in the slab as minimum reinforcement.

3.2.2 Shear Reinforcement Design and Detailing. Design of shear reinforcement for Specimen 1 was based on the maximum quantity of shear reinforcement allowed by the AASHTO shear design provisions. This quantity, which is specified as ($V_s=8\sqrt{f'_c}b_w d$), corresponded to a spacing of 2 3/8 in. and was provided throughout portions of the girder which would be tested in shear. Shear reinforcement for Specimen 2 was one half of this quantity, resulting in a spacing of 4 3/4 in. Girder reinforcement for the scale model is shown in Fig. 3.4.

For Specimen 1, different stirrup details were used at each end. A stirrup modelled after the standard Texas open stirrup was used at the south end, and a stirrup which crossed beneath the center column of strands and hooked up at the edges of the section was used at the north end (Fig. 3.5). The second stirrup detail was expected to provide more confinement for the strands. For Specimen 2, the standard Texas stirrup detail was used in the shear span at both ends, but a 6-in. overhang was provided for the shear test of the north end in order to study the effect of strand bond on the shear capacity of the section.

End reinforcement details used in the specimens, which are shown in Fig. 3.6 and 3.7, were based on the standard Texas detail for a Type IV girder, which appears in Fig. 3.8. For Specimen 2, an extension of the standard detail was provided for the overhang. At locations where interior supports were to be located for shear tests, additional stirrups and mild steel longitudinal reinforcement was provided to limit cracking during the flexure test. Stirrup spacing was reduced in the central region of the specimens, as shown in Fig. 3.4.

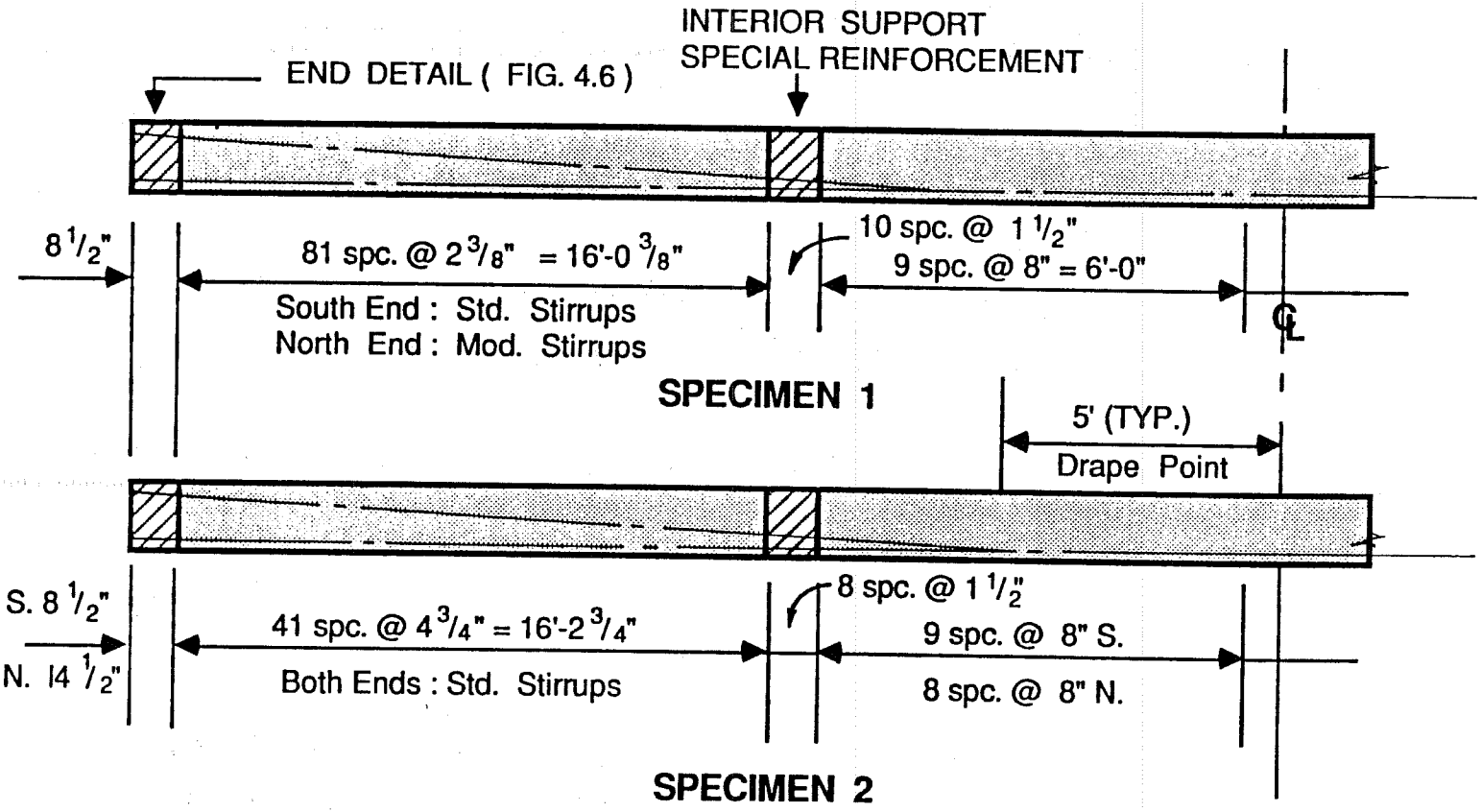

Fig. 3.4 Scale model girder reinforcement

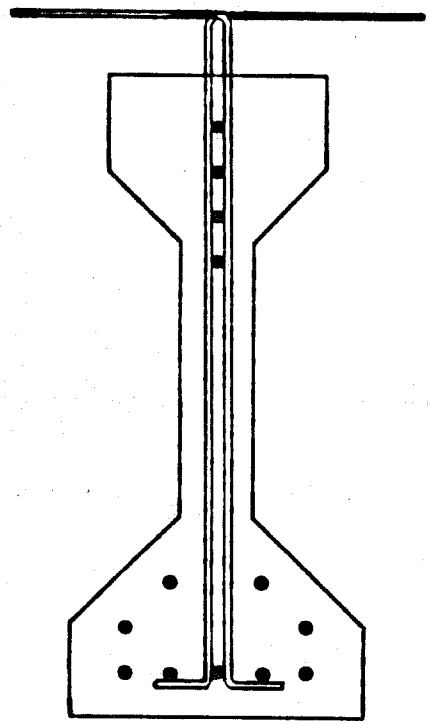

STANDARD
SPECIMEN 1, SOUTH END
SPECIMEN 2

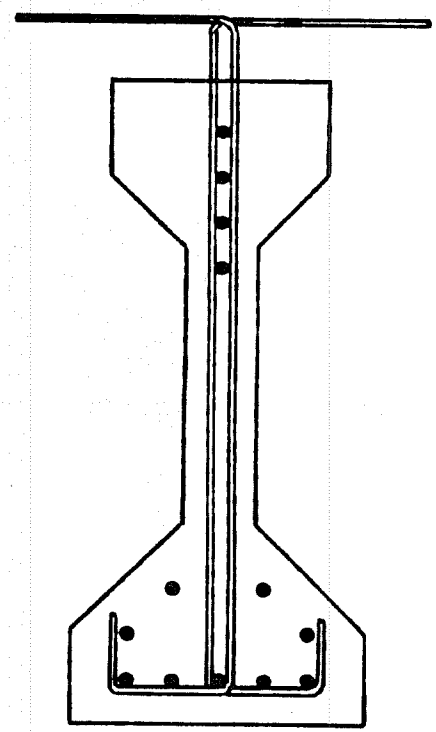

MODIFIED
SPECIMEN 1, NORTH END

Fig. 3.5 Stirrup details

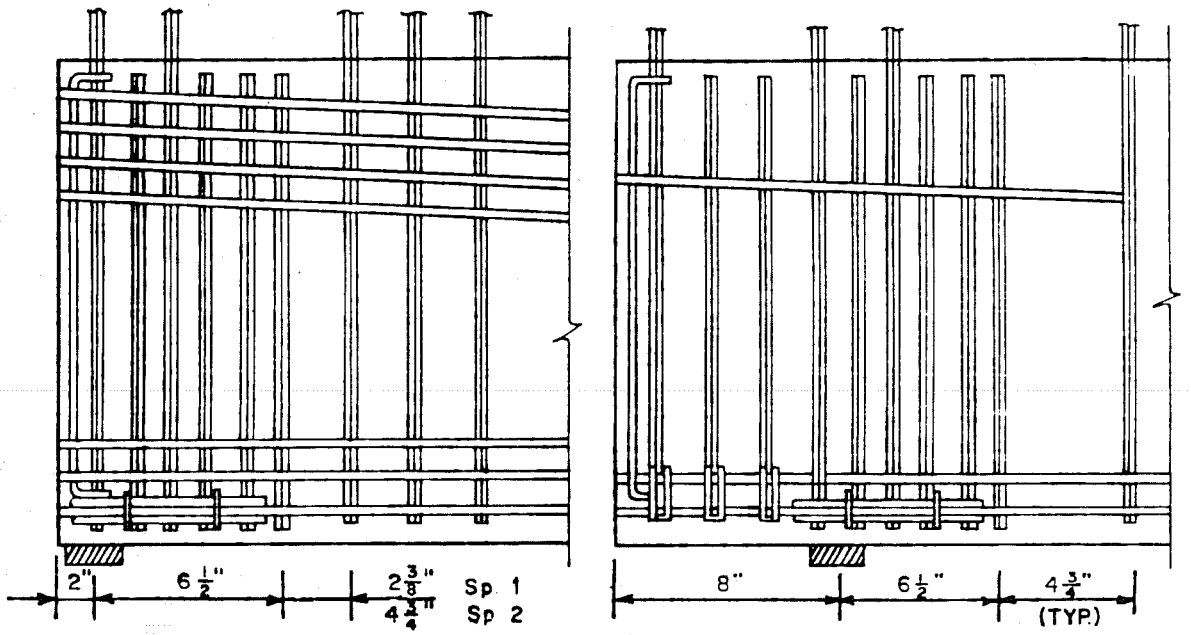

SPECIMEN 1

SOUTH END-SPECIMEN 2

NORTH END-SPECIMEN 2

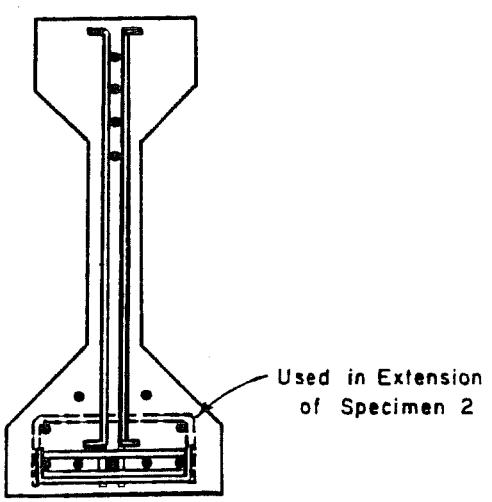

END VIEW

All Reinforcing Bars are No. 2
Prestressing Strands are 3/8" diam.

Fig. 3.6 Scale model end reinforcement details

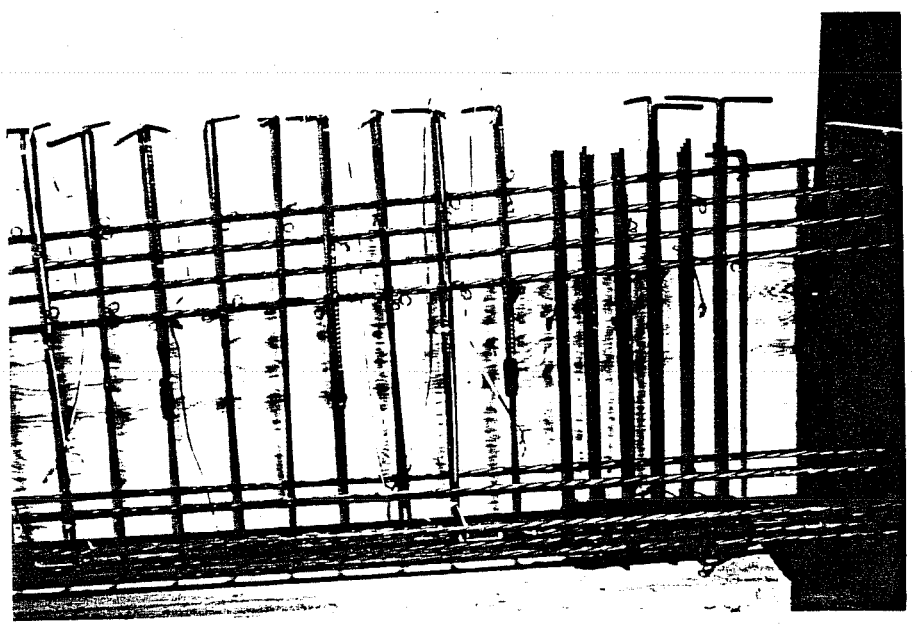

Fig. 3.7 Photograph of end reinforcement detail - south end, Specimen 1

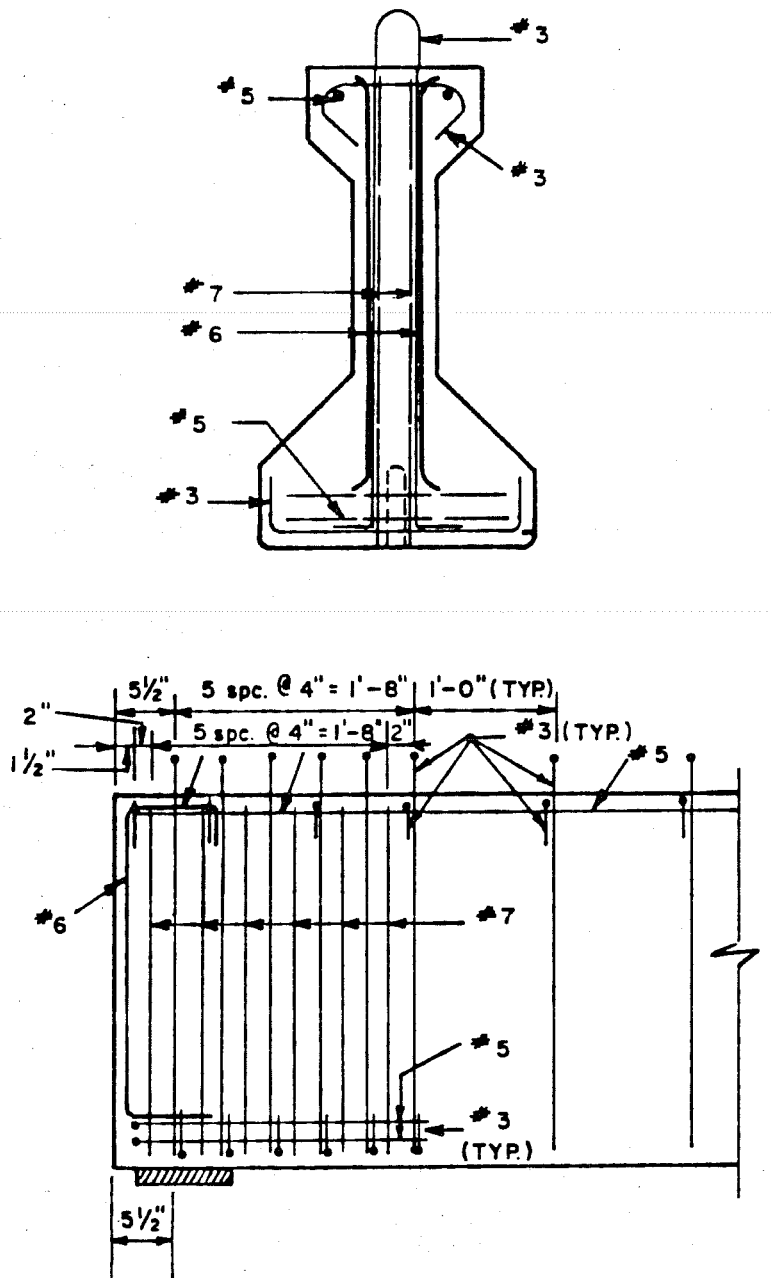

Fig. 3.8 Texas SDHPT standard end reinforcement detail for Type IV girder

3.3 Materials

3.3.1 Concrete. A high strength concrete with a design strength of 12,000 psi at 28 days was used for the girders. To determine the mix design for this concrete, 22 trial batches were produced and tested. Data from these trial batches are reported in Ref. [35]. Strength data for the girder and deck concrete at critical events during fabrication and testing for Specimen 1 and 2 in Table 6.1 and 6.7, respectively. Complete strength data and information regarding the mix design for the high strength concrete used in the specimens appear in Appendix A. The normal strength concrete mixes used for the deck, which were designed to have a strength of 3,600 to 4,000 psi at the time of the flexure test, were standard mixes and contained entrained air. Different mixes were used for the two specimens to satisfy testing schedule requirements. All mixes were batched at a ready mix plant and were transported to the laboratory in a mixer truck.

Properties of the concrete were determined by testing 6 by 12-in. cylinders under axial compression and 6 by 6 by 21 in.- beams loaded at third points. Steel and plastic molds were used for the cylinders. Some cylinders were cured in a lime bath, while most were air cured with the specimens after receiving a coat of curing compound after removal from the molds. The modulus of elasticity for the concrete was determined using a compressometer or strain gages applied to the cylinders.

3.3.2 Prestressing Strand. The prestressing strand was 3/8-in. Grade 270 ksi seven wire low-relaxation strand donated by Florida Wire and Cable Company. The strand was lightly rusted with some light pitting.

Load-strain characteristics of the strand were given in the mill test report supplied with the strand, and were supplemented by tests conducted in the laboratory with electronic strain gages attached to single wires of the strand. The load-strain curve and other test data provided with the mill report appear in Fig. 3.9, along with the average apparent modulus determined from strand tests using strain gages. The average cross sectional area of the strand was 0.0845 $in.^2$, which was determined by weighing and measuring lengths of strand and then computing the area by assuming the unit weight of steel to be 490 pcf.

3.3.3 Nonprestressed Reinforcement. The small size of deformed reinforcement required for model construction is not produced

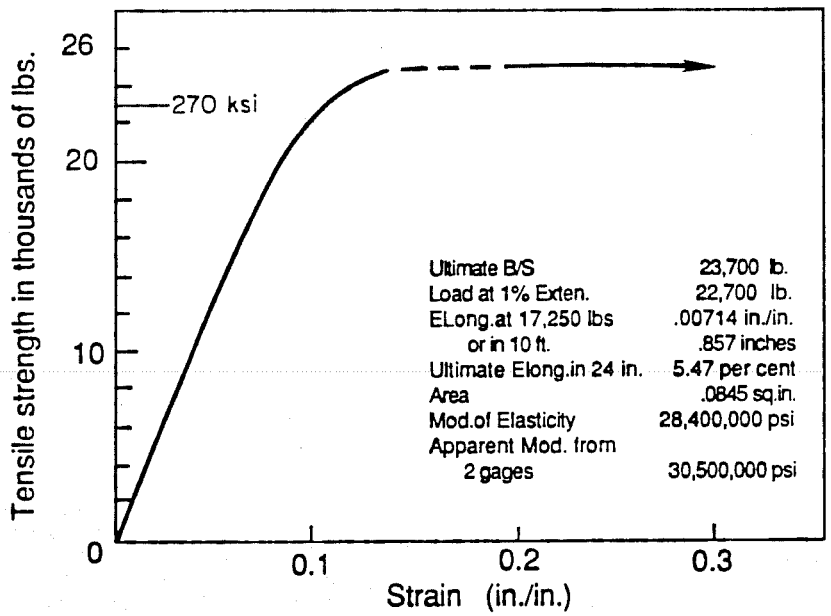

Fig. 3.9 Load-strain curve and associated data for prestressing strand

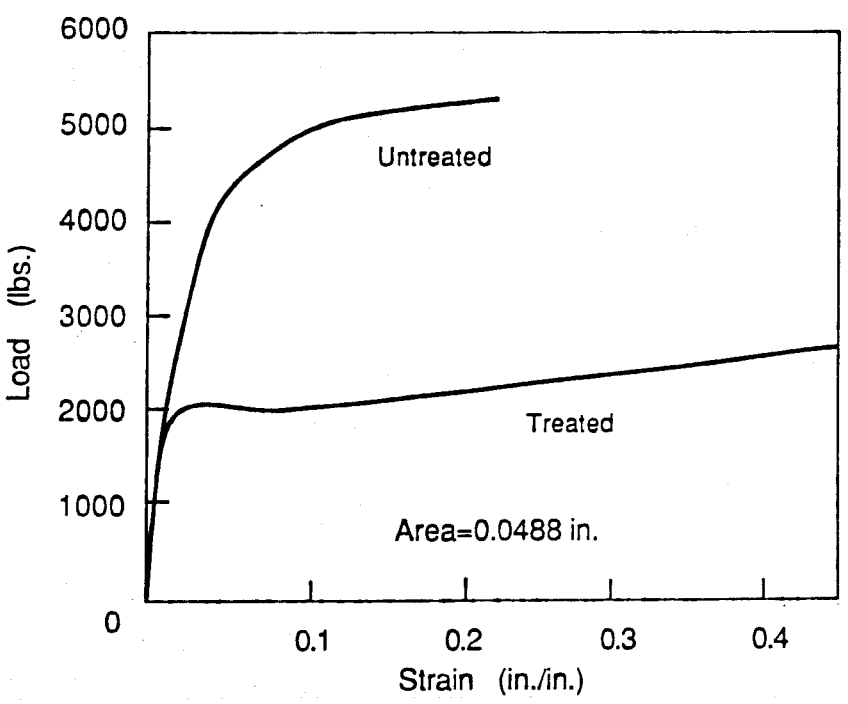

Fig. 3.10 Typical load-strain curves for No. 2 deformed bars

domestically. However, it was discovered that a mill in Mexico was producing small sizes of deformed reinforcement. The name and address of the mill was:

Alta Resistencia, S.A.
Sucursal Monterrey
Abraham Lincoln 4016
Fraccionamiento Lincoln
Monterrey, N.L.
Telephone: 70-32-23

Quantities of this steel were obtained in sizes corresponding to No. 2, No. 1.5, and No. 1.25, although only No. 2 bars were used in the specimens. As received, this steel had a high yield strength and limited ductility. Heat treatment at a local commercial characteristics typical of domestic reinforcement. After treatment, the steel yielded at an average stress of 44 ksi and had a significant yield plateau. Typical load-strain curves for the untreated and treated No. 2 reinforcing bars are shown in Fig. 3.10, which also gives the average area for these bars. The area was determined using the weighing method described in the preceding section.

3.4 Fabrication

3.4.1 Prestressing Operation. Strands were tensioned in the prestressing bed at the laboratory. A post-tensioning ram, loaned to the laboratory by the VSL Corporation, was used to apply an initial tension to each strand. This ensured a uniform stress in the strands. Chucks and wedges were donated by the Great Southwest Marketing Company.

Initial tensioning was achieved in stages. First, a strand was tensioned to the full prestressing force of 17 kips to set the wedges in the chucks at the far end of the bed. The force was then released and a chuck and wedges were placed on the strand at the tensioning end. The strand was then stressed to a partial load of 10 kips, which provided a greater margin of safety while tying stirrups to the strands. Finally, the wedges were power-seated by releasing the pressure in the ram.

To remove slack and provide a repeatable reference for elongation measurements, an initial force corresponding to 500 psi in the ram was applied to each strand before tensioning to both the 17

and 10 kip level. Pressure in the ram and movement of both ends of each strand were monitored and checked for agreement during the stressing operation. Strain gages on the two instrumented strands, which were the first strands to be tensioned, were read at each stage of their tensioning and at intervals during the remainder of the tensioning procedure.

Hold-down points for draped strands were located 5 ft each side of midspan. Drape hardware was fabricated at the laboratory and supported the strands on rollers (Fig. 3.11). The hold-down hardware bolted to an anchor block attached to the strong testing floor. At one end of the prestressing bed, the same hardware was used to hold up draped strands to obtain the desired strand profile.

After stirrups and detail reinforcement were tied to the strands, a 200-ton ram pulled all strands simultaneously to a final stress of approximately 200 ksi, which corresponded to a force of 17 kips per strand. This tensioning was controlled by strand elongation and change in strain in the strands. Friction in the tensioning system precluded use of the ram pressure for load control. After full stress was achieved, elongation was maintained by tightening restraining nuts. Pressure in the ram was then released.

Transfer of the prestress force to the girder was begun by releasing the hold-down hardware near midspan. This applied an upward force on the section, which had no precompression. In Specimen 1, which had four draped strands, this force was sufficient to cause cracking over the first hold-down to be released. Dead load blocks were placed on Specimen 2 at release although the force was much less because only one strand was draped. Following release of the draping hardware, the large stressing ram was repressurized, restraining nuts were loosened, and the ram was slowly depressurized to transfer the prestress force gradually. Strands were then cut with a torch at each end to free the girder. Later, the strands were ground off flush with the end of the girder.

3.4.2 Girder Fabrication. Girder forms were constructed in three parts. The soffit form, which was bolted to the base, ran the full length of the girder, with cut-outs for the drape hardware. Side forms were built up from layers of plywood to obtain the desired contour. Each side form was built in two sections to facilitate handling. Side forms were held in place by threaded rods passing through the soffit and through angles bolted to the top of the side forms. Plywood end forms were bolted to ends of the side forms. The forms received several coats of lacquer before each use.

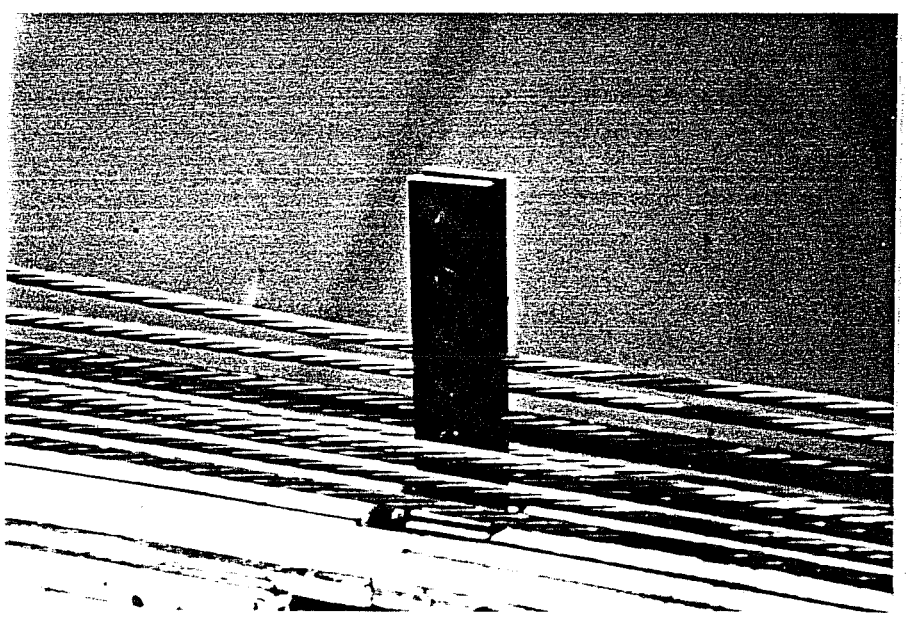

Fig. 3.11 Photograph of hold-down hardware

Stirrups and detail reinforcement were cut and bent in the laboratory. Strain gages were attached to stirrups and strands where desired. After initial tensioning of the strands was completed, stirrups and detail reinforcement was tied to the strands. After full tension was applied to the strands, girder forms were lightly oiled and then secured in place.

Concrete was placed in three lifts using a small concrete bucket or shovels. Internal vibrators were used to consolidate the concrete, although the tight clearances between strands, stirrups and forms made them difficult to use. However, consolidation was very good and damage to the forms was limited. The concrete was struck off level with the top of the forms, then roughened to ensure proper composite action.

Forms were covered with wet burlap and plastic for curing. Specimen 1 was cast in January when the ambient temperature in the laboratory was maintained between 50 and 70xF. Specimen 2 was cast in July with a temperature range of 75 to 100xF. Forms were removed in three to five days, and the burlap and plastic were replaced for a few more days.

Electrical resistance strain gages and mechanical strain gage (demec) points were applied to the surface of the girder each side of midspan and near the ends. After release, the girder was moved to the location where the slab was cast and the completed specimen was tested.

3.3.3 Slab Fabrication. Slab forms were constructed in sections that connected together and were supported by the girder. Support was provided by coil rod hangers that crossed over the girder, and by knee braces that propped the forms against the bottom flange of the girder. Dead load blocks required to compensate for the lack of dead load in both the slab and girder were placed on the forms until the slab was cast and cured.

Concrete was placed in the deck forms using an overhead crane and a small concrete bucket. Internal vibrators and a vibrating screed were used to consolidate the concrete. The surface was trowelled then covered with wet burlap and plastic to cure for three to five days. Temperature ranges during deck curing were similar to those for the corresponding girders.

When initial curing was complete, dead load blocks were removed while the forms were stripped. Dead load blocks were

immediately reapplied by hanging them beneath the specimen (Fig. 3.12). Dead load blocks were uniformly distributed until they were rearranged for placement of the loading system.

While coil rod form hangers protruded slightly from the slab in some locations and voids were present where coil rods had been removed, it did not appear that the ultimate behavior of the specimens was significantly affected.

3.5 Test Setup and Testing Procedures

3.5.1 Long-Term Deflections. Girder deflections at midspan were monitored from release until flexure tests were completed. Movement was measured using dial gages. This worked well except when the girder was moved from the prestressing bed to the test location.

3.5.2 Flexure Tests. Load for the flexure tests was applied by two equal concentrated loads placed symmetrically about midspan as shown schematically in Fig. 3.13, creating a constant moment region between load points. Spacing between loads was representative of a simplified AASHTO truck loading. Dead load blocks were removed from the constant moment region and concentrated just outside the load points to maintain the moment at midspan. The weight of the loading system was considered part of the dead load compensation. The distribution of dead load compensation during the flexure tests is also shown in Fig. 3.13.

Load was applied through the system of cross heads, threaded rods, and hydraulic rams shown in Fig. 3.14. At each load point, threaded rods, which were anchored to the load floor, restrained upper crossheads. A ram and load cell were suspended from the crossheads. The two lower cross heads were tied together by a beam to form a frame to prevent the cross heads from overturning. The lower cross heads, which rested on neoprene pads placed at each load point, were used to maintain the deflection of the specimen while the upper cross heads were lowered when rams reached the limit of their stroke. Rollers were attached to ends of the lower cross heads in such a way that lateral movement was restrained by a pair of braced columns, but vertical movement was unrestricted (Fig. 3.15).

The girder was supported by neoprene bearing pads that measured 3 by 7 by 2-in. thick. The pad footprint was scaled from

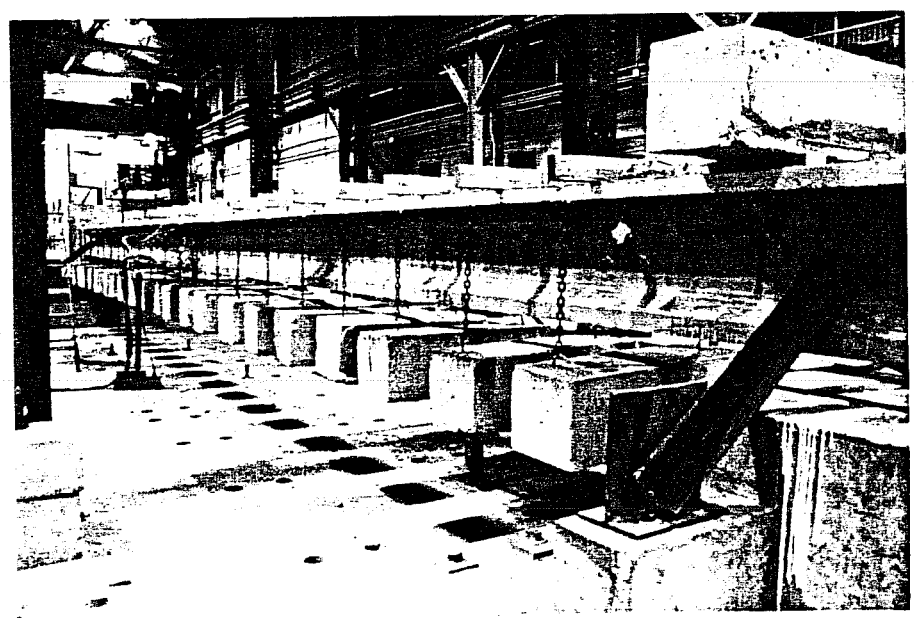

Fig. 3.12 Photograph of specimen with dead load blocks in place

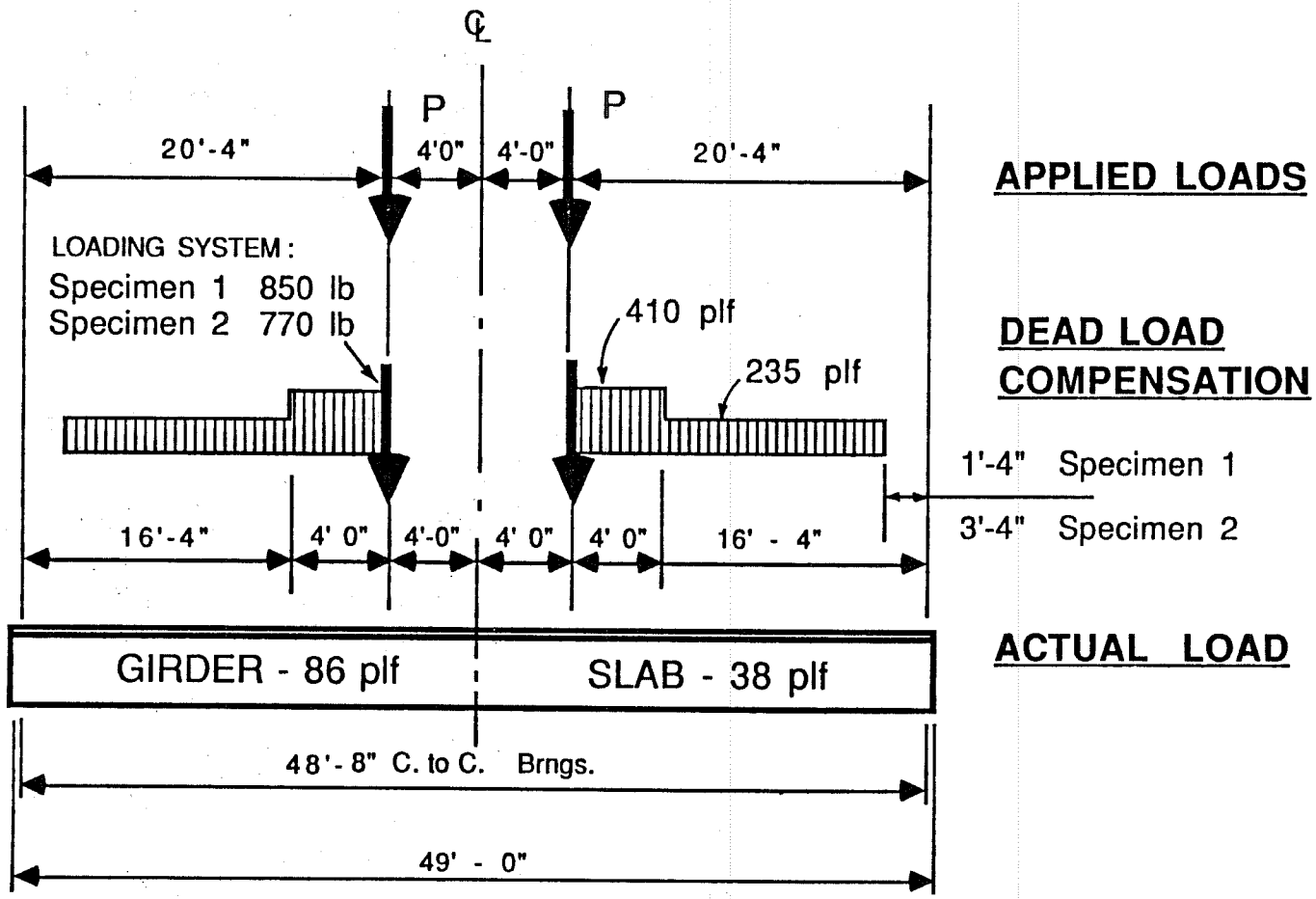

Fig. 3.13 Loads present during flexure tests

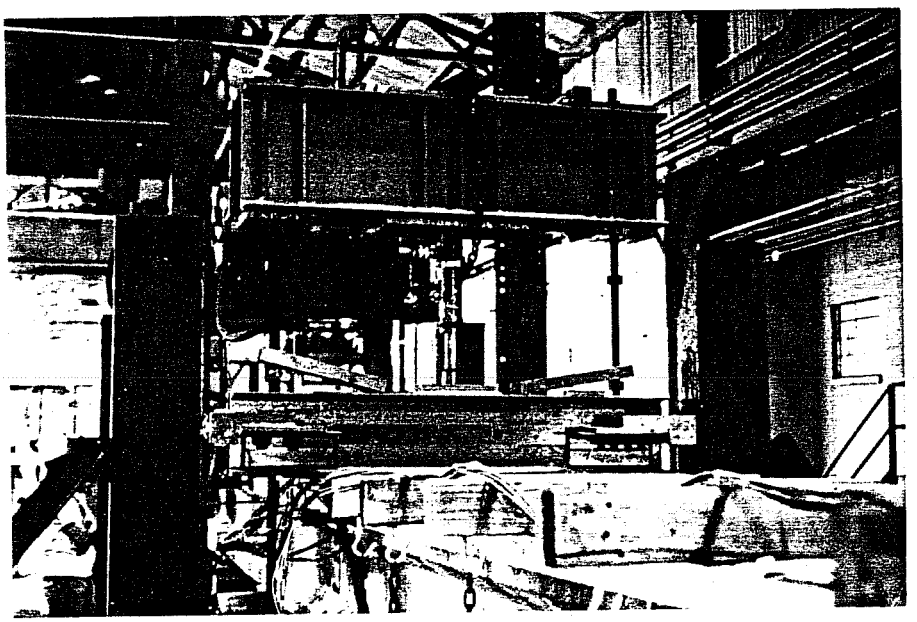

Fig. 3.14 Photograph of loading system for flexure tests

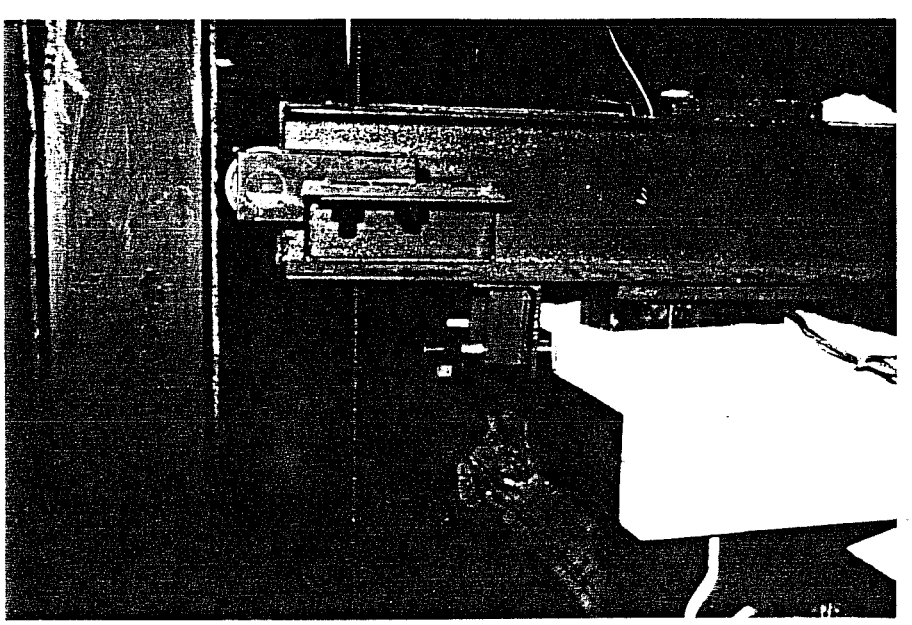

Fig. 3.15 Photograph of roller, crosshead, and braced column for lateral restraint

the prototype. These pads, and those under the load points which were 3 by 11 by 2-in. thick, were designed by the manufacturer, Oil States Rubber Co., for the expected loads and rotations and contained nine steel shim plates.

Loading was controlled by monitoring pressure in the rams, which were connected to a common manifold. Load cells were also used during the test of Specimen 1. When a desired level of load was reached, pressure was maintained for approximately 10 seconds, then valves in the hydraulic loading system were closed and readings were taken.

Specimen 1 was loaded initially to a level above the cracking load and then completely unloaded, so that when the specimen was reloaded to failure, cracked section behavior could be observed. The initial cracking test was omitted for Specimen 2 because of the extensive shrinkage cracking that occurred prior to release. Cracks were marked at each load level.

3.6 Specimen and Test Setup Instrumentation

3.6.1 Reinforcement. Electrical resistance strain gages were attached to strands and stirrups at locations near midspan and each end as shown in Fig. 3.16 and 3.17. Foil backed temperature compensating gages with a gage length of 6 mm were used. Gages were applied to prepared surfaces on the steel using standard strain gaging procedures. Strand gages were placed on a single wire of the strand. Readings were taken using switch and balance boxes and strain indicator boxes, and were adjusted by readings taken on precision resistors connected to a channel in each switch and balance box.

Some strand gages were connected and read during stressing operations and more were connected before release. One or two stirrups at each end were connected and read beginning at release. These gages were monitored through the conclusion of the flexure test. For each shear test, strand and stirrup gages for the end being tested were connected and read.

3.6.2 Concrete Strains. Concrete strains were measured using a mechanical strain measuring device (demec gage) and electrical resistance strain gages mounted on the surface of the concrete at locations shown in Fig. 3.16, 3.17, and 3.18. Electrical resistance gages were paper backed with a gage length of 60 mm. Mechanical strain measurements were made using a 200 mm (8 in.) demec gage with a

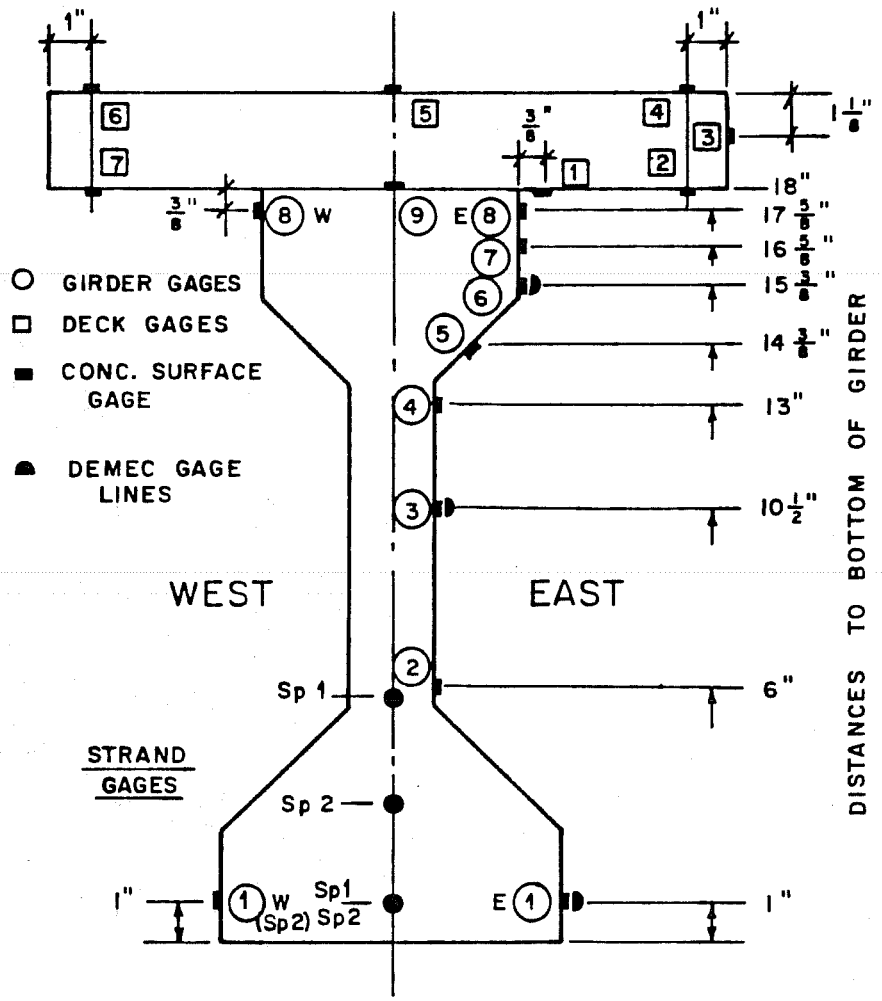

Electrical Resistance Gages are placed in locations shown 9" each side of midspan.

Concrete Gages : PL-60-11
Strand Gages : MM EA-06-062AP-120 L

Fig. 3.16 Strain gage locations near midspan

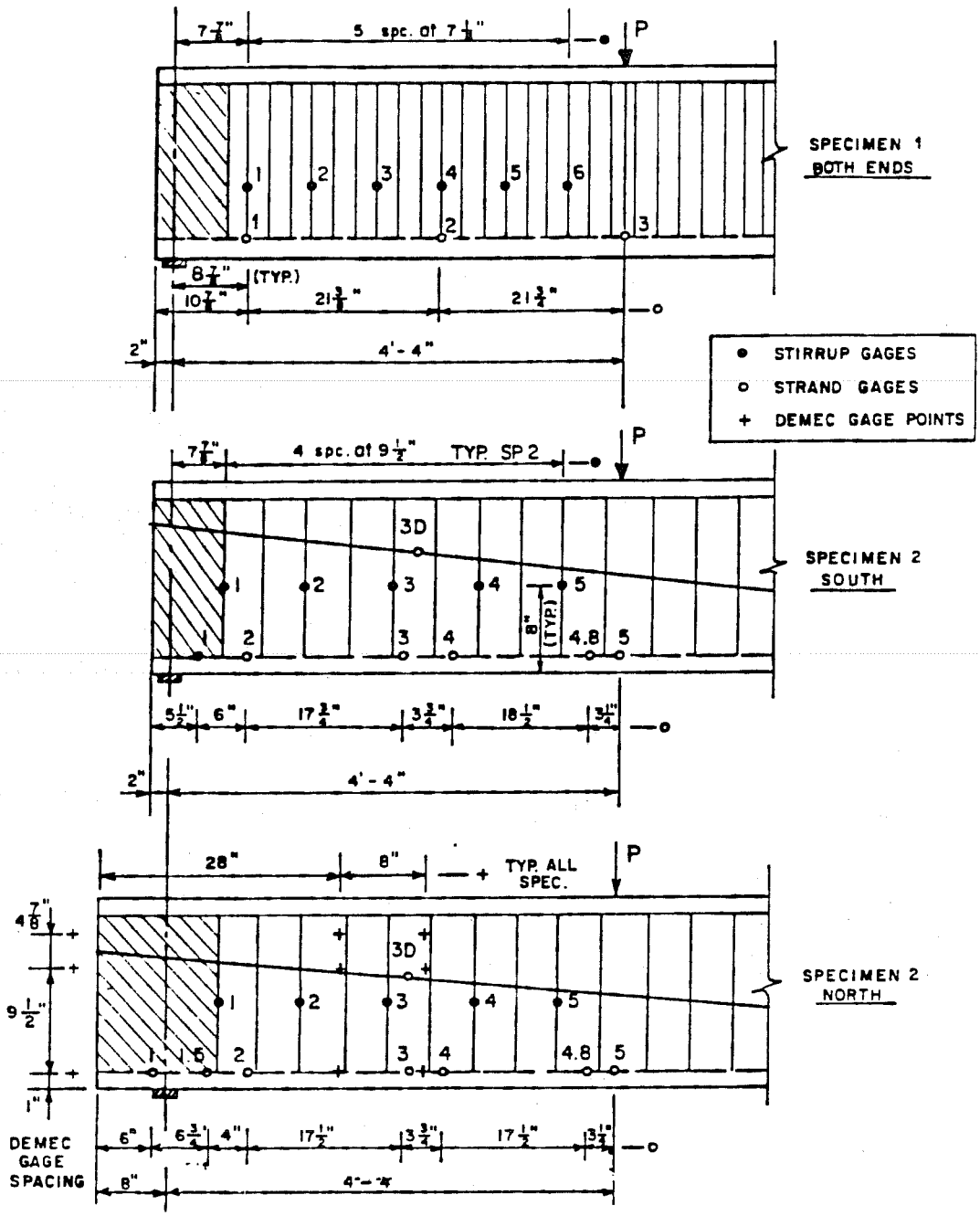

Fig. 3.17 Instrumentation near ends of girder

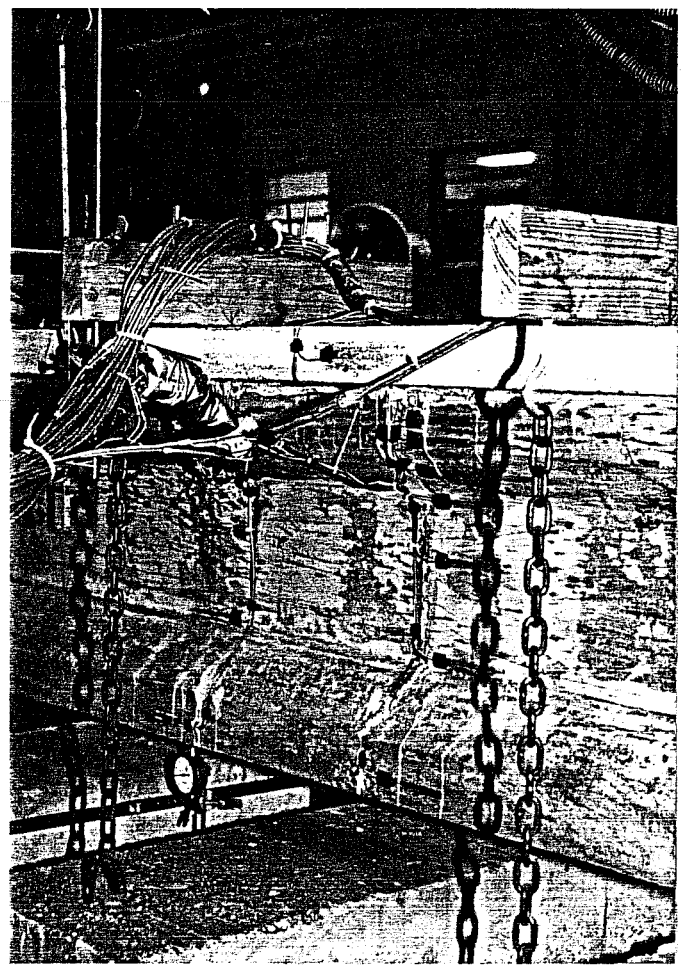

Fig. 3.18 Photograph of concrete surface gages at midspan

sensitivity of approximately 8 microstrains. Both types of gages were attached to specimens using model cement or epoxy. For electrical resistance gages, the surface was ground smooth and a layer of cement or epoxy was applied to seal the surface. After this coat was allowed to dry, the gage was applied using another layer of cement or epoxy. Electrical gages were connected to switch and balance boxes and strain indicators.

Prior to release, demec and electrical resistance gages were attached to the girder and initial readings were taken. The remaining electrical gages were applied after the slab was cast. All electrical gages were read through completion of the flexure test, while demec gages were read occasionally up to the time of the flexure and shear tests, but not during the tests.

3.6.3 Test Setup.

3.6.3.1 Deflections. A number of types of deflection measurements were taken during flexure tests. At midspan, dial gages were used to measure vertical deflection, sidesway, and roll. At ends of the girder, dial gages were used to measure bearing pad compression and roll. A surveying level was used to remotely monitor pad compression and midspan deflection during flexural tests to failure. A string line was stretched between ends of the specimen for photographs and to make rough deflection measurements at midspan. A line was drawn on the girder beneath the string line with no load applied so that deflection of the specimen could be observed as the two lines diverged. String lines were also used to detect lateral deflections (sweep). Sections of steel tape were attached to the threaded loading rods mentioned earlier to monitor travel of the lower cross heads. Readings were taken for all deflection measuring devices at all load stages.

During shear tests, deflections were measured at the load point and midspan using dial gages. Lateral and roll motions were detected with dial gages at each end and at midspan. For Specimen 1, additional measurements were taken using a plumb bob at the load point to detect longitudinal or transverse movement of the specimen, and using a string line for approximate deflection measurements and photographic purposes. All deflection measuring devices were read at each increment of load.

3.6.3.2 Strand and Slab Slip. Frames were epoxied to ends of the girder to support dial gages that were used to measure both strand

and slab slip (Fig. 3.19). The dial gages were capable of reading to within 0.001 in. These gages were read after each increment of load.

3.7 Data Reduction

All data was recorded manually during the tests and was then processed by hand or entered into a microcomputer for manipulation and plotting. When data from more than one source was available to obtain a specific quantity, such as the prestress force or deflection at midspan, an attempt was made to reconcile any differences in readings in order to obtain the best estimate for the quantity.

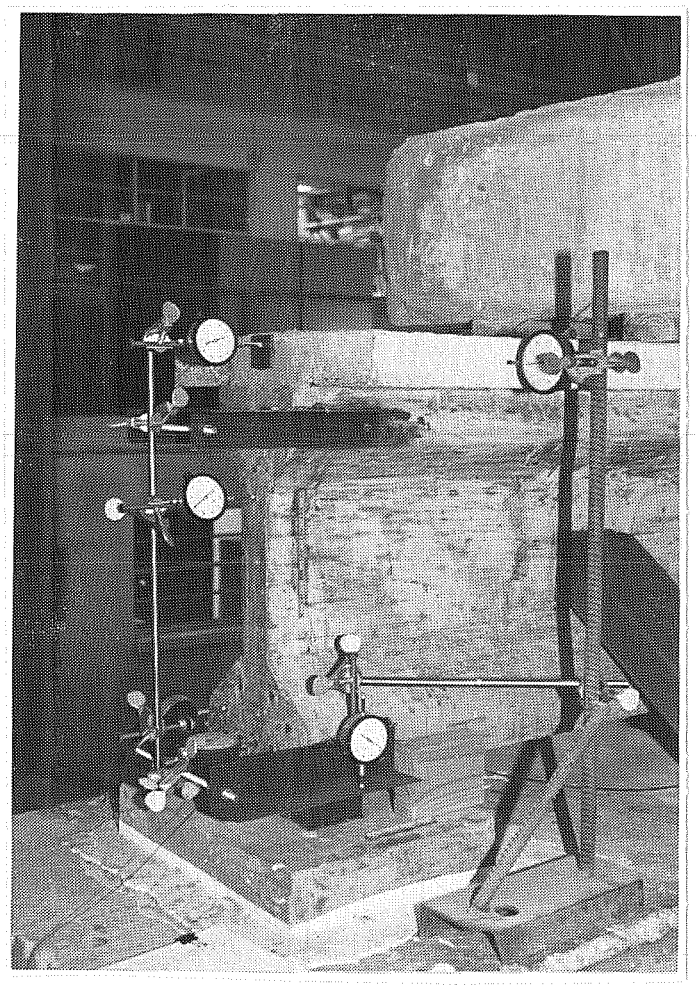

Fig. 3.19 Photograph of instrumentation at end of girder

CHAPTER 4

PRESENTATION OF LONG-SPAN GIRDER TEST RESULTS

4.1 Introduction

In this chapter, results of the long-span girder test series are presented. Each test is presented separately and in chronological order of testing. Where information or analysis procedures apply to more than one test, they will be described fully for the first use and the reader will be referred to that description for subsequent applications. Figures will contain an identifier in a box in one corner of the figure with "Sp 1" or "Sp 2" to represent Specimen 1 or 2, respectively. A suffix of "-N" or "-S" attached to the identifier indicates the end of the specimen being considered for shear test results.

The pretensioned, high strength concrete portion of each specimen is referred to as the "girder" throughout the fabrication and testing of the specimen. The completed composite section is composed of the pretensioned girder and the composite deck, and the extreme fiber of the composite section is the top of the deck.

A detailed chronology of the construction and testing of both specimens is given in Appendix B.

Following the presentation of test data, results of the tests will be compared. Examination of these data with respect to the topics considered in Chapter 3 is reserved for Chapter 5.

4.2 Specimen 1 (13 Strands)

In this section, behavior and properties of Specimen 1 prior to and during flexure and shear tests will be discussed. While the span of time from casting the girder to the flexure test was only approximately two months, a discussion of specimen behavior during that time period is included because of its significance in establishing effective stresses and strains at the time of the flexure test and in understanding the long-term behavior of the structure.

Specimen 1 was designed to fail near the balanced condition and therefore required more strands than the minimum needed to satisfy

allowable stress design criteria. Four of the 13 strands were draped to control stresses at the ends of the section.

The first attempted flexure test, which will be referred to as the "initial flexure test" in the following discussion, was halted because of excessive lateral movement of the specimen and instability in the loading system. After this test, the loading system was redesigned so that the specimen could be pushed and then restrained laterally at the load points to maintain the reduced sweep (lateral deflection) and prevent lateral motion during the subsequent flexure test. The second flexure test, which will be referred to as the "flexure test", was conducted in two stages: the first was the loading to the cracking load, after which the specimen was completely unloaded; and the second stage, in which the specimen was loaded to failure.

Shear tests of the two ends of the flexure specimen also included cracking and failure tests. The tests are referred to by the location (south or north) of the end during the flexure test. At both ends, stirrups were provided at a spacing that corresponded to approximately $V_s=8\sqrt{f'_c}b_w d$, which is the maximum quantity allowed by the codes. Standard open stirrups were used in the south end and stirrups which crossed under the center column of strands and were bent up at the corners of the section were used at the north end (see Fig. 5.5).

4.2.1 Prior to Flexure Test. This section presents material properties and reports observed behavior of the specimen prior to the flexure test.

4.2.1.1 Concrete Material Properties. Properties of girder and deck concrete were measured at intervals throughout the life of the specimen. Measured and estimated data at significant events are given in Table 4.1. Values were estimated when data was not available for the date on which an event occurred. Estimates were based on data presented in Appendix A. Strength gain with age curves are shown for both types of concrete in Fig. 4.1. Average stress-strain curves for the concrete at the time of the flexure test are shown in Fig. 4.2. Data for the curves were obtained from electrical resistance strain gages mounted on the surface of 6 by 12-in. cylinders. More data on the mix design and material properties are given in Appendix A.

4.2.1.2 General Description of Behavior. A summary of specimen history, including times at which dead load compensation and deck formwork was added or removed, is given in Appendix B.

Table 4.1 Concrete properties at significant events - Specimen 1

Event	Age (days)	f'_c (psi)	E_c (ksi)	f'_r (psi)
Release				
Girder	7	10,200	(5,750)	
Deck Cast				
Girder	16	(12,000)	(6,250)	
Flexure Test				
Girder	64	12,500		
		12,900 S	6,400	(1,000)
Deck	48	3,260		
		3,490 S	3,800	
Shear Test of South End				
Girder	93	13,000		
Deck	77	(3,300)		
Shear Test of North End				
Girder	113	13,160		
Deck	97	3,300		

() - Estimated values, based on additional data presented in Appendix A.

S - Steel cylinder molds; otherwise plastic molds were used.

Note: All data are for cylinders cured with the Specimen 1 under ambient conditions.

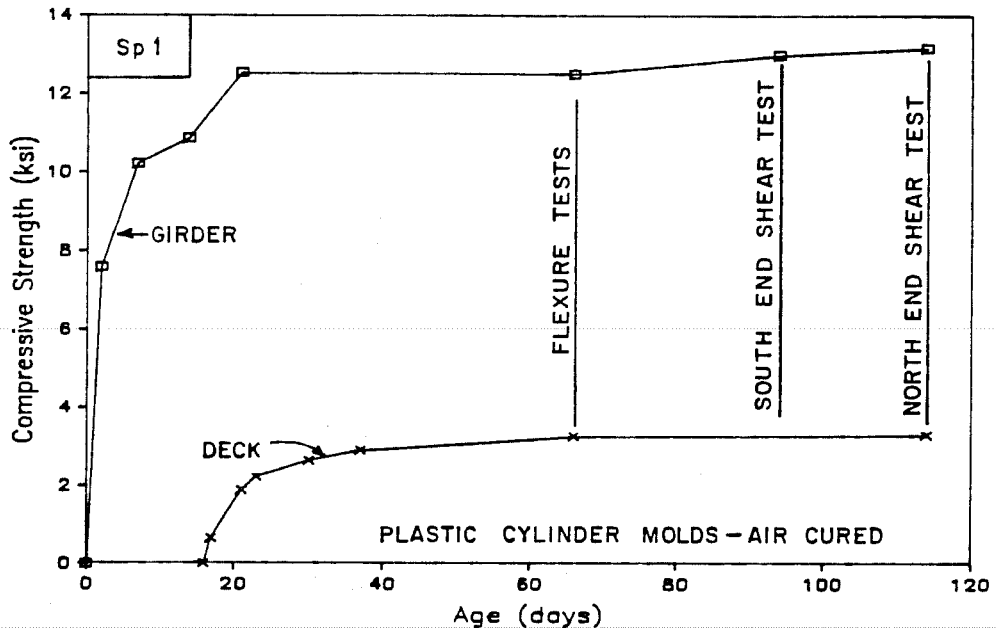

Fig. 4.1 Girder and deck concrete strength gain with age- Specimen 1

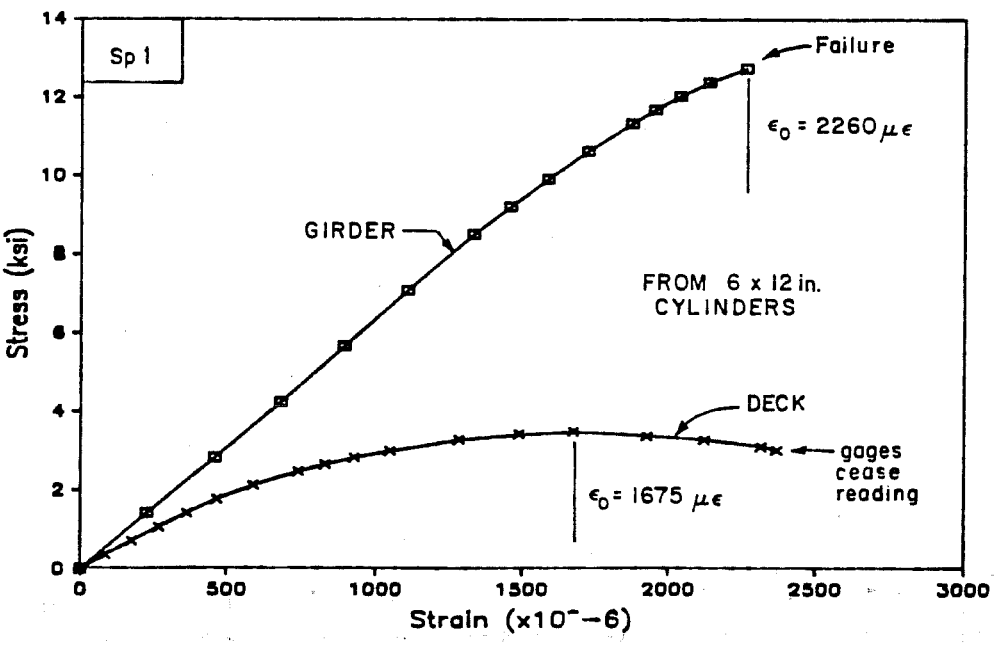

Fig. 4.2 Girder and deck concrete stress-strain curves at flexure test - Specimen 1

During initial stages of the transfer of prestress to the girder, a large crack and several smaller cracks formed at the south strand hold-down device, which was the first to be released (Fig. 4.3). Dead load compensation had not been placed on the girder prior to release because it had been determined that stresses after complete release were not sufficient to cause cracking of the girder. The crack formed because there was no precompression and insufficient dead load moment to resist the uplift force caused when the hold-down was released. Since there was no reinforcement in the top of the girder to limit its growth, the crack passed completely through the thickness of the girder and extended from the top of the girder into the taper of the bottom flange. No cracking was observed at the second hold-down because a longer span was available to produce dead load moment. The cracks closed when the prestress was fully released. Because the cracks closed and were located at a drape point outside the constant moment region of the flexure test, the cracks were expected to have no adverse effect on test results. Girder dead load compensation was added when deck forms were put in place three days after release.

The specimen was very flexible laterally. This, coupled with a significant sweep in the girder, caused excessive lateral movement in the specimen during the initial flexure test. The loading system was modified to restrain lateral movement during testing and to allow reduction of the sweep, which was accomplished by pushing the specimen laterally at the level of the deck and maintaining the new position with the loading system.

Actual specimen are summarized in Table 4.2.

4.2.1.3 Deflections. Midspan girder deflections from time of release until the flexure test are shown in Fig. 4.4. Significant events are indicated on the figure. A deflection measurement using an optical level, which is also shown on the figure, agreed well with the data shown.

The effect of creep was evident as deflections increased significantly with time for the bare girder. After the deck was added deflections stabilized.

At release, a sweep of approximately 0.5 in. to the west was observed at midspan. While no measurement was made prior to the initial flexure test, at the maximum load of the initial flexure test, a sweep of 1.375 in. was measured. This reading decreased to 1.19 in. when the load was removed. After forcing the specimen laterally

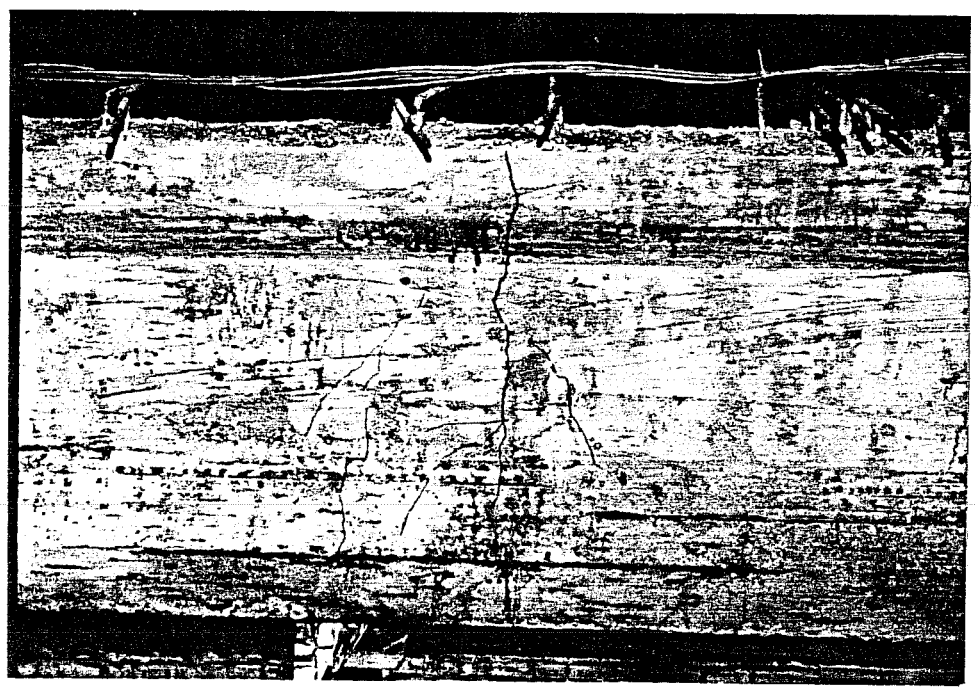

Fig. 4.3 Photograph of cracking at strand hold-down device at release

Table 4.2 Actual section dimensions - Specimen 1

Girder

Use Nominal Dimensions

Strand Placement

	Distance from strands to bottom of girder, g		
	Straight	Draped	Total
No. of Strands	9	4	13
North End	2.10"	14.71"	5.98"
Midspan	2.07"	4.58"	2.84"
South End	2.19"	14.91"	6.11"

Drape locations are 19.5' from ends of girder.

Deck

Width	16 5/8"
Thickness	2 5/16"
Offset *	5/16"

Overhang at Interior End during Shear Tests

North End	7'-7"
South End	5'-0"

Distance measured from center of support at interior end.

* - Offset is the distance from top of girder to bottom of deck. This area is filled with deck concrete and is as wide as the girder top flange.

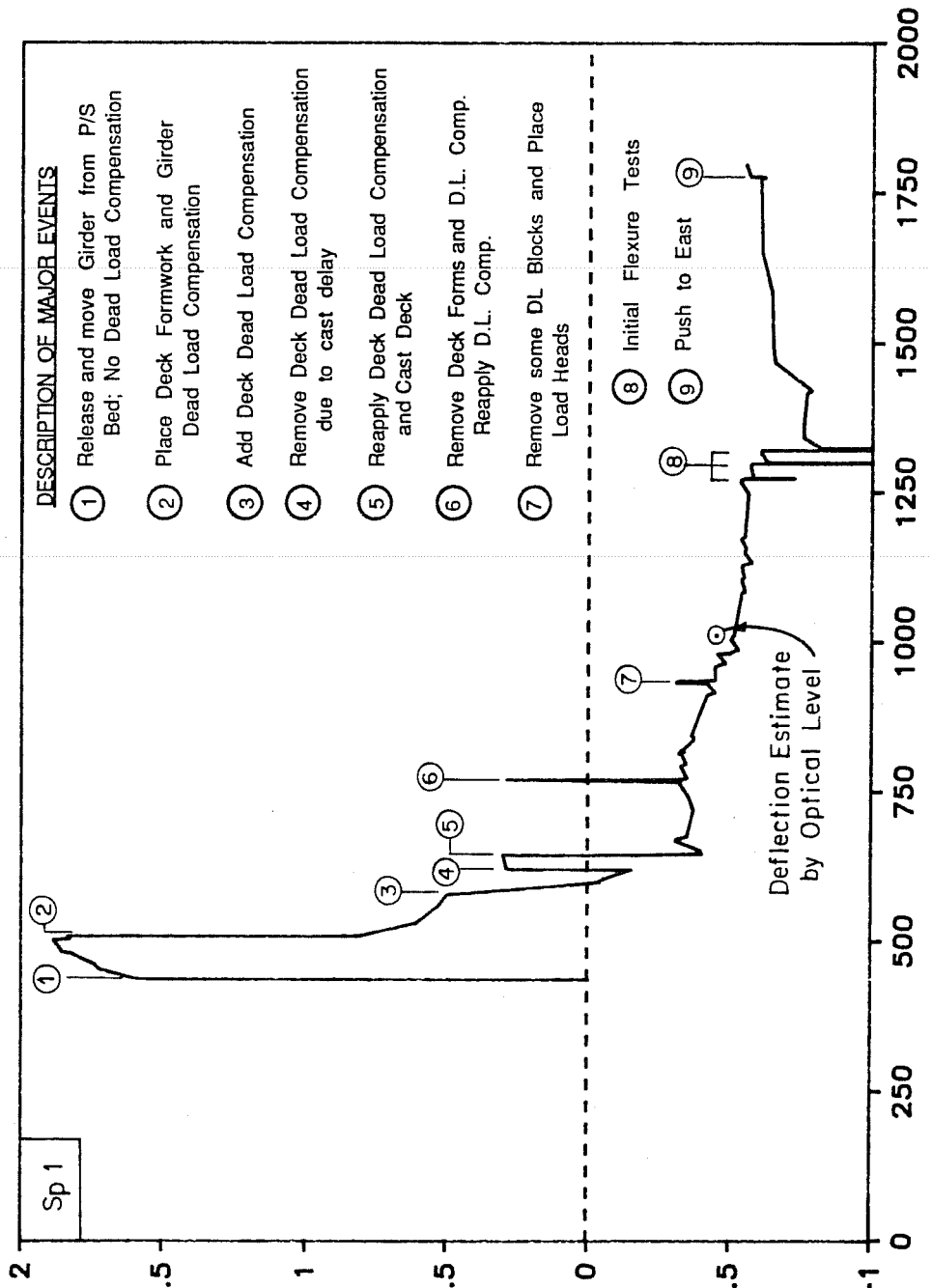

Fig. 4.4 Midspan deflection with time

(to the east) at the load points, the sweep was decreased to about 0.375 in.

4.2.1.4 Effective Stresses and Strains. Strain readings for strands, girder concrete and deck concrete were corrected for time effects and discontinuities to obtain an "effective" strain for each gage. Corrected strains therefore represent an estimate of the elastic strain at a specific time.

For the strands, an effective strain was determined following full tensioning using elongation and strain data and considering the order of prestressing. Readings were adjusted to compensate for erratic losses in strain observed following placement of the girder concrete. Corrected strains were multiplied by the ratio of the "apparent" strand modulus (determined using strain gages attached to a single wire) to the "true" strand modulus (provided by the strand manufacturer) to obtain "true" strains. These true strains were used to determine strand stresses from the load-strain curve provided by the manufacturer and were compared with strains measured elsewhere in the specimen. Corrected strand strains at midspan for a typical straight and draped strand are shown in Fig. 4.5. The corrected strains and corresponding stresses were not adjusted for strand relaxation.

The strain at each row of strands was determined by interpolating between measured changes in strain for the two instrumented strands. These strains were used to determine an "average" strain at the centroid of all strands. Effective strand stresses and forces computed from the "average" strand strains are summarized in Table 4.3. Effective strand stresses at release were also computed using an elastic analysis and the effective strand stresses prior to release. Measured losses in strand stress were closely approximated when computed losses were increased by 25 percent. Therefore, this additional loss was added to obtain the computed stresses at both midspan and end to account for creep losses that occurred before readings were taken, and to provide a consistent basis for determining the effective strand stress.

Changes in strand strain at release near ends of the girder indicate a transfer length of less than 10 in. Combined data for active gages at both ends of the girder is shown in Fig. 4.6. Agreement between gages is quite good.

Girder concrete strains required correction for effects of creep which can be seen in the typical girder strain data shown in

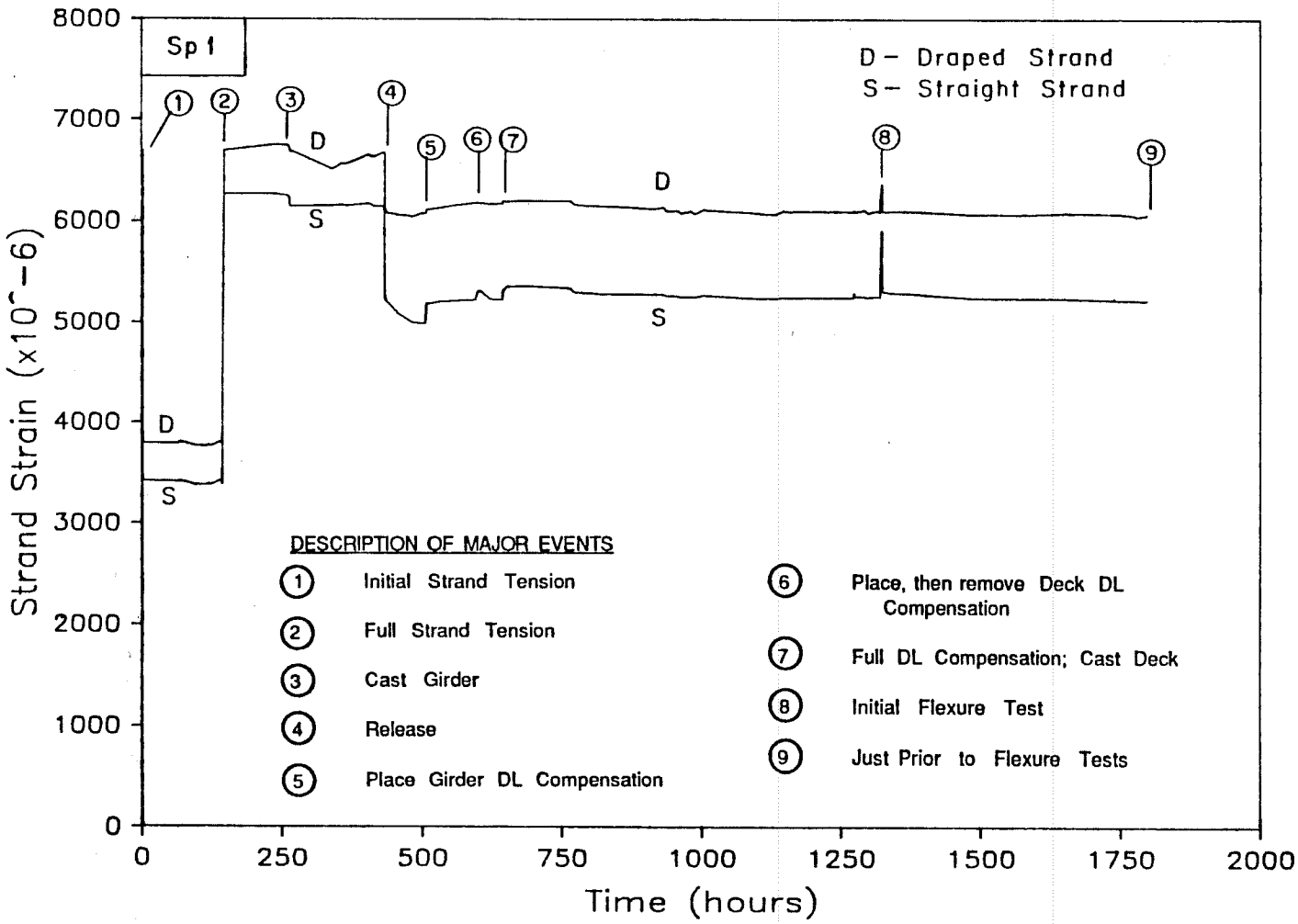

Fig. 4.5 Typical corrected midspan strand strains with time

Table 4.3 Effective strand stresses and forces - Specimen 1

	Stress (ksi)	Force (kips)
Full Tensioning		
All Locations	187.6	206.1
Prior to Release		
All Locations	181.7	199.6
After Release		
Midspan	159.6	175.3
Midspan *	159.6	175
North End *	164.2	180
South End *	164	180.6
Flexure Test		
Midspan	152.5	167.5
North End	147.5	162.0
South End	143.6	157.7
Shear Tests		
North End	143.1	157.2
South End	140.5	154.3

* - These values represent computed instantaneous elastic prestress losses plus 25%. The computed loss was increased by 25% to provide better agreement with the limited measured strain data. The elastic losses were calculated using the "Prior to Release" prestress force and gross section properties.

Area of prestressing steel = $13(0.0845 \text{ in.}^2) = 1.0985 \text{ in.}^2$

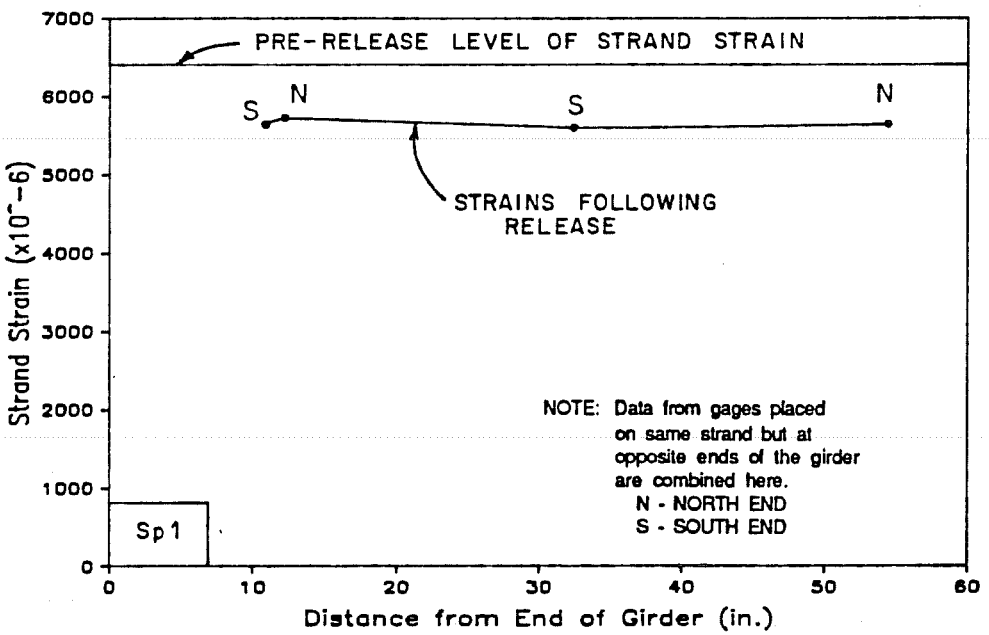

Fig. 4.6 Strand strains near ends of girder before and after release

Fig. 4.7. Correction was complicated by a strong sensitivity of many gages to temperature which caused readings to fluctuate as much as 100 microstrains during a day. Initial creep corrections were made by subtracting changes in strain over periods where there was no change in load. When changes in load occurred, corrections were made by subtracting the difference between measured and computed changes in strain. Computed strains generally showed good agreement with measured data.

Measured and computed girder concrete strains at release are shown in Fig. 4.8a as they vary with the depth of the girder. Agreement between lines of gages at different locations is good. Agreement is also reasonable between measured strands and computed strains. Strain readings were taken shortly after release and may contain some creep. In the second plot (Fig.4.8b), corrected and uncorrected strains for both sets of gages prior to the flexure test are compared with computed strains. Agreement of the corrected strains is good between the two lines of gages and reasonable for computed strains. The variation between measured and computed strains at release and between corrected and computed strains at test are similar.

Most of the creep in the girder concrete had occurred by the time of the flexure test as indicated by Fig. 4.7. The magnitude of creep during this period was approximately 600 microstrains and was fairly uniform across the section (Fig. 4.8b).

The deck concrete was instrumented after removal of the deck forms and replacement of the dead load compensation. Typical top and bottom deck strain data prior to the flexure test are shown in Fig. 4.9. Strains and changes in strain are shown for all deck gages at three times in Fig. 4.10. Measured strains were caused mostly by creep because the only sustained elastic change in load that the deck experienced while gages were active was due to forcing the specimen to the east to reduce the sweep. Effective strains at the beginning of the flexure test were therefore considered to be the strains caused by the lateral push (Fig. 4.10), and the elastic strains caused by removal of the deck forms were neglected because calculations showed that the strains were insignificant.

Deck strains were not as well behaved as the girder strain data. Some gages were erratic and some trends in the data could not be explained. Data indicate that the deck was either previously cracked or cracked when pushed to the east, because compression strains measured on the west side of the deck were significantly

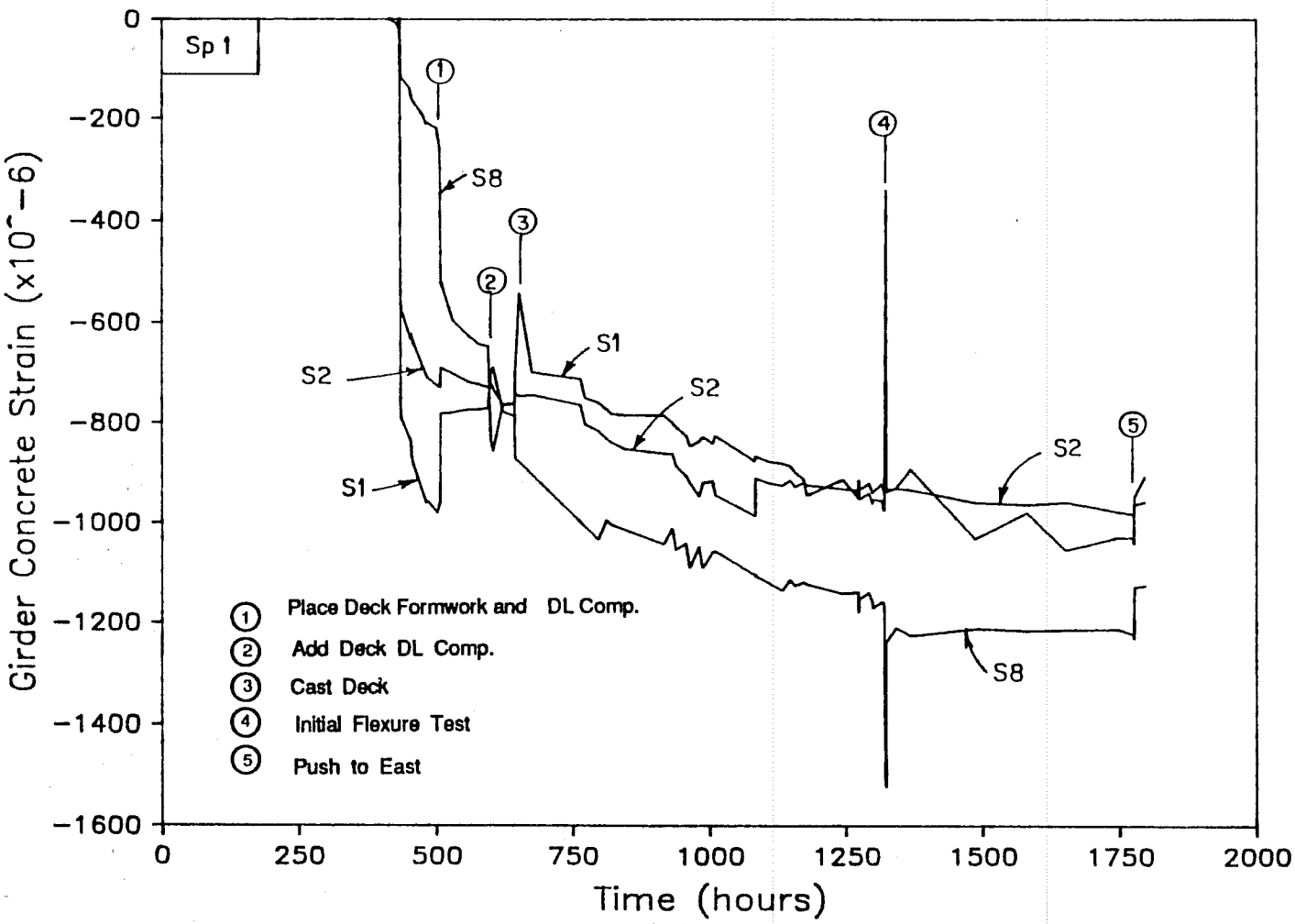

Fig. 4.7 Girder concrete strains with time for typical gages

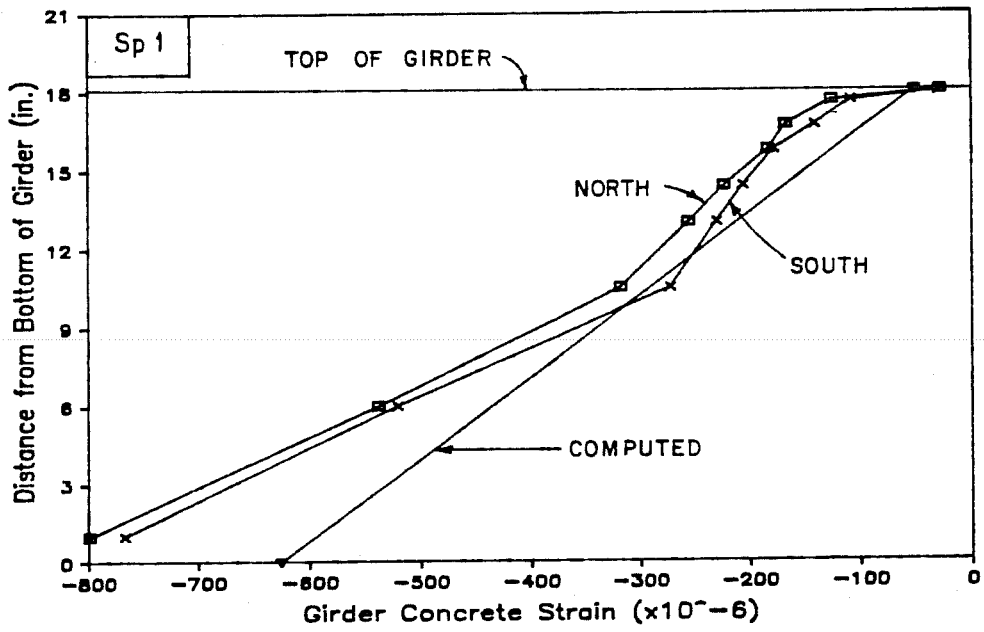

(a)

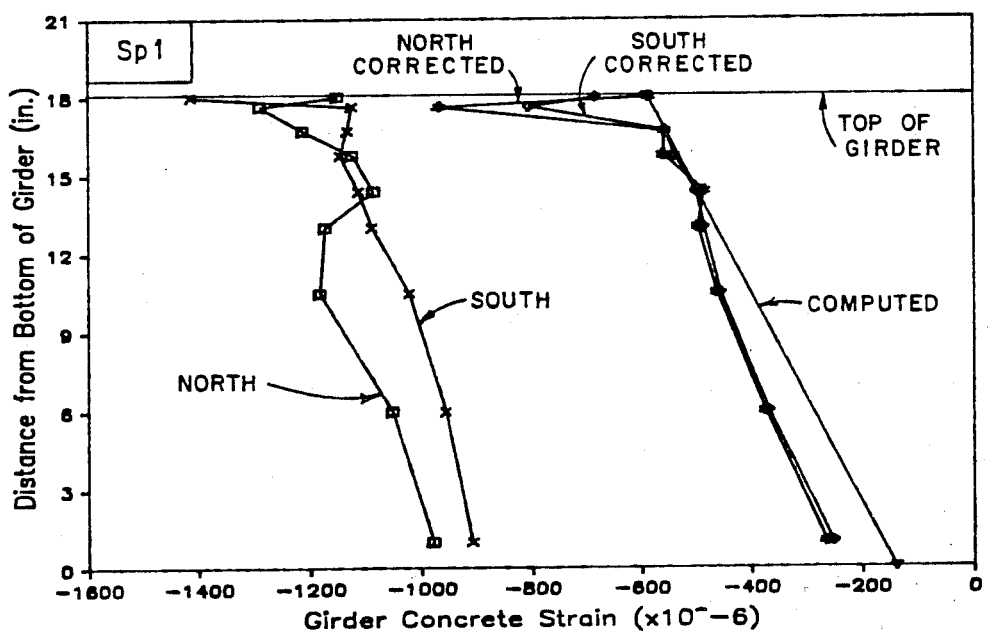

(b)

Fig. 4.8 Computed and measured girder concrete strains at release and prior to flexure tests: a) at release; b) prior to ultimate flexure test

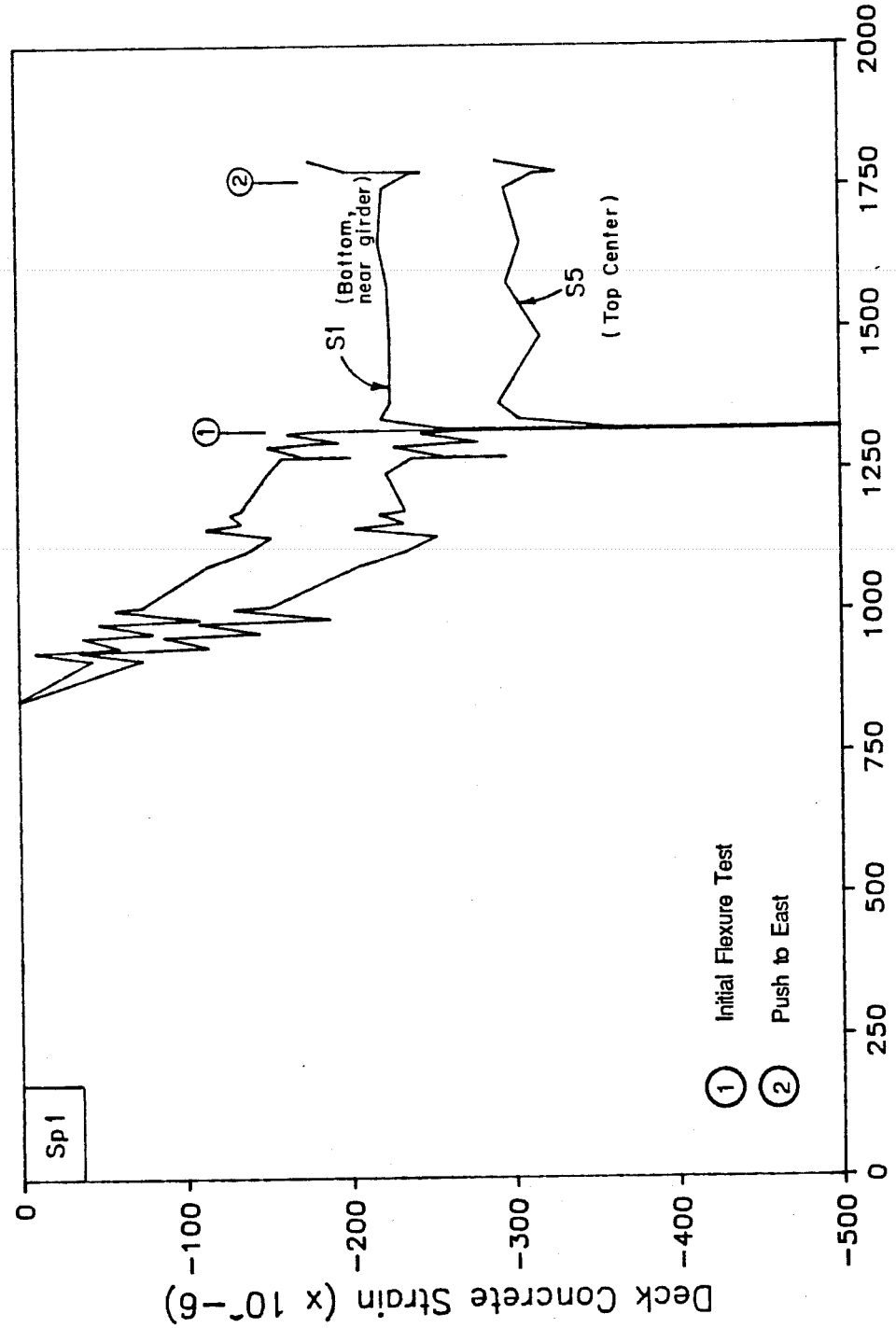

Fig. 4.9 Deck concrete strains with time for typical gages

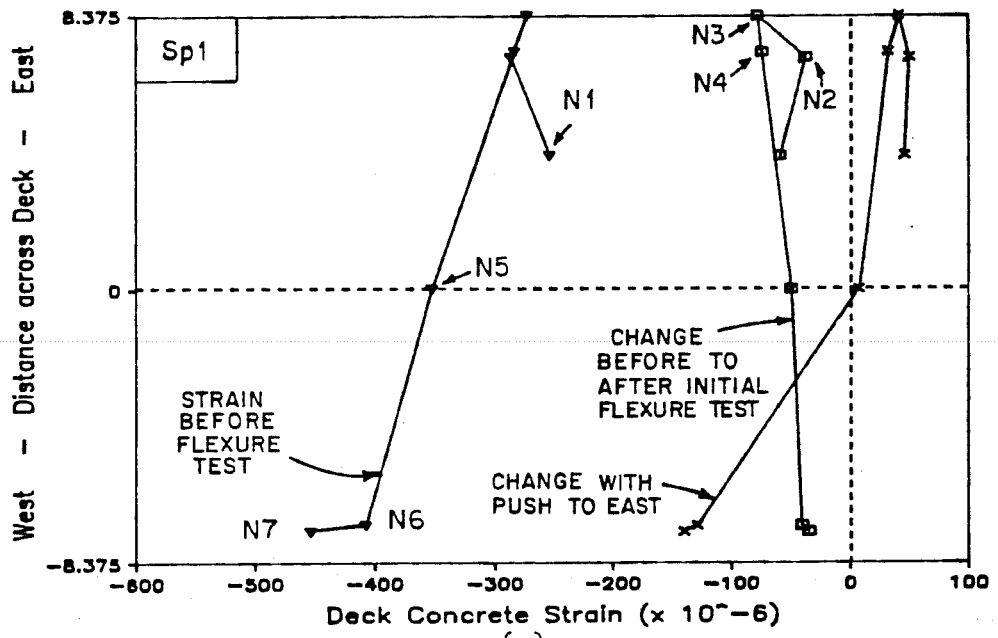

(a)

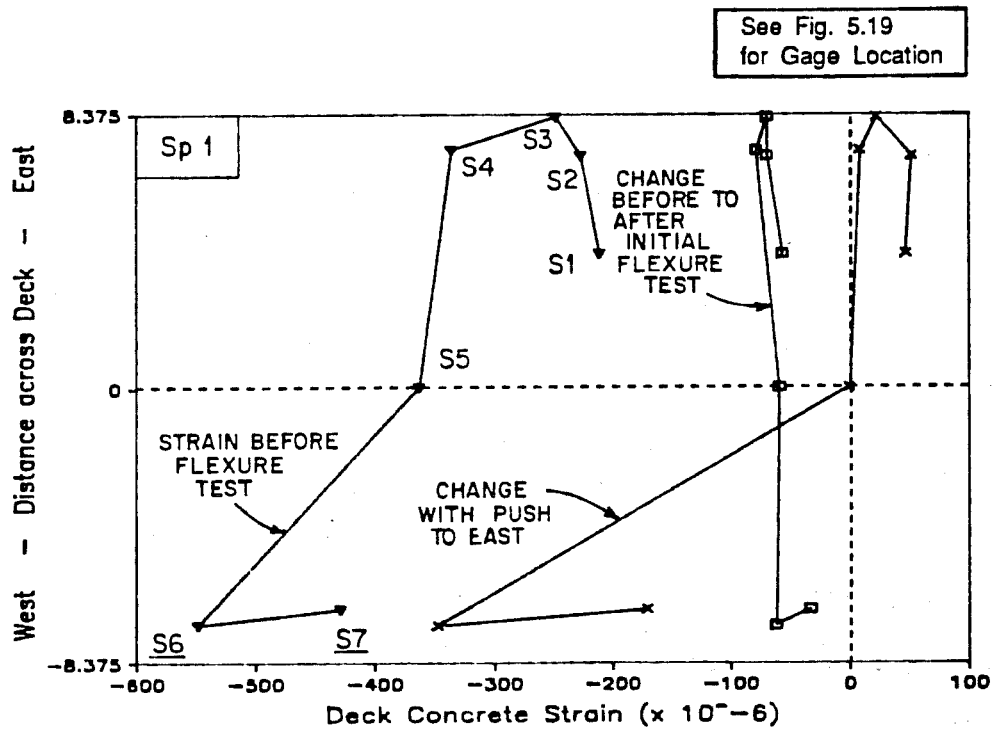

(b)

Fig. 4.10 Deck concrete strains at selected time: a) north gages; b) south gages

larger than the tensile strains measured on the east side. No deck cracking was detected before or after the lateral push. Any deck cracking would affect behavior and strains measured during early stages of the flexure test because cracks would have to close before the east side could develop additional strain.

Creep strains before the flexure test amounted to nearly 400 microstrains at the top of the deck and 250 microstrains at the bottom of the deck. By the time of the test, creep had slowed significantly, which agreed with similar behavior observed in the girder. Nearly 100 microstrains of the creep occurred during the initial flexure test.

Stirrup strains from just prior to release until the time of the shear tests are shown in Fig. 4.11 for active gages at each end. No corrections to the readings were necessary. Gage N3 appeared unreliable and was disregarded. At release, small tensile strains were recorded in the stirrups, but no cracking in the web of the girder was detected. By the time of the flexure test, stirrup strains had changed approximately 200 microstrains in compression which indicates continuing shrinkage in the concrete. These strains do not include shrinkage strains that occurred prior to release. A large increase in strain occurred at the end of the flexure test and is discussed later in this chapter.

4.2.2 Flexure Test.

4.2.2.1 General Description of Behavior. The initial flexure test was halted due to excessive lateral movement of the specimen and rolling of the cross heads. After modification of the load system, the flexure test was performed in two stages: cracking and ultimate (failure). Load stages and corresponding times are given for both stages of the flexure test in Appendix B. Deflection readings were taken at all load stages while strain readings were taken at selected loads. Load stage designations represent the applied load at each load point. Load stages used in marking cracks are slightly higher than actual loads because of a later calibration of the load system.

The initial flexure test was conducted in the same manner as the later tests. At a load of 5.66 kips, a single crack appeared on the west side of the girder under the south load point and extended to the bottom of the web. The next cracks were found three load stages later at 6.40 kips, and an additional crack was observed at 6.89 kips. These cracks were also located near the load points, appeared only on the west side, and were limited to the bottom flange. Two of

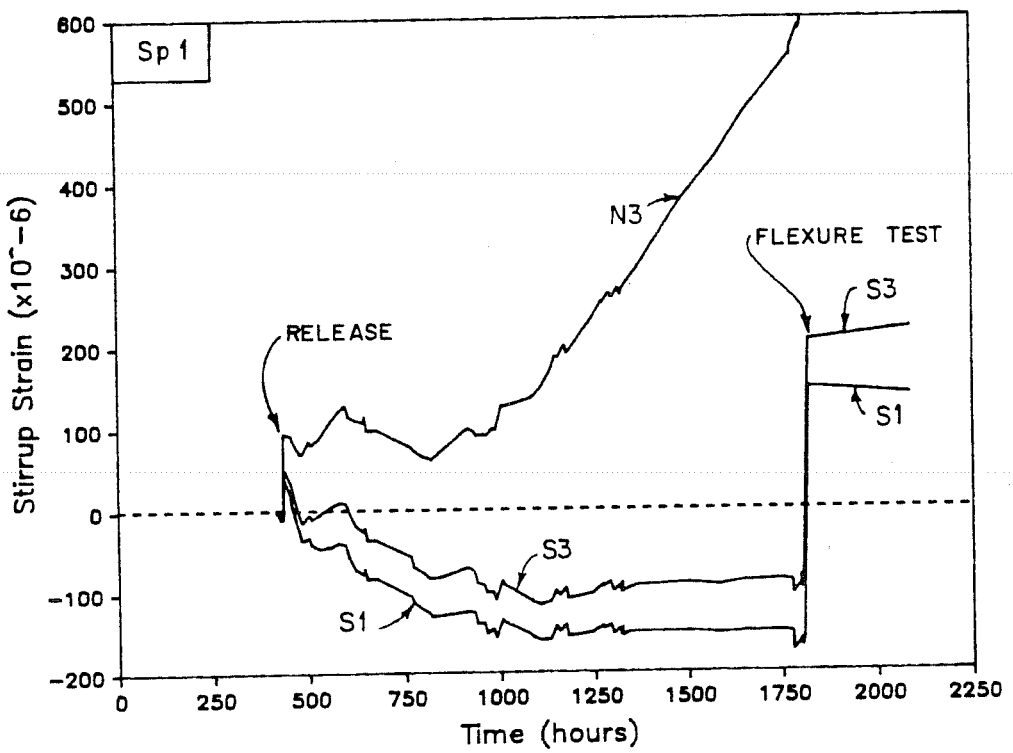

Fig. 4.11 Stirrup strains with time

the cracks were extensions of the cracking which occurred at release. After a load of 7.14 kips was reached, the load was removed.

An altered load system was then constructed. Prior to the flexure test, the specimen was pushed laterally to remove some of the sweep. The modified load system provided restraint to maintain the reduced sweep.

A separate cracking test was performed in order to make possible the observation of cracked section behavior in the subsequent ultimate test. The limited cracking which occurred during the initial flexure test had a minor effect on the results of the cracking test. The loading system and procedure were identical to those used in the ultimate test.

Loading for the cracking test commenced by placing the weight of the upper cross heads on the specimen. Because this weight completed the full dead load compensation, this condition was considered to be zero applied load. Cracking of concrete was heard at 5.41 kips but no cracks were observed. At the next load stage, 5.66 kips, cracks present from the initial flexure test began to open. At 6.15 kips, cracking was observed on the east side which was uncracked during the initial flexure test. These cracks extended across the bottom of the girder and were limited to the bottom flange. After a maximum load of 7.38 kips was reached, the specimen was unloaded.

The second stage of the flexure test, the ultimate test, was then begun. The first new crack observed during the ultimate test occurred at 6.89 kips. Cracks extended into the web at 7.87 kips. At 9.35 kips, cracks reached midheight of the web (Fig. 4.12), and the deflection was held by the lower cross head while the rams were retracted and the upper cross head was reset. Cross heads and rams were reset again at 12.30 kips. At 12.79 kips a few cracks extended to the bottom of the taper of the top flange, while most ended approximately one in. below the taper (see Fig. 4.13). Cracks were well distributed but were not wide even though the deflection had increased noticeably in reaching this load stage. Inclined flexure cracks outside the constant moment region also increased in length during this load stage. As a load of 13.29 kips was reached, the specimen failed explosively in compression less than one foot south of midspan. The only warning of collapse was a small quantity of concrete dropping to the floor seconds before crushing. It was not clear whether the falling concrete was from the deck or girder.

The failed specimen is shown in Fig. 4.13. Although the specimen fell only approximately one in. to the cribbing placed beneath it, the force of impact was sufficient to straighten steel hooks from which the dead load blocks were hung. Secondary failure cracks formed along the junction of the web and bottom flange, and branched upward into the web. The ends of the girder were thrown up

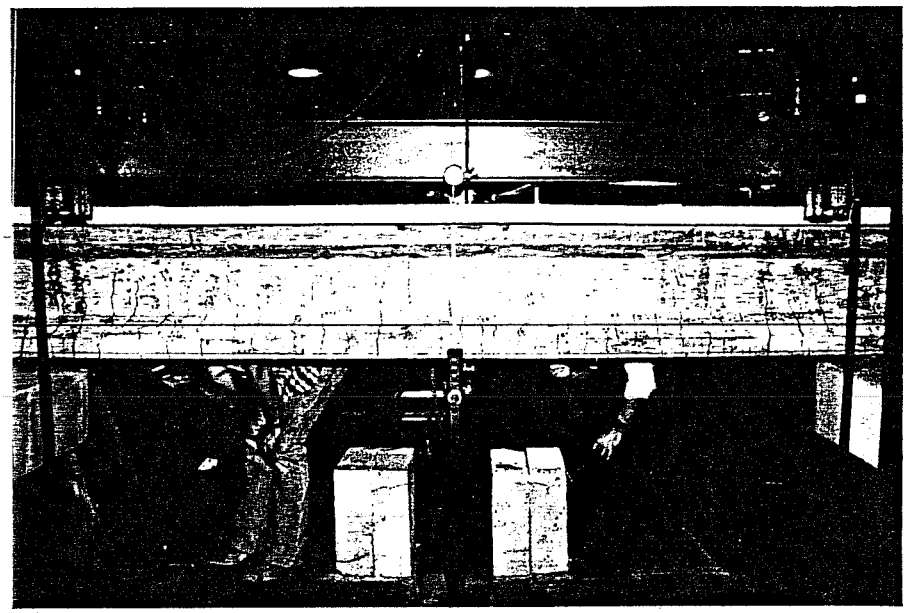

Fig. 4.12 Photograph of crack pattern at load of 9.35 kips during ultimate flexure test - Specimen 1

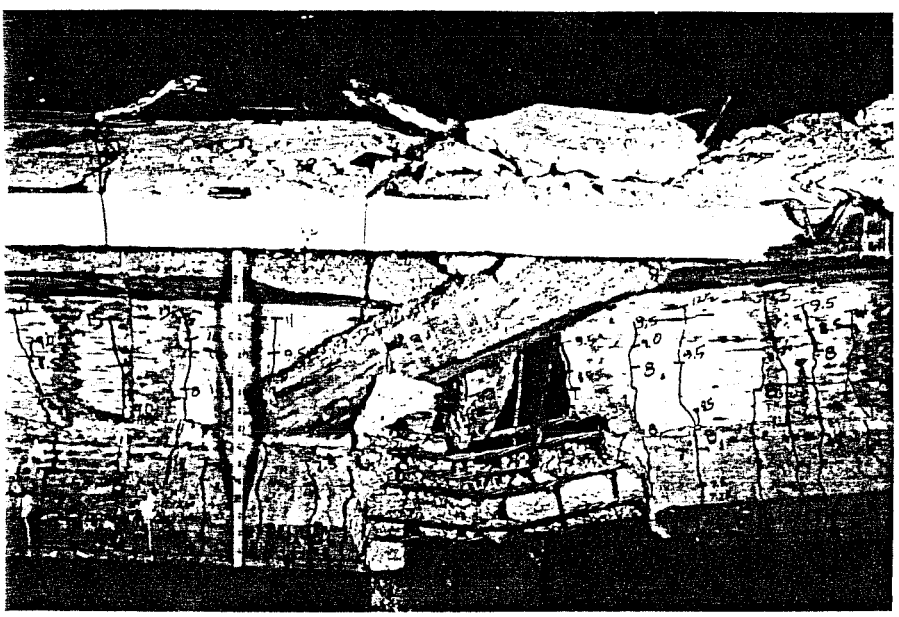

Fig. 4.13 Photograph after flexural failure - Specimen 1

into the air and drawn inward causing the bearing pads to roll off the concrete support pedestals. The sudden increase in stirrup strain after failure, which was mentioned earlier (Fig. 4.11), suggests that the ends of the girder may have cracked sufficiently at failure to leave permanent strains in the stirrups. However, no shear cracks were found in the web after failure. A dead load block that had been resting on the deck at the north end was thrown off, landing on the edge of the deck and knocking out a v-shaped piece of the deck. This was later patched and did not affect the shear test.

The failure surface was typical of a compression failure. The surface was an inclined plane originating in the top of the girder and continuing through the deck (Fig. 4.14a). When viewed from above, the failure surface was wedge-shaped with its point over the girder (Fig. 4.14b). The appearance of the failure surface did not provide conclusive evidence for determining whether the girder or deck concrete crushed first.

Flexure cracks were well distributed during the test and remained narrow at all levels of load. At the conclusion of the cracking test, cracks near midspan were spaced at approximately 7.5 in. Prior to failure, cracks formed in the bottom flange between load points at a uniform spacing of approximately 3 in.

The loading system was successful in preventing excessive sway during the test.

Significant events during the flexure test are summarized in Table 4.4, which also includes computed and design loads of interest. The computed and design loads were based on the effective prestress force and material and section properties given earlier in this chapter. Live load plus impact was the applied load at which bottom fiber stress was computed to be $6\sqrt{f'_c}$. The impact factor was computed using the prototype span of 146 ft. AASHTO load factors were used to determine the factored load. Nominal capacity was computed using AASHTO and ACI procedures because application of AASHTO equations was not clear in this case. Test results are compared with computed and design loads later in this chapter and in the next chapter.

4.2.2.2 Deflections. Net deflection at midspan is shown in Fig. 4.15 for both cracking and ultimate flexure tests with loads from Table 4.4 indicated on the figure. Readings were corrected for compression of the bearing pads. Cracking apparently occurred prior to visual detection because the curves deviate from initial linear behavior at 3.5 to 4 kips. Agreement between the cracking and ultimate test data is good with the ultimate test data showing slightly greater flexibility. Some difference in the plots is caused by a lack of readings at low loads, which may obscure actual behavior.

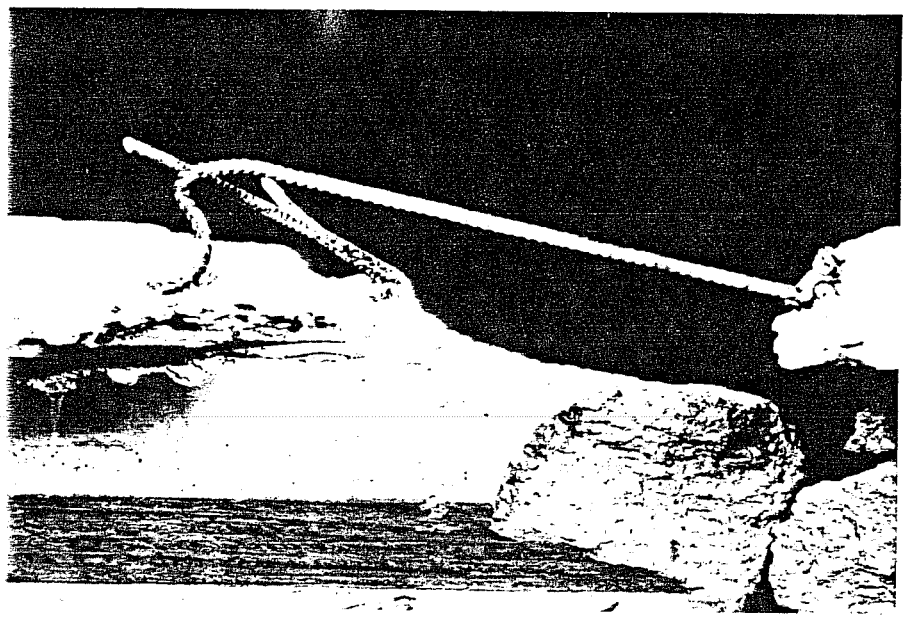

(a)

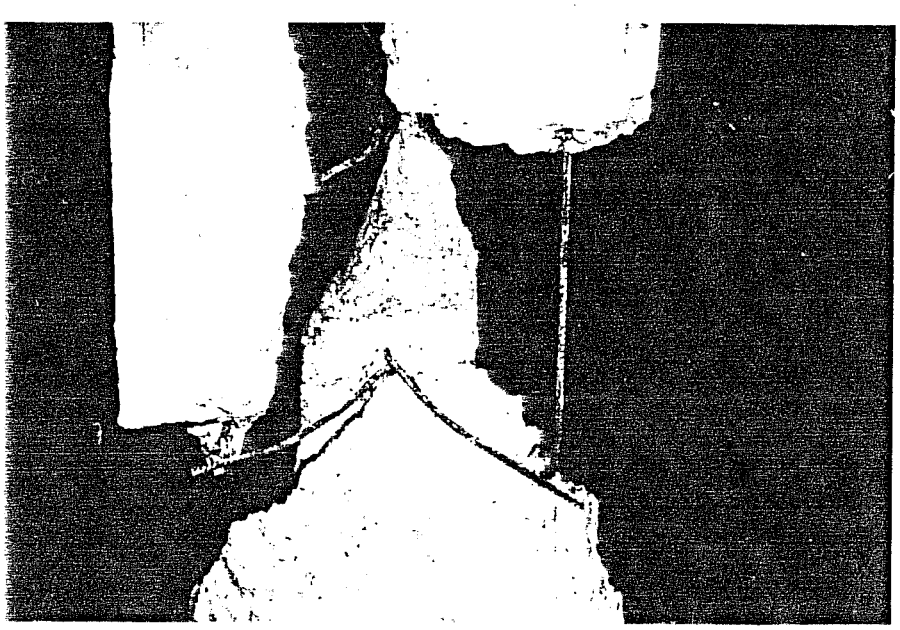

(b)

Fig. 3.14 Photographs of concrete failure surface after flexural failure - Specimen 1: a) side view; b) top view

Table 4.4 Load stages of interest during flexure tests - Specimen 12

Key (Fig. 6.15)	Description of Load Stage		Load (kips)
Computed and Observed Behavior			
CD	Computed Decompression	$0\sqrt{f'_c}$	1.89
CC	Computed Cracking	$(7.5\sqrt{f'_c}$	3.69
O	Observed Crack Opening		5.66
C	Observed Cracking	$(17.8\sqrt{f'_c}$	6.15
R	Reset Loading System		9.35
R	Reset Loading System		12.30
U	Ultimate (Maximum and Failure Load		13.29
CW	Computed Web Cracking at h/2		25.16
Design Loads			
	Service Loads:		
LL	Live Load		2.81
LI	Live Load + Impact	$(6\sqrt{f_c'}$	3.33
FL	Factored Load (AASHTO)		8.79
NC	Computed Nominal Capacity (ϕ = 1.0)		11.14
Total Reaction at Ultimate Load			21.85

* - Impact factor computed using prototype span of 146 ft.

Note: "Load" is the force applied at each load point.
"Computed Nominal Capacity" is the difference between the nominal moment capacity computed using AASHTO procedures and the actual dead load moment divided by the shear span during the flexure test

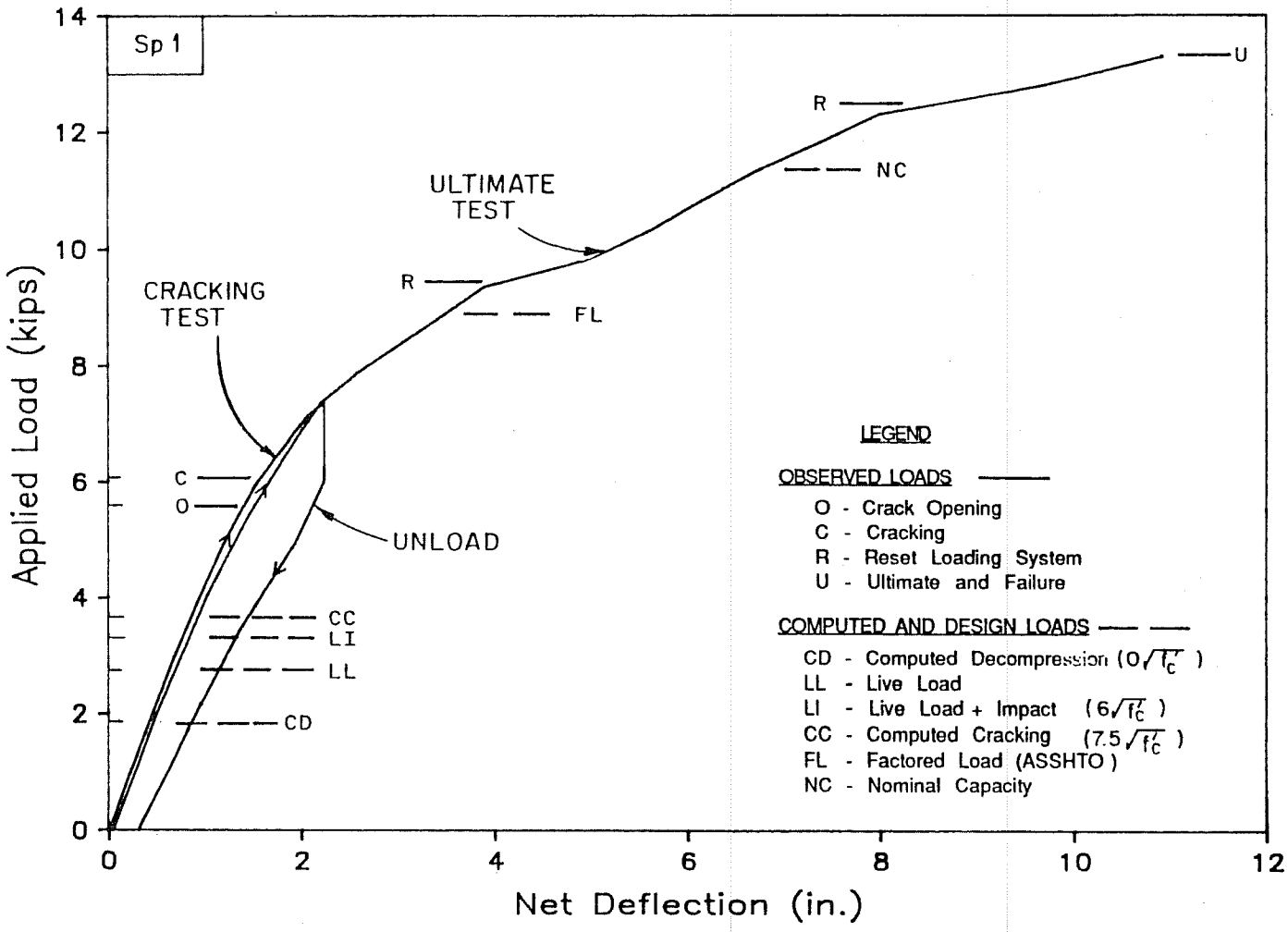

Fig. 4.15 Net deflection at midspan during flexure test

Resetting the load system clearly affected specimen behavior as evidenced by the offsets in the curve. These offsets indicate that, while the deflection was held constant, time effects allowed the stresses, and therefore the load, to drop. This required additional deflection to regain the load that had been on the structure, thus producing the observed offset. Readings were not taken during reloading after resetting the loading system.

The shape of the curve near failure indicates that yielding did not occur. This is corroborated by the observation that crack openings were not wide prior to failure. However, the deflection at failure was large, indicating a substantial capacity for energy absorption, and providing ample warning of impending collapse in a structure in service.

4.2.2.3 Strand and Concrete Strains. Corrected strand strains for the instrumented strands are shown in Fig. 4.16 with the average strain which represents the strain at the centroid of the strands. Because strain data at failure were not available but the deflection was known, strains at failure were estimated by applying the ratio of the increase in deflection during the final load increment to the increase in deflection during the preceding load increment to the strain readings from the preceding load stage. Points or groups of points corresponding to these estimated values are enclosed in parentheses. Average strand stresses are shown in Fig. 4.17.

At failure, the average strand strain exceeded 1 percent, which is the strain used to define yield in ASTM A416 [25]. However, both the bottom strand strain and the average strand strain failed to reach a strain corresponding to the 0.2 percent offset.

Corrected girder concrete strains during the flexure test appear in Fig. 4.18. Strains at failure are estimated from load-deflection data as previously mentioned. Strains for the upper gages are presented with respect to gage location for selected loads in Fig. 4.19. The gages behaved well throughout the test as demonstrated by the net strain plots of Fig. 4.20 and 4.21 which correspond to plots of corrected strains in Fig. 4.18 and 4.19. Strains from both sides of the girder near the top are shown in Fig. 4.22 and indicate that the girder was not experiencing significant lateral movement during the flexure test.

At failure the strain at the top of the girder was nearly 2000 microstrains, which is close to the strain at maximum stress and failure for cylinder tests of girder concrete. Strains at the top of girder are consistent with nearby gages as demonstrated by comparing them with strains computed for the top of the girder using net strain data from two lower gages shown in Fig. 4.23.

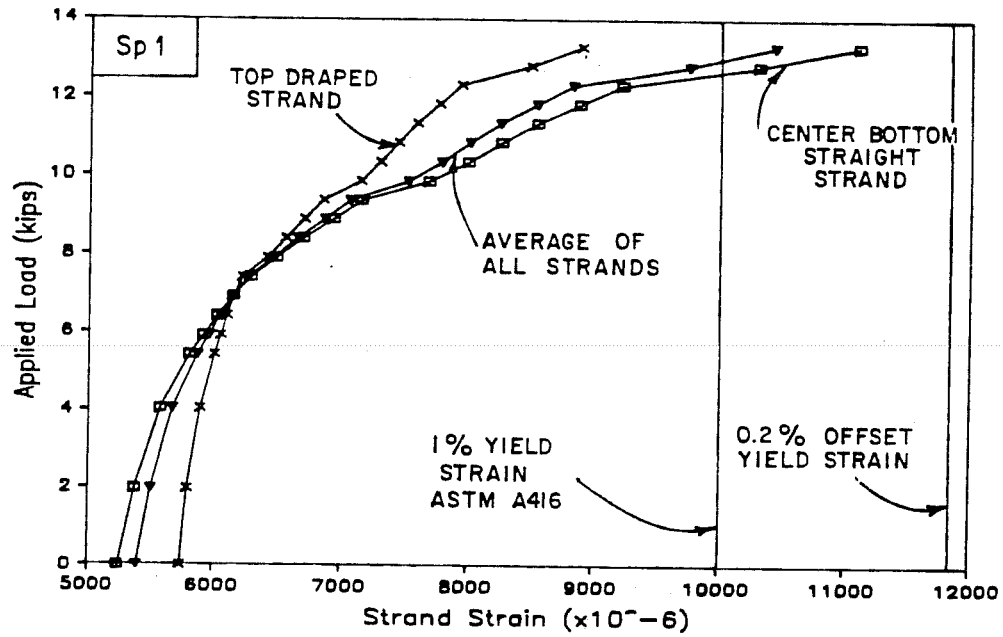

Fig. 4.16 Corrected and average strand strains during ultimate flexure test

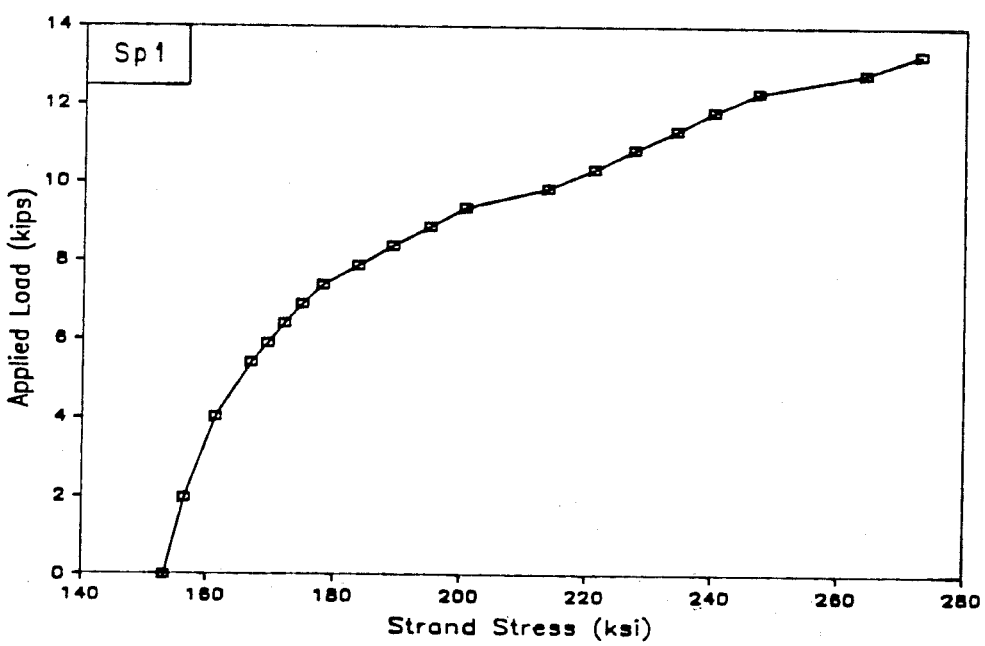

Fig. 4.17 Average strand stress during ultimate flexure test

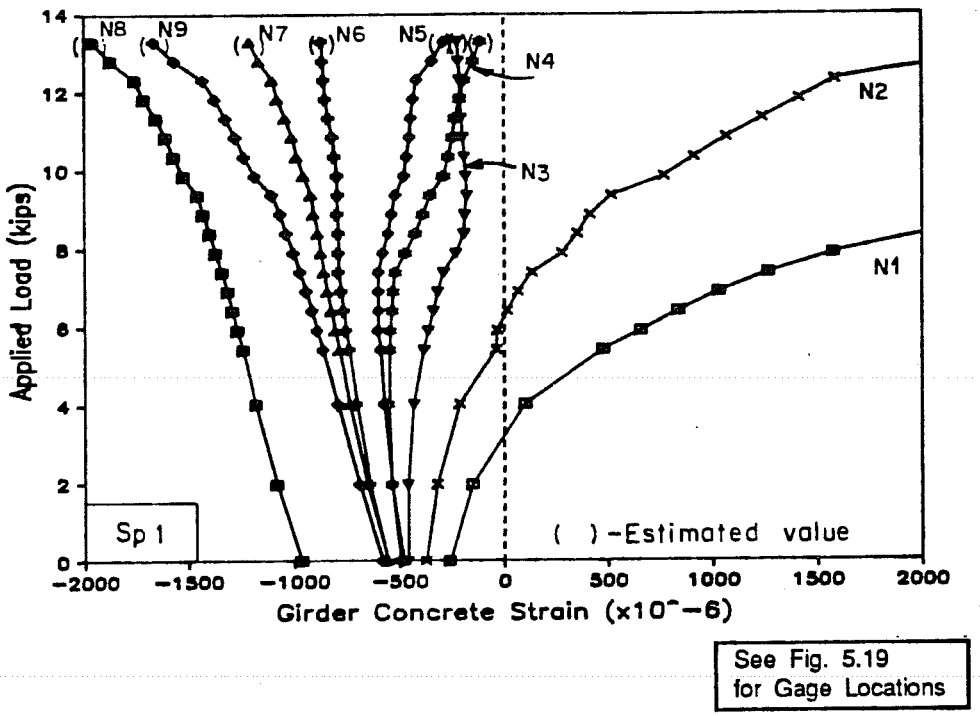

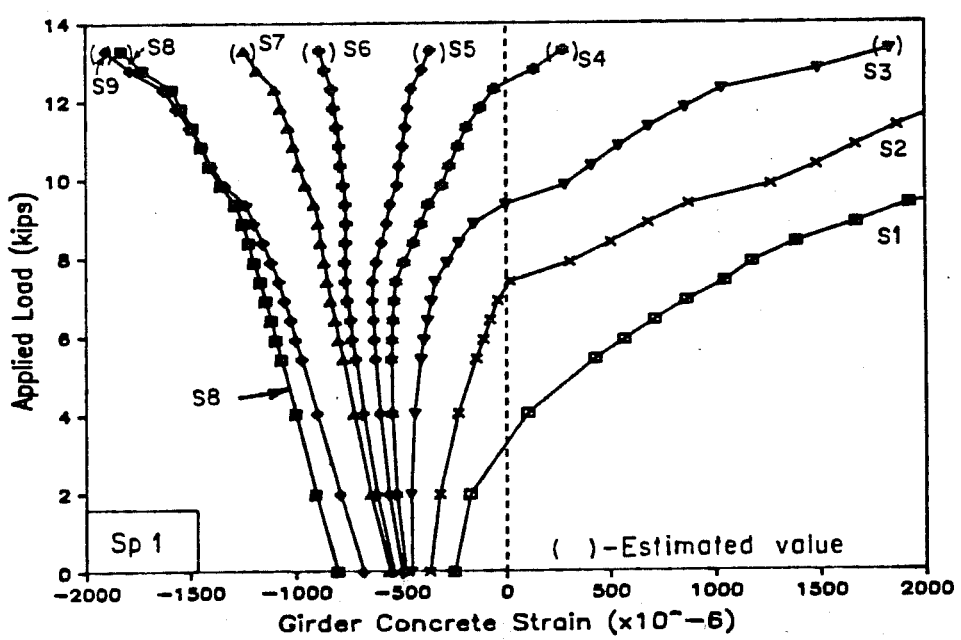

Fig. 4.18 Corrected girder concrete strains during ultimate flexure tests: a) north gages; b) south gages

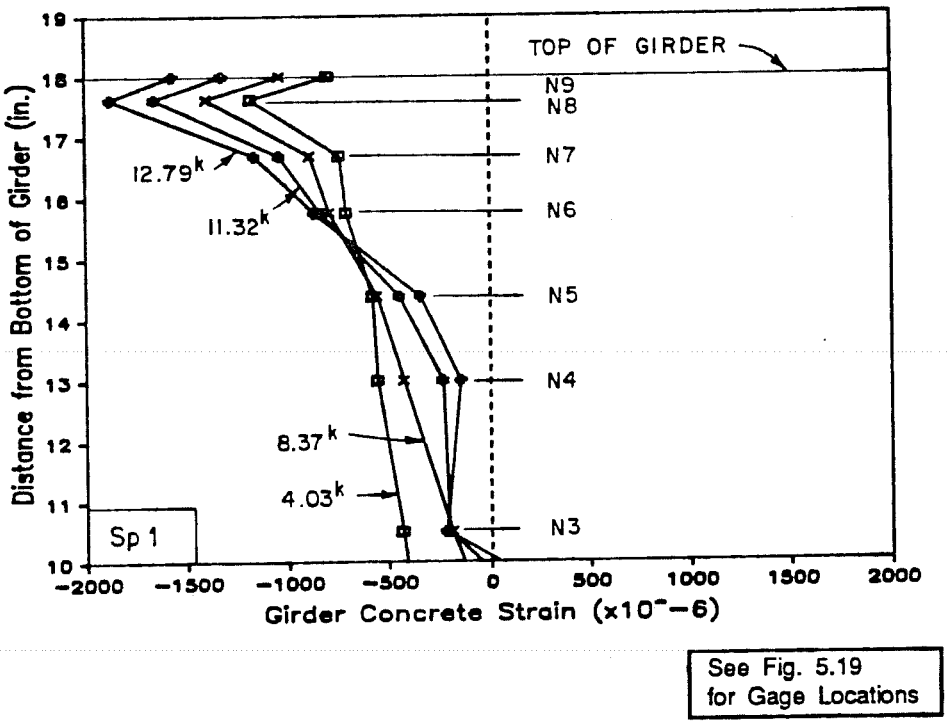

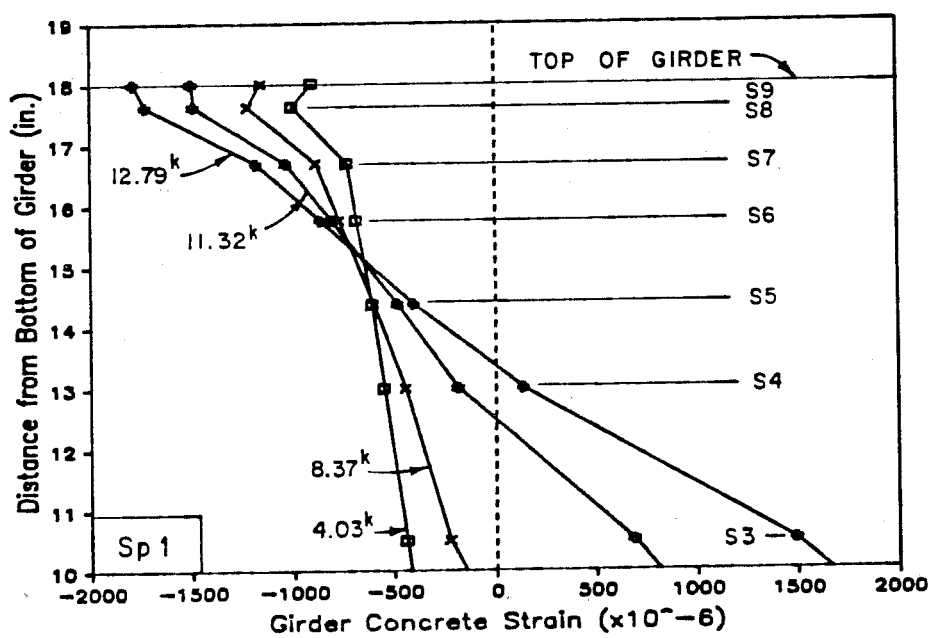

Fig. 4.19 Corrected girder concrete strains at selected loads during flexure test: a) north gages; b) south gages

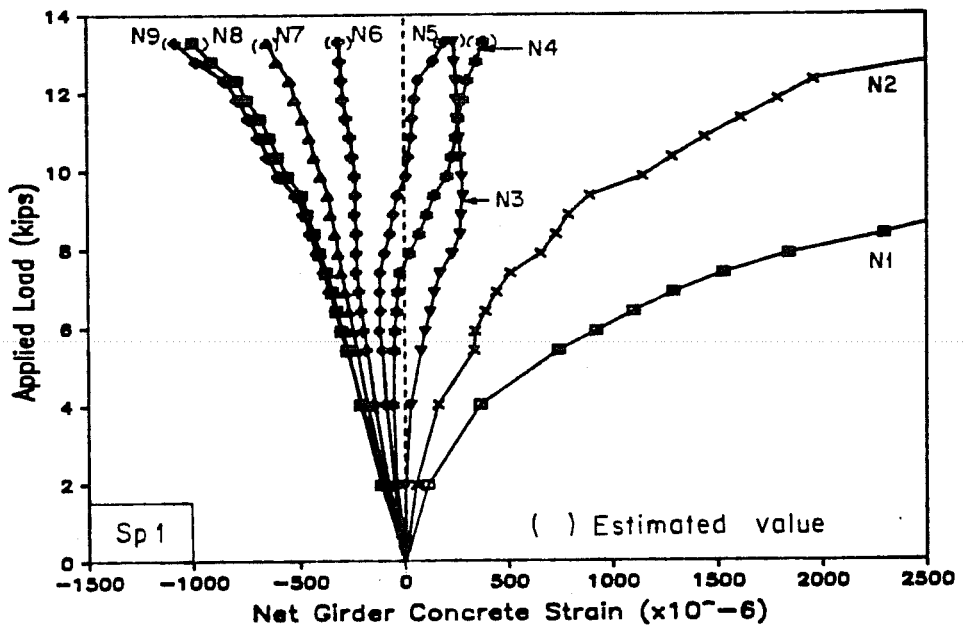

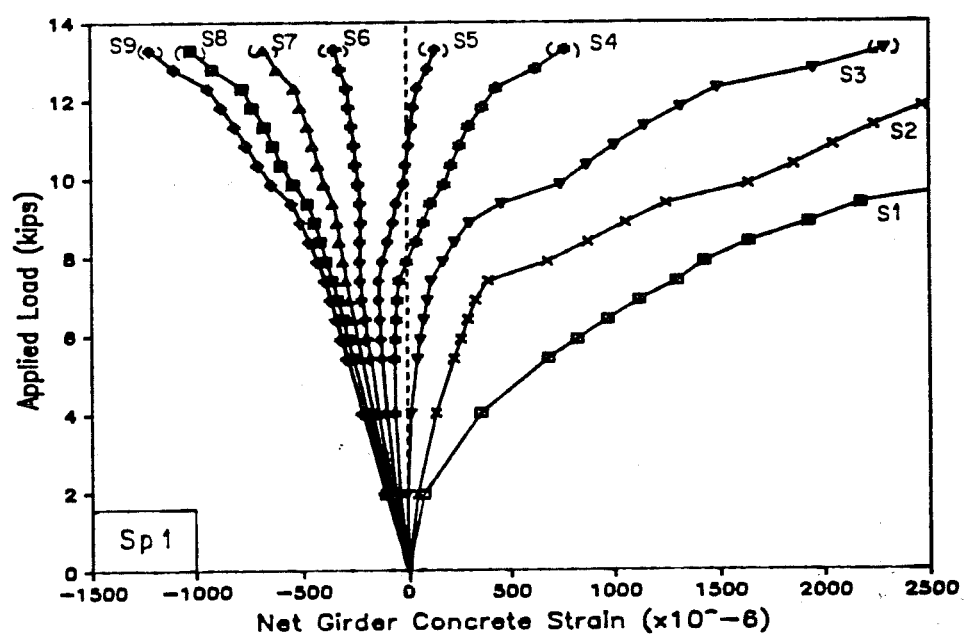

Fig. 4.20 Net girder concrete strains during ultimate flexure test: a) north gages; b) south gages

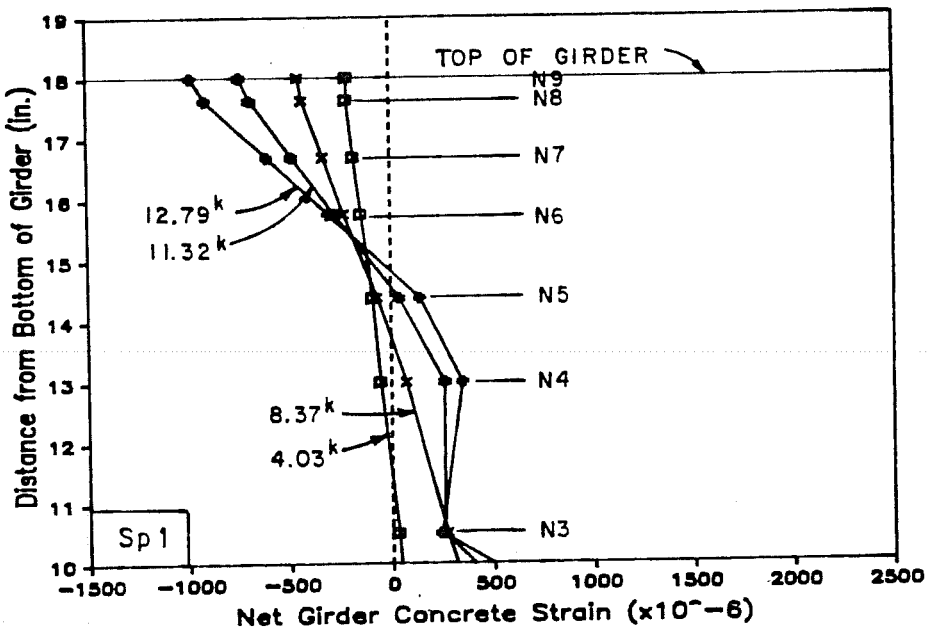

See Fig. 5.19 for Gage Locations

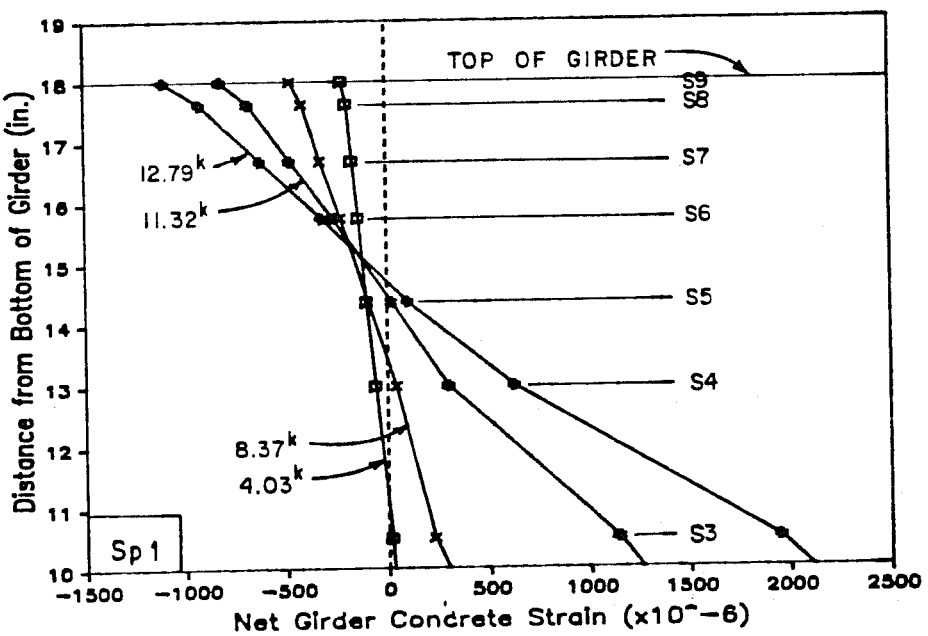

Fig. 4.21 Net girder concrete strains at selected loads during ultimate flexure test: a) north gages; b) south gages

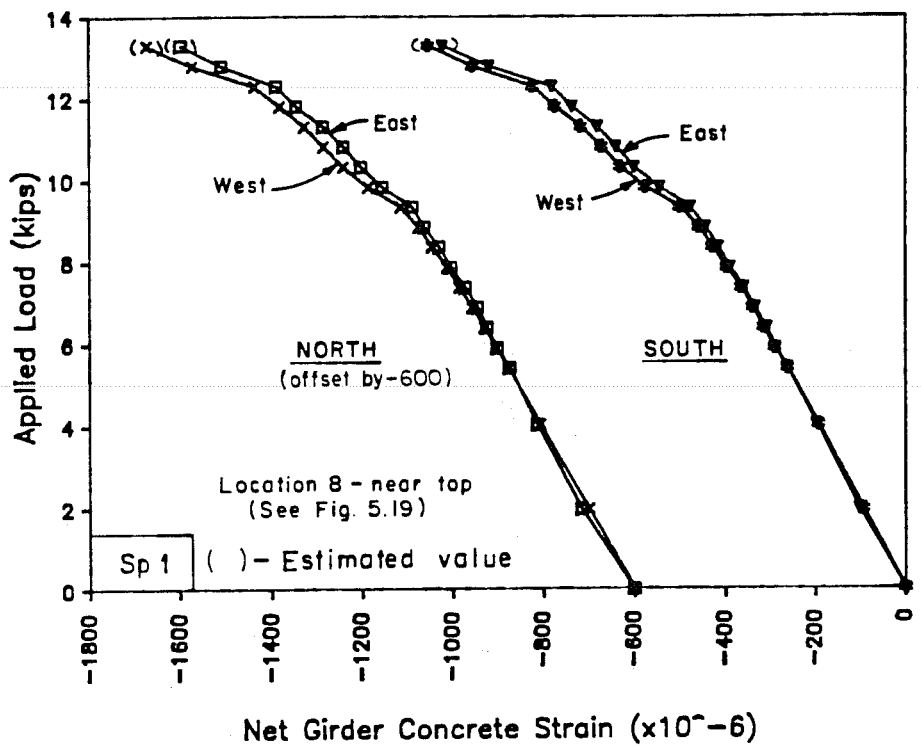

Fig. 4.22 Net concrete strains on opposite side of girder during ultimate flexure test

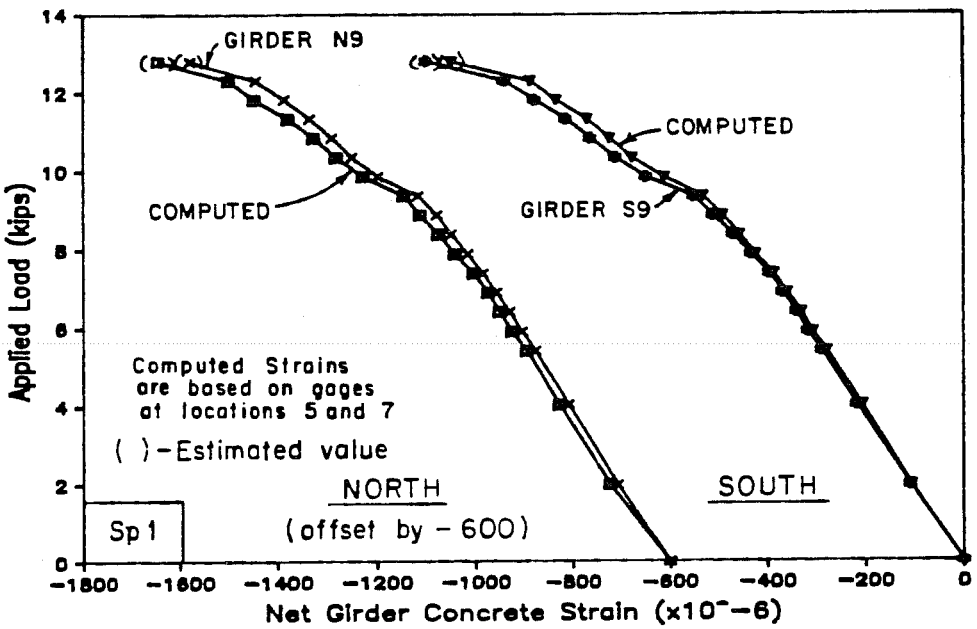

Fig. 4.23 Measured and computed top of girder concrete strains

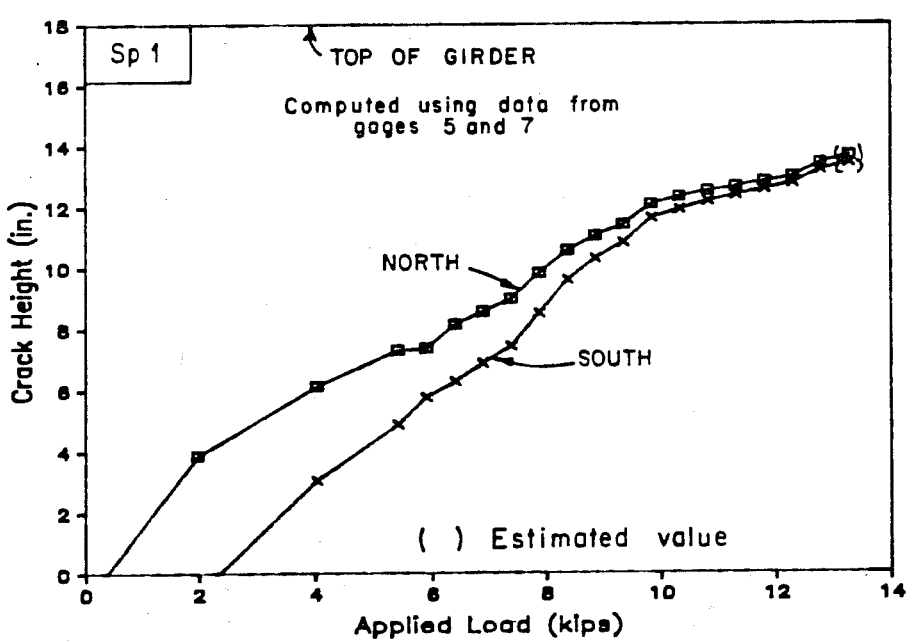

Fig. 4.24 Computed crack height

The crack height computed using corrected girder strains is shown in Fig. 4.24. The computed crack height was approximately 13.5 in. at failure, which is at the bottom of the taper of the top flange and agrees with visual observations.

Corrected deck concrete strains are shown for typical top and bottom gages in Fig. 4.25. Data from all deck strain gages are presented in Fig. 4.26 with respect to the gage location for selected loads. The increasing and pronounced strain gradient across the deck indicates asymmetrical behavior. Some of the gradient was caused by the lateral push of the specimen, but this would be a small, constant value. Lateral movement during the test did not appear sufficient to produce a strain gradient of this magnitude and no other explanation was found.

At failure, strain at the top of the deck was estimated to be between 1600 and 2400 microstrains. These strains equalled or exceeded the strain at maximum stress and approached the maximum strains which were measured during cylinder tests (see Table 7.3). However, maximum strains measured during cylinder tests were limited by failure of the strain gages rather than failure of the cylinder (see Sec. 7.3.2) and were therefore significantly less than expected. Similar concrete for Specimen 2 achieved strains in excess of 0.003.

Estimates of corrected strains at the top of the girder and deck were similar at failure. Strains measured at crushing of cylinders for the two concretes were also similar. Therefore, on the basis of these strains, it is not possible to determine which concrete initiated crushing.

Top of girder and bottom of deck net strains are shown in Fig. 4.27 with respect to their location across the deck for selected loads. Net strains for girder gages and the center top deck gage at different levels of load are plotted in Fig. 4.28. The data in the two figures demonstrate that agreement between the deck and girder strains at the level of the bottom of the deck was good and that the strain gradient through the full depth of the section for different stages of applied load remained approximately linear up to failure. This verifies that full composite action was present up to failure.

Curvature of the section was computed using strains from a pair of girder gages and three pairs of deck gages. The average of the three bottom deck gages was used with the top center deck gage because no deck gage was available directly below it. The resulting net curvatures are presented with increasing load in Fig. 4.29 and the total curvatures are shown versus total moment in Fig. 4.30. Total curvatures were computed by adding net curvatures to a computed curvature at the beginning of the flexure test. The girder data is a

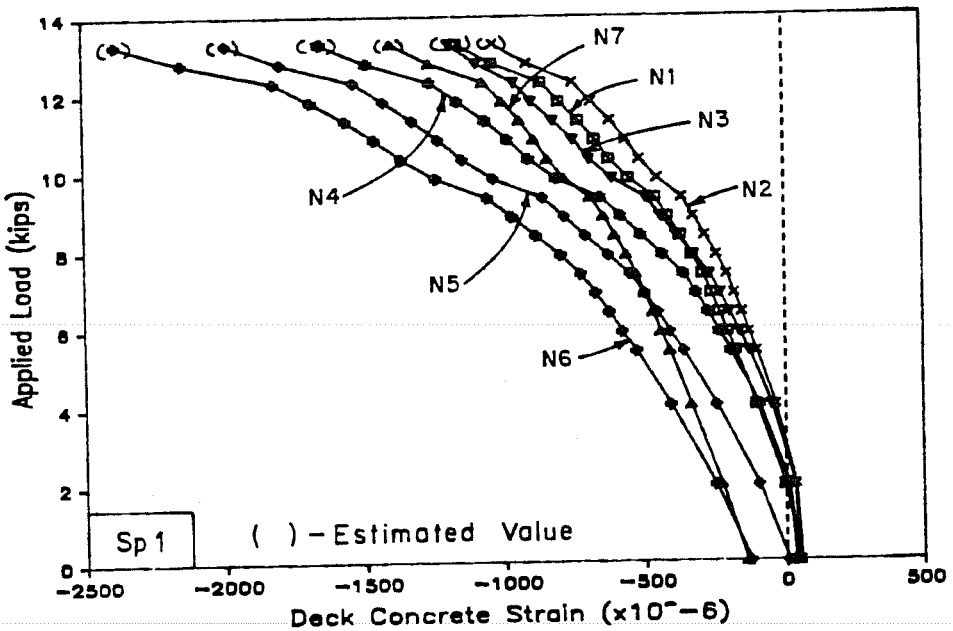

(a)

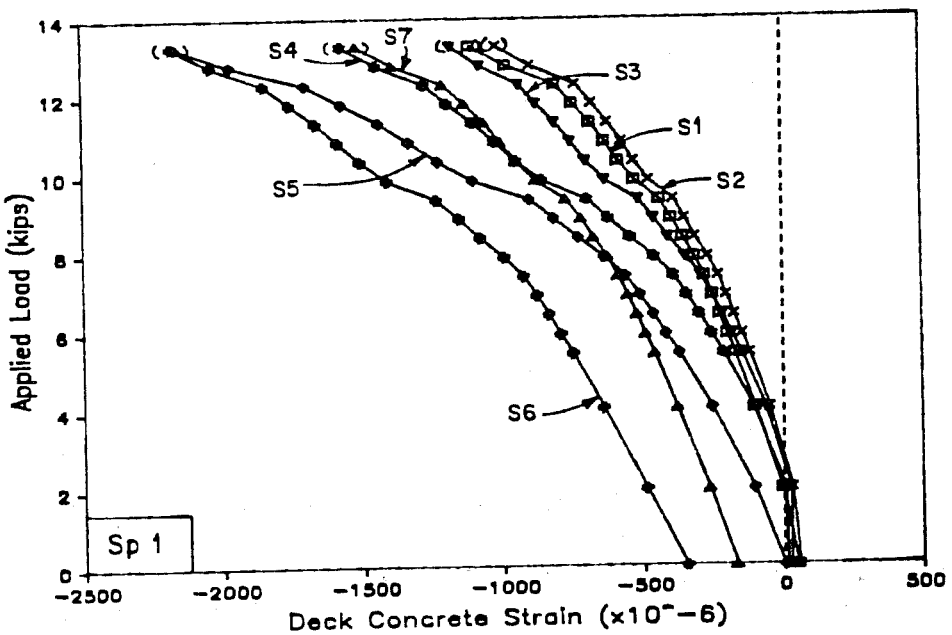

(b)

Fig. 4.25 Corrected deck concrete strains during ultimate flexure test: a) north gages; b) south gages

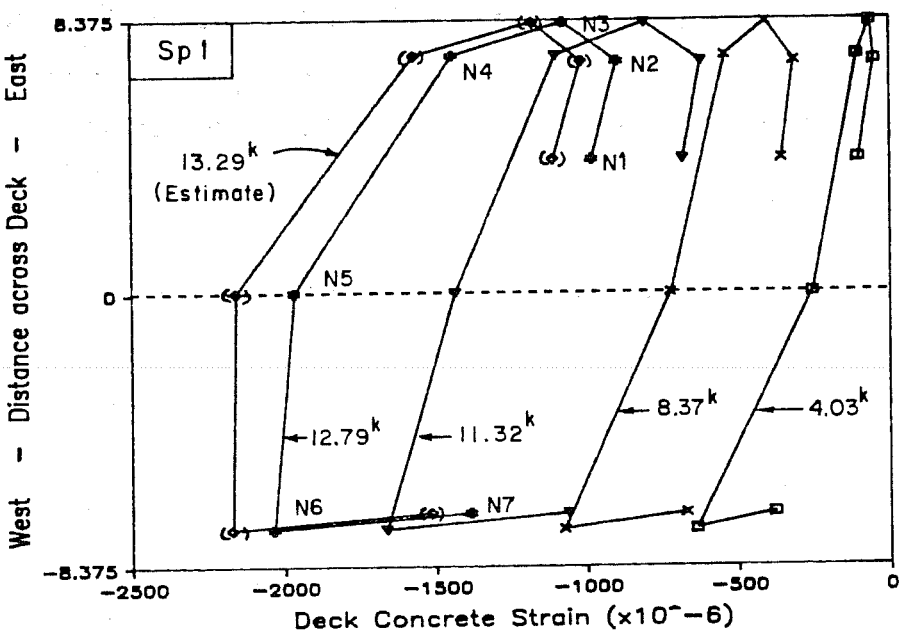

(a)

See Fig. 5.19 for Gage Locations

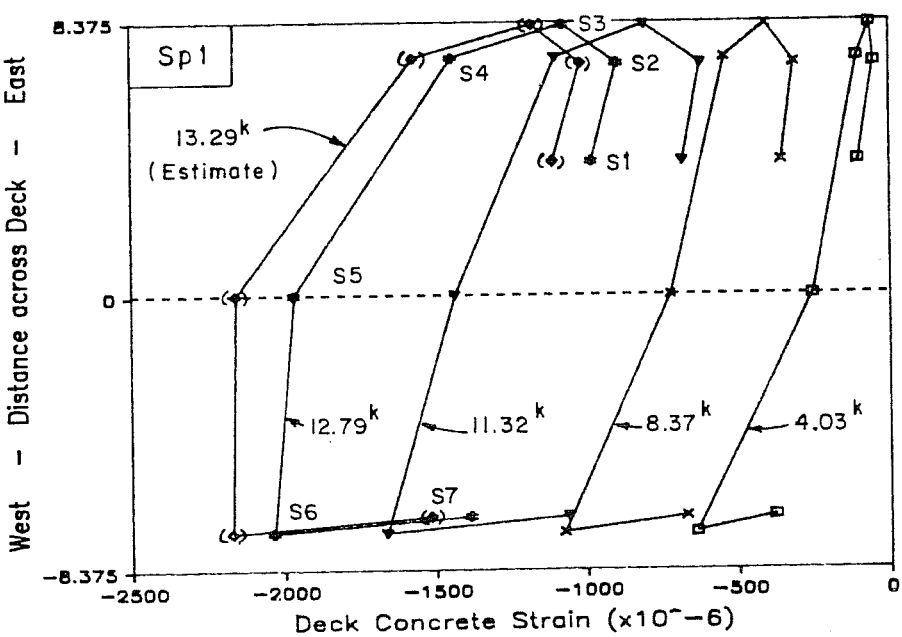

(b)

Fig. 4.26 Corrected deck concrete strains at selected loads during ultimate flexure test: a) north gages; b) south gages

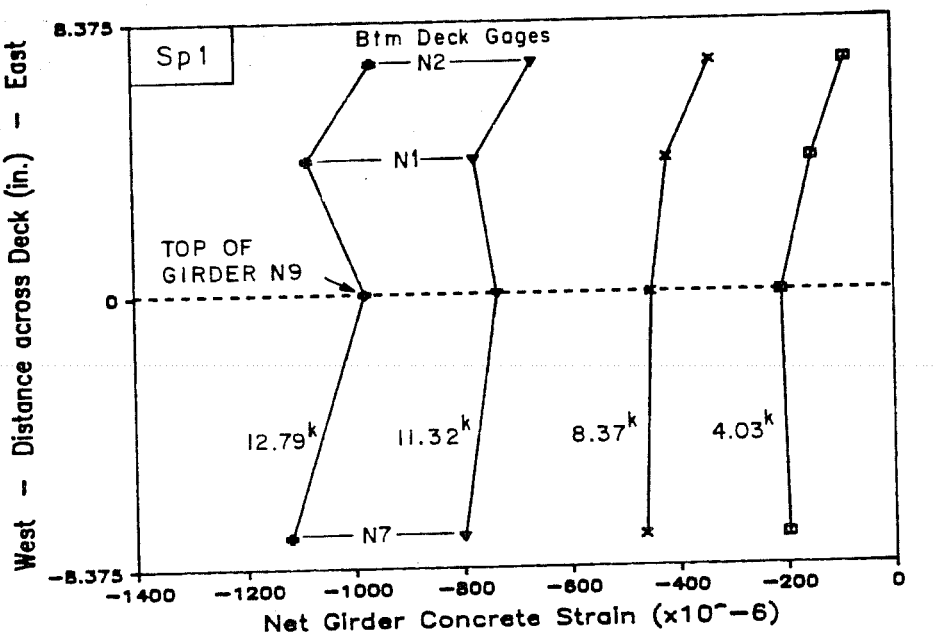

(a)

See Fig. 5.19
for Gage Locations

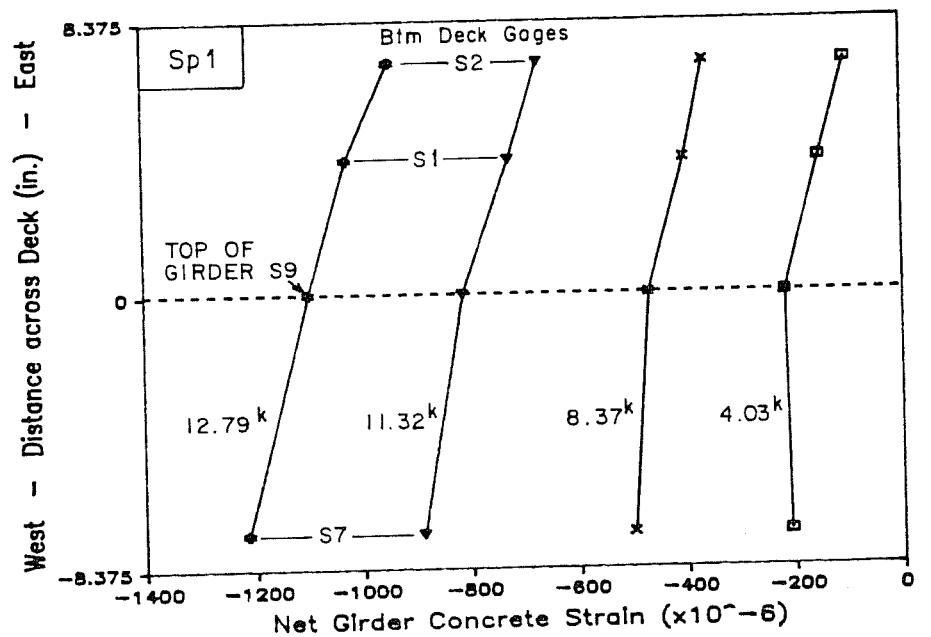

(b)

Fig. 4.27 Net concrete strains at top of girder and bottom of deck at selected loads during ultimate flexure test: a) north gages; b) south gages

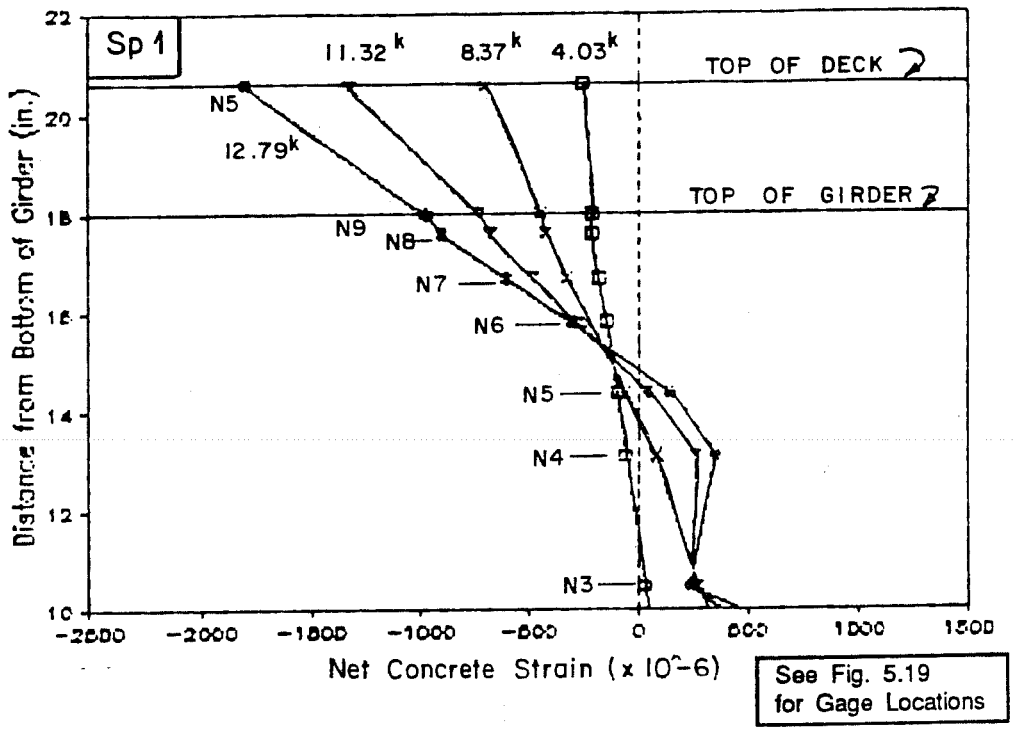

(a)

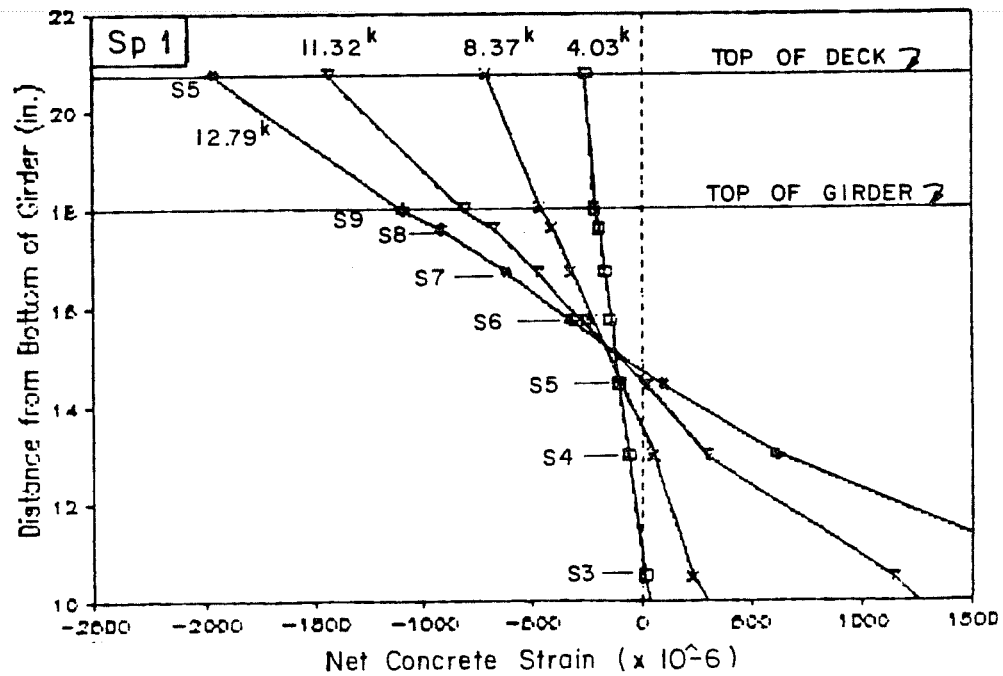

(b)

Fig. 4.28 Net girder and deck concrete strains at selected loads during ultimate flexure test: a) north gages; b) south gages

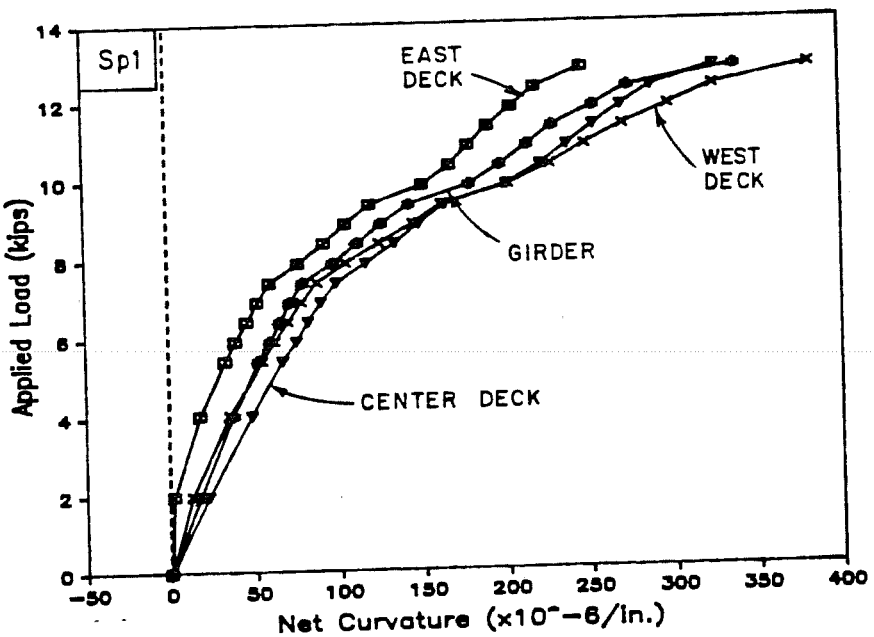

(a)

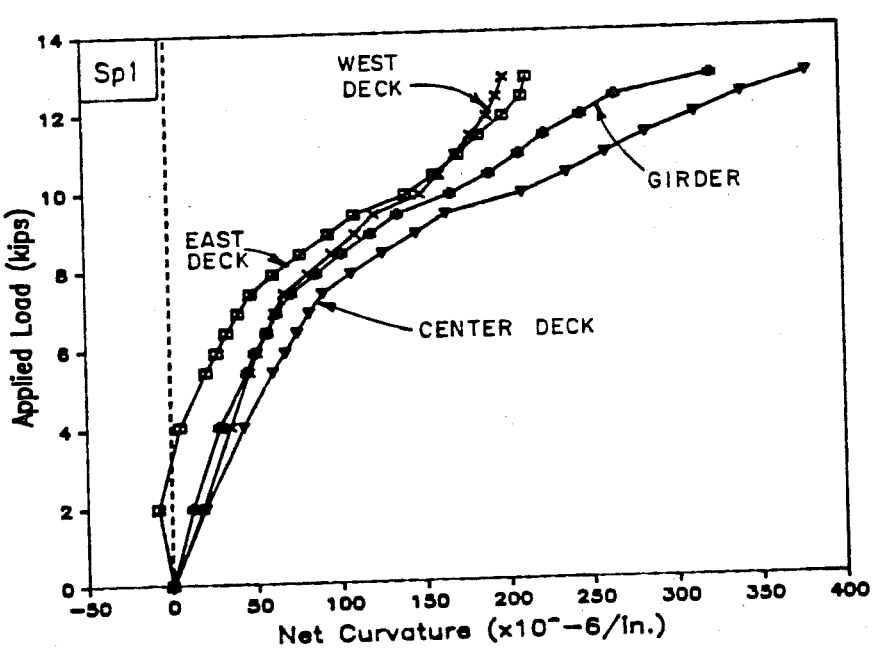

(b)

Fig. 4.29 Load-net curvature curves during ultimate flexure test: a) north gages; b) south gages

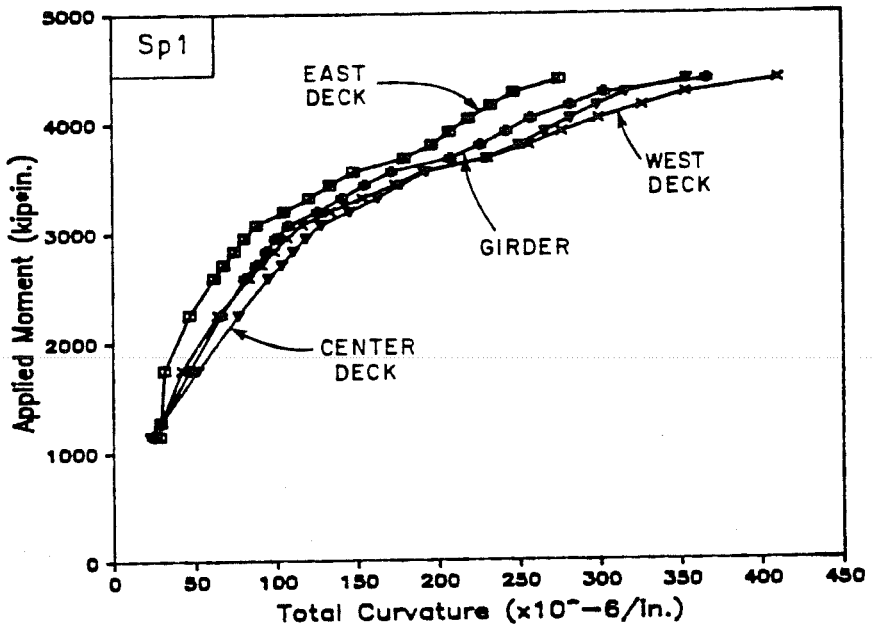

(a)

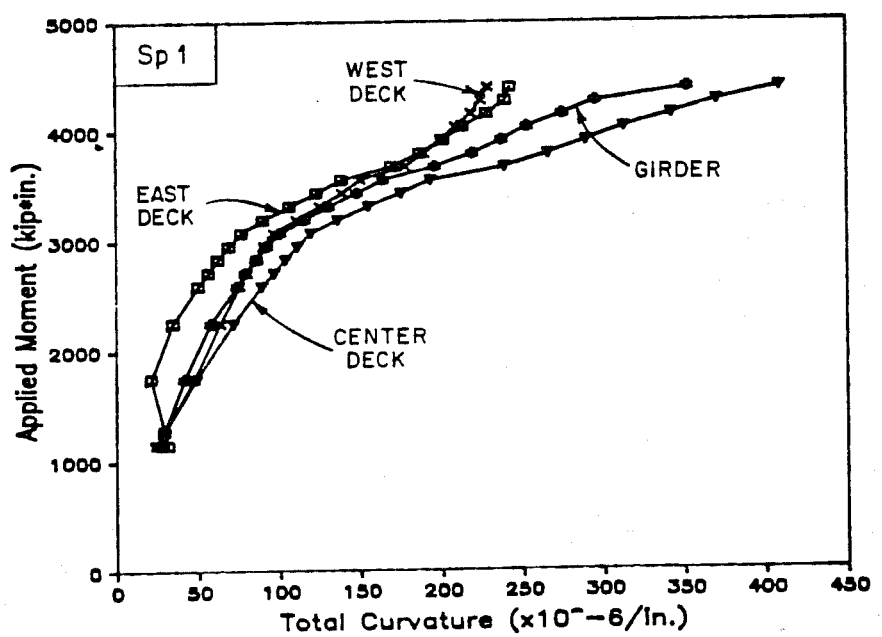

(b)

Fig. 4.30 Moment curvature curves during ultimate flexure test: a) north gages; b) south gages

reasonable average of the curves and will be used to represent specimen curvature during the flexure test.

Measured strand strains are compared with strand strains computed using girder curvature data in Fig. 4.31. Data for both lines of gages are shown on the same plot by adding an increment to the south data. These plots show that measured strand strains are consistent with the overall behavior of the specimen and that no debonding of the strands occurred during the test.

Strand strains, girder concrete strains, deck concrete strains, girder curvature, and midspan deflections are combined in Fig. 4.32. The data is normalized with respect to readings at the load stage prior to failure because data was not available for quantities other than deflection at failure.

4.2.2.4 Stirrup Strains and Strand Slip at Ends. Strains in the stirrups were negligible, indicating that no significant shear cracking occurred (Fig. 4.33). However, the large increase in strains measured at the south end after failure indicates that cracking may have occurred due to the violent flexural failure. Data was not available after failure for the north end because the gage lead was severed during failure.

No slip was measured in the strands at ends of the girder.

4.3 Specimen 2 (9 strands)

In this section, behavior and properties of Specimen 2 prior to and during flexure and shear tests will be discussed. While the span of time from casting the girder to the flexure test was only approximately two months, a discussion of specimen behavior during that time period is included because of its significance in establishing effective stresses and strains at the time of the flexure test and in understanding the long-term behavior of the structure.

Since the flexural failure of Specimen 1 was near the balanced condition, Specimen 2 was designed to produce a more ductile failure. The design used the minimum number of strands required to satisfy allowable stress design criteria. One of the nine strands was draped to control stresses at the ends of the section. The flexure test consisted only of an ultimate test because the girder suffered extensive cracking prior to release due to shrinkage.

Shear tests of the two ends of the flexure specimen also included only ultimate tests because of the prior cracking of the girder. The tests are referred to by the location (south or north) of the end during the flexure test. At both ends, stirrups were provided at a spacing that corresponded to approximately $V_s=4\sqrt{f'_c}b_w d$, or half

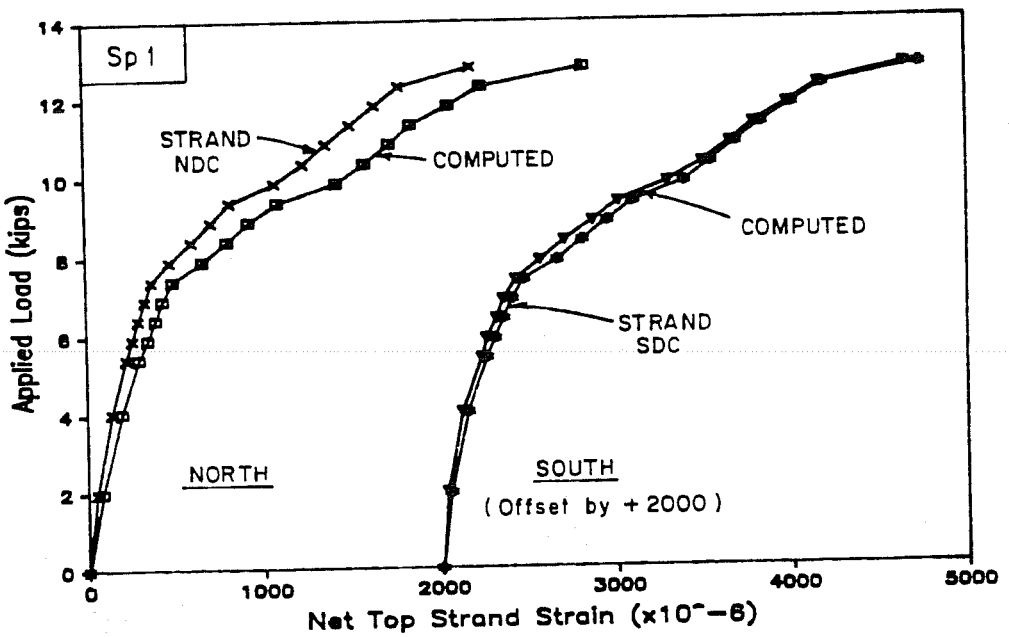

(a)

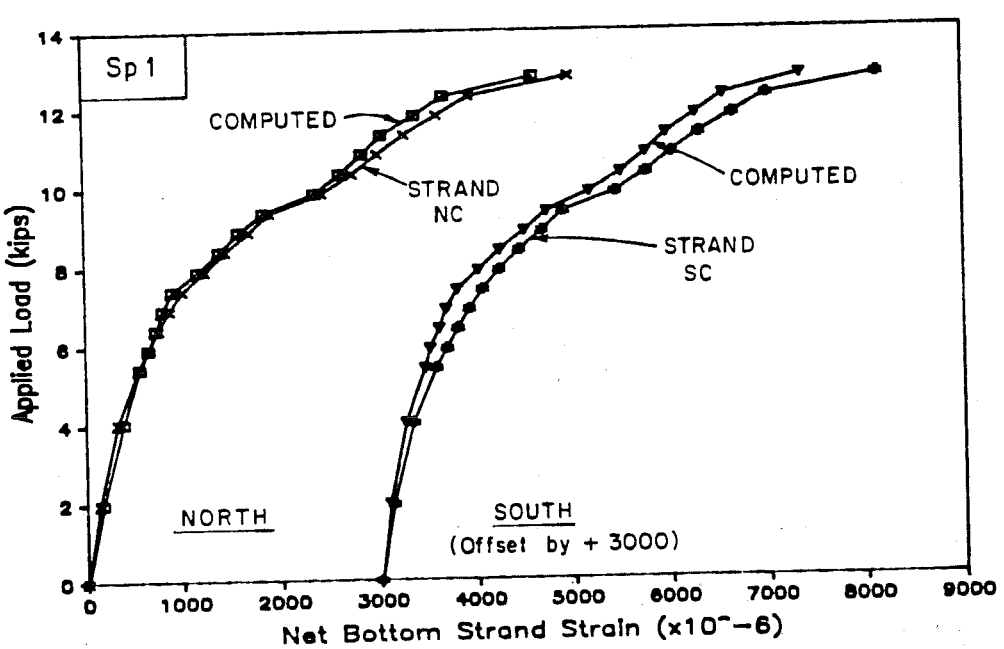

(b)

Fig. 4.31 Measured and computed strand strains during ultimate flexure test: a) measured and computed top strand strain; b) measured and computed bottom strand strain

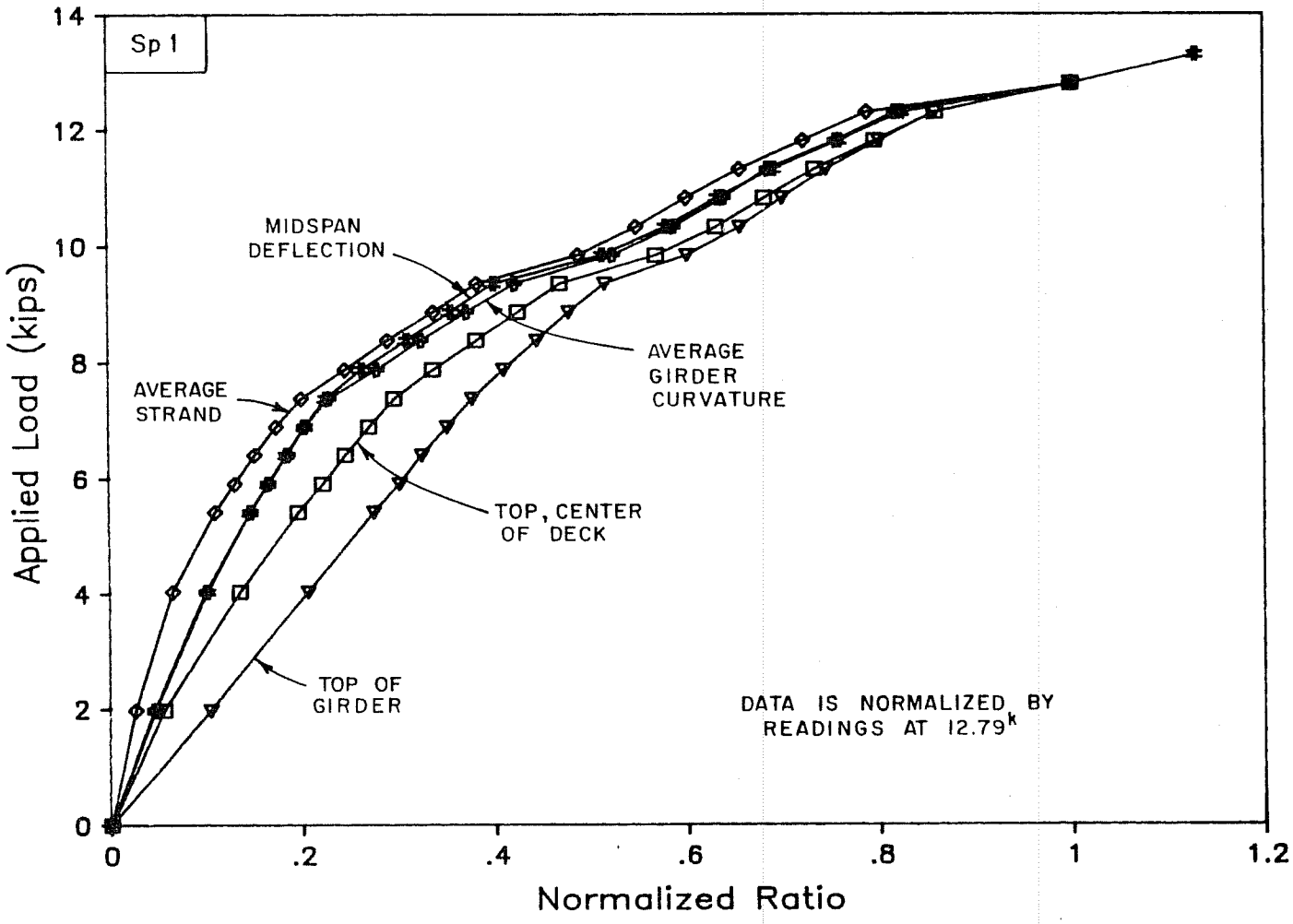

Fig. 4.32 Comparison of different types of data during ultimate flexure test

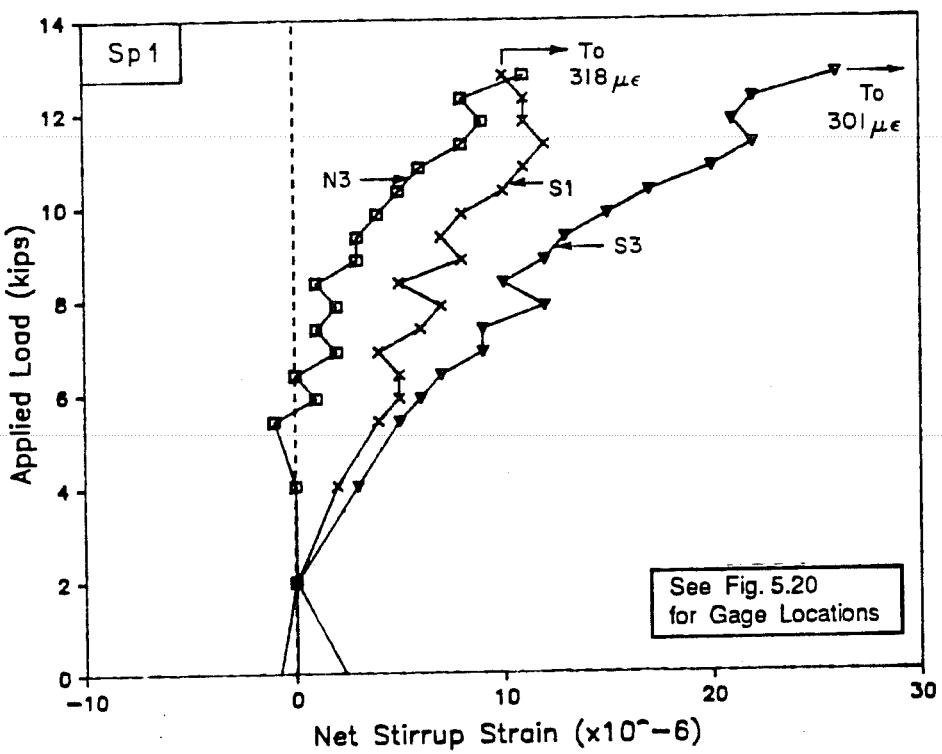

Fig. 4.33 Net stirrups strains during ultimate flexure test

the quantity of stirrups used in Specimen 1. Standard open stirrups were used for both ends, but an additional 6 in. extension beyond the support was provided at the north end in order to study the effect of bond on shear capacity.

4.3.1 Prior to Flexure Test.

4.3.1.1 Concrete Material Properties. Properties of girder and deck concrete were measured at intervals. Measured and estimated data at specific times are given in Table 4.7. Values were estimated when data were not available for the date on which an event occurred. Estimates were based on data presented in Appendix A. Strength gain with age is shown in Fig. 4.34. Average stress-strain curves at the time of the flexure test are shown in Fig. 4.35. Stress-strain curves were obtained using compressometer and head displacement data for tests of 6 by 12-in. cylinders and head to head displacement data for 3 by 6- in. and 4 by 8-in. cylinders (high strength concrete only). More information on mix design and material properties is given in Appendix A.

4.3.1.2 General Description of Behavior. A summary of the specimen history is given in Appendix B including times at which dead load compensation and deck formwork were added and removed.

When the forms were removed the girder was found to have extensive shrinkage cracking. The forms were left in place four days to improve curing. However, it appeared that the surface of the forms, which was roughened by vibrators during placement of the girder concrete, may have absorbed water instead. The forms and the unreleased prestressing strands served as the restraint required to cause cracking from shrinkage strains. The probable magnitude of shrinkage strains is considered in Sec. 4.3.1.4 with the discussion of stirrup strains prior to the flexure test.

Shrinkage cracks in the web were regularly spaced at about 7.5 in. for the full length of the specimen. Most cracks were vertical, but inclined near the ends. Horizontal cracks appeared at the junction of the web and flanges. Web cracks averaged about 0.010 in. wide with a maximum crack width of 0.035 in. A number of small cracks 0.002 in. wide or less crossed the bottom flange. The top flange cracked in few locations with cracks ranging from 0.002 in. to 0.018 in. wide. It is not known whether cracks completely penetrated the web and flanges, although some cracks did cross the top of the girder. Because the cracks were not expected to significantly affect ultimate test results, testing proceeded as planned. At release the cracks closed but the strain distribution across the section was very non-linear.

Table 4.5 Concrete properties at significant events - Specimen 2

Event	Age (days)	f'_c (psi)	E_c (ksi)	f'_r (psi)
Release				
Girder	7	9,200	(5,290)	880
Deck Cast				
Girder	48	(10,120)	(5,500)	
Flexure Test				
Girder	56	10.800	5,675	1,100
Deck	8	4,350	4,370	
Shear Tests				
Girder	265	11,300	(5,800)	1,275
Deck	217	5,350		

() - Estimated values, based on additional data presented in Appendix A.

Note: All data are for cylinders cast in plastic molds and cured with Specimen 2 under ambient conditions.

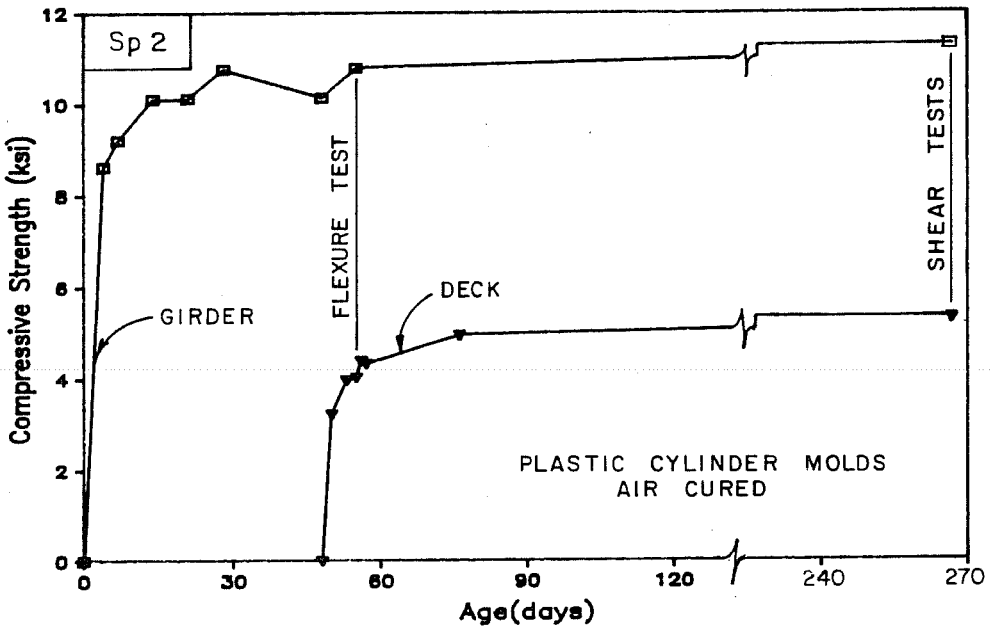

Fig. 4.34 Girder and deck concrete strength gain with age-Specimen 2

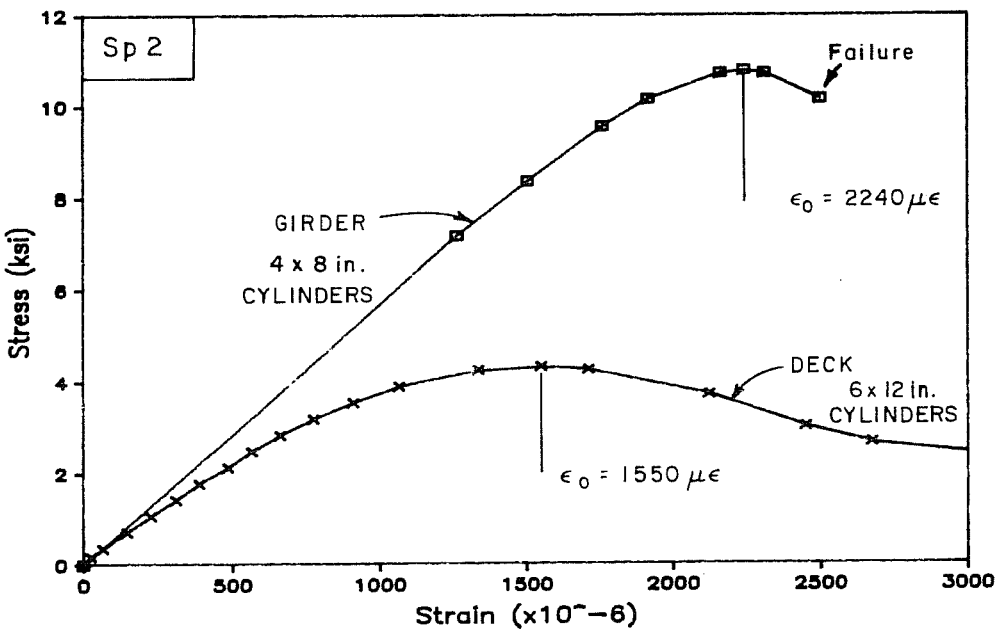

Fig. 4.35 Girder and deck concrete stress-strain curves at flexure text - Specimen 2

Half of the girder dead load compensation was in place at release with the remainder being put in place the following day. No additional cracking was observed at the time of release.

A second episode of unanticipated cracking occurred when deck forms were removed. Forms and dead load compensation were removed in stages with the dead load blocks replaced as soon as possible to prevent deck cracking. However, cracking was observed as blocks were removed from midspan. When the dead load was replaced, the cracks did not close fully. These cracks affected early behavior of the specimen during the flexure test but had no effect on ultimate behavior.

Prior to the flexure test, the specimen was pushed laterally to the west at the level of the deck to reduce sweep. No additional deck cracking was observed. Sweep was not large at release but increased after addition of the deck.

Actual specimen dimensions are summarized in Table 4.6.

4.3.1.3 Deflections. Midspan girder deflections from release until the flexure test are shown in Fig. 4.36. Significant events are indicated on the plot. A deflection measurement using an optical level was 0.236 in. greater than the data shown. This indicates possible movement in the dial gage stand or a change in deflection when the specimen was moved out of the prestress bed.

Camber at release was much smaller than for the first specimen because dead load compensation was present and there was a lower level of prestress. Creep caused significant increases in deflection that continued until the time of the flexure test. The deck was not available to arrest the continuing sag because it was applied just over a week prior to the flexure test.

At release, a sweep at midspan of 0.02 in. to the east was observed. This increased to 0.03 in. during the month over which readings were taken. However, after the deck was added, the sweep was large enough to necessitate pushing the specimen approximately 3/8 in. to the west, leaving the specimen essentially straight.

4.3.1.4 Effective Stresses and Strains. Strain readings for strands, girder concrete and deck concrete were corrected for time effects and discontinuities to obtain "effective" strain for each gage. Corrected strains therefore represent an estimate of the elastic strain at a specific time. Methods described in 4.2.1.4 for Specimen 1 were also used for Specimen 2.

Typical corrected strains for straight and draped strands prior to the flexure test are shown in Fig. 4.37. A summary of the effective strand stresses and forces computed from the "average" strand strain is given in Table 4.7. Because consistent data was not

Table 4.6 Actual section dimensions - Specimen 2

Girder

Use Nominal Dimensions

Strand Placement

No. of Strands	Distance from strands to bottom of girder, g Straight 8	 Draped 1	 Total 9
North end	1.72"	14.31"	2.84"
Midspan	1.72"	3.81"	1.95"
South end	1.80"	14.25"	2.90"

Drape locations are 19.5' from ends of girder

Deck

Width	16-3/8 "
Thickness	2-1/4 "
Offset *	3/8 "

Overhang at Interior End During Shear Tests

North end	3' 3"
South end	9' 2"

* - Offset is the distance from top of girder to bottom of deck. This area is filled with deck concrete and is as wide as the girder top flange

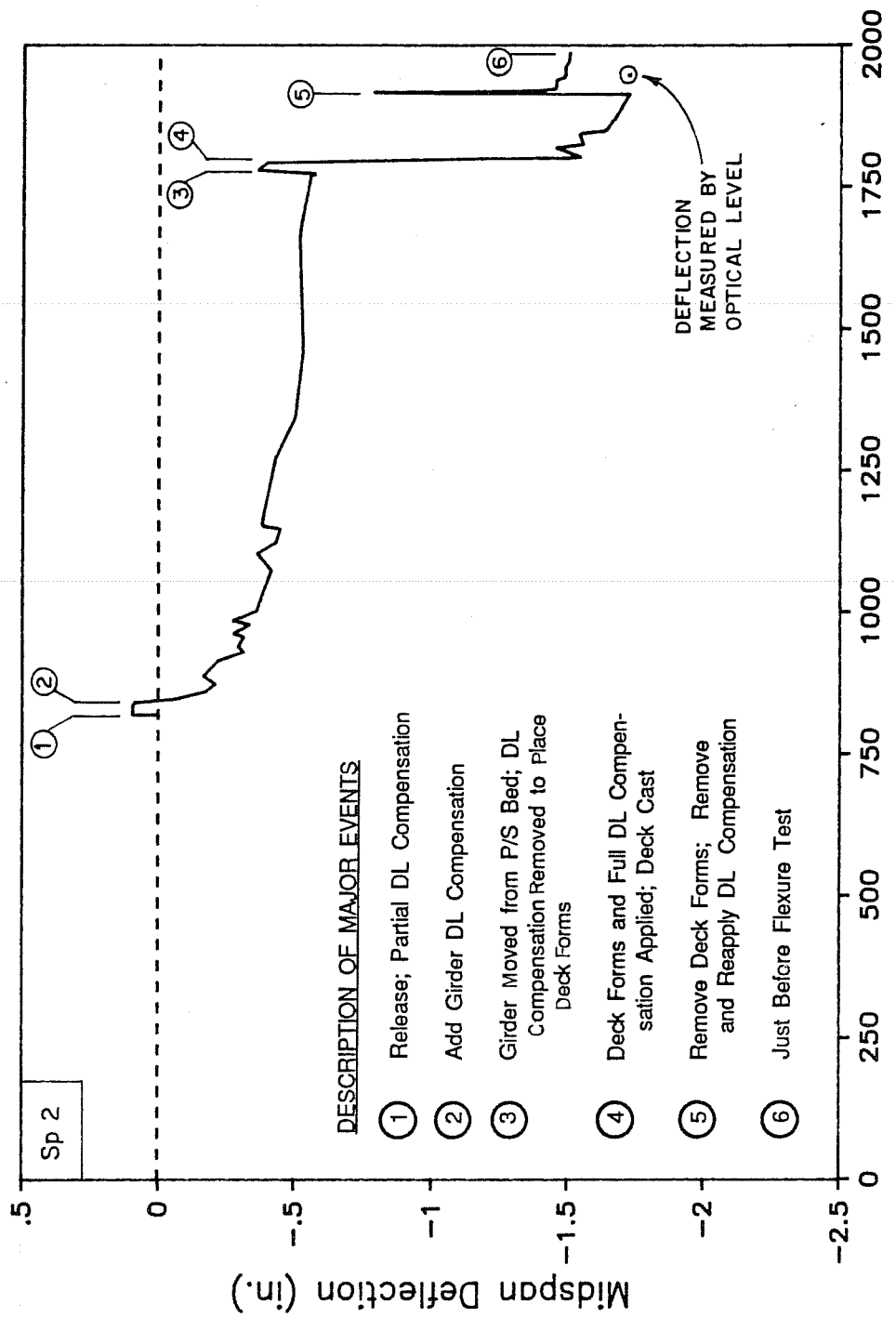

Fig. 4.36 Midspan deflection with time

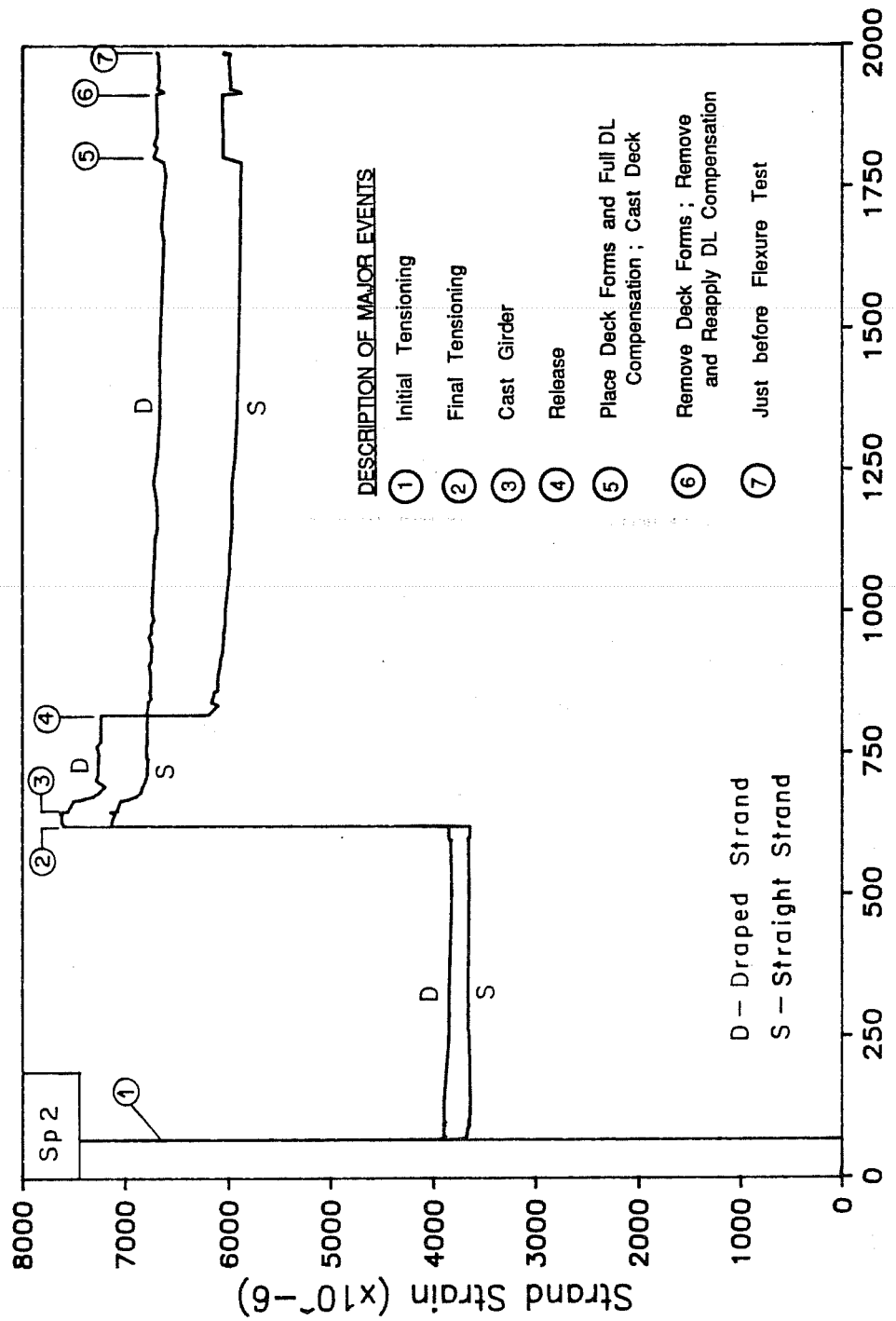

Fig. 4.37 Typical corrected midspan strand strains with time

Table 4.7 Effective strand stresses and forces - Specimen 2

	Stress (ksi)	Force (ksi)
Full Tensioning		
All locations	206.7	157.2
Prior to Release		
All locations	193.6	147.2
After Release		
Midspan	177.6	135.0
Midspan *	179.4	136.4
At both ends *	173.5	131.9
Flexure Test		
Midspan	173.1	131.7
At both ends	156.8	119.2
Shear Tests (estimated)		
At both ends	156.8	119.2

* - These values represent computed instantaneous elastic prestress losses plus 25% to provide better agreement with the limited measured strain data. The elastic losses were calculated using the "Prior to Release" prestress force and gross section properties.

Area of prestressing steel = $9(0.0845 \text{ in.}^2) = 0.76905 \text{ in.}^2$

available for determining the effective strand stress at the shear tests, the value used at the flexure tests was used as an estimate.

Changes in strain at release for strand gages near the ends of the girder indicate a transfer length of less than 12 in. Fig. 4.38 shows the data for active strand gages at both ends of the girder. Data for the two ends are very consistent.

Typical girder concrete strain data is presented in Fig. 4.39. Readings were again susceptible to large variations due to changes in temperature. Figure 4.40a shows measured and computed girder concrete strains at release as they vary with location on the girder. Agreement is fair between lines of gages, and poor when comparing measured and computed strains because of the effects of shrinkage cracking. The nonlinear strain gradient is a result of the top and bottom flanges receiving load at release while the cracks in the web were closing. Strain readings were taken shortly after release and may contain some creep. The second plot (Fig. 4.40b), compares uncorrected and corrected strains prior to the flexure test with computed strains across the depth of the girder. Agreement of corrected strains is again fair between the two lines of gages and poor for the computed strains with the effects of shrinkage still obvious. Corrected strains at the time of the flexure test are related to computed strains in much the same way as measured and computed strains at release.

Creep in the girder concrete had slowed by the time of the flexure test, as indicated by Fig. 4.39. The magnitude of creep during this period ranged from about 250 microstrains near the bottom of the girder to 450 microstrains near the top, although the data were erratic (Fig. 4.40b).

Strain gages were applied to the top of the deck prior to removal of deck forms, and the remaining deck gages were applied after form removal. Typical top and bottom deck strains prior to the flexure test are shown in Fig. 4.41, and strains and changes in strain are shown for all deck gages in Fig. 4.42. While the top gages were present to measure the elastic change in strain at removal of the forms, these strains were small and were obscured by large strain variations caused by temperature (Fig. 4.41). Effective strains at the beginning of the flexure test were determined to be the strains caused by the lateral push for the same reasons given for Specimen 1.

Data indicate the presence of existing deck cracks or that additional deck cracks formed when the specimen was pushed to the west, because compression measured on the east side of the deck was significantly larger than the tensile strains measured on the west side. The difference in strains between east and west sides of the deck affected strains measured during early stages of the flexure test

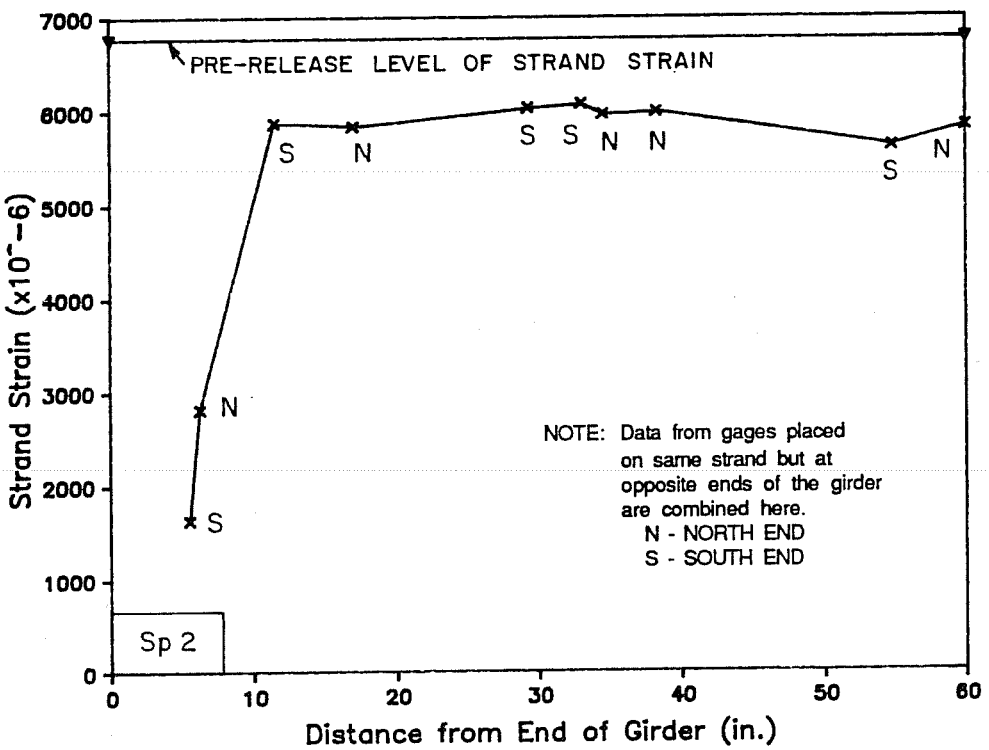

Fig. 4.38 Strand strains near ends of girder before and after release

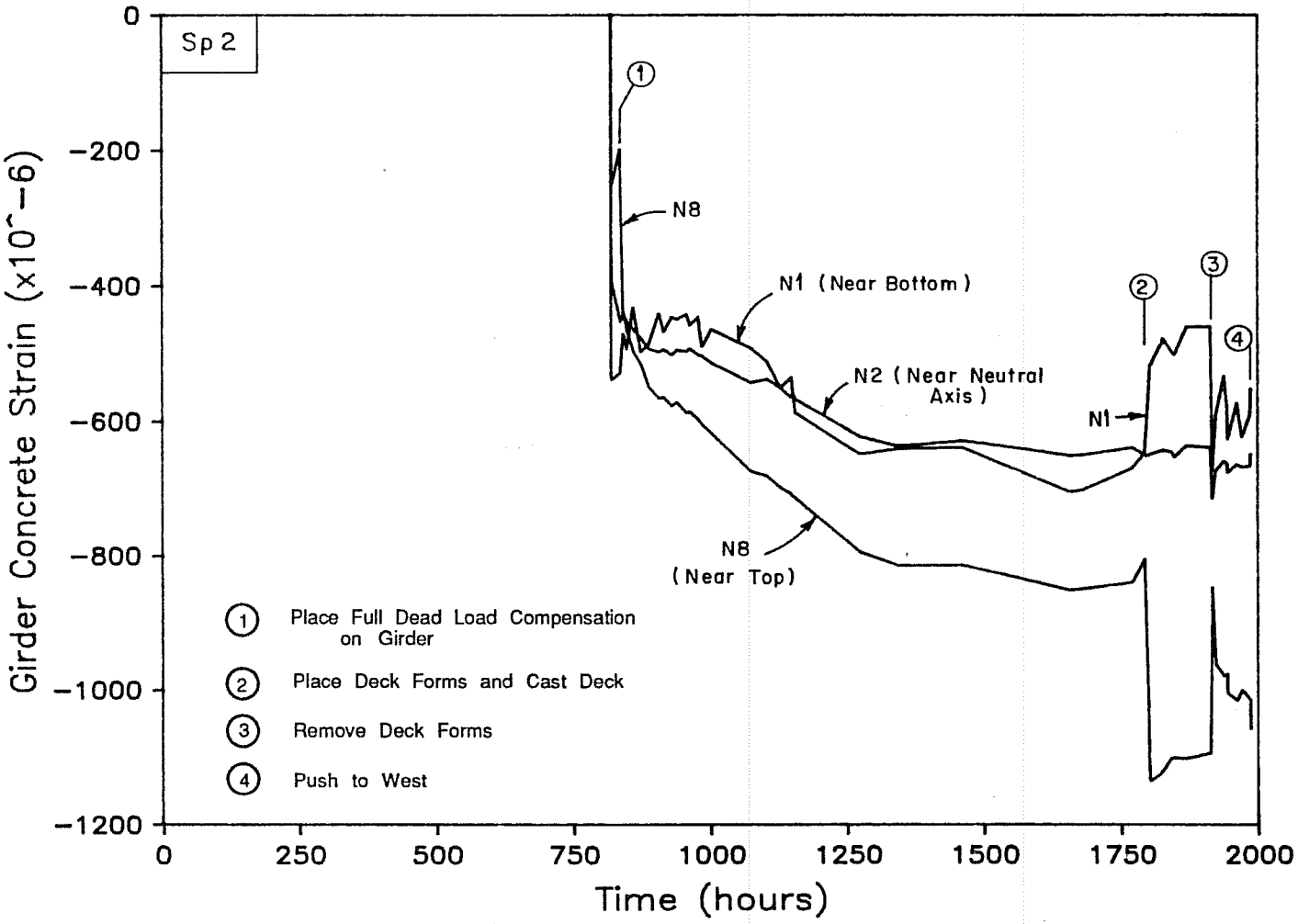

Fig. 4.39 Girder strains with time for typical gages

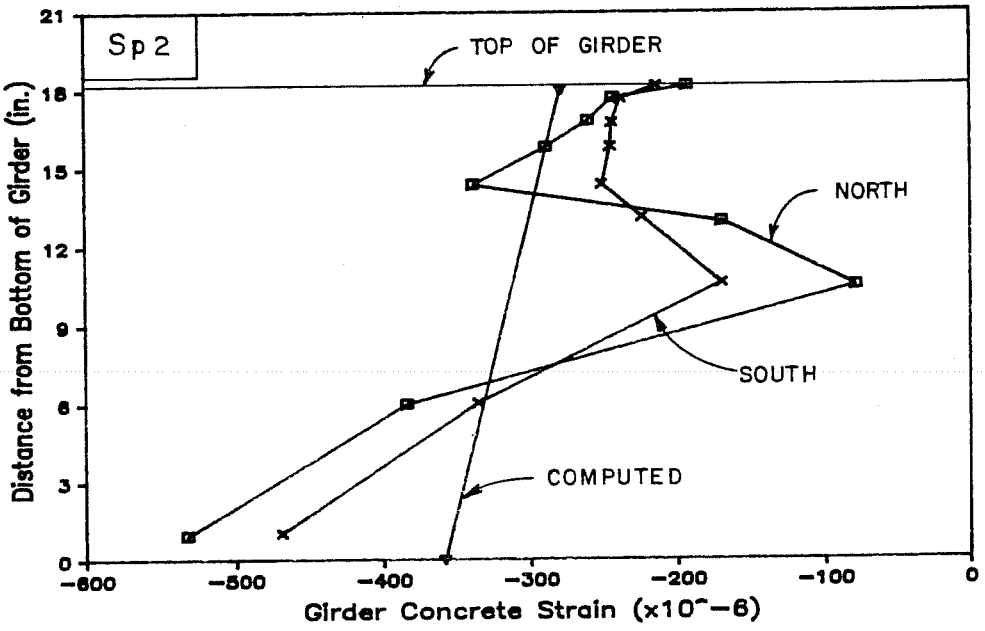

(a)

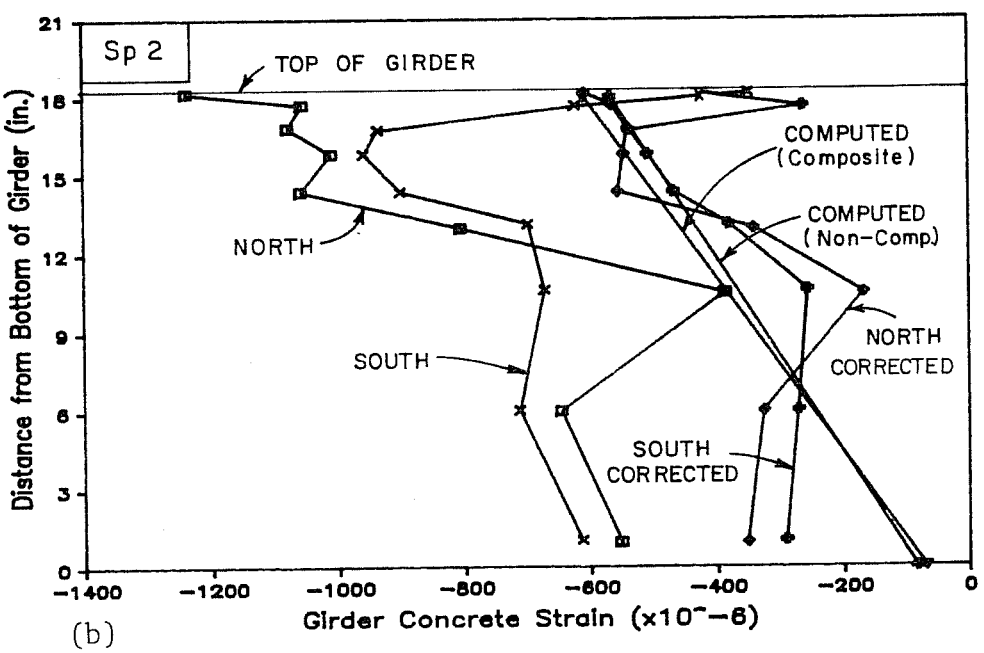

(b)

Fig. 4.40 Computed and mesured girder concrete strains at release and prior to flexure test: a) at release; b) prior to ultimate flexure test

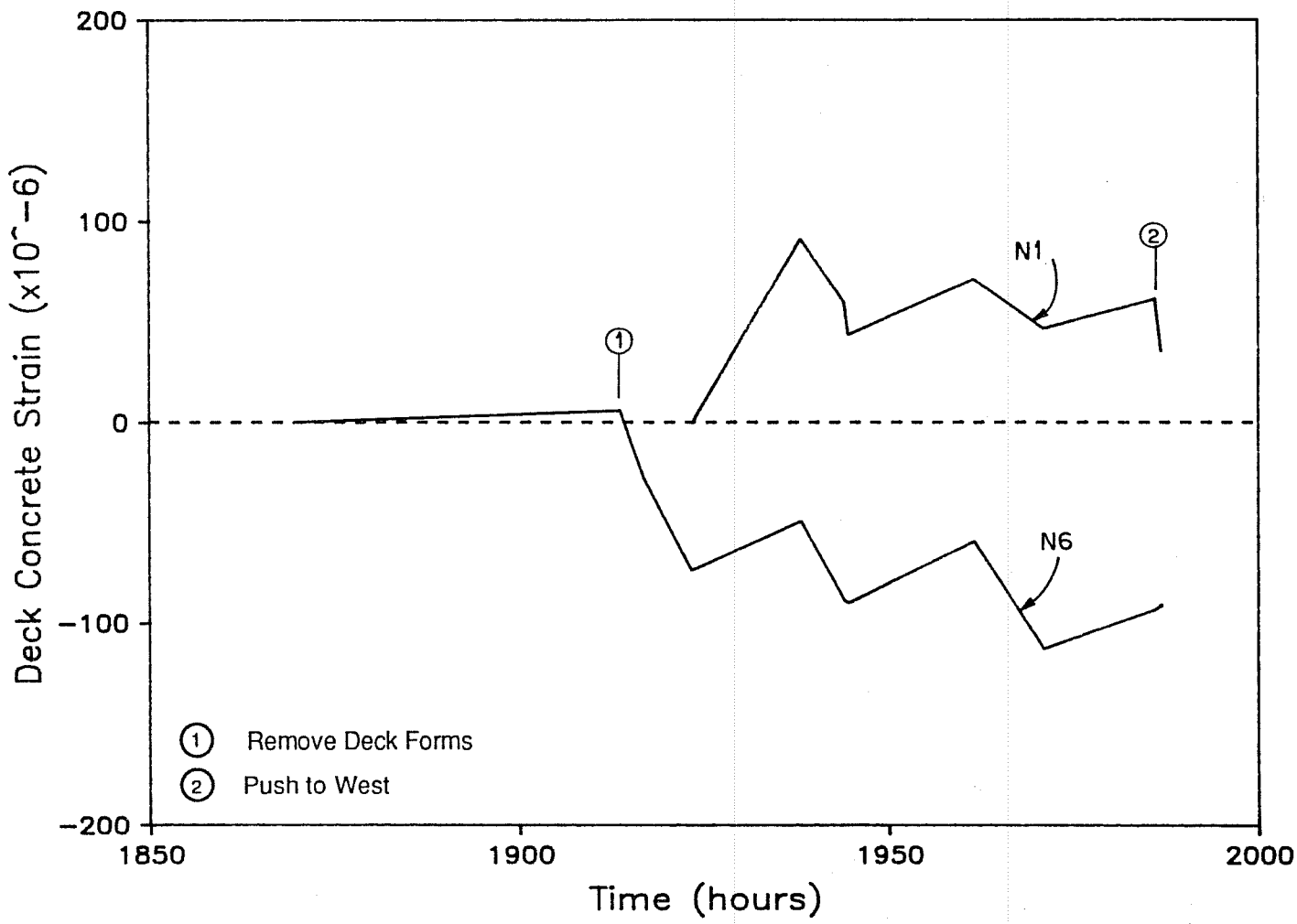

Fig. 4.41 Deck concrete strains with time for typical gages

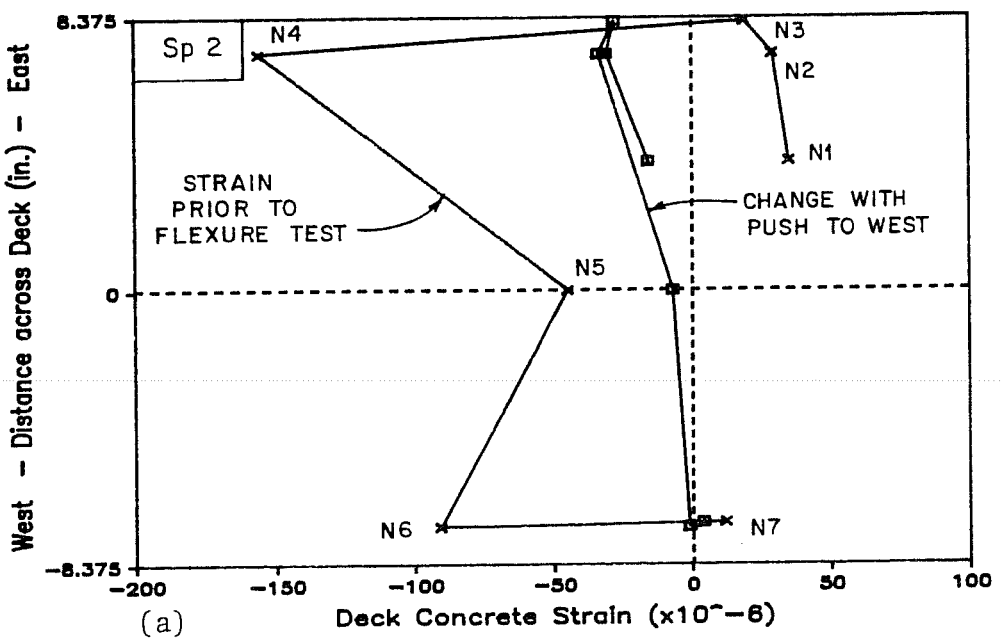

See Fig. 5.19
for Gage Locations

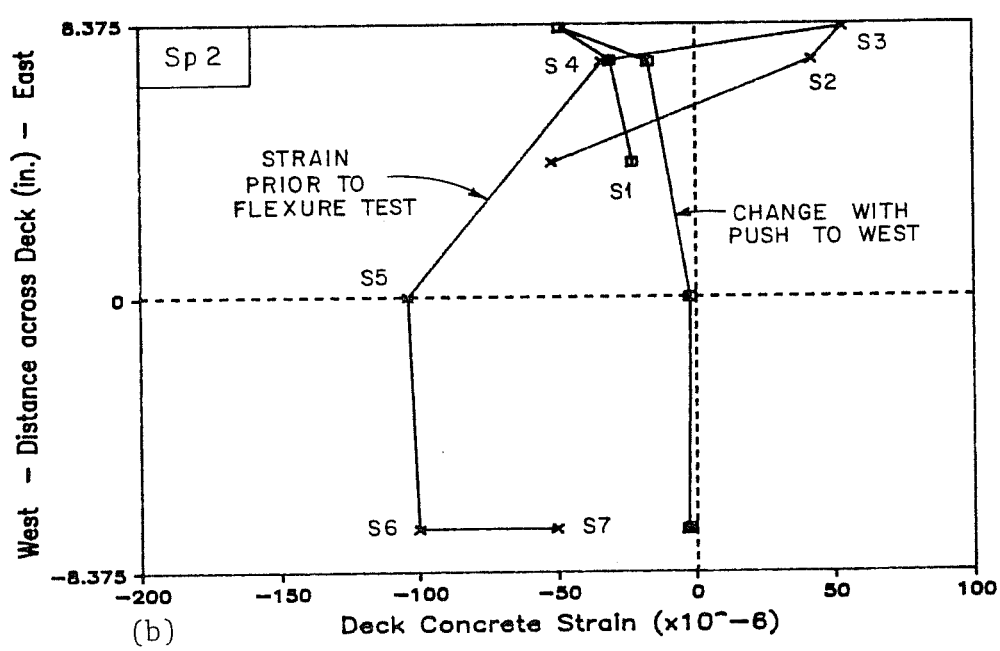

Fig. 4.42 Deck concrete strains at selected times: a) north gages; b) south gages

because cracks had to be closed before the west side could pick up additional strain.

Creep strains in the deck prior to the flexure test were about 100 microstrains at the top and negligible at the bottom. Creep was still increasing slowly at the time of the flexure test.

Stirrup strains for one stirrup at each end of the girder are shown in Fig. 4.43. The large displacement in strains shortly after placement of girder concrete appears to be caused by shrinkage in the concrete. From this data, shrinkage strains of approximately 250 microstrains occurred within a day after casting with an additional 50 microstrains occurring prior to release. Using the girder concrete modulus at release, the total shrinkage strain would correspond to a stress of 1.6 ksi which is nearly twice the measured modulus of rupture at release (see Table 4.7). This high shrinkage strain with the restraint provided by forms and unreleased strands caused the cracking. After release, strains remained fairly constant until the flexure test, except for a change when the deck was cast that was probably caused by disturbing the leads during placement of the concrete.

4.3.2 Flexure Test.

4.3.2.1 General Description of Behavior. Because of the widespread shrinkage cracks only an ultimate flexure test was conducted on Specimen 2. Load stages used during the flexure test and times at which they occurred are given in Appendix B. Frequency of readings and designation of load stages are the same as Specimen 1 except loads used during the test required no correction.

Flexure cracks were first detected in the constant moment region at 4 kips. Some cracks were directly below shrinkage cracks, but others were independent of prior cracking. Cracks extended into the web at 6 kips. At 7.5 kips load the deflection was held by the lower cross heads, rams were retracted and upper cross heads were reset. Web shear cracks about 3 in. long formed near the ends of the girder as inclined extensions of shrinkage cracks at 8 kips. Flexure cracks reached the top of the web at 8.5 kips and entered the taper of the top flange at 9.25 kips. At this load, crack widths near midspan were approximately 0.02 in. and cross heads were reset.

At the next load stage, 9.44 kips, cracks progressed through the taper and into the top flange. The deflection was maintained at this load stage while a leaking hose was replaced. Load was then brought back to 9.44 kips. At 9.67 kips cross heads were reset. Cracking in the constant moment region and the large deflection of the specimen at this load are shown in Fig. 4.44. Cracks extended nearly an inch into the top flange at this load as shown in Fig. 4.45, which was taken after failure. While attempting to bring the load back to

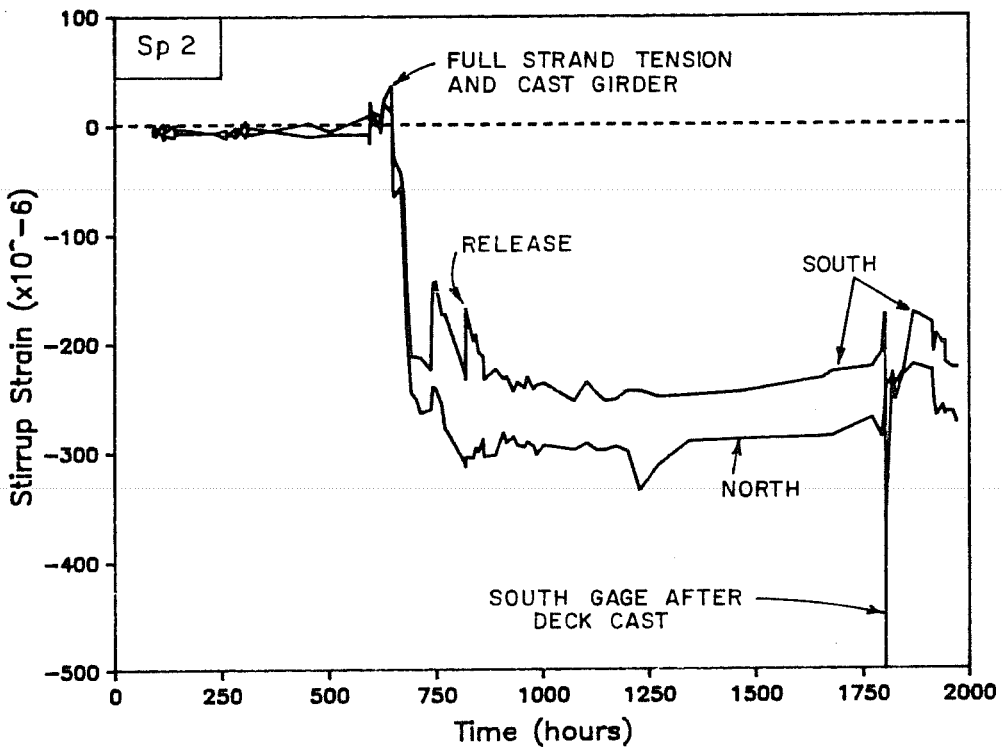

Fig. 4.43 Stirrup strains with time

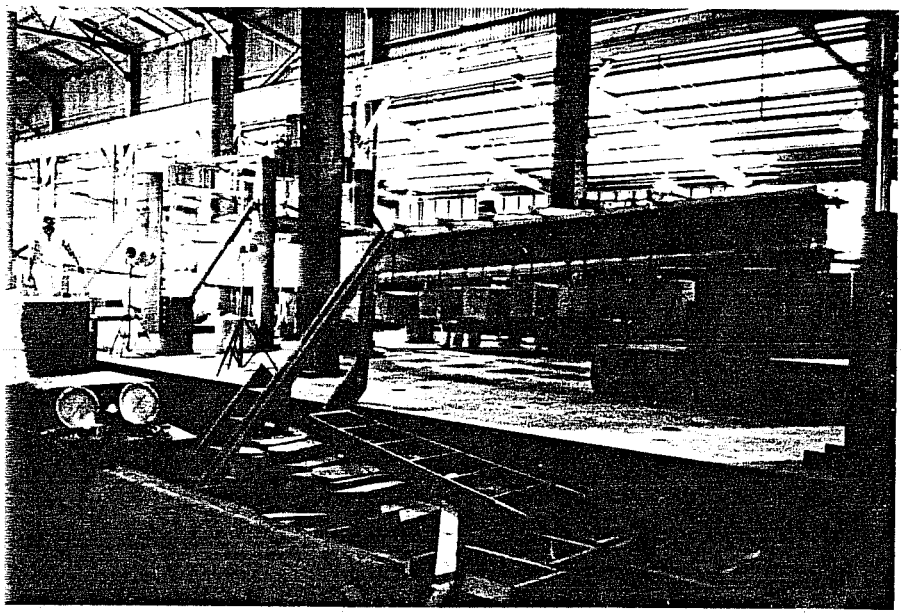

(a)

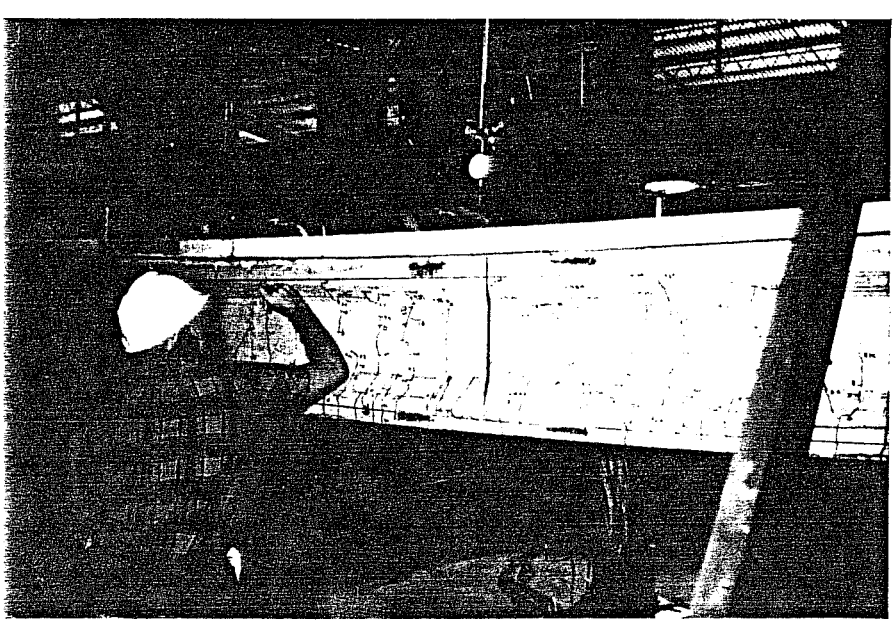

(b)

Fig. 4.44 Photographs prior to flexural failure (9.67 kips)- Specimen 2: a) entire specimen; b) midspan

Fig. 4.45 Photograph of extent of cracking of top flange prior to flexural failure - Specimen 2

9.67 kips, failure occurred at a load of 9.59 kips. The specimen failed explosively in compression midway between the north load point and midspan. There was no warning of collapse other than the large deflection and many cracks.

Failure was violent and very similar to the failure observed for Specimen 1 (Fig. 4.46). Dead load blocks were again stripped from their hangers. Secondary failure cracks formed at the junction of the web and bottom flange and branched upward into the web. The ends of the girder were again thrown up into the air and drawn inward, causing the bearing pads to roll off the supports. The failure surface was typical of a compression failure. The surface was an inclined plane originating near the top of the girder and continuing through the deck (Fig. 4.47a). Viewed from above, the failure surface was wedge-shaped as shown in Fig. 4.47b. The appearance of the failure surface did not provide conclusive evidence for determining whether the girder or deck concrete crushed first.

At failure, spacing of flexure cracks crossing the bottom flange averaged 2.7 in. in the constant moment region. The flexure cracks nearest the supports were located 13 ft from the ends of girder and were extensions of shrinkage cracks.

Significant events during the test and design loads are summarized in Table 4.8. Loads were determined as described for Specimen 1 (Table 4.4). Test results are compared with computed and design loads later in this chapter and in the next chapter.

4.3.2.2 Deflections. Net deflection at midspan, adjusted for bearing pad compression, is shown in Fig. 4.48. Loads from Table 4.8 are indicated on the figure. Observed cracking coincided well with the onset of nonlinear behavior. The specimen exhibited a limited yield plateau and large deflections before reaching the ultimate load, which demonstrates a significant capacity for energy absorption and also indicates that such a structure in service would provide ample warning of impending collapse. While post-ultimate capacity is shown, this is illusory since the choice of load stages and the necessity of resetting the load system made this possible. If load had been applied continuously, no post-ultimate behavior would be expected, as was observed with the first specimen.

Locking the deflection to reset the loading system clearly affected the behavior of the specimen, as the presence of offsets in the load-deflection curve indicate. This phenomena was discussed during the consideration of Specimen 1 data.

4.3.2.3 Strand and Concrete Strains. Corrected strand strains for instrumented strands are shown in Fig. 4.49 with the average strain which represents the strain at the centroid of the strands. Strains for the top draped strand were estimated using bottom strand

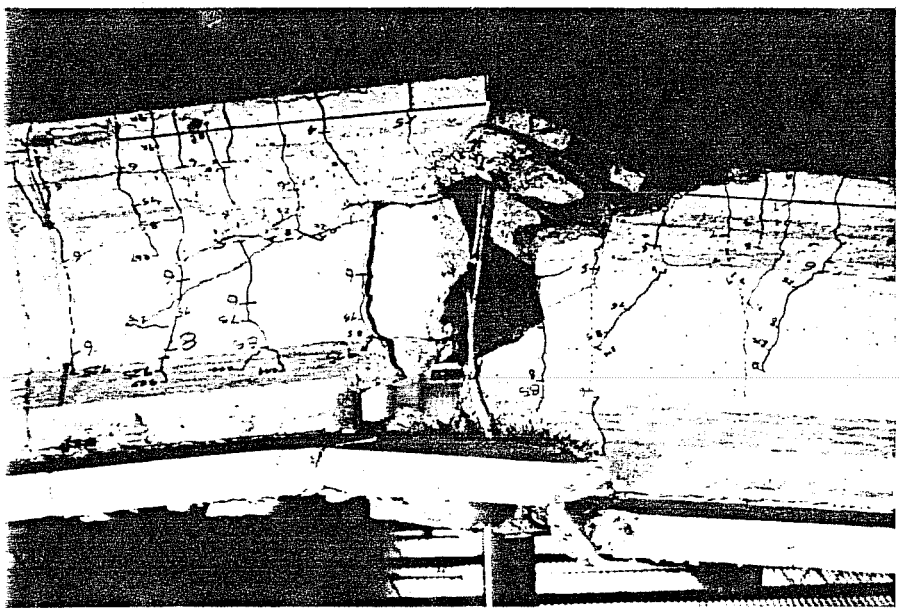

(a)

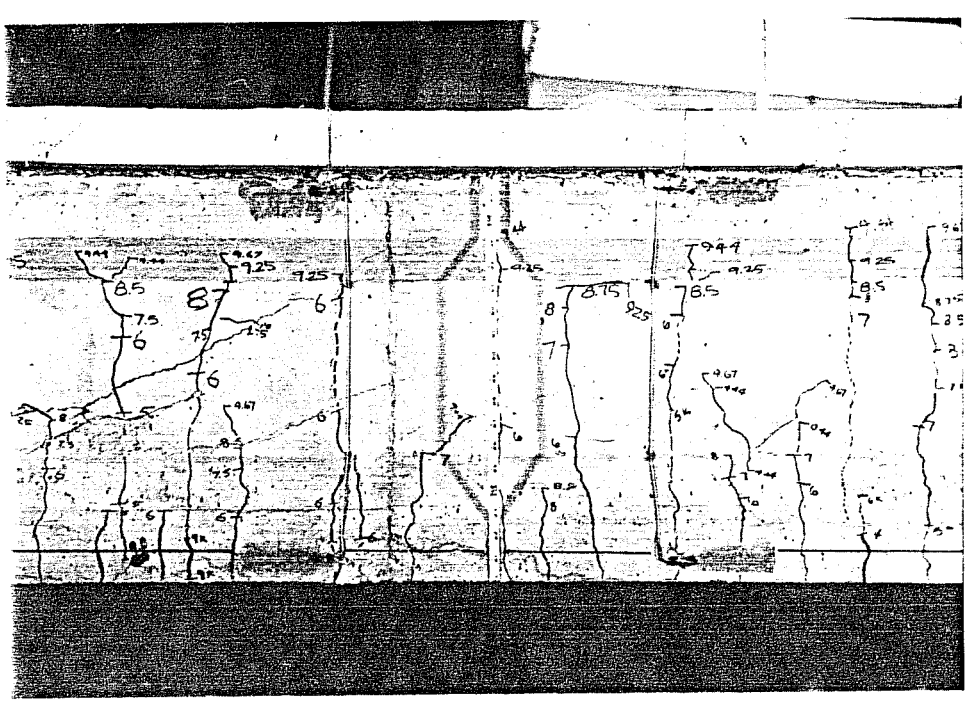

(b)

Fig. 4.46 Photographs after flexural failure - Specimen 2: a) at failure; b) at midspan

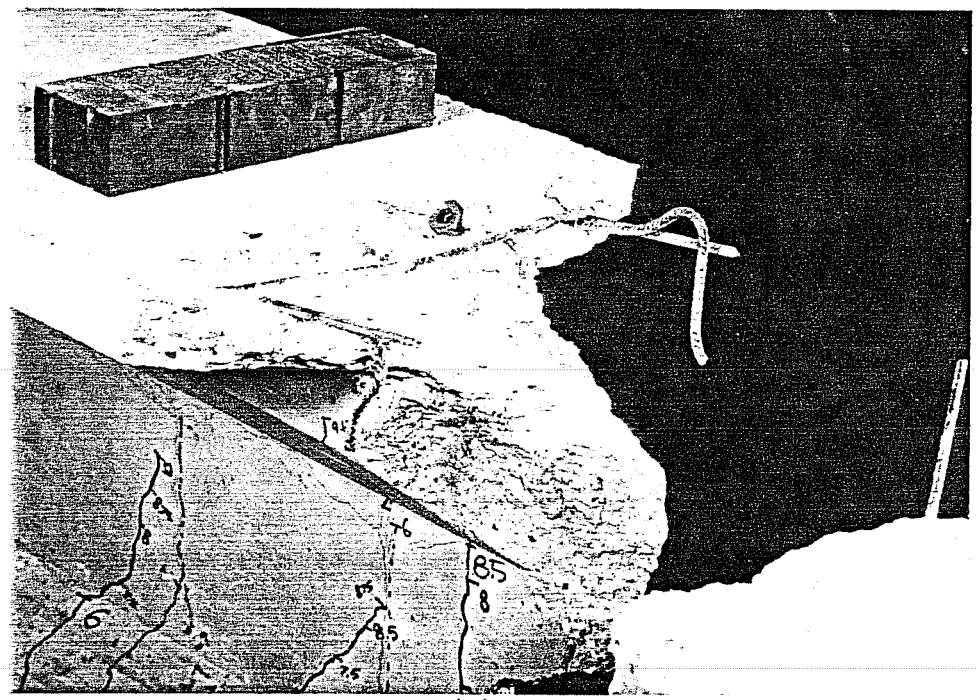

(a)

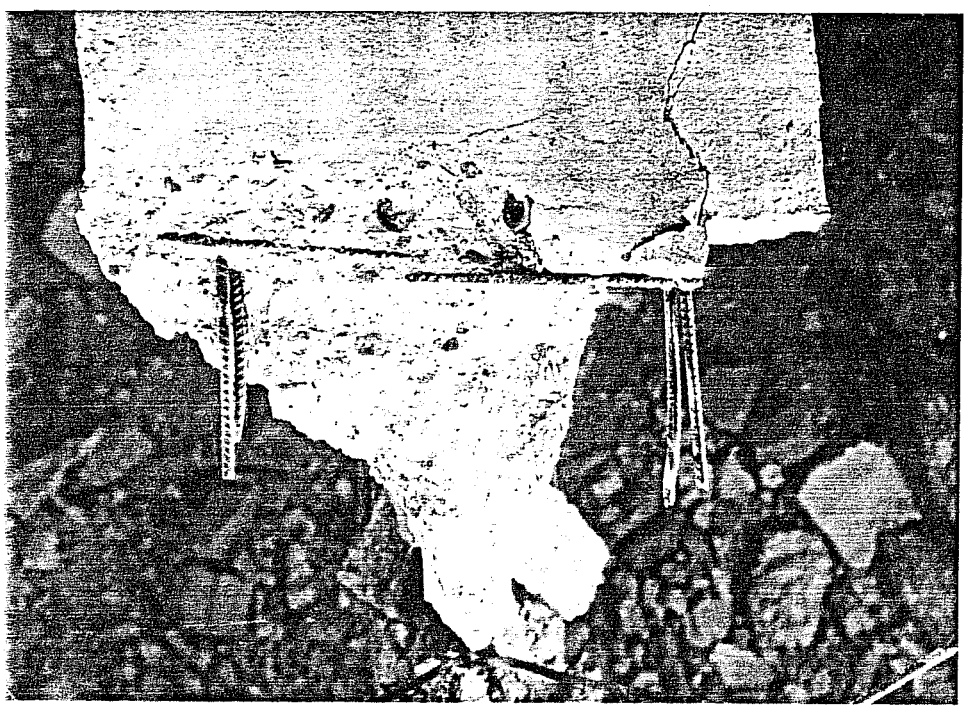

b)

Fig. 4.47 Photographs of concrete failure surface - Specimen 2: a) side view; b) top view

Table 4.8 Load Stages and interest during flexure test - Specimen 2

Key (Fig. 6.65)	Description of Load Stage	Load (kips)
Computed and Observed Behavior		
CD	Computed Decompression ($0\sqrt{f_c'}$)	0.86
CC	Computed Cracking ($7.5\sqrt{f_c'}$)	2.56
C	Observed Cracking ($10.4\sqrt{f_c'}$)	4.00
R	Reset Loading System	7.50
R	Reset Loading System	9.25
L	Lock off Loading System	9.44
U	Ultimate (Maximum) Loading	9.67
F	Failure Load	9.59
CW	Computed Web Cracking at h/2	15.86
Design Loads		
LL	Live Load	1.87
LI	Live Load + Impact * ($6\sqrt{f_c'}$)	2.22
FL	Factored Load (AASHTO)	6.34
NC	Computed Nominal Capacity ($\phi = 1$)	8.56
Total Reaction at Ultimate Load		17.67

* - Impact factor computed using prototype span of 146 ft.

For Notes, See Table 6.4

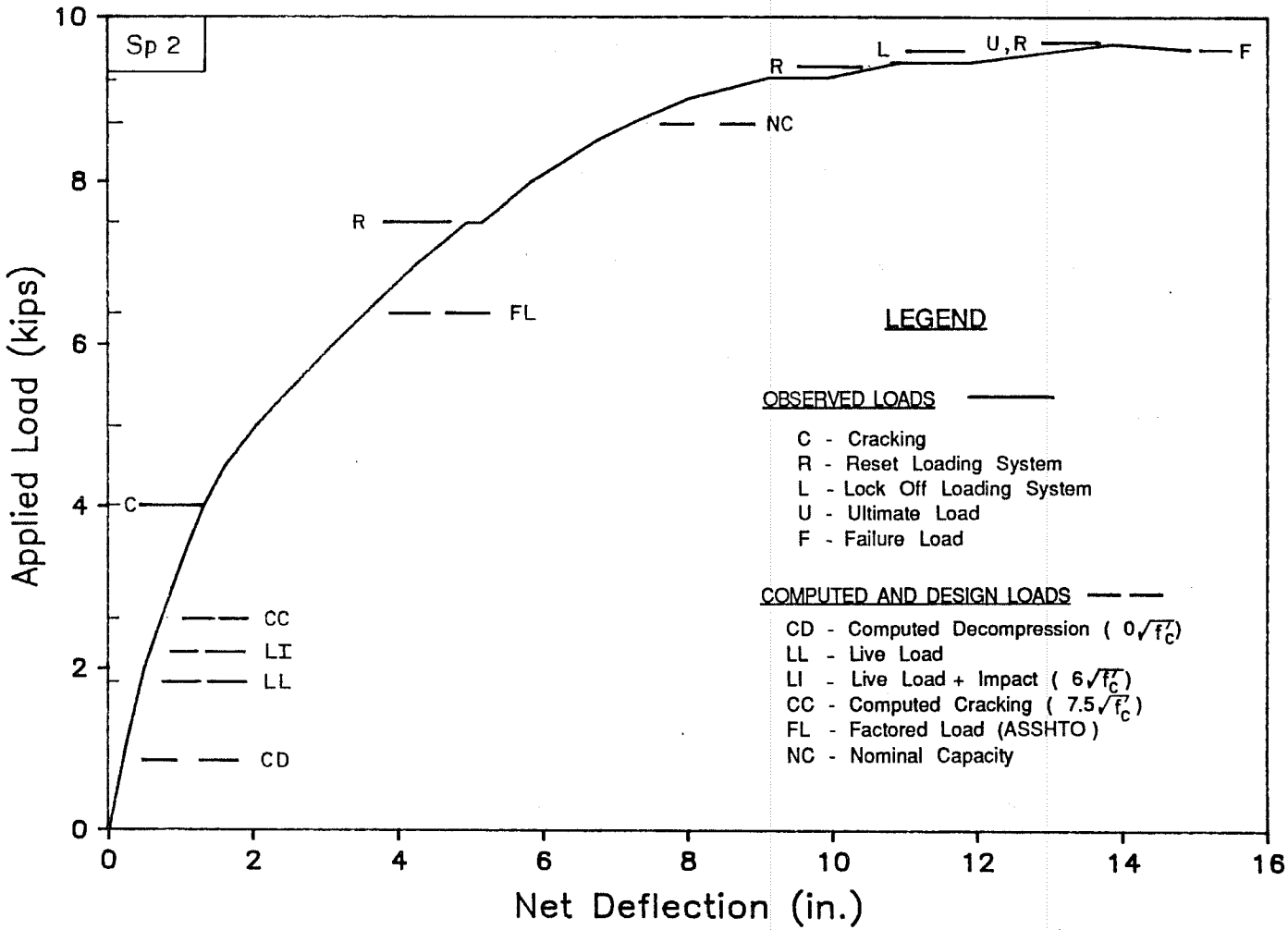

Fig. 4.48 Deflection at midspan during flexure test

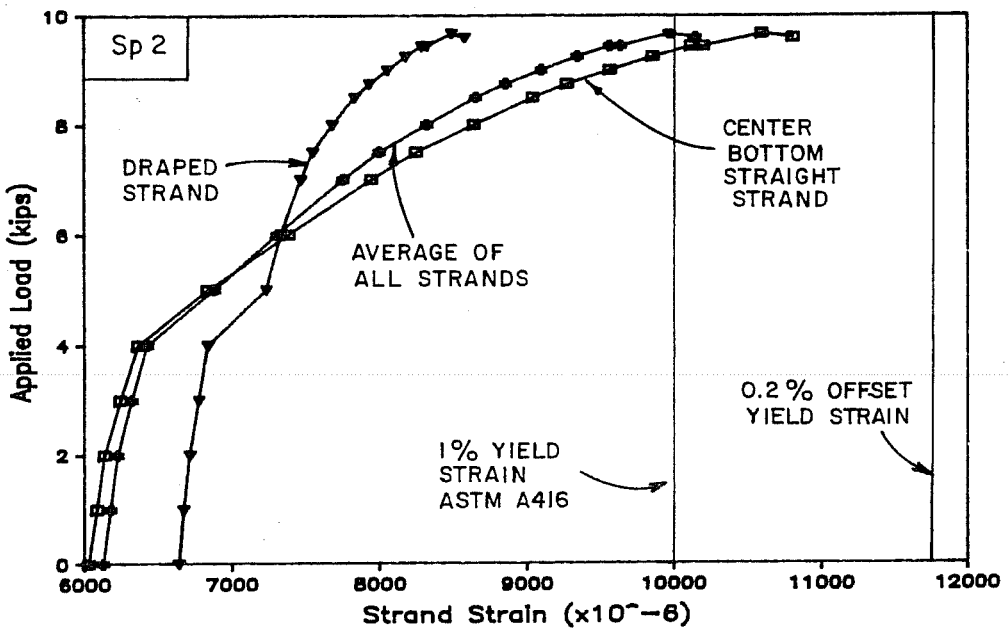

Fig. 4.49 Corrected and average strand strains during flexure test

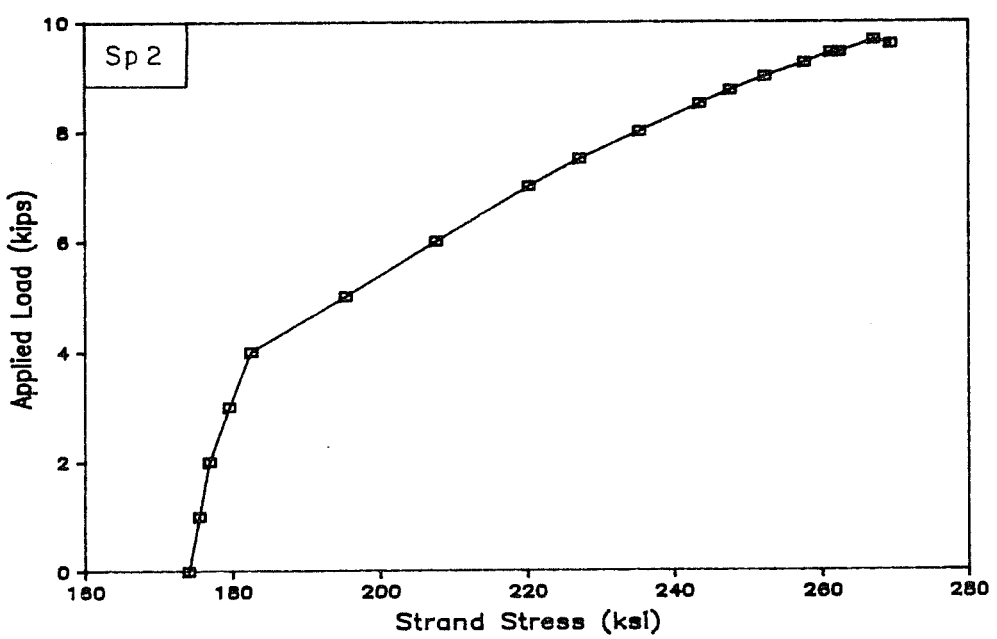

Fig. 4.50 Average strand stress during flexure test

data for loads above 8.75 kips. Strains at failure were estimated using load-deflection data. Average strand stresses during the test are shown in Fig. 4.50.

Strains at ultimate and failure differed very little. At failure, the average strand strain reached 1 percent, which is the strain used to define yield in ASTM A416 [25]. However, both the bottom strand and the average strand strains failed to reach a strain corresponding to the 0.2 percent offset.

Corrected girder concrete strains are shown in Fig. 4.51. Strains at failure are estimated using load-deflection data. Strains for the upper gages are presented with respect to gage location on the girder for selected loads in Fig. 4.52. The gages behaved well during the test as shown by the net strain plots in Fig. 4.53 and 4.54, which correspond to plots of corrected strains in Fig. 4.51 and 4.52. Strains from both sides of the girder near the top and bottom (Fig. 4.55) indicated that the girder was not moving laterally during the flexure test.

At ultimate load, strain at the top of the girder was less than 1100 microstrains and perhaps as low as 700 microstrains. At failure, data were available from only one gage and this indicated a decrease in strain of less than 30 microstrains from ultimate. These values are about half the strain measured at maximum stress and failure for cylinder tests of this concrete. Top of girder strains at the north location are consistent with nearby gages as demonstrated by comparing these strains with strains computed for the top of the girder using net strains from two lower gages as shown in Fig. 4.56. The top of girder gage at the south line was not functioning properly. Therefore, the top of girder strain at ultimate can be taken as 1100 microstrains based on north gage data and the computed change in strain at the south location.

The crack height computed using corrected girder strains is shown in Fig. 4.57. At failure, the computed crack height was approximately 16 in. which is 2 in. below the top of the girder and agrees well with visual observations.

Corrected deck concrete strains are shown for typical top and bottom gages in Fig. 4.58. Data for all deck strain gages are presented in Fig. 4.59 with respect to gage location for selected loads. The uniform increase in strain across the section indicated that behavior was symmetrical. The east gage at the north line on the top of the deck appears to be faulty since no reason was arrived at to explain the high strains. Both bottom gages on the west side of the deck also displayed unexplainable behavior by lagging behind the corresponding gages on the east side.

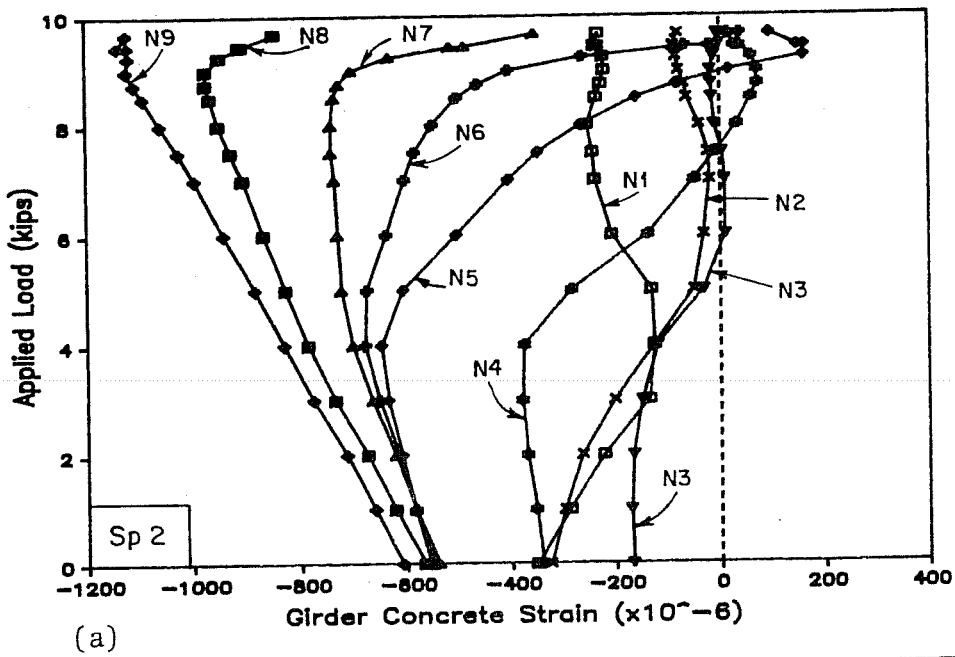

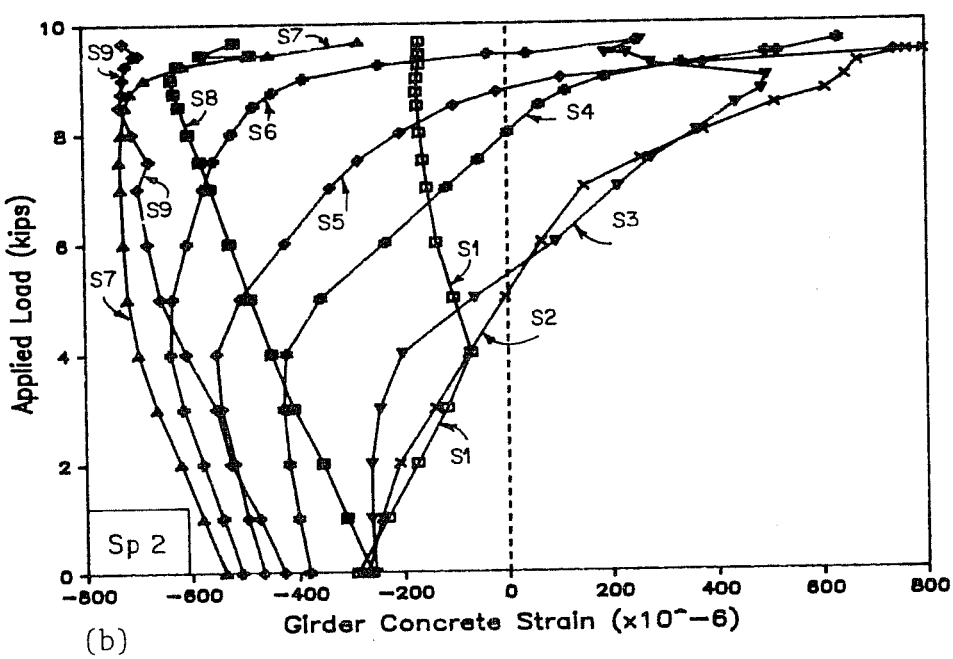

Fig. 4.51 Corrected girder concrete strains during flexure test: a) north gages; b) south gages

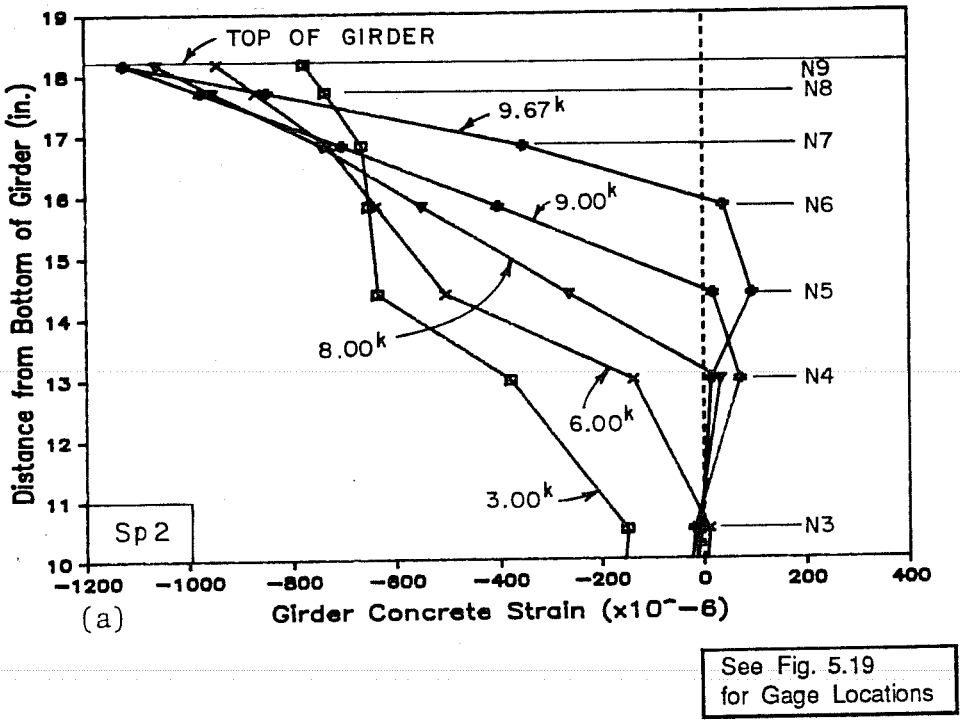

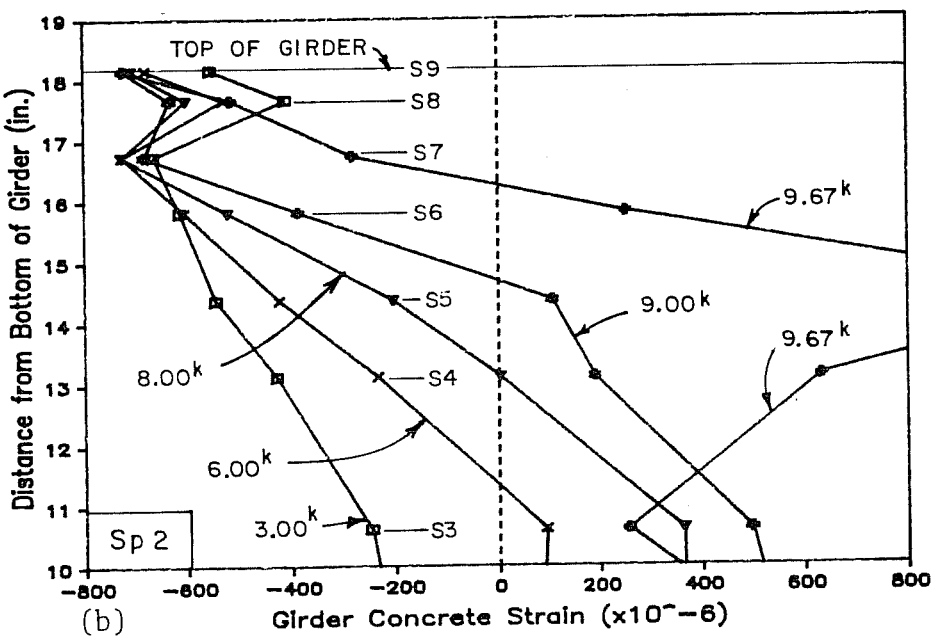

Fig. 4.52 Corrected girder concrete strains at selected loads during flexure test: a) north gages; b) south gages

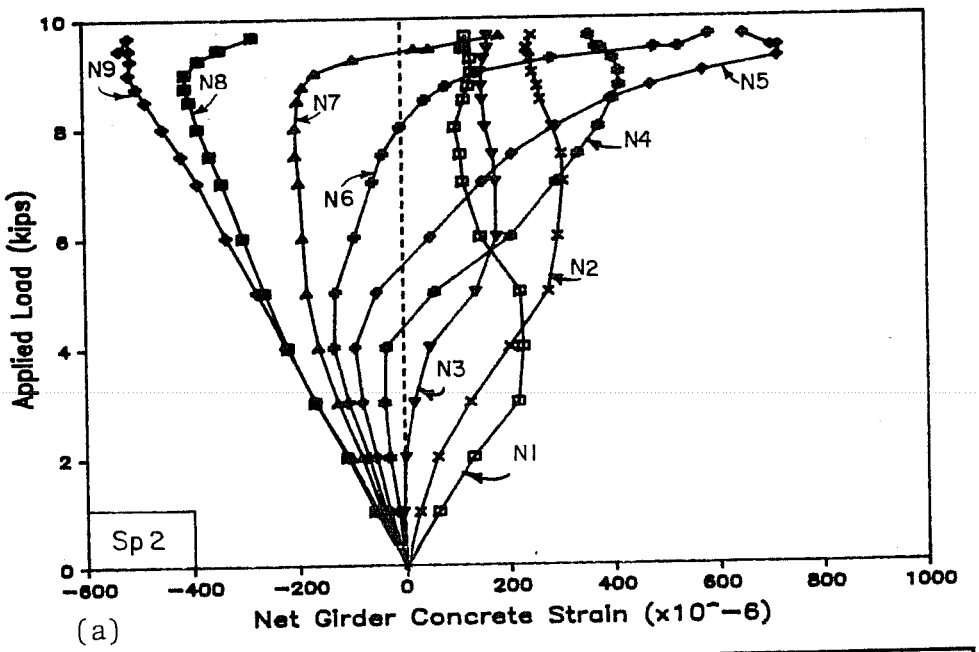

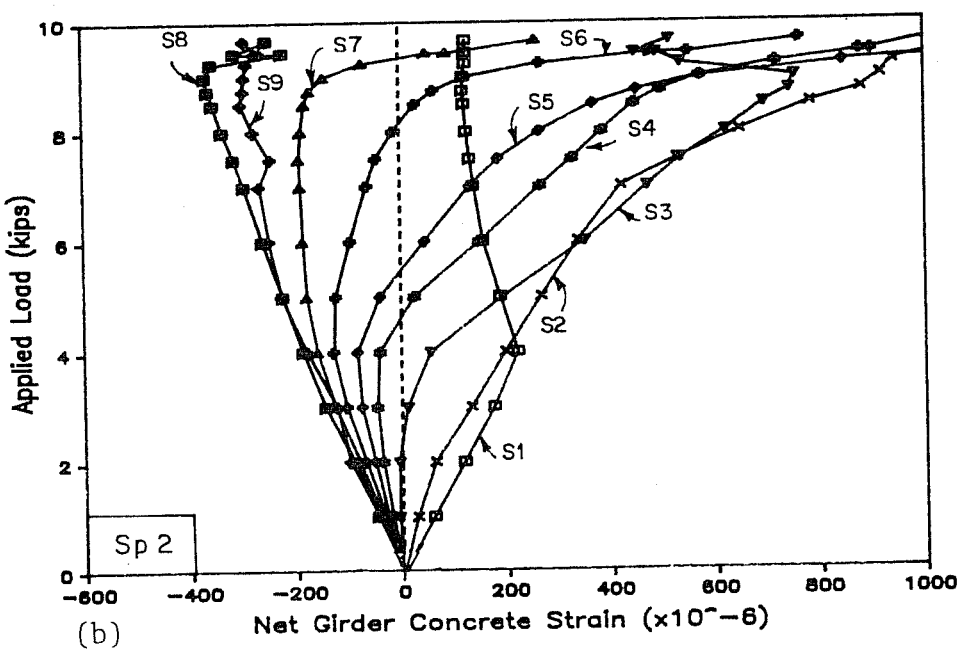

Fig. 4.53 Net girder concrete strains during flexure test: a) north gages; b) south gages

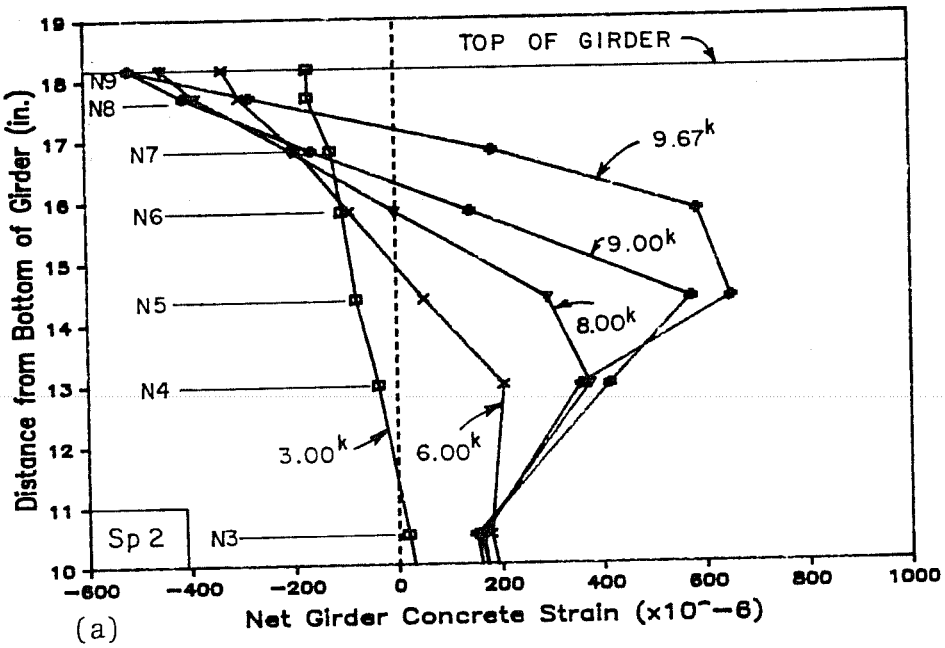

See Fig. 5.19 for Gage Locations

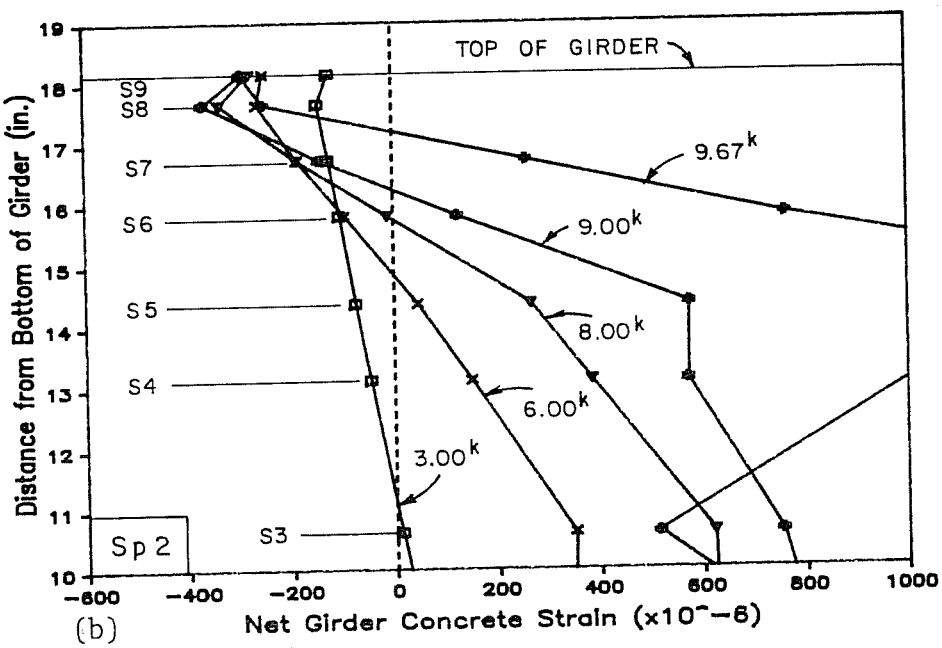

Fig. 4.54 Net girder concrete strains at selected loads during flexure test: a) north gages; b) south gages

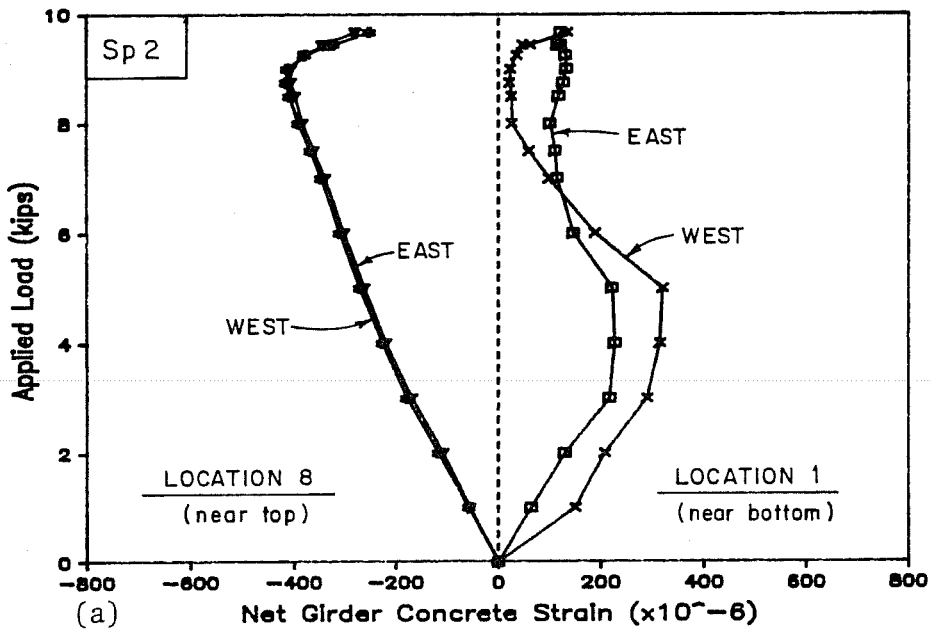

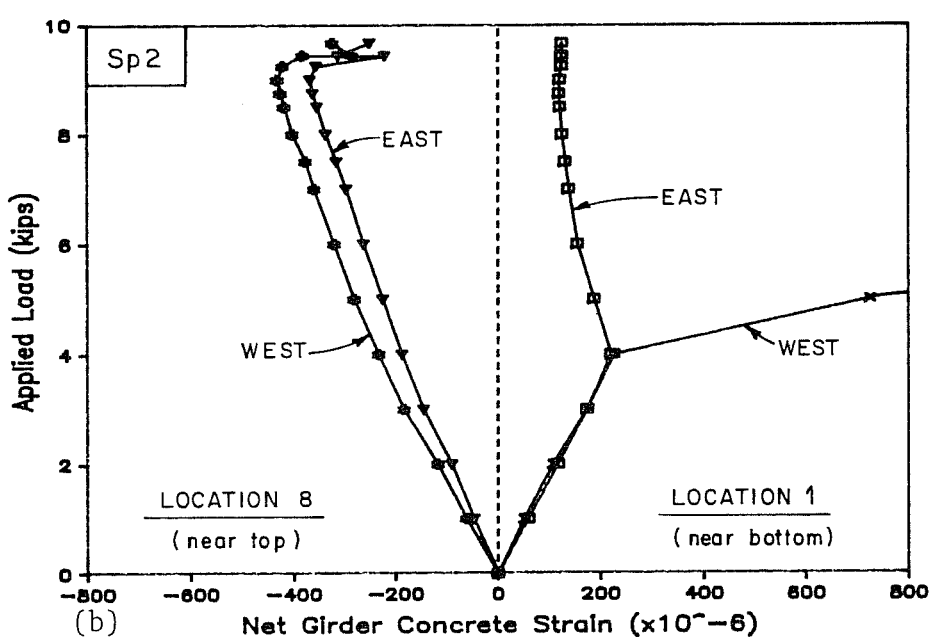

Fig 4.55 Net concrete strains on opposite sides of girder during flexure test: a) north gages; b) south gages

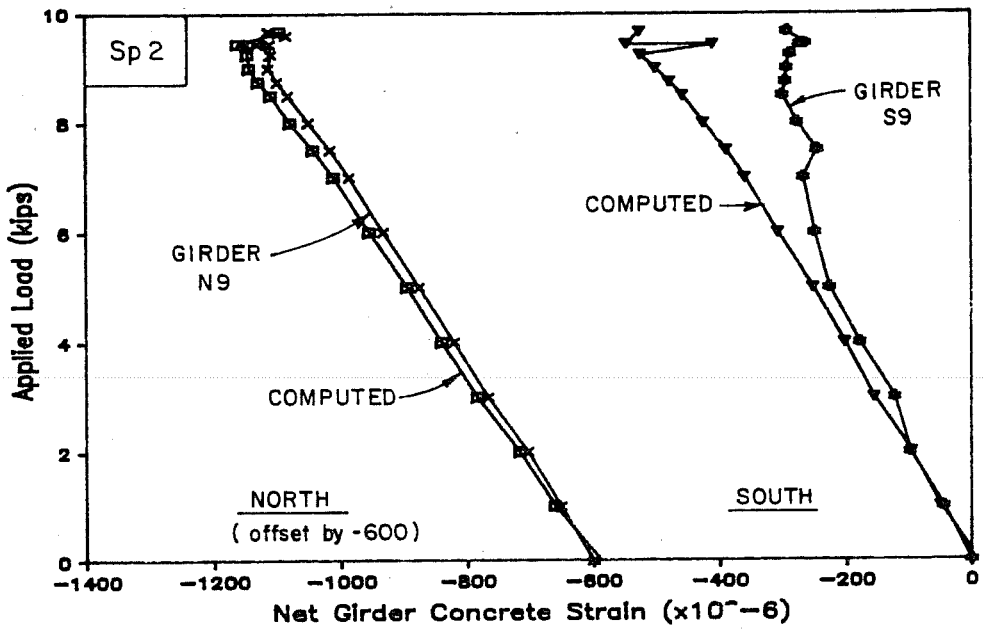

Fig. 4.56 Measured and computed top of girder concrete strains

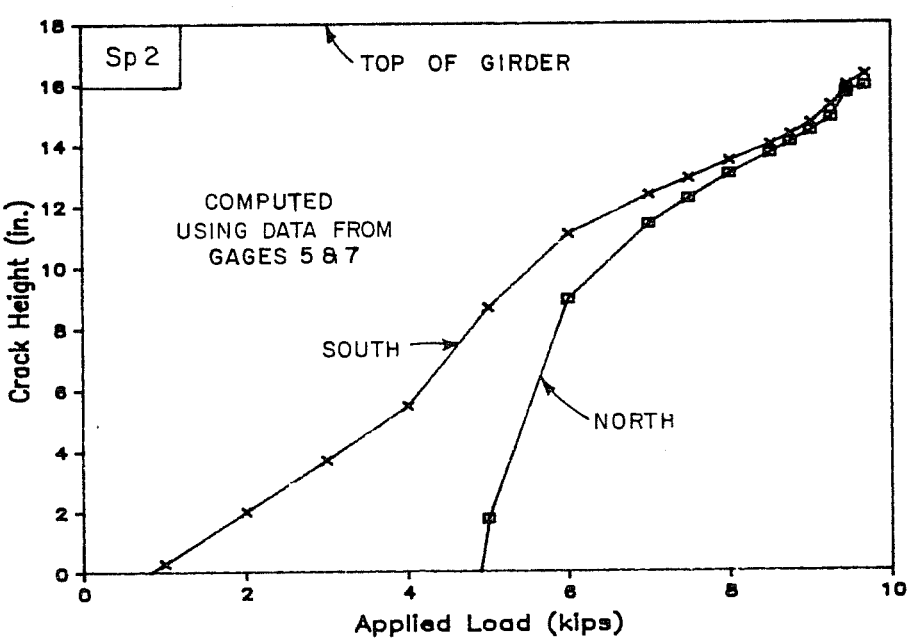

Fig. 4.57 Computed crack height

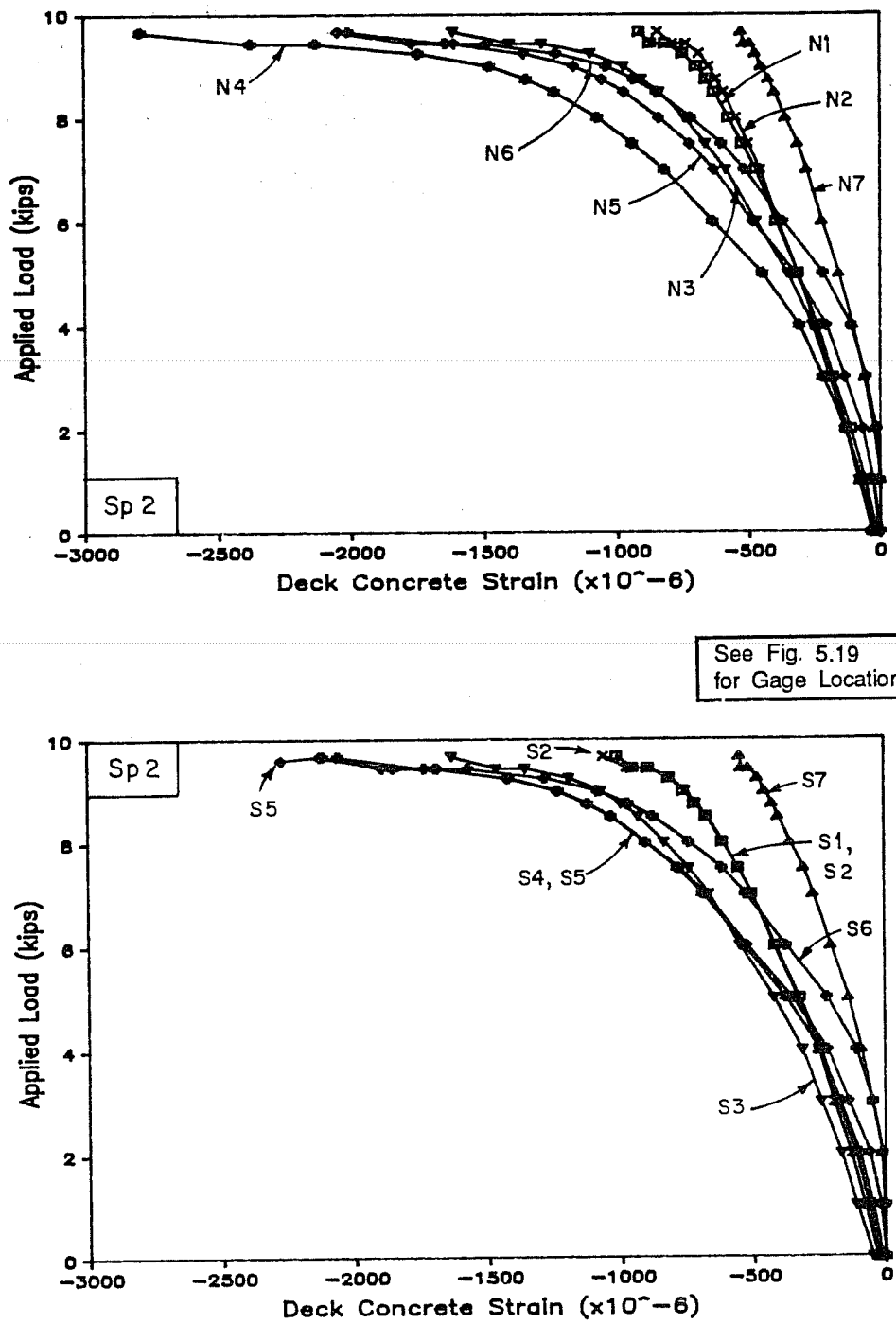

Fig. 4.58 Corrected deck concrete strains during flexure test: a) north gages; b) south gages

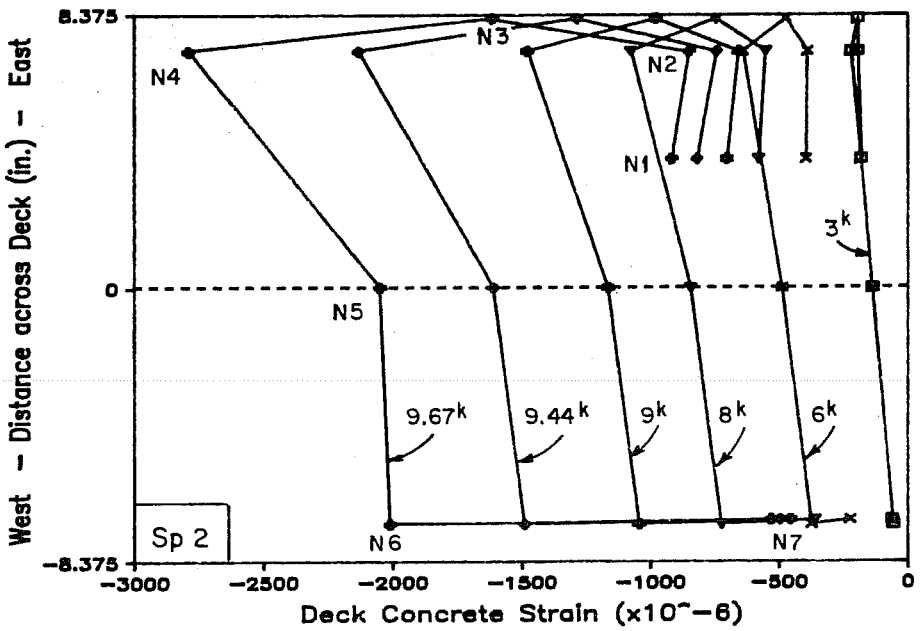

See Fig. 5.19
for Gage Locations

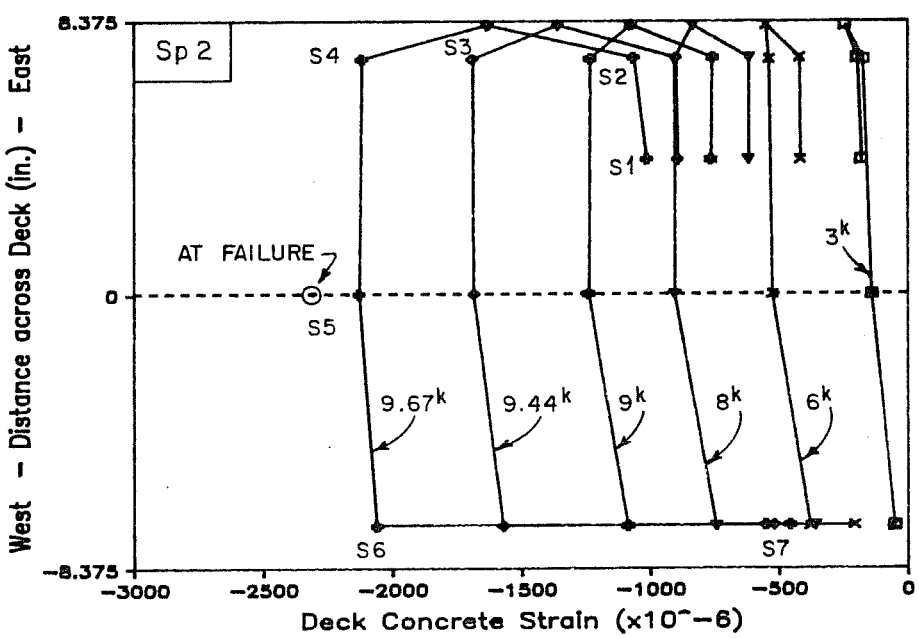

Fig. 4.59 Corrected deck concrete strains at selected loads during flexure test: a) north gages; b) south gages

Strain at the top of the deck was 2100 microstrains at the maximum load and 2280 microstrains at failure. The strain at failure was based on a reading from a single gage. The strains at the maximum and failure loads are above the strain at maximum stress measured in cylinder tests but below the maximum strain recorded in the cylinder tests.

Net strains at the top of girder and bottom of deck at selected loads are shown with respect to their location across the deck in Fig. 4.60. However, the combined plots of girder strains and the strain at the center of the top of the deck during the flexure test, which are shown in Fig. 4.61, reveal that the strain profile measured over the full depth of the specimen was nearly linear for the south set of data. This indicates that the reason for nearly constant strain at the top of the girder was due to the rising neutral axis and that full composite action was present up to failure. A reason for the strains at the bottom of the deck being significantly greater than those at the top of girder, which was especially evident at later load stages, was not identified.

The girder and deck strain data presented above do not clearly indicate which concrete initiated crushing, since neither concrete appeared to be near the limiting strains obtained during cylinder tests. The high strain gradient across the deck and girder at failure and the fact that sections were unconfined and thin in some dimensions may have affected member behavior. The fact that a high level of load was maintained on the specimen for a relatively long period of time may also have affected the behavior and capacity of the member.

Curvature of the section was computed using a pair of girder gages and pairs of deck gages. The average of all bottom gages was used with the top center gage because no deck gage was available directly below it. The resulting net curvatures are presented with increasing load in Fig. 4.62, and total curvatures are shown versus total moment in Fig. 4.63. Total curvatures were computed by adding net curvatures to a computed curvature at the beginning of the flexure test. Deck curvature changes very little during initial load stages while girder curvature steadily increases. This behavior probably reflects the closing of deck cracks during the early load stages. Because the plot of girder curvature shows steady change, it is the most representative of overall specimen behavior.

Measured strand strains are compared with strains computed using girder curvature data in Fig. 4.64. These plots show that the measured strand strains are consistent with the overall behavior of the specimen for the ranges of load in which gages were functioning. The top north gage does not appear to function properly at any time during the test. Both the top south and bottom north gages appear to have failed at a load near 8 kips. In addition, the bottom south gage

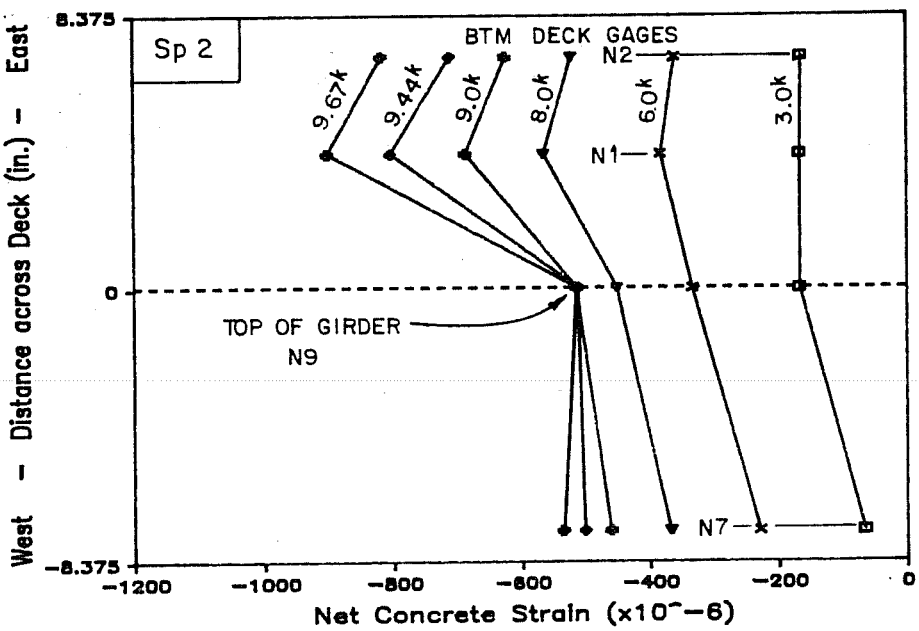

See Fig. 5.19
for Gage Locations

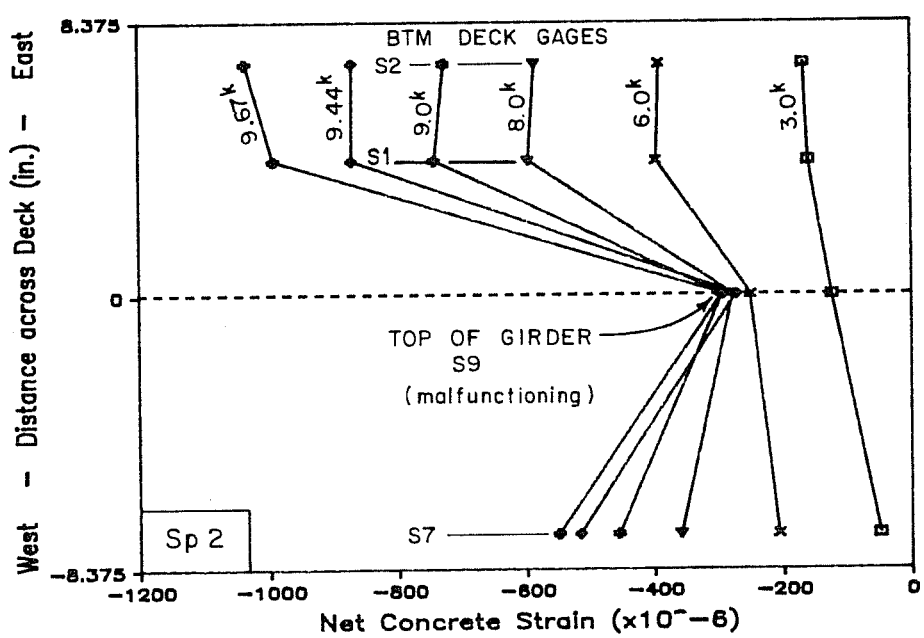

Fig. 4.60 Net concrete strains at top of girder and bottom of deck during flexure test: a) north gages; b) south gages

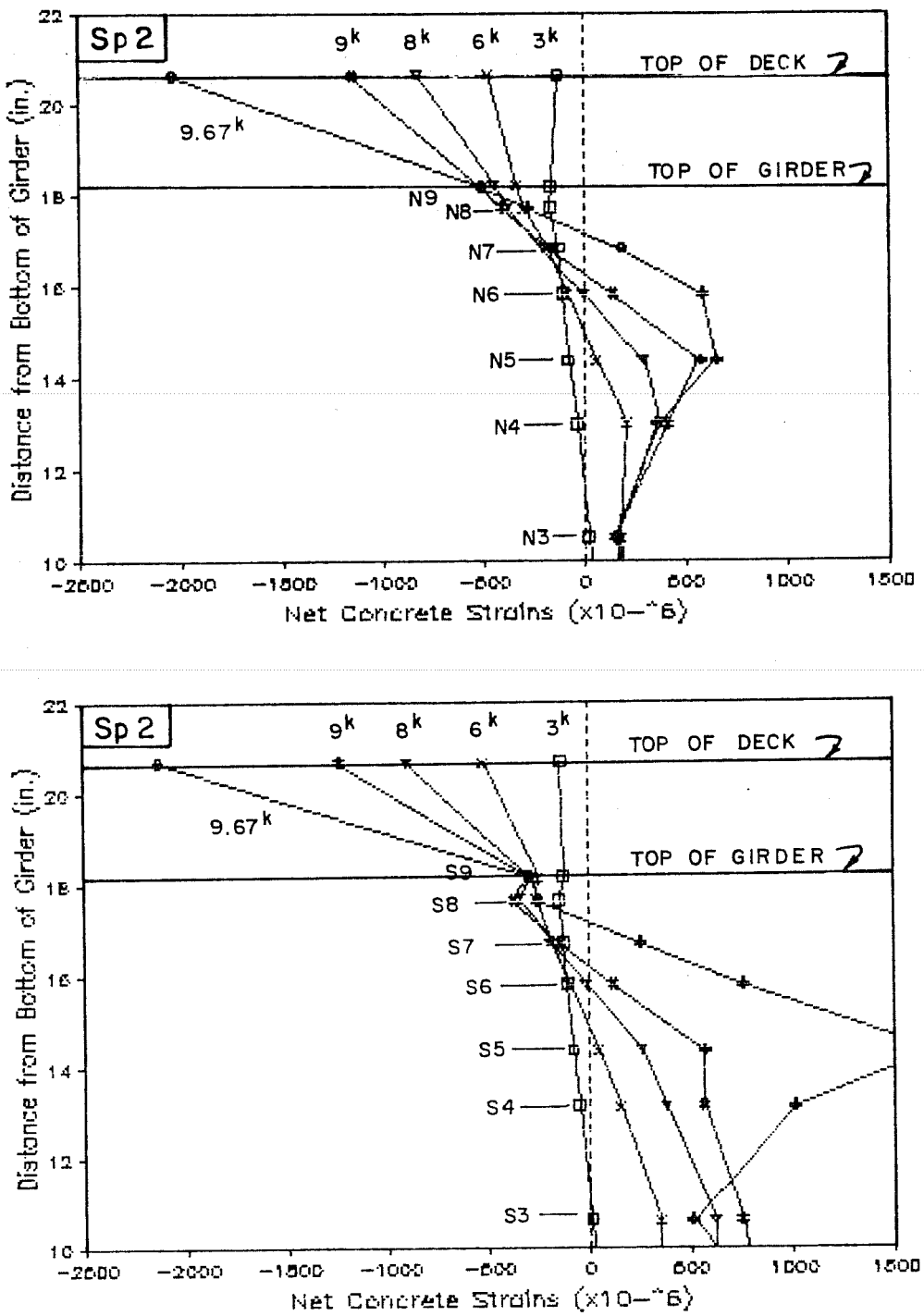

Fig. 4.61 Net girder and deck concrete strains at selected loads during flexure test: a) north gages; b) south gages

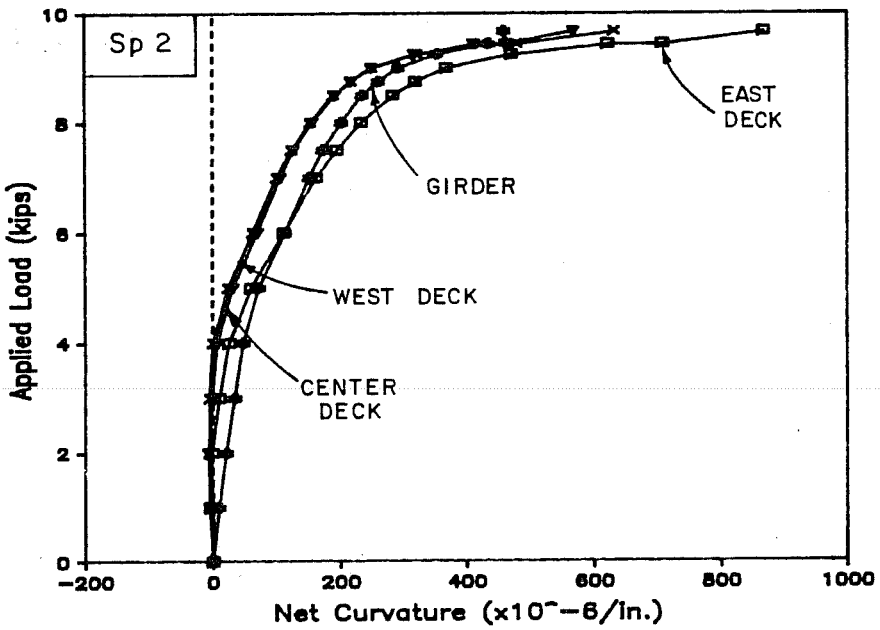

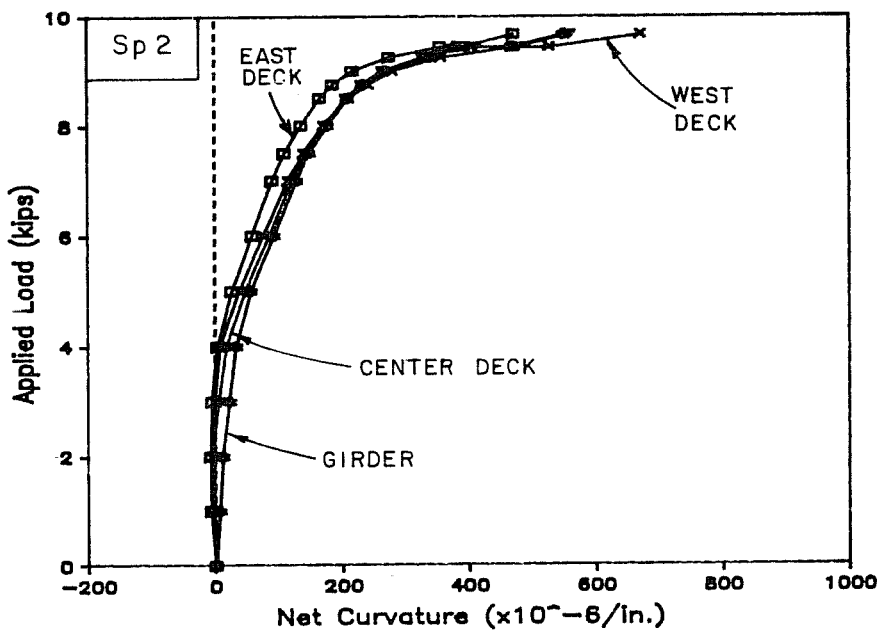

Fig. 4.62 Load-net curvature curves during flexure test: a) north gages; b) south gages

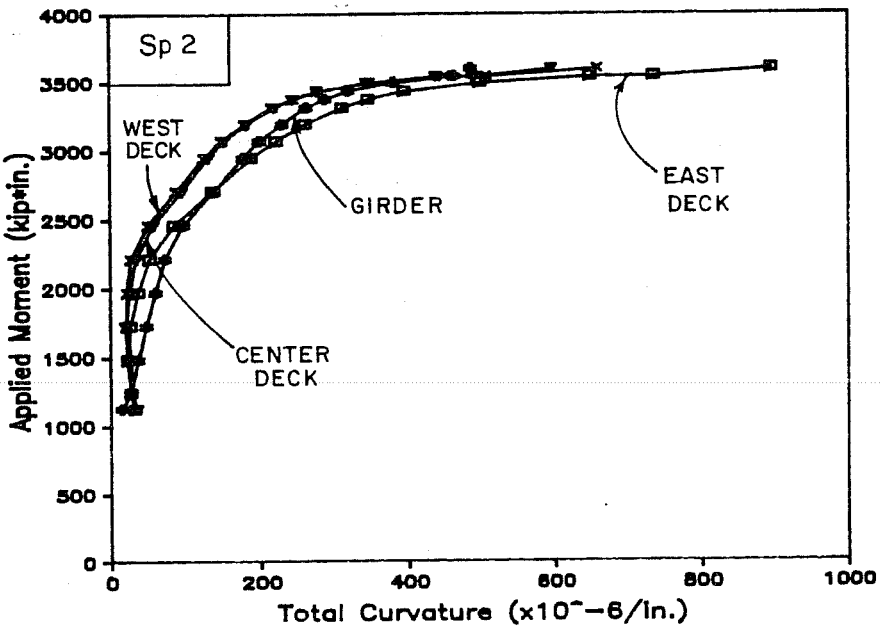

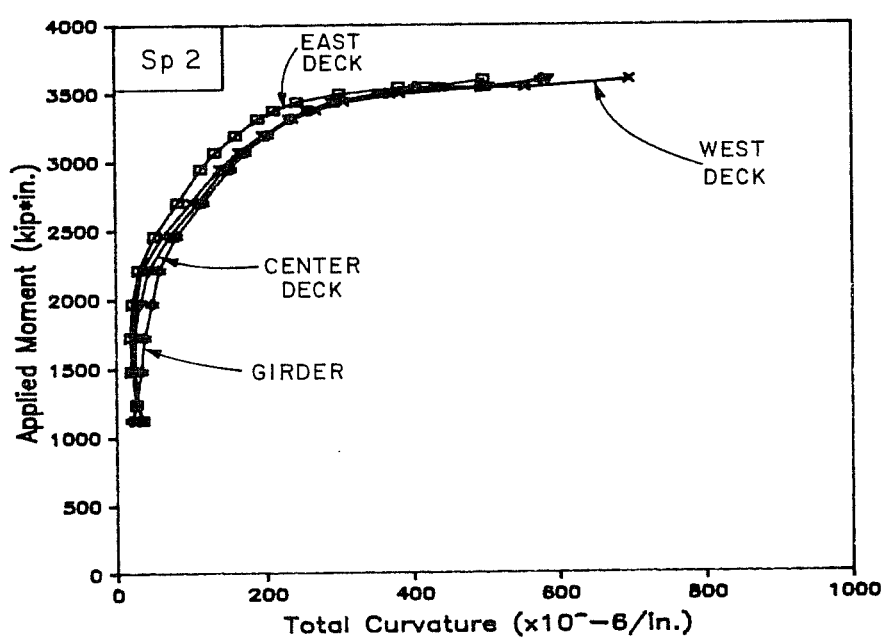

Fig. 4.63 Moment-curvature curves during flexure test: a) north gages; b) south gages

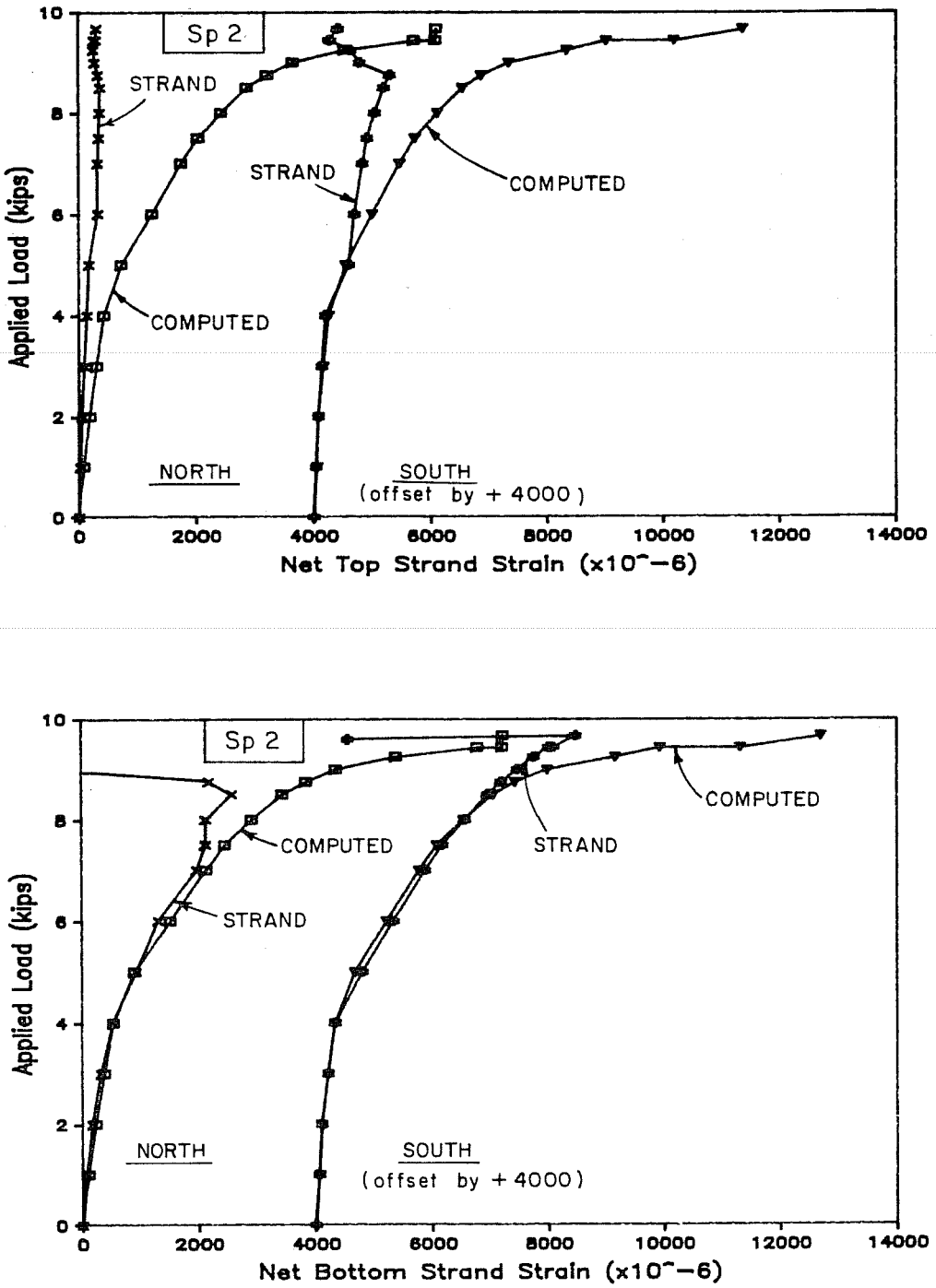

Fig. 4.64 Measured and computed strand strains during flexure test: a) top strand strains; b) bottom strand strains

appeared to fail just prior to ultimate as indicated by the retreat of the strain readings following gage failure.

The departure of the south gage data (both top and bottom) from the computed strains appears to indicate that the strands debonded in the concrete and therefore failed to experience the increase in strain consistent with the increasing section curvature. A similar trend appears in the bottom north gage data, although it is not as clear or long-lived. Slip in the top strand appears to have occurred near 5 kips while the bottom strand departs from the computed curve at 8.5 kips. This behavior was not expected but can be explained by the presence of many closely spaced flexure cracks that elevated bond stresses to a point where debonding occurred between cracks. The high shrinkage strains may have also adversely affected strand bond. The top strand may have debonded at a lower load because it was close to the more severe shrinkage cracking of the web.

Strand strains, girder concrete strains, deck concrete strains, girder curvature and midspan deflections are combined in Fig. 4.65. Data is normalized with respect to readings at the ultimate load.

4.3.2.4 Stirrup Strains and Strand Slip at Ends. Stirrup strains were significant which indicates that shear cracking occurred or that shrinkage cracks were opening under the influence of shear (Fig. 4.66). The south gage data appears to indicate cracking at 7.5 kips while the steady increase of the north gage data is evidence that a shrinkage crack was opening under the influence of shear.

No strand slip was measured at the ends of the girder during the flexure test.

4.4 Comparison of Specimens 1 and 2

4.4.1 Prior to Flexure Tests.

4.4.1.1 Concrete Material Properties. Stress-strain curves for both specimens are compared in Fig. 4.67. The girder concrete for Specimen 1 appears to be more brittle than the weaker Specimen 2 concrete because the curve deviated little from linear response at failure and no unloading branch was recorded.

4.4.1.2 Effective Stresses and Creep Strains. Effective stresses and losses are presented in Table 4.9. The effect of shrinkage on Specimen 2 is evident in increased losses prior to release. Losses at release were higher for Specimen 1 because of a higher prestress force. Strand stresses remained at reasonable levels for both specimens.

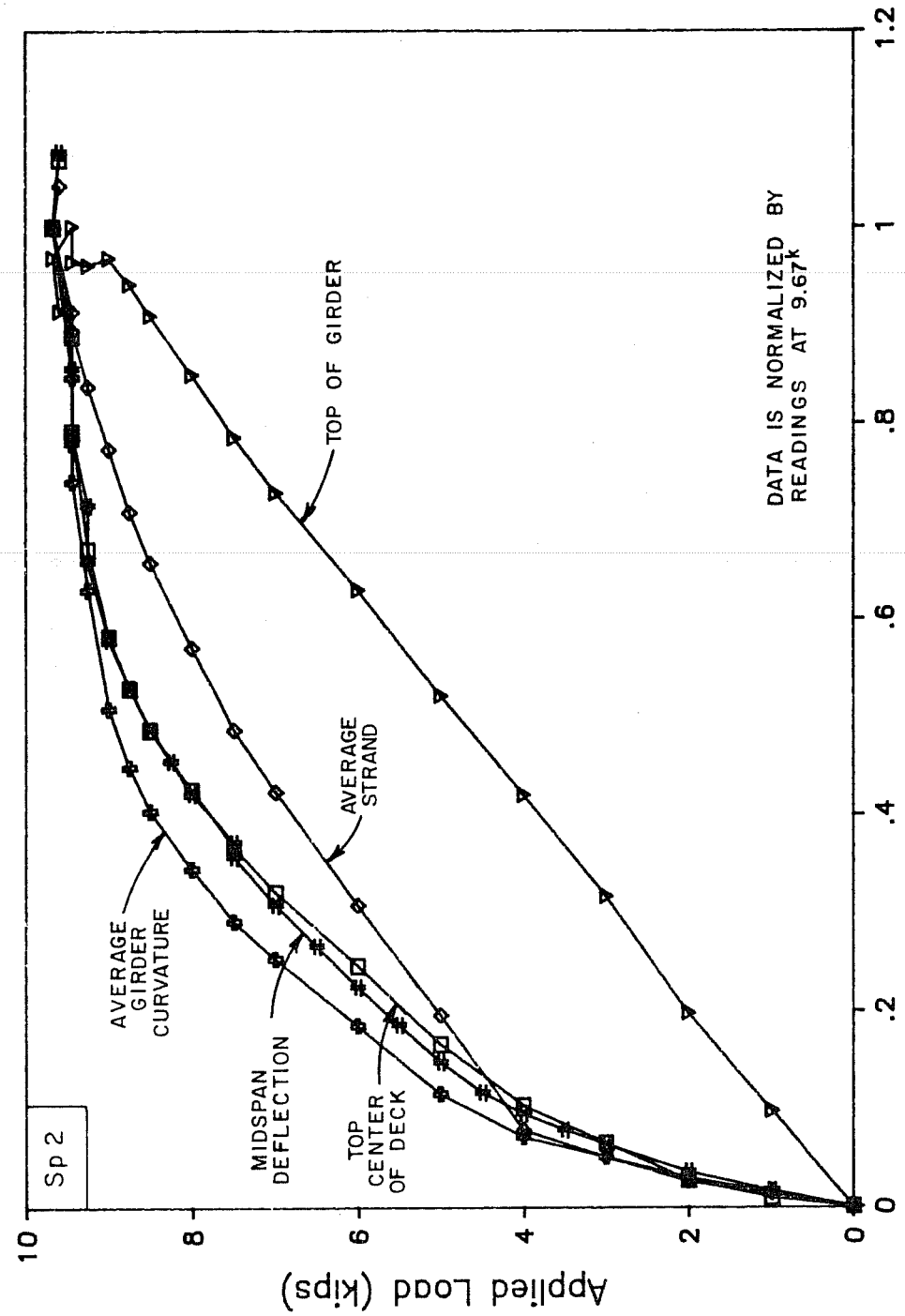

Fig. 4.65 Comparison of different types of data during flexure test

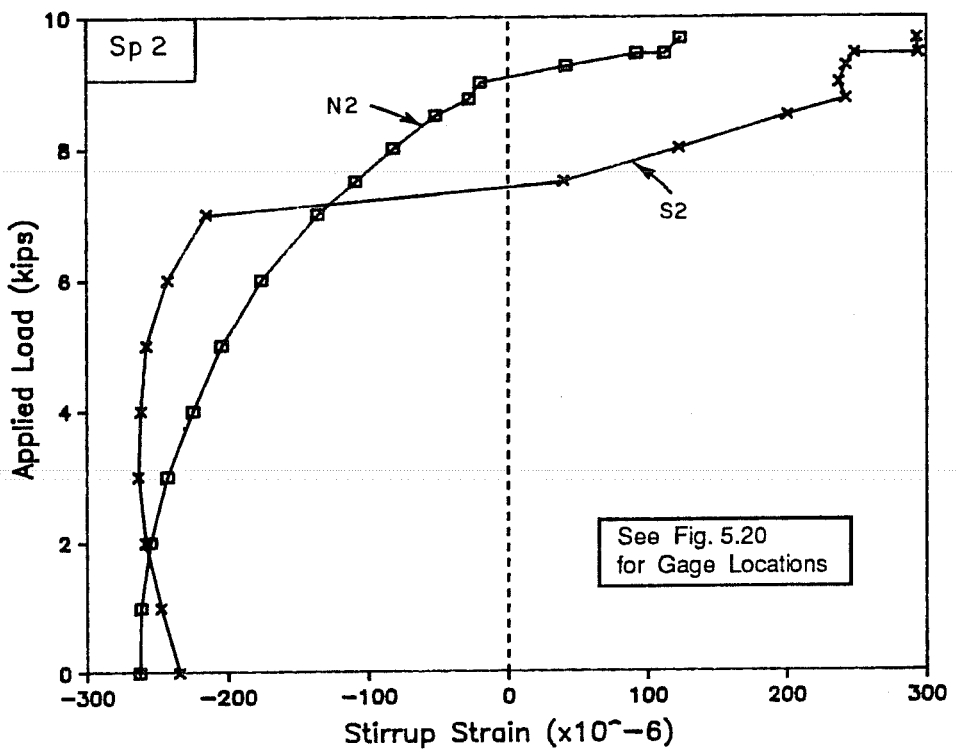

Fig. 4.66 Stirrups strains during flexure test

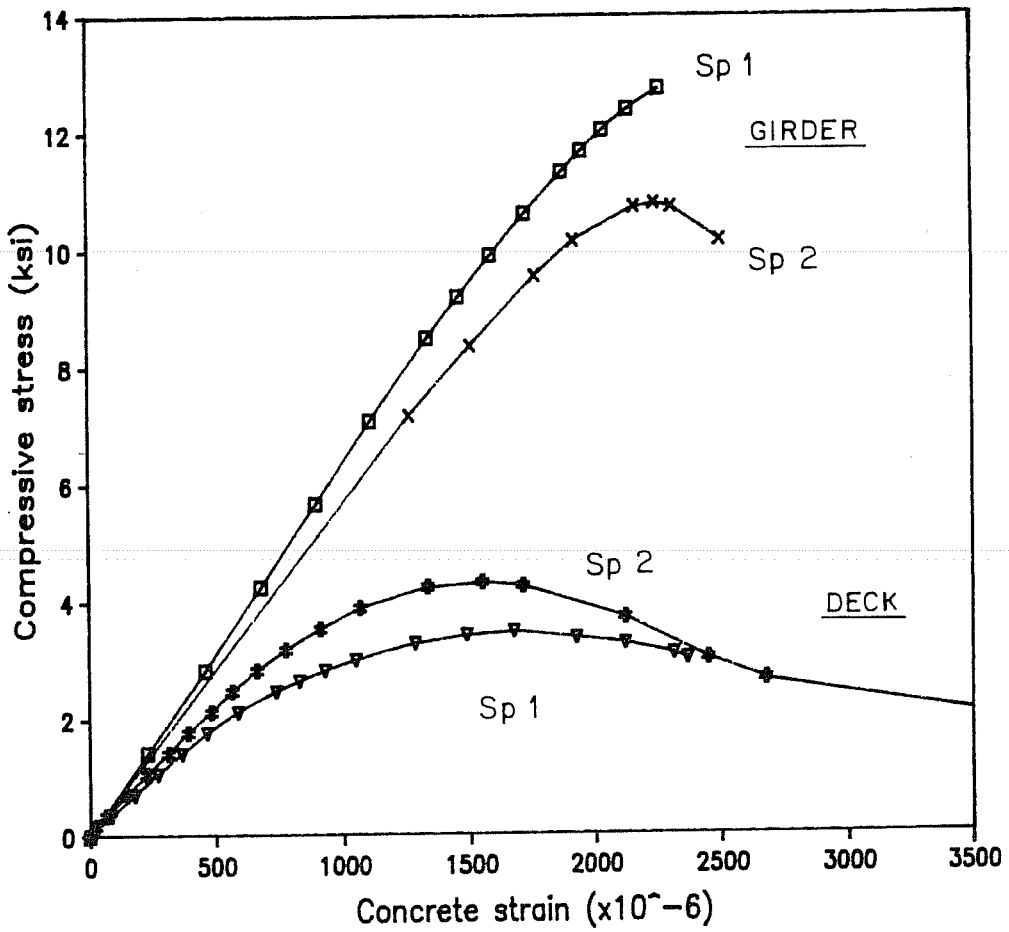

Fig. 4.67 Comparison of concrete stress-strain curves

Table 4.9 Comparison of effective strand stresses and losses

	Specimen 1 (Table 6.3)		Specimen 2 (Table 6.9)	
	Stress (ksi)	Loss (ksi)	Stress (ksi)	Loss (ksi)
Full Tensioning				
All locations	187.6	---	206.7	---
Prior to Release				
All locations	181.7	5.9	193.6	13.1
After Release				
Midspan	159.6	28.0	177.6	29.1
Midspan *	159.6	28.0	179.4	27.3
North end *	164.2	23.4	173.5	33.2
South end *	164.4	23.2	173.5	33.2
Flexure Test				
Midspan	152.5	35.1	173.1	33.6
North end	147.5	40.1	156.8	49.9
South end	143.6	44.0	156.8	49.9
Shear Tests				
North end	143.1	44.5	156.8	49.9
South end	140.5	47.1	156.8	49.9

* - These values represent computed instantaneous elastic losses plus 25% and were calculated as noted in Tables 6.3 and 6.9.

Note:

Losses were computed by subtracting effective stresses from the stress present when strands were fully tensioned.

While the specimens were scale models, some of the factors that affect prestress losses could not be properly scaled. For example, the volume to surface ratio of the modified Type IV prototype girder is 4.19 while the ratio is 1.39 for the scale-model girder. This difference, which approximately corresponds to the scale factor, could result in nearly three times more shrinkage for the model than for the prototype for the time scale involved in the testing schedule according to test data presented in Ref. [51]. The same test data [51] also indicated that creep tends to be greater for sections with smaller volume-to-surface ratios. Therefore, losses of the magnitude found in these girders should not be expected in a prototype structure.

Girder creep strains, which are the difference between corrected strains before the flexure tests and after release, are compared in Fig. 4.68. Specimen 1 experienced creep of approximately 600 microstrains which was uniform with depth. Creep experienced by Specimen 2 amounted to about 400 microstrains and increased toward the top of the girder. The lower creep for Specimen 2 was expected because of the lower prestress force.

Deck creep strains are presented in Fig. 4.69. Creep for Specimen 1 was approximately 350 microstrains at the top of the deck and about 300 microstrains at the bottom. Because the deck for Specimen 2 was added only eight days before the flexure test, the creep was much lower, only reaching about 100 microstrains.

4.4.2 Flexure Tests.

4.4.2.1 General Description of Behavior. Behavior of the two specimens was very similar. Cracking progressed similarly with cracking loads being higher for Specimen 1 due to the higher prestress force. The most striking aspect of the behavior of the specimens was that the failures were nearly identical. The failure surfaces were nearly indistinguishable.

Computed and observed cracking loads and ultimate loads are compared in Fig. 4.70 using computed values as the basis for comparison. Observed cracking loads exceed computed loads by a large margin for both specimens. This is probably because actual tensile capacity was higher than the assumed value. Any error in estimates of prestress force would also affect cracking loads. Observed ultimate loads exceeded computed values by 20 percent or less which is reasonable.

Design and ultimate loads are compared in Fig. 4.71 using factored load as the basis for comparison. Factored load is nearly three times the live load due to the high dead load to live load ratio. The figure also shows the considerable excess nominal capacity provided because allowable stress criteria control the design. The

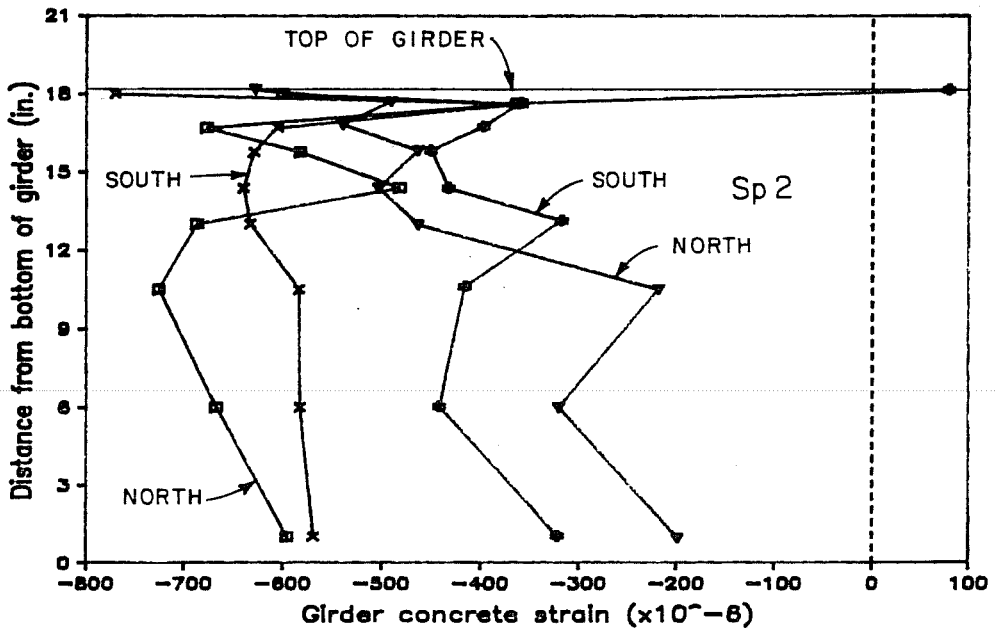

Fig. 4.68 Girder concrete creep strains at midspan at ultimate flexure tests

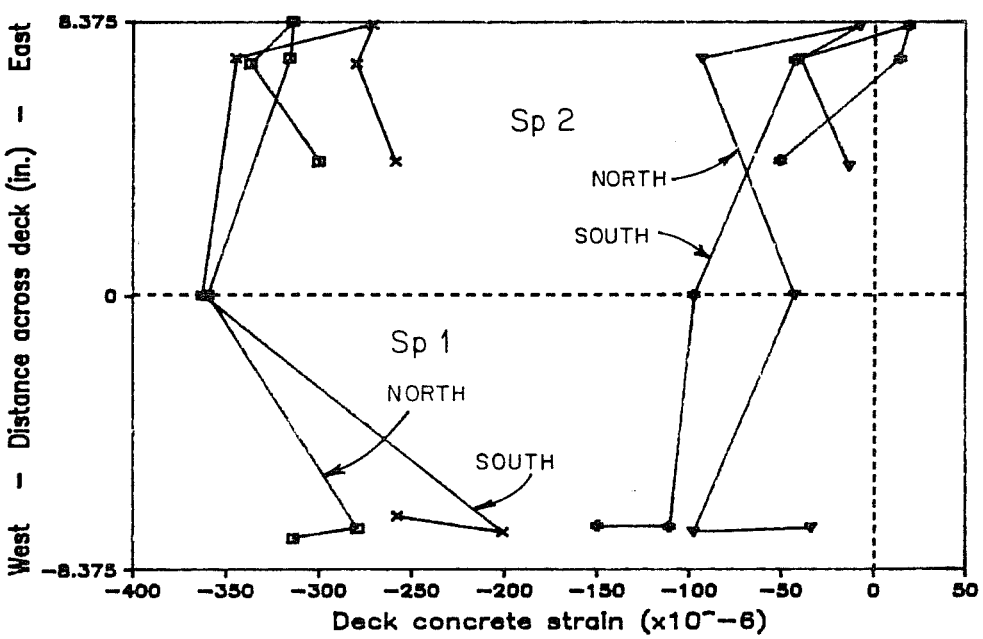

Fig. 4.69 Deck concrete creep strains at midspan at ultimate flexure tests

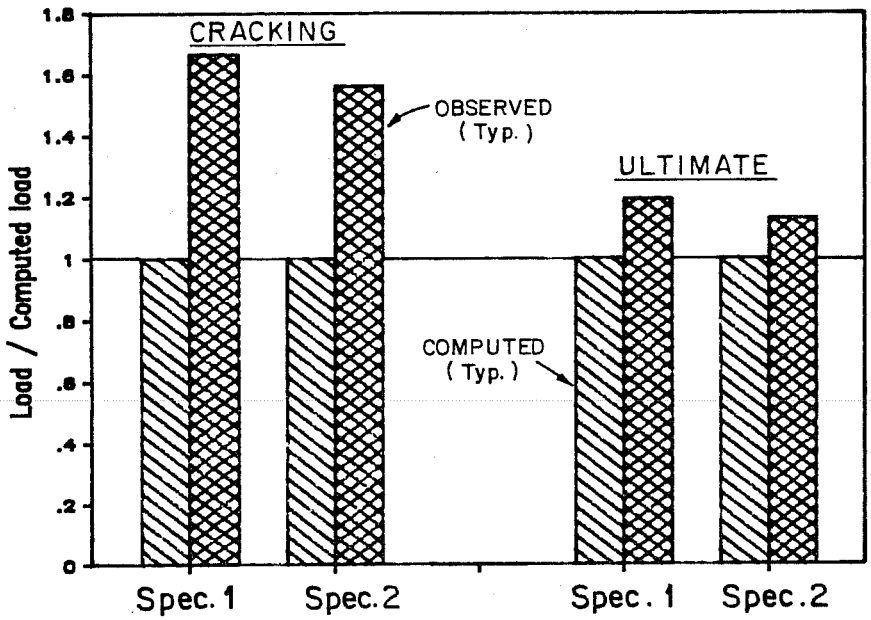

Fig. 4.70 Relative comparisons of computed and observed loads at cracking and ultimate

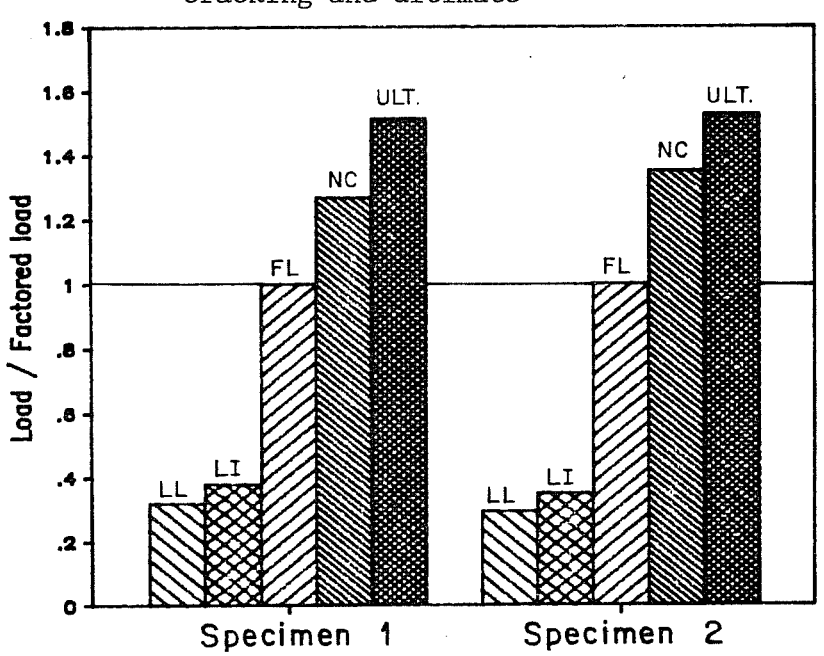

Fig. 4.71 Comparisons of design and ultimate loads

computed nominal capacity exceeds the factored load by 25 to 35 percent. Where computed and observed capacity should be equal, since $\phi = 1.0$ for laboratory tests, the observed ultimate exceeded the computed value for both specimens.

4.4.2.2 Deflections. Midspan deflections are plotted in Fig. 4.72 which also shows some of the significant loads. At low loads, the stiffnesses are similar because specimens were essentially uncracked. Specimen 2 appears more ductile because it has an apparent yield plateau, although it was rather limited. Deflections at design, ultimate, and failure loads are summarized and compared with the span length as an index of their relative magnitude in Table 4.10.

The area beneath the load-deflection curve, which is an index of ductility, is shown in Fig. 4.73 for the specimens. At ultimate the areas beneath the load-deflection curves were nearly identical, indicating similar energy absorption capacities.

4.4.2.3 Strand and Concrete Strains. Average and net average strand strains are shown in Fig. 4.74. At failure, strains, and therefore stresses (Fig. 4.75), reached nearly the same level although the change in strain during the test for Specimen 2 was less than for Specimen 1. While it was expected that Specimen 2 would reach higher strains because of its lighter reinforcement, the suspected debonding of the strands limited the strains to values lower than expected when considering overall member behavior (see Fig. 4.64 for comparison of measured and computed strand strains for Specimen 2). Stresses in both specimens reached or exceeded 95 percent of the measured ultimate stress and came very close to or exceeded the specified ultimate stress of 270 ksi.

Corrected concrete strains at the top of the girder, which appear in Fig. 4.76, show that Specimen 1 reached much higher strains than Specimen 2 even though the curves are nearly identical for the range of loads encountered by Specimen 2. This is found to be reasonable if crack height and curvature data are considered.

Typical corrected strains for the top of the deck are shown in Fig. 4.77. Both specimens reached similar levels of strain at failure which were well below the expected ultimate strain capacity of the concrete.

Strain gradients at selected loads are shown for girder and top of deck strains in Fig. 4.78. These plots demonstrate that the strain gradient for the section due to applied load remained linear to failure. Therefore, full composite action was present for both specimens at all levels of load.

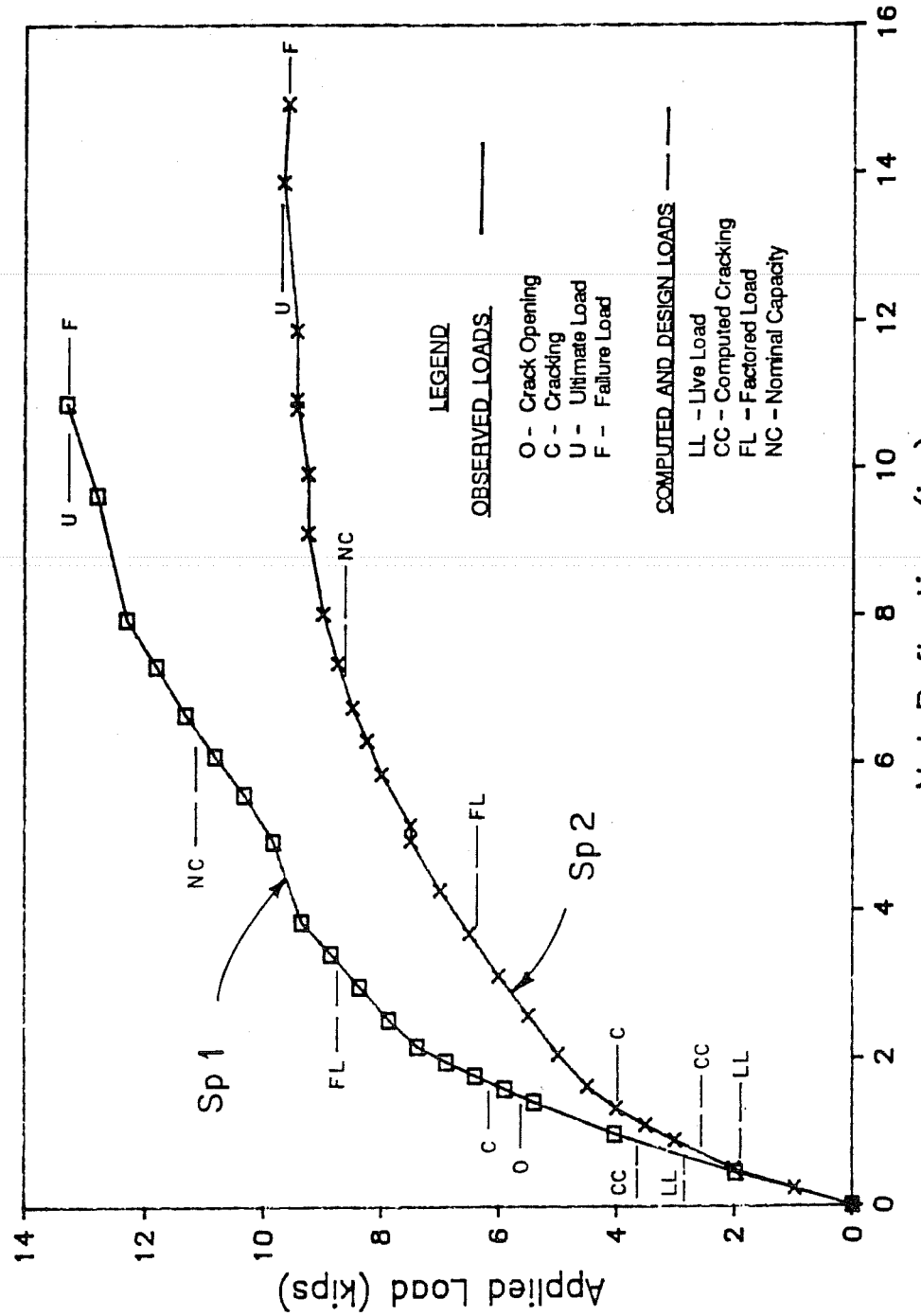

Fig. 4.72 Net deflection at midspan during ultimate flexure tests

Table 4.10 Comparison of deflections to span length during ultimate flexure tests

Load Stage	Load (kips)	Deflection (in.)	% of Span	Span/Defl.
Specimen 1				
Live Load	2.81	0.668	0.11	874.4
Live + Impact	3.33	0.801	0.14	729.2
Factored Load	8.79	3.354	0.57	174.1
Ultimate Load	13.29	10.880	1.86	53.7
Failure Load	13.29	10.880	1.86	53.7
Specimen 2				
Live Load	1.87	0.464	0.08	1258.6
Live + Impact	2.22	0.585	0.10	998.3
Factored Load	6.34	3.501	0.60	166.8
Ultimate Load	9.67	13.863	2.37	42.1
Failure Load	9.59	14.925	2.56	39.1

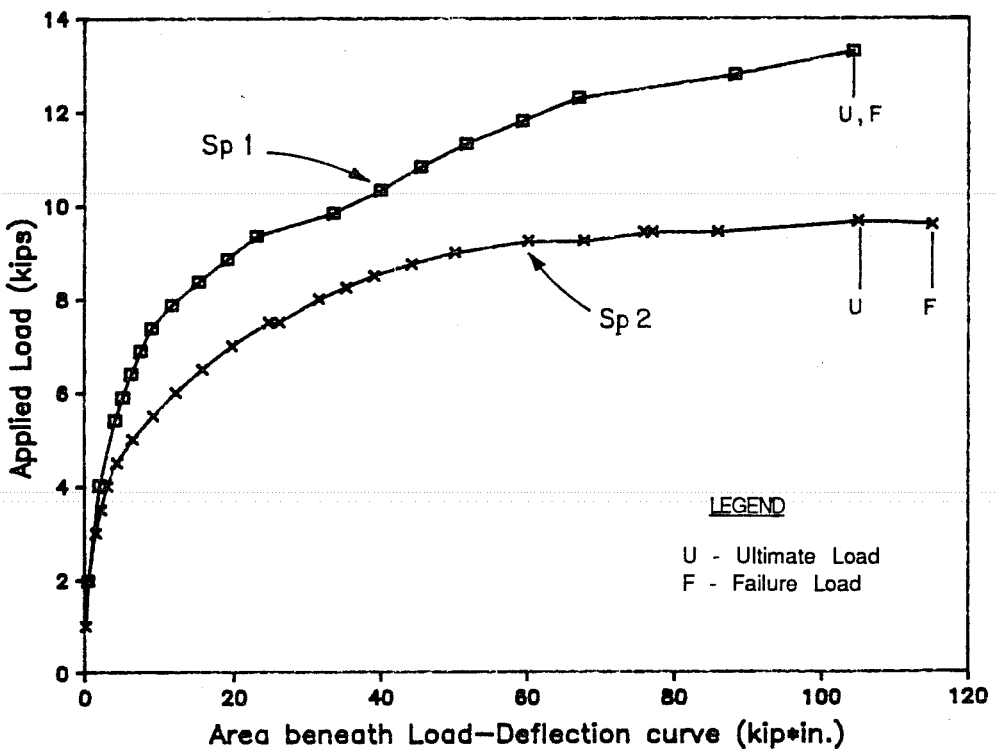

Fig. 4.73 Area beneath load-deflection curves

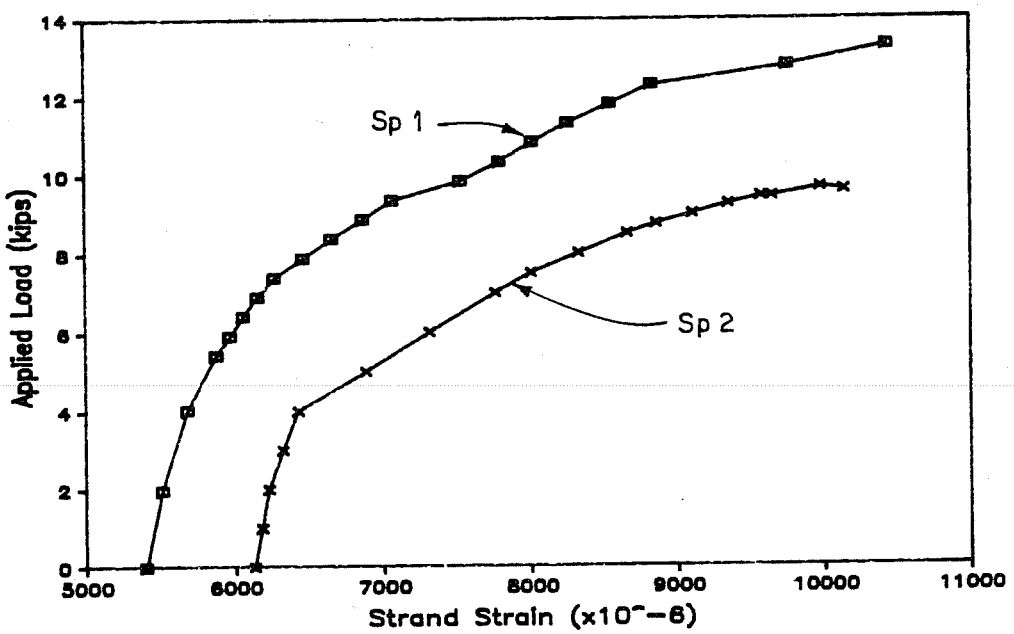

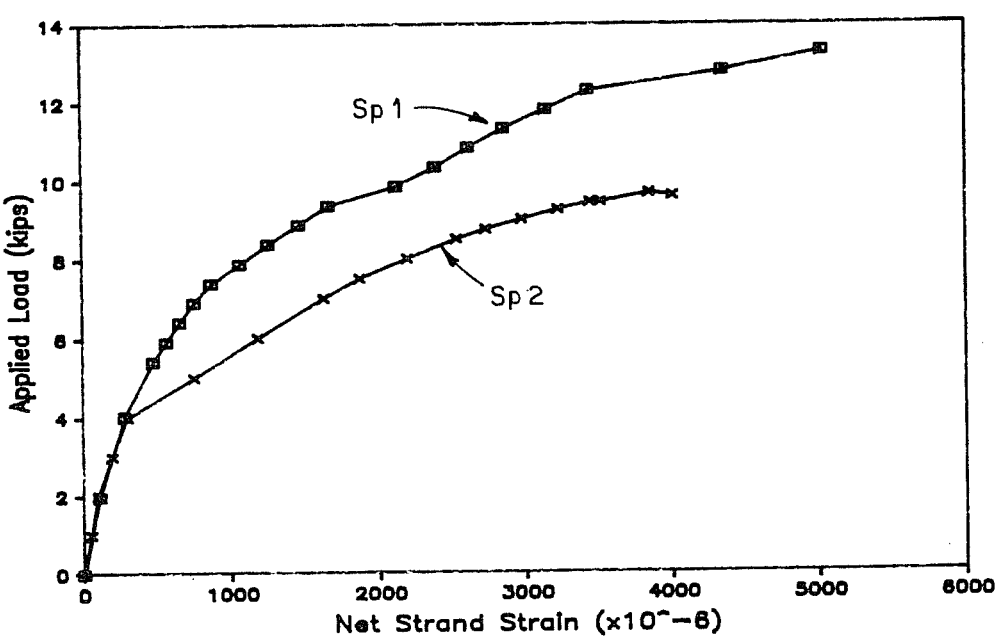

Fig. 4.74 Average strand strains during ultimate flexure tests: a) average strains; b) net average strains

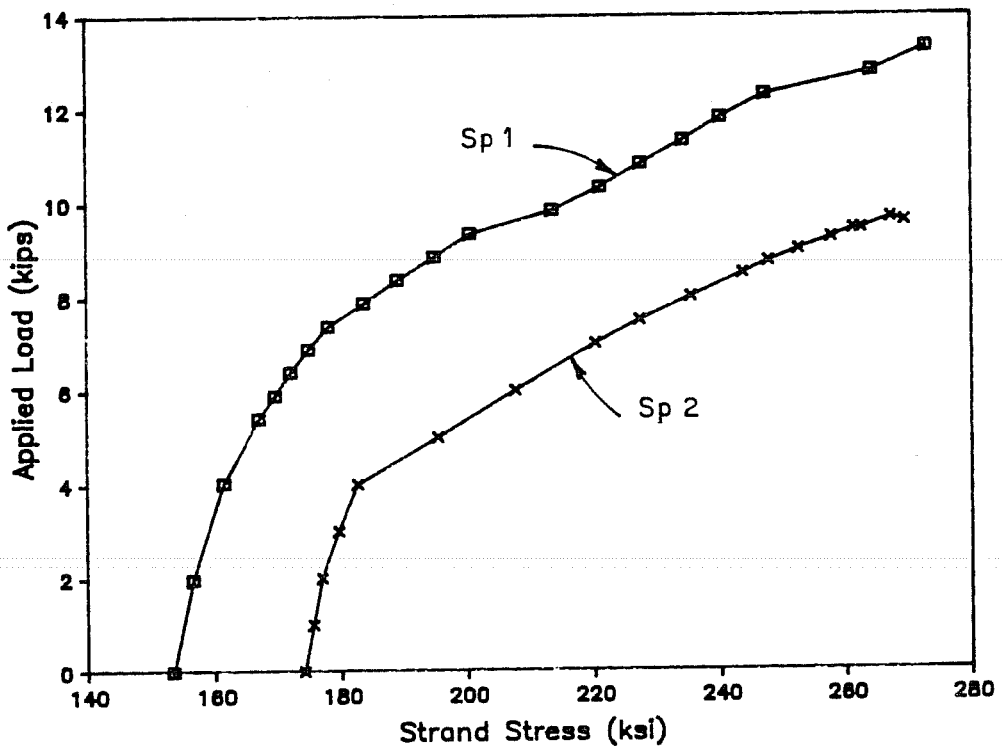

Fig. 4.75 Average strand stresses during ultimate flexure tests

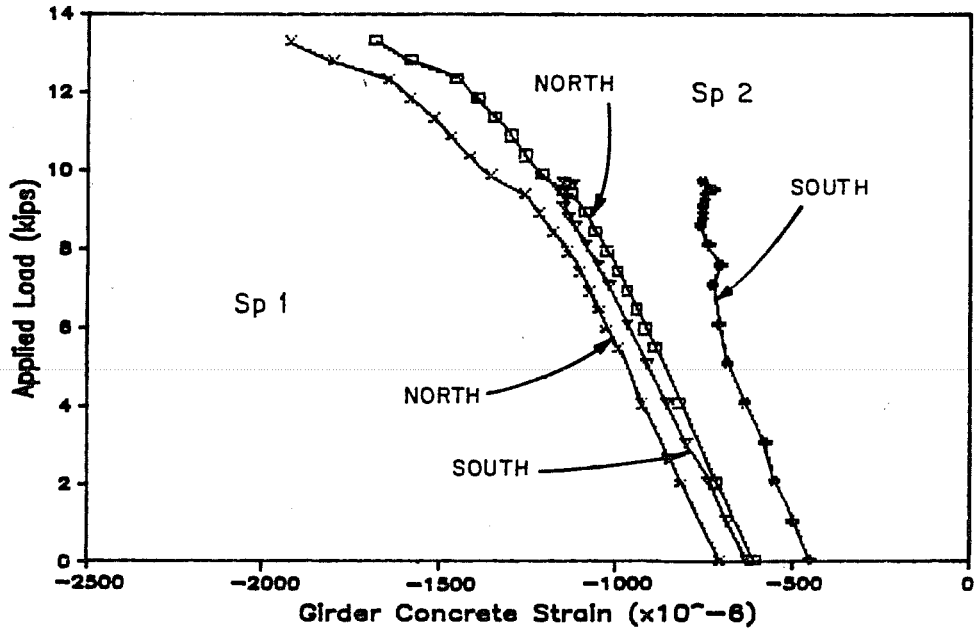

Fig. 4.76 Corrected top of girder concrete strains during ultimate flexure tests

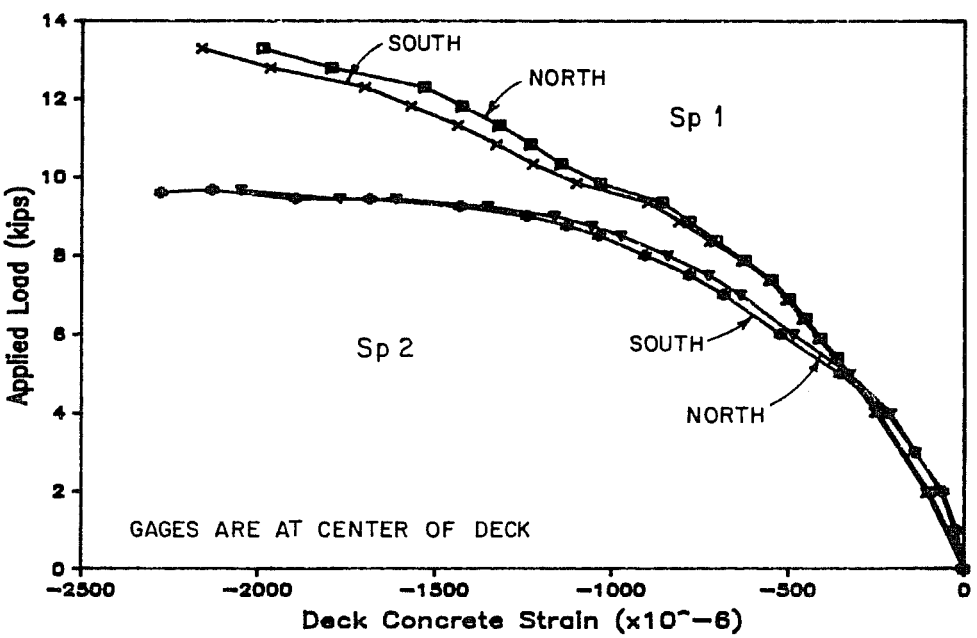

Fig. 4.77 Corrected top of deck concrete strains during ultimate flexure tests

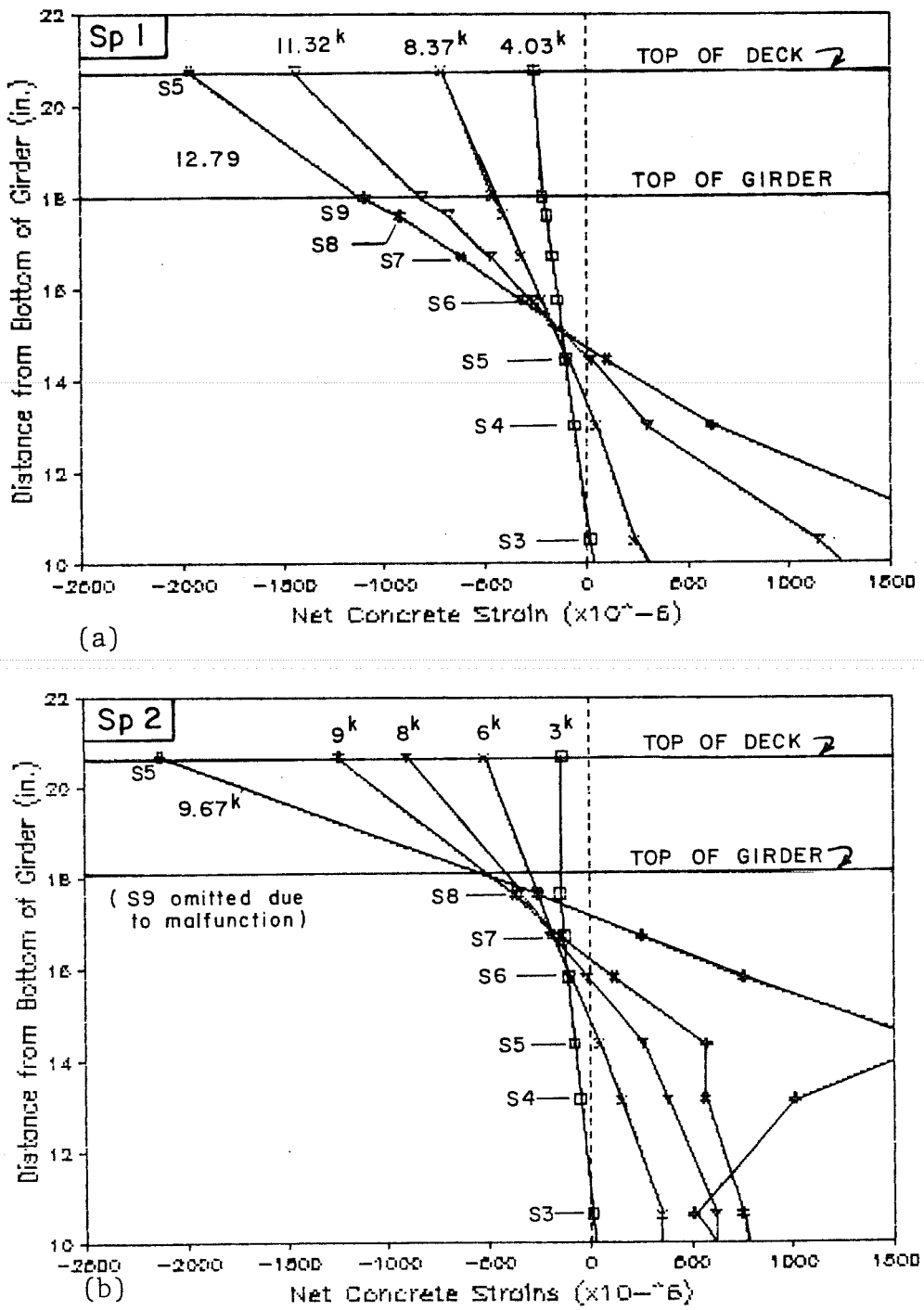

Fig. 4.78 Net girder and deck concrete strains at selected loads during flexure test: a) south gages, Specimen 1; b) south gages, Specimen 2

Crack heights computed using corrected girder strains are shown in Fig. 4.79. Cracks rose higher in Specimen 2 with less reinforcement. The crack height was rising rapidly as failure was approached for Specimen 2 while the crack height was more stable for Specimen 1 at high loads.

Moment-curvature plots are compared in Fig. 4.80. The curvature at ultimate for Specimen 2 is 22 percent greater than for Specimen 1; at failure, the curvature is 42 percent higher for Specimen 2 than for Specimen 1. This indicates greater ductility in Specimen 2, but it is less of a difference than expected.

All types of data for each specimen are shown in Fig. 4.81. These curves demonstrate some basic differences in behavior between the specimens. For Specimen 1, the strand strain increased most slowly at first and the deflection and curvature were nearly indistinguishable, which is surprising. After a load of about 9.5 kips, the curves all follow the same path as they converge on the load stage prior to failure. Specimen 2 behavior is different with the curvature being the quantity to increase most slowly and the midspan deflection and the top of deck strain being almost indistinguishable. The average strand strain followed the girder curvature up to 4 kips, then departed as it began to change more rapidly. The top of girder strain was striking in that it remained essentially linear up to the ultimate load. Identifying the reasons for the differences in behavior is not simple due to the complex interrelation of the quantities.

4.4.3 Shear Tests. A general discussion of the behavior observed during the four shear tests will be presented in this section. These tests were preliminary in nature and were used to provide background for a more complete study of shear that followed in this overall test program.

The complete analysis of the shear tests from the ends of these girders is contained in Ref. 138 and only a brief summary of the ultimate shear strength is given here, Fig. 4.82. For a complete discussion of the shear behavior and strength of high strength concrete, additional tests were needed. The total test program for shear is presented in Ref. 138.

Testing the ends of the flexural test specimens proved to be quite successful. While formation of cracks in the shear spans of interest during flexure tests precluded determination of cracking loads in some cases, the total capacity was apparently unaffected. Load-deflection curves obtained during the tests were affected by the presence of cracks in the deck due to insufficient dead load moment as a result of the shortened span. However, the capacity of the member was unaffected. The end of the shear specimen that was near midspan

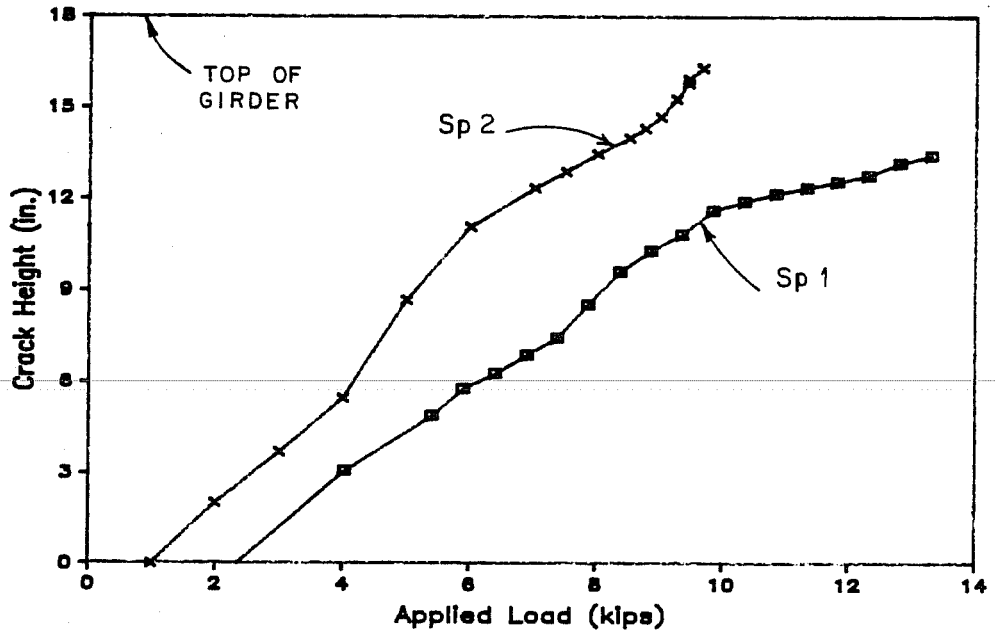

Fig. 4.79 Computed crack height during ultimate flexure tests

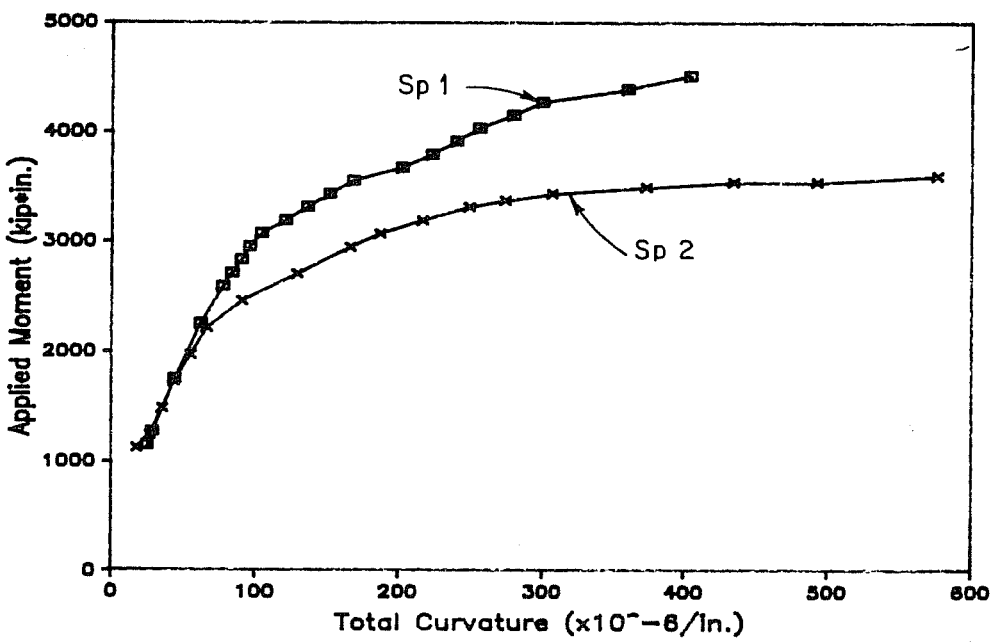

Fig. 4.80 Moment-curvature curves during ultimate flexure tests

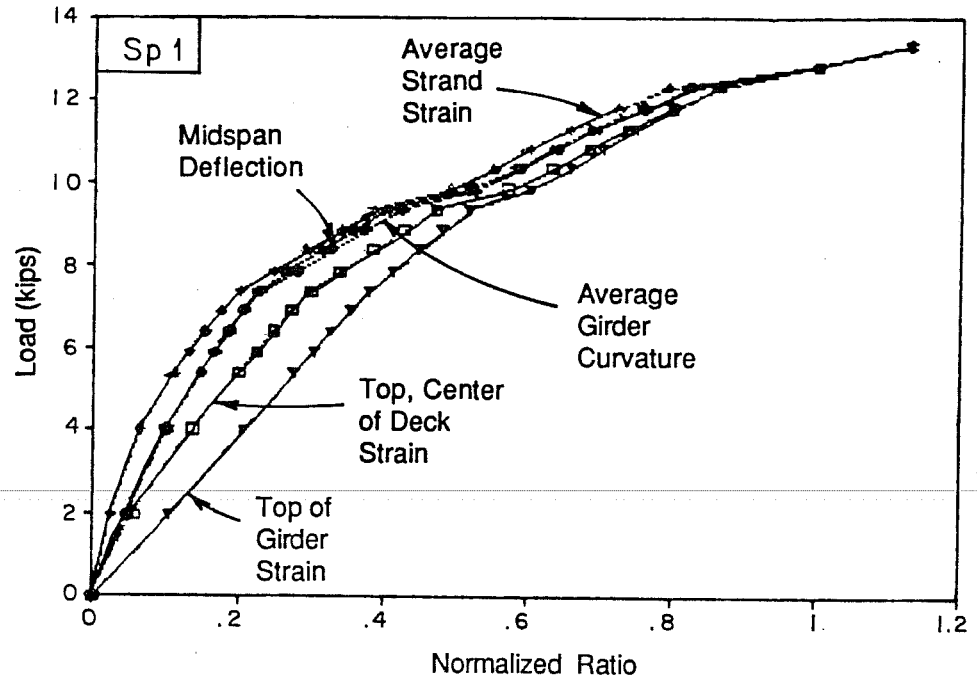

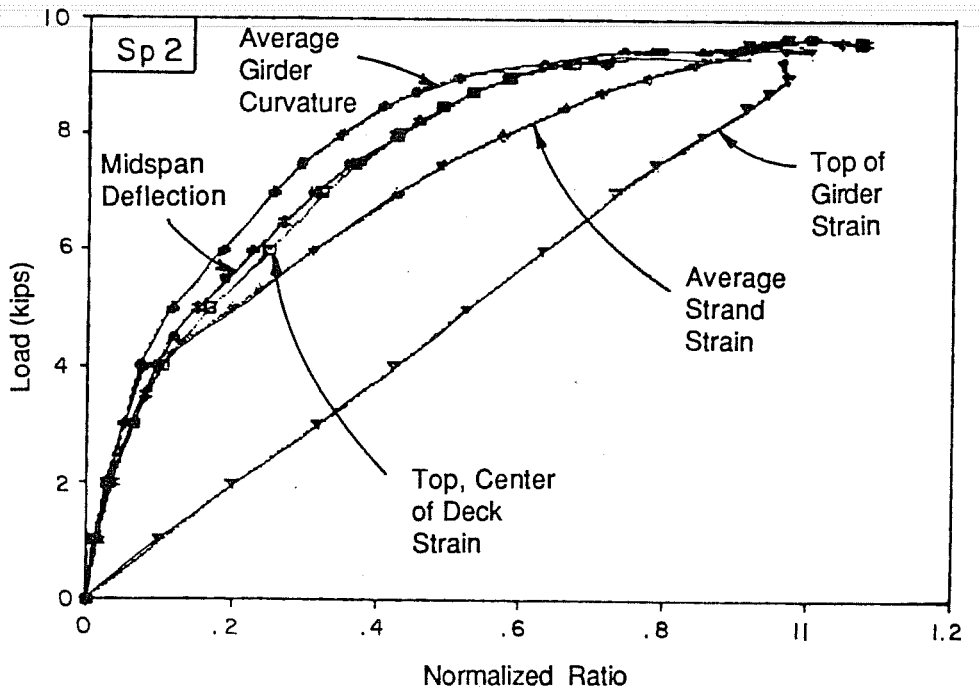

Fig. 4.81 Comparison of different types of data during ultimate flexure tests: a) Specimen 1; b) Specimen 2

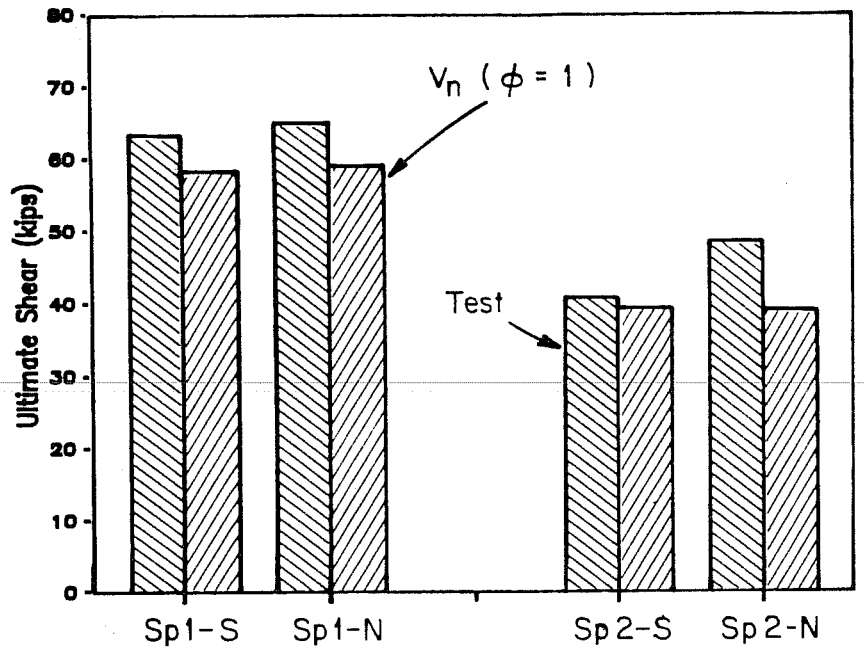

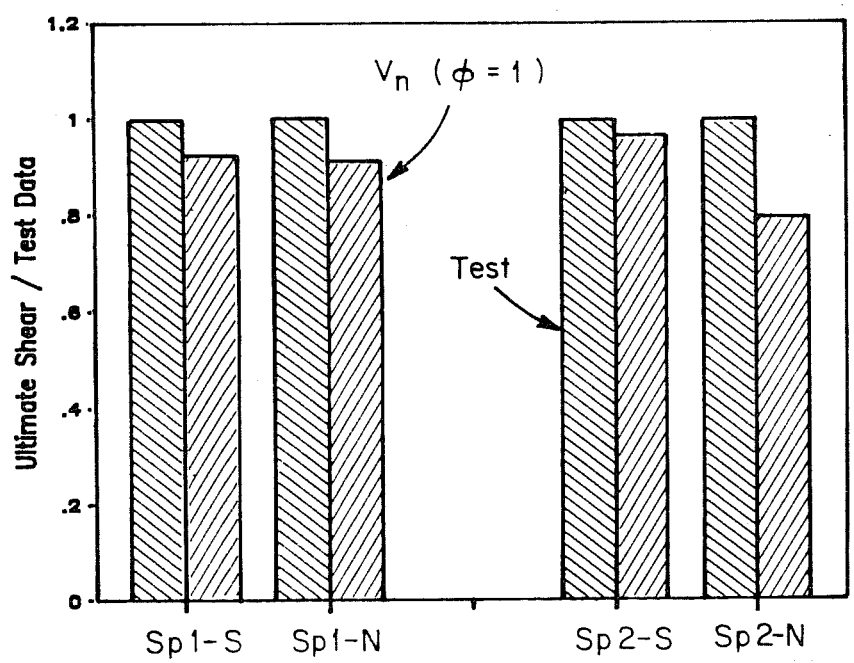

Fig. 4.82 Comparison of measured and predicted capacities for shear tests: a) ultimate shear capacity; b) normalized with respect to test data

of the complete flexure specimen experienced little additional cracking during shear tests, and existing cracks were unaffected.

Measured and predicted shear capacities of the specimens are compared in Fig. 4.82. Predicted ultimate shears were computed using the ACI equation for web cracking with a capacity reduction factors (ϕ) of 1.0, as appropriate for laboratory tests. The upper half of the figure compares the actual shear values while the lower half contains data normalized using the test results. In all four tests, the predicted values were reasonably conservative when compared with the test data. The predicted values were most conservative for the north end of Specimen 2 where strand slippage did not occur. It is expected that, if strand slippage had been prevented for the other specimens, the predicted capacities would be more conservative.

A similar comparison was made between observed shears at web cracking and shears at which the ACI equation predicted web cracking (Fig. 4.83). In all cases the computed value greatly exceeded the observed cracking shears. The large discrepancy between observed and computed shears causing web cracking may be partially due to the presence of prior cracking resulting from the violent flexural failures and shrinkage.

Load-deflection behavior of the specimens during the four ultimate shear tests is shown in Fig. 4.84. As mentioned above, the curves include the effect of deck cracks closing as load was added. Flexural cracking played a more significant role in the Specimen 1 tests as indicated by the more clearly bilinear shape of the curves. Both shear tests for Specimen 1 ended in strand slippage which is a brittle failure that led to a sudden departure from the linear behavior of the member. Significant capacity remained after slip occurred, although loading was not continued to complete failure. The south end of Specimen 2 displayed similar behavior with the capacity controlled by strand slippage. While the north end of Specimen 2 failed in web crushing, the capacity continued to increase slightly as crushing began and decreased only gradually as crushing became widespread. This failure mode led to a load-deflection curve (Fig. 4.118) that exhibited a degree of ductility. Flexural cracking was not a significant factor in the behavior of either end of Specimen 2.

Failure modes were basically brittle where strand slippage was involved since shear decreased immediately following the slip, although the shear resisted by the member decreased only slightly. The web crushing failure proved to be more ductile because the shear resisted initially continued to increase slightly as deflection continued.

Other aspects of behavior of the specimens were quite similar. Most instrumented stirrups yielded during the four shear tests,

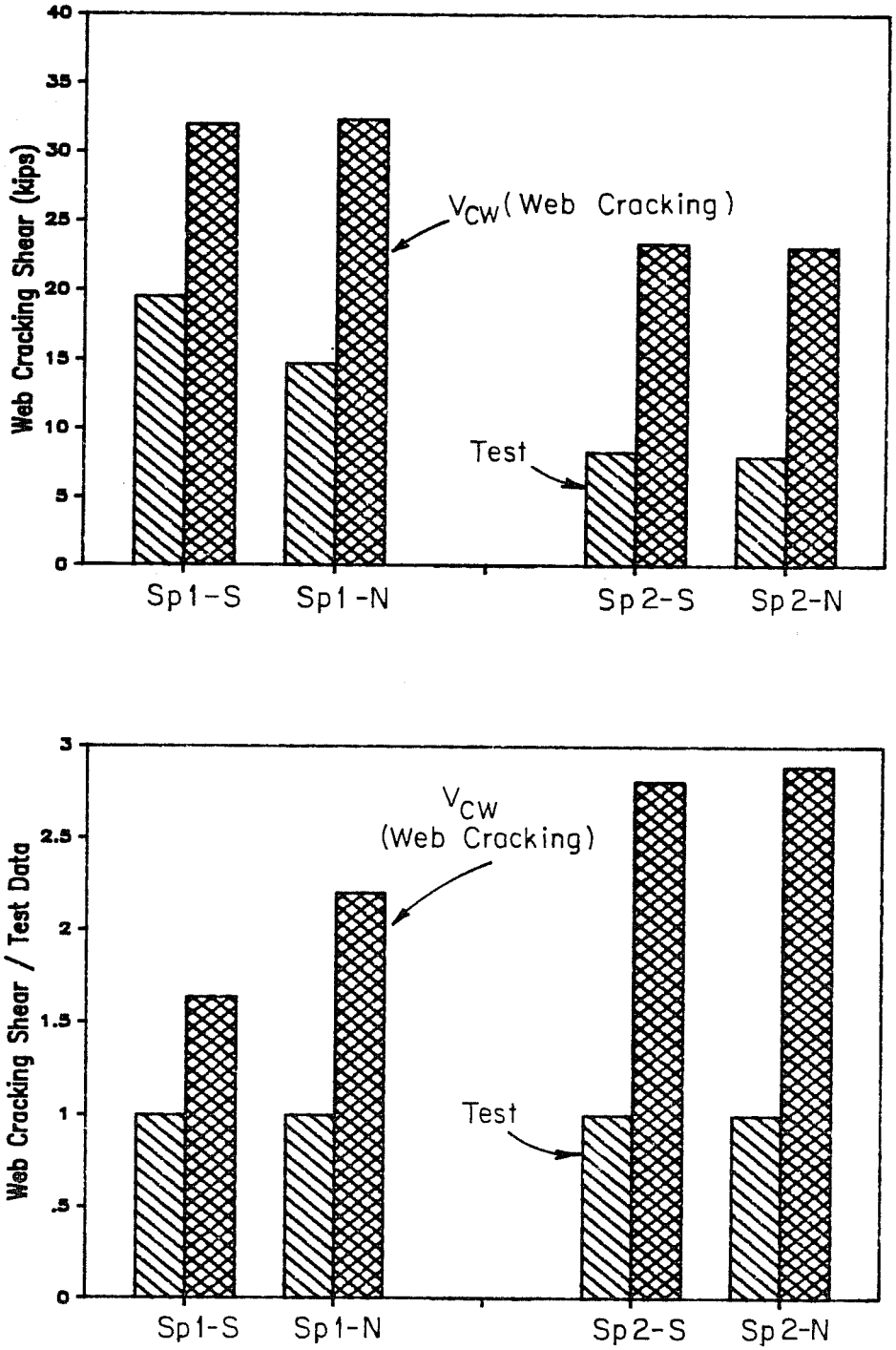

Fig. 4.83 Comparison of measured and predicted web cracking shears for shear tests: a) web cracking shear; b) normalized with respect to test data

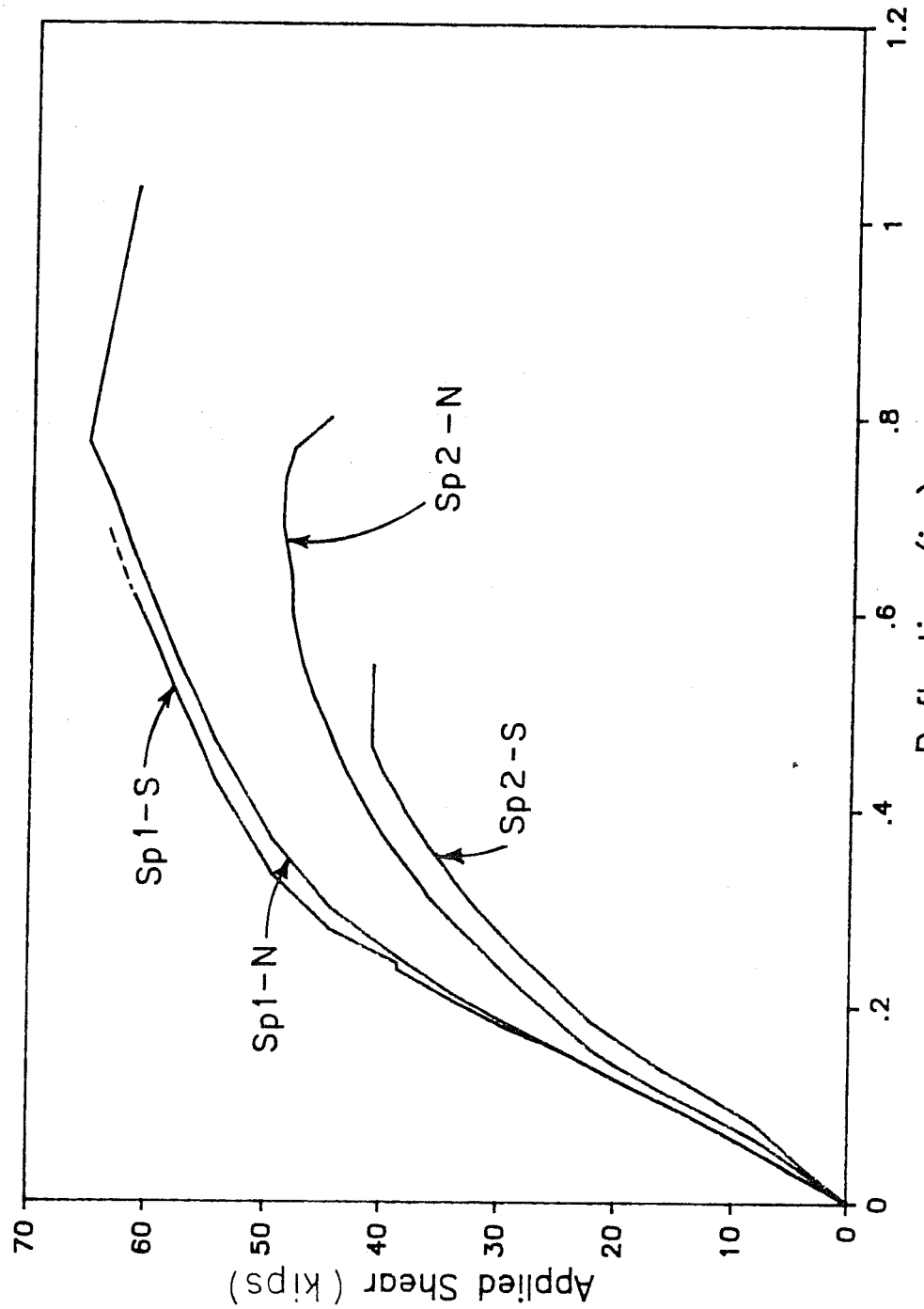

Fig. 4.84 Deflection at load point during ultimate shear tests

especially those in the central portion of the shear span. Strand strains were also approximately the same for Specimen 1 and the north end of Specimen 2 even though the load applied to Specimen 2 at failure was approximately 75 percent of the maximum load applied during both tests of Specimen 1. The maximum strand strain for the south end of Specimen 2 was lower than for the north end, although it corresponded well with the strains measured at the same load for the test of the north end.

CHAPTER 5

EVALUATION OF TEST RESULTS AND CURRENT DESIGN PRACTICE

5.1 Introduction

In this chapter, results of the literature review Ref. 139 and data gathered during the test programs are compared and evaluated with emphasis on the effect of high strength concrete on design. The organization parallels that of Ref. 139. Major sections conclude with a summary and recommendations where appropriate.

5.2 Philosophy of Design

The use of allowable stress and ultimate strength criteria as the basis for design of prestressed members is reasonable and has served the industry well. However, other aspects of design must also be considered if a bridge is to give satisfactory performance. Therefore, consideration of other important aspects of member design and behavior should be clearly and directly addressed. This is especially necessary as structures extend customary limits and become increasingly complex. Analysis capabilities have also become more sophisticated, enabling designers to directly determine quantities that have often been entirely neglected or indirectly limited due to a lack of computational methods. The intent of the code must be clear so that designers can correctly apply the code in unusual situations.

The topic of ductility is one such area that must be adequately addressed in a manner that can be understood and correctly applied by the designer. The current indirect approach of limiting the reinforcement index has apparently been sufficient, but the intent of the limit is not clear to the designer and may be misinterpreted. New limits are proposed and it is suggested that the basis or derivation of the limits be included in codes or commentaries. In this way, the intent of the provisions can be understood and applied where the specific limits are not applicable or where a more complete analysis is used, which would permit direct application of limits for which the code provisions are approximations.

Other areas in which the design of highway bridges should take a more direct approach are deflections, stability, and fatigue. In

the sections that follow, direct approaches for determining member behavior in these areas will be presented and discussed.

With these considerations, codes would move toward a more complete consideration of member behavior and would therefore produce structures that have been directly examined for all aspects of behavior.

5.3 Basic Properties of High Strength Concrete

This section presents a further review of the data presented in Ref. 139 and compares that information with data and observations collected during construction and testing of the long-span girder specimens.

5.3.1 Compressive Strength. The limited data reported from this study in Appendix A indicates that the mean variation between strengths for the two sizes of cylinders is small (<3.5 percent) with 4 x 8-in. cylinders giving higher strengths than standard cylinders. The magnitude of variation between the two sizes of cylinders is in agreement with data reported in Sec. 3.3.1, although the reported strengths for 4 x 8-in. cylinders are higher instead of lower than strengths for 6 x 12-in. cylinders. Therefore, because available data are limited and inconsistent, it is recommended that a correlation between 4 x 8-in. and 6 x 12-in. cylinder strengths should be determined on a local basis when 4 x 8-in. cylinders will be used. Because of the increased 3 variability in tests of 4 x 8-in. cylinders reported by Malhotra [78], which may contribute to the inconsistency between results reported by investigators, it is also recommended that at least twice as many 4 x 8-in. cylinders should be tested as the number of 6 x 12-in. cylinders currently tested in order to obtain the same level of confidence [78].

Use of a later design age for concrete strengths does not appear to be of great consequence but may be desirable when a mix shows a large increase in strength with time and the design strength is not required until the later date. Proper controls on the strength must be developed in order to determine satisfaction of design criteria at early ages as discussed by Drake [43].

Data presented in Appendix A indicate that curing cylinders in ambient conditions following the application of curing compound after stripping the molds reduced the strength of the concrete by less than 5 percent when compared with cylinders cured in a lime bath.

This agrees with data reported by other investigators. Therefore, cylinders cured in a wet or moist environment can be used to estimate the concrete strength in girders cured under ambient conditions, although the cylinders will have a somewhat higher strength than the girder, assuming that cylinders cured with the girder give a good indication of girder strength.

Greater reductions in strength may be possible between ambient and moist- or wet-cured cylinders because of the severe curing conditions to which some girders are subjected. While most girders are removed from forms less than 24 hours after casting and are immediately placed in an open yard for storage, the girders in this study remained in the forms for two or four days after casting, received a liberal coat of curing compound, and were stored and tested under the shelter of a roof, which prevented direct exposure to sunlight. Further study is needed to determine the effect of severe curing conditions on concrete strength. However, for pretensioned girders, the design strength is generally not critical because concrete strength requirements at release control the mix design. This results in a concrete strength at the design age significantly greater than the strength required in almost all cases.

5.3.2 Modulus of Elasticity and Stress-Strain Curve. Average modulus of elasticity data for the girder concrete of Specimens 1 and 2 at various ages are summarized in Table 5.1. This data for 6 x 12-in. cylinders, was obtained with a mechanical extensometer (compressometer) with an 8-in. gage length, or for a single case, strain gages attached to the cylinders. Data for Specimen 1 at 66 days were inconsistent, with the compressometer data giving lower modulus values than those determined using strain gages. Strain gage measurements agreed closely with compressometer measurements taken at 44 days. The discrepancy between moduli determined using strain gage and compressometer measurements was unexpected because in previous tests where both strain gage and compressometer readings were made for the same cylinders, agreement was very good.

After adjustment for unit weight, the average data given in the table was added to previously required data and appears here as Fig. 5.1. Air cured cylinders are positioned between the ACI and Cornell equations while the single wet cured data point is significantly above the ACI equation. In this case, the modulus is much more sensitive to curing conditions than the strength. However, two air cured cylinders from the final trial batch for the girder concrete had moduli of 8,160 and 8,680 ksi for cylinder strengths of

Table 5.1 Average Modulus of Elasticity Data for Girder Concrete - Specimens 1 and 2

Age (days)	Curing	Strength (ksi)	Average Modulus (ksi)	$E_c/\sqrt{f'_c}$ (x10^3)
Specimen 1 - Steel molds				
44	Air	13.02	6,380	55.9
66	Air	12.91	5,980	52.6
66 *	Air	12.91	6,430	56.5
Specimen 2 - Plastic molds				
7	Air	9.20	5,300	55.3
21	Air	10.12	5,550	55.2
28	Air	10.75	5,720	55.2
28	Wet	10.66	7,000	67.8
56	Air	10.78	5,675	54.7

Note: Unit weight of concrete is approximately 150 pcf.

* - Modulus determined using two electronic strain gages on each cylinder. All other data taken using a compressometer.

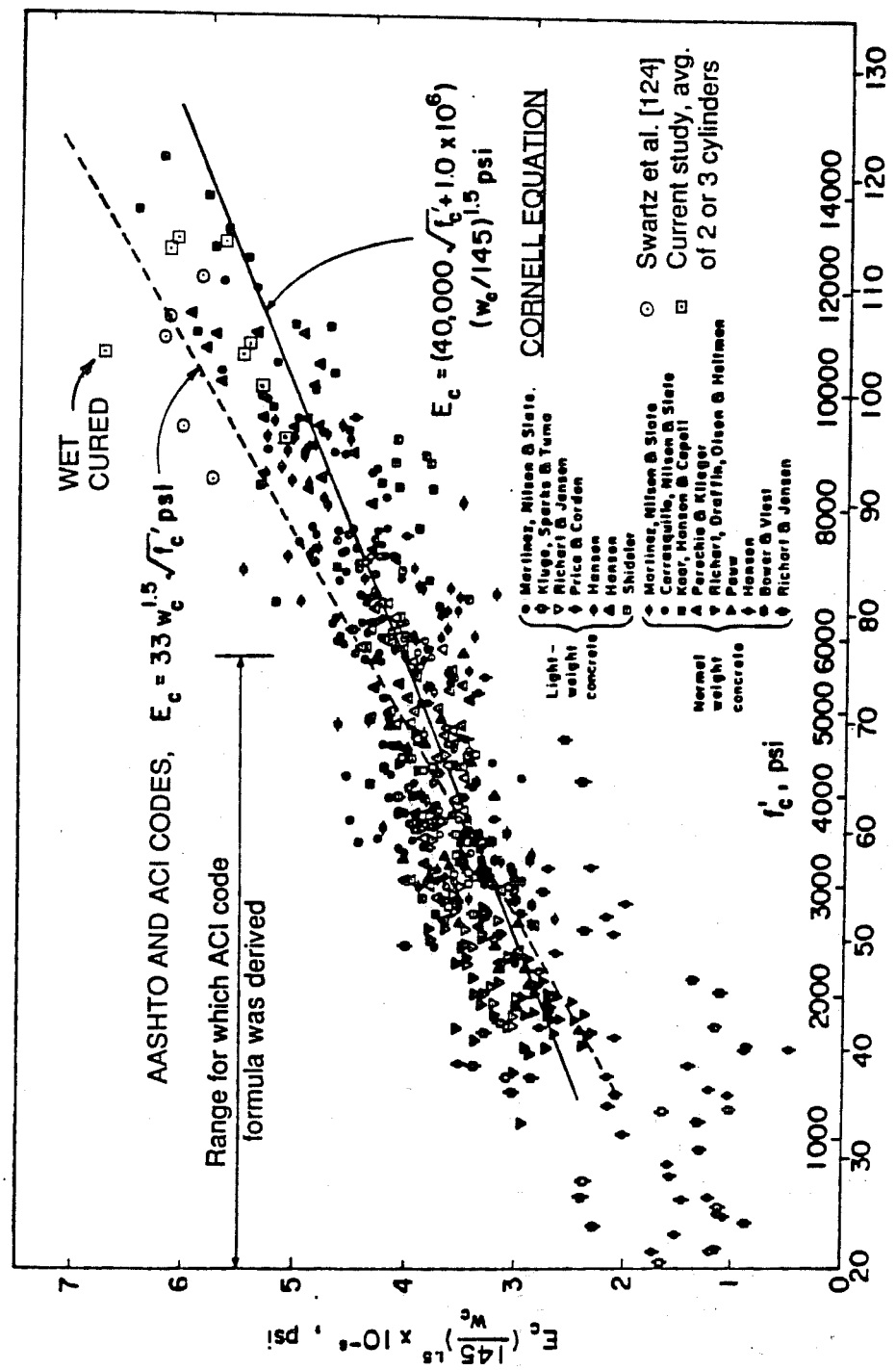

Fig. 5.1 Modulus of elasticity versus concrete strength including data from current study [79, 122]

12,410 and 14,000 psi, respectively. These data points are well above the ACI equation but were not included on Fig. 5.1 because they were obtained using strain gages rather than a compressometer. Unit weight for this batch at casting was 153.8 pcf.

The data of Fig. 5.1 and the additional data mentioned above confirm the potential for wide scatter in modulus values due to differences in curing conditions and materials. Also, it should be noted that the data from which the proposed Cornell equation was developed were obtained from a limited variety of aggregate sources. Therefore, it appears prudent, in situations where the modulus is a critical factor in design, to determine the effect of specific materials and conditions by measuring the modulus for high strength concrete. The current AASHTO and ACI expression for modulus of elasticity appears sufficiently accurate for estimating the modulus if data on a specific mix are not available. The effect that using the current modulus equation or the equation proposed by investigators at Cornell has on designs is considered in Sec. 5.4.5.4.

Average stress-strain curves for the girder and slab concrete at the time of the flexure tests are shown in Fig. 5.2. Curves for Specimen 1 were obtained using strain gages attached to manual strain indicators while data for Specimen 2 were obtained using a plotter to record head displacement of the testing machine. The method of measurement was changed to permit determination of the stress-strain curve approaching and beyond the peak stress. This was not possible for Specimen 1 using strain gages because of spalling of the concrete surface to which the gages were attached, and because the data recording device used with the gages did not permit accurate, continuous monitoring of strain. Plots obtained for Specimen 2 cylinders were calibrated using modulus measurements made with a compressometer. While cap deformation was included in strains measured for Specimen 2, the error introduced was estimated to be less than 2 percent. The shapes of the curves are similar to the typical curves shown in Fig. 3.3, although the strains at maximum stress are lower. Curves for high strength concrete end with the sudden destruction of the cylinder while low strength cylinders continue to resist load beyond the strains shown, although the concrete is badly crushed and the usefulness of such data is questionable.

The shape and extent of the descending branch of the stress-strain curves are affected by the stiffness of the testing machine and the testing method. When the stiffness of the descending branch of the stress-strain curve for a concrete cylinder approaches the stiffness of the testing machine, energy in the testing machine is

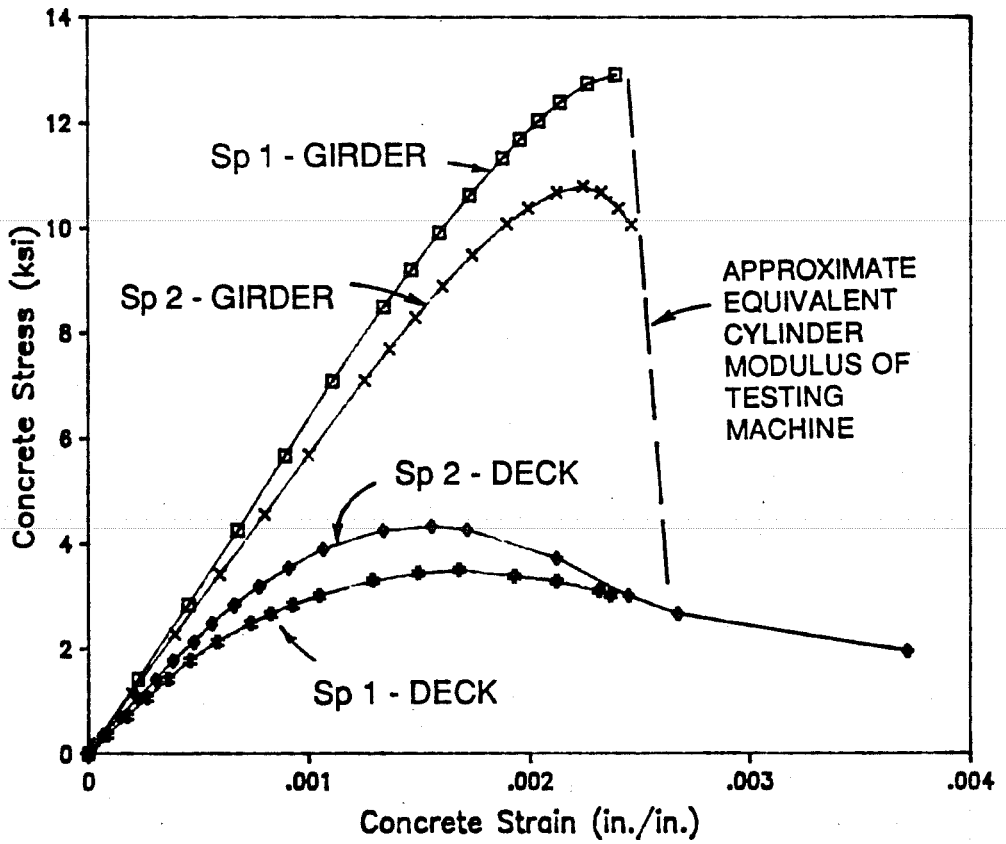

Fig. 5.2 Average stress-strain curves for concrete at time of flexure test for Specimens 1 and 2

unloaded on the cylinder resulting in the sudden destruction of the cylinder. An equivalent cylinder modulus of elasticity of 51,000 ksi was computed for the testing machine considering only the axial stiffness of the sidewalls of the machine. A dashed line corresponding to this equivalent modulus is indicated on Fig. 5.2. Since the descending branch for the low strength deck concrete was less stiff, the stress-strain curve was minimally affected by the properties of the testing machine. The descending branch of the stress-strain curves for the high strength girder concrete cylinders, however, was apparently very steep and was therefore strongly influenced by the machine. Use of a stiffer machine may have resulted in a longer descending branch for the high strength concrete.

Measured strains at maximum stress and ultimate strains for the girder concrete of Specimen 2 are summarized for three 4 x 8-in. cylinders in Table 5.2. These values were obtained from measurements of the testing machine head displacement at an age of 56 days. This data is used for the following comparisons because it appears more reliable than the data obtained for Specimen 1 using strain gages. As described earlier, the strain monitoring device could not be expected to give accurate data as the peak of the stress-strain curve was approached or exceeded.

Strains at maximum stress from Table 5.2 are compared with compression (cylinder) data and combined flexure and compression data from the literature in Fig. 5.3. The current data are among the highest reported concrete strengths and lowest strains.

Ultimate strains from Table 5.2 are compared with cylinder data and combined data from the literature in Fig. 5.4. The current data are representative of cylinder data for comparable concrete strength and are low for combined data, which is expected because ultimate strains for cylinder data are typically lower than for flexural data.

Estimated and measured values for the deck and girder concrete strains at failure are given for Specimens 1 and 2 in Table 5.3 along with strains at maximum stress and failure for corresponding cylinder tests. These data are presented graphically in Fig. 5.5. The estimated strains at failure for Specimen 1, which represent an average for a number of gages, were computed using measured changes in deflection (see Sec. 6.2.2.3). The strain at the top of the Specimen 2 girder was estimated using data for the single active gage for which readings had been essentially constant for load stages preceding failure. The deck strain at failure of Specimen 2 was

Table 5.2 Strain at Maximum Stress and Ultimate Strain for Girder Concrete - Specimen 2

f'_c	ϵ_0	ϵ_{cu}
(ksi)	(in/in)	(in/in)
10.72	0.002240	0.002500
10.95	0.002290	0.002480
10.73	0.002190	0.002400

Note: Data shown are for 4 x 8-in. cylinders.

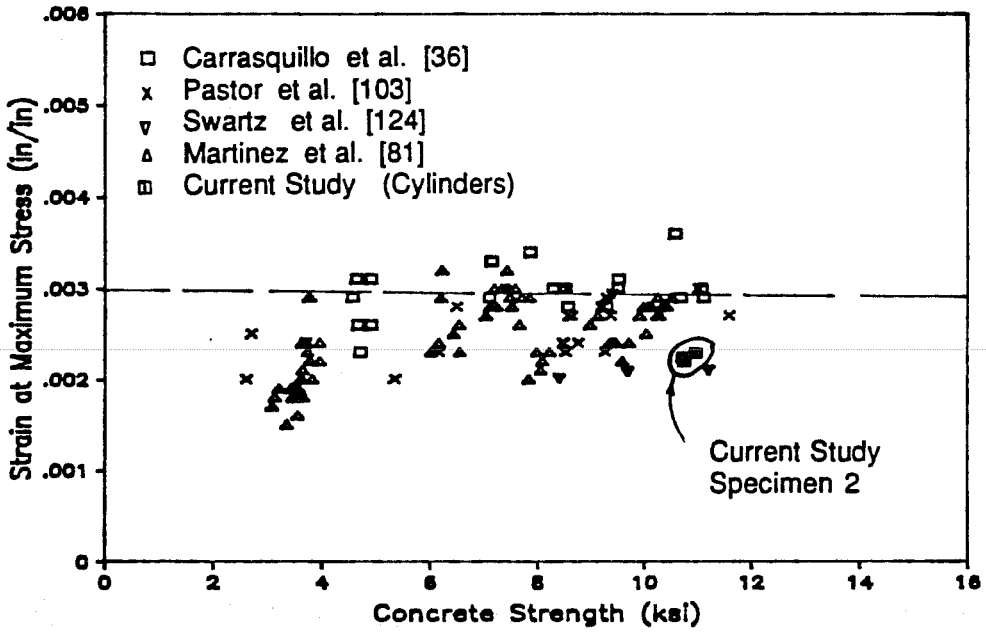

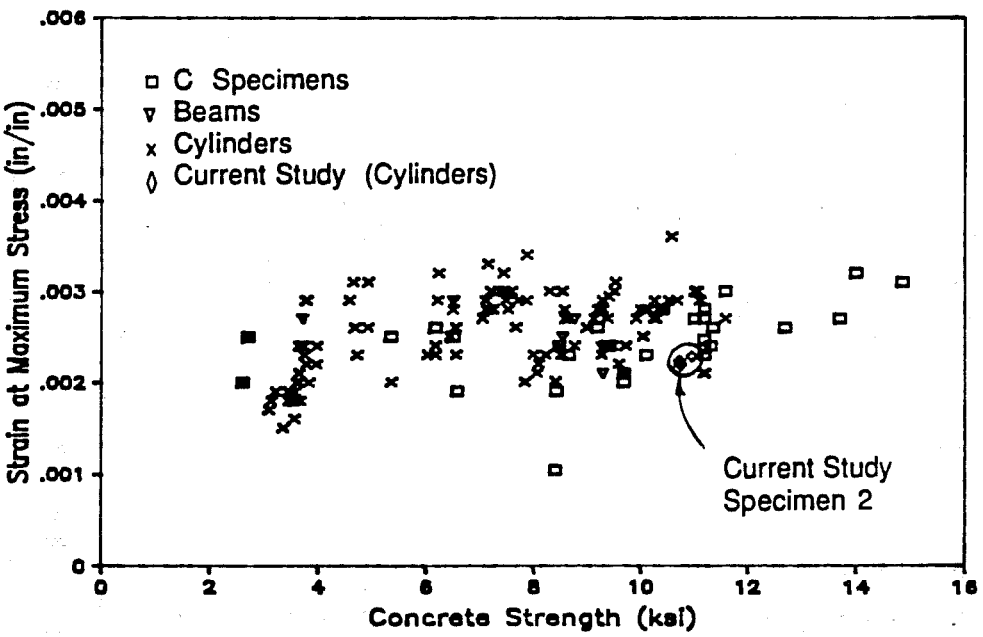

Fig. 5.3 Comparison of Specimen 2 data for strain at maximum stress with other data: a) cylinder data; b) combined data

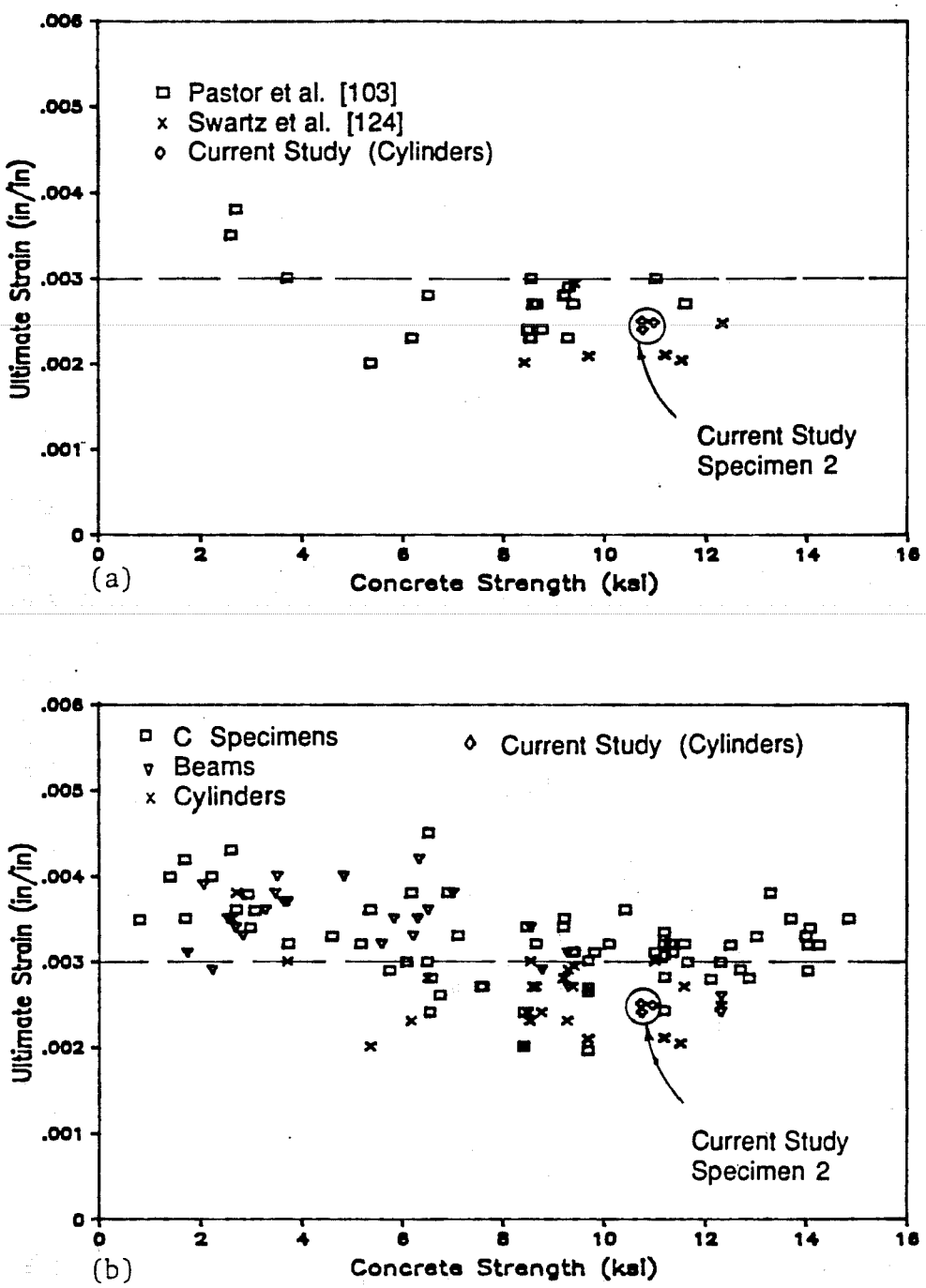

Fig. 5.4 Comparison of Specimen 2 data for ultimate strain with other data: a) cylinder data; b) combined data

Table 5.3 Critical Strains for Specimens and Related Cylinders

	Test Specimens	----- Cylinders -----		
	f'_c	ϵ_{max}	ϵ_0	ϵ_{cu}
	(ksi)	(in./in.)	(in./in.)	(in./in.)
Specimen 1				
Girder	12.90	0.001900 E	0.002400	0.002400
Deck	3.50	0.002080 E	0.001600	0.002370 *
Specimen 2				
Girder	10.80	0.001090 E	0.002240	0.002460
Deck	4.35	0.002240 M	0.001550	0.003710 **

ϵ_{max} = corrected strain at top fiber of element at failure of member.

E = Estimated strain

M = Measured strain

ϵ_0 = strain at maximum stress in cylinder.

ϵ_{cu} = strain at failure of cylinder.

* - strain limited by failure of strain gages rather than failure of cylinder.

** - strains in excess of this value were recorded, but concrete was badly crushed.

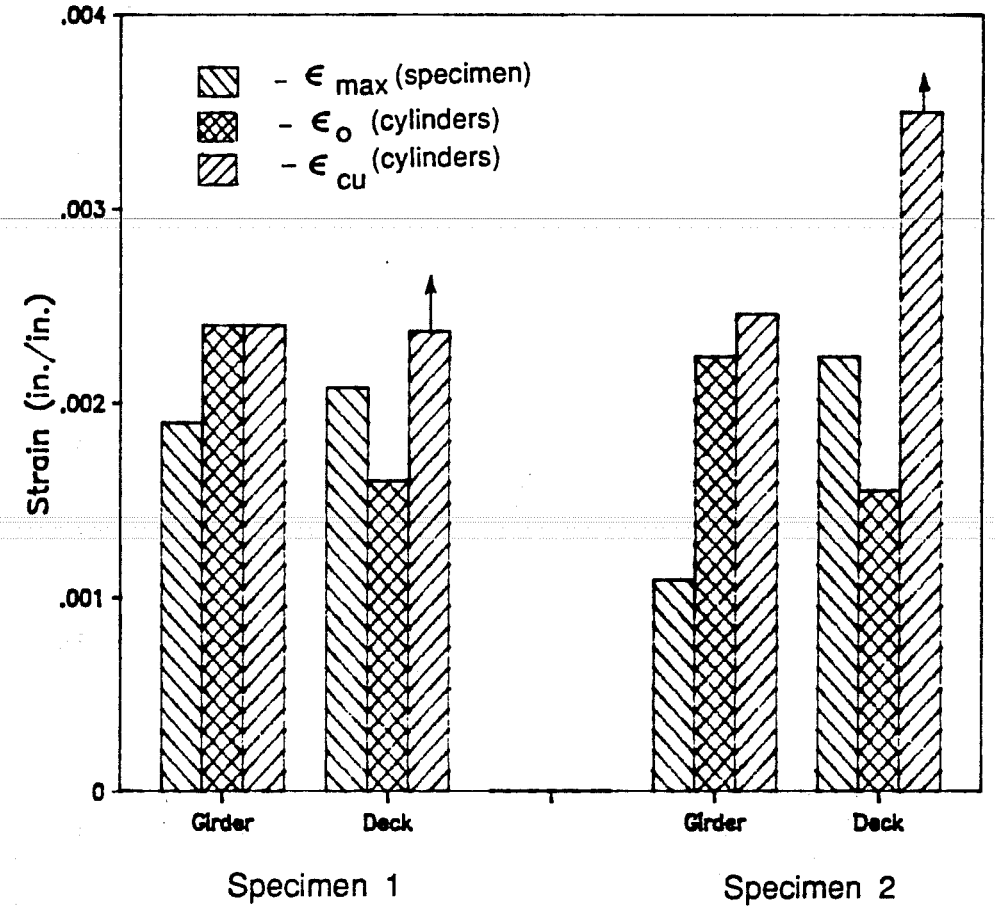

Fig. 5.5 Comparison of critical strains for specimens and related cylinders

measured by manually following the reading for a single gage with a strain indicator as load was being applied. This gage was representative of most other deck gages on the top of Specimen 2, although one gage gave readings that were approaching 3000 microstrains at the load stage preceding failure (see Fig. 6.76). All specimen strains were corrected as described in Chapter 6 to by eliminate strains related to time effects. These corrections were relatively large for girder strains (Fig. 6.102) but relatively small for deck strains (Fig. 6.103) when compared with the strains in Table 5.3.

Considering all available data and the limitations on accuracy of measurements from this study, the strains given in Table 5.3 are good estimates of strains at failure reflecting overall member behavior. However, they are not necessarily representative of locations where failure at each girder occurred. Strains might be elevated due to special conditions at the failure section in a composite member. Further study should be conducted to more closely define strains at failure in composite pretensioned members.

The strains at failure for the specimens given in Table 5.3 are well below ultimate strains measured in cylinder tests of the same concrete. This is opposite the trend reported in the literature where ultimate strains measured in flexure tests are generally greater than those from cylinder tests (Fig. 3.11).

While the available data are not conclusive, it appears most likely that crushing of the deck concrete initiated failure of both specimens. This is based on the fact that strains in the deck at failure were 30 and 45 percent (for Specimens 1 and 2, respectively) higher than the strain at maximum stress. Since high levels of load, which corresponded to strains in the deck approaching maximum levels, were maintained for significant periods of time during the tests (see Appendix B), it appears likely that sustained loading effects contributed to the crushing of the deck concrete.

Considering all available data (see also Fig. 3.7), use of the current maximum usable concrete strain of 0.003 for ultimate flexural design in all cases appears questionable for both normal and high strength concrete. Significant variations in both the strain at maximum stress and the ultimate strain result from use of different aggregates and mix designs as demonstrated by the differences in the curves of Fig. 3.3 and 5.1. For composite, pretensioned structures the ultimate strain for high strength concrete will most likely not be critical because a girder will seldom approach even a reduced limiting

strain prior to the deck reaching its limiting strain. If the deck concrete crushes at strains below the specified limiting strain, which appears possible in light of the preceding data and discussion, the girder strain would be lower with respect to its limiting strain when the deck concrete crushes. However, in non-composite structures, the maximum usable strain is critical and should be investigated further. Data from other investigators (Fig. 3.7), which indicate that beam specimens have failed at strains below 0.003, support this concern. High strength concrete with a high modulus of elasticity appears most likely to have reduced strains at maximum stress and failure and should therefore be the object of special concern. The effect of using a reduced maximum usable concrete strain on design is discussed in Sec. 5.4.4 and 5.4.5.

5.3.3 Tensile Strength. Table 5.4 contains a summary of tensile strength measurements made for Specimens 1 and 2. The last column of the table provides a comparison between measured strengths and those predicted using current equations. In all cases the current coefficient of 5.5 for modulus of rupture is conservative. However, the coefficient of 6.7 for the split cylinder tests was unconservative in one case and was only slightly conservative for the remaining cases. Curing conditions greatly affected the beam specimens as demonstrated by the modulus of rupture for wet specimens exceeding those for air cured specimens by an average of about 70 percent. For the single comparison available, split cylinders showed much less sensitivity with a difference of only about 5 percent between air and wet cured tests.

Observed cracking loads during specimen flexure tests were quite high as shown in Tables 6.4 and 6.10. High cracking loads may be due to undetected cracking at lower load stages, cracking occurring early in a load increment, or errors in determining the effective prestress.

Therefore, the estimate of cracking stress currently used in the Codes, $5.5\sqrt{f'_c}$ is conservative for use with high strength concrete cured under normal conditions encountered in the production of prestressed members.

5.3.4 Creep, Shrinkage, and Thermal Effects. A detailed study of the creep of high strength concrete was not conducted as part of the current study. However, data for the high strength concrete girders indicate that creep strains prior to the flexure test were roughly equal to the elastic strains. This means that the creep coefficient, Ccu, is approximately 2, which is slightly higher than

Table 5.4 Average Tensile Strength Data for Specimens

	Age	Cure	f_r	f'_c	$f_r\sqrt{f'_c}$
	(days)		(ksi)	(ksi)	
Beams					
Specimen 1	28	Air	0.908	12.00	8.29
		Wet	1.650	12.42	14.81
	44	Air	1.019	13.02	8.93
		Wet	1.715	13.66	14.67
Specimen 2	7	Air	0.879	9.20	9.16
		Wet	1.598	8.90	16.94
	28	Air	0.965	10.75	9.31
		Wet	1.533	10.66	14.85
	55	Air	1.100	10.78	10.59
Split cylinders					
Specimen 1	114	Air	0.724	13.16	6.31
Specimen 2	29	Air	0.722	10.75	6.96
		Wet	0.756	10.66	7.32

Note: Above tensile data are averages of two tests.

values given in Table 3.1. Since deflection-time plots indicate that most of the creep had occurred by the time of the flexure tests, this estimate for the creep coefficient is a reasonable estimate for the total creep. On the basis of this limited data, it appears that use of a creep coefficient of 2 for high strength concrete is appropriate and probably conservative.

While no direct measurements of shrinkage were made, the formation of widespread shrinkage cracks in the Specimen 2 girder prior to release indicates that this property of high strength concrete should be explored further. It should be noted, however, that the scale-model specimens, because of their thin (2 in.) webs and a volume to surface ratio approximately one-third that of the prototype girder, could be expected to experience shrinkage up to three times greater than a prototype girder [51]. The cracking did not appear to significantly affect member behavior, as indicated by the fact that prestress losses were not excessive.

No data on thermal properties of high strength concrete were obtained in this study. It is recommended that the same thermal properties used for normal strength concrete be used for high strength concrete [22].

5.3.5 Cover and Durability. Current limits on cover over reinforcement are appropriate for use with high strength concrete because of its improved impermeability and durability. In order to further improve the durability of high strength concrete, use of entrained air is suggested where the accompanying reduction of strength is tolerable.

5.3.6 Unit Weight. The unit weight of the high strength concrete used in this study was 150 pcf. This is similar to the findings of Carrasquillo et al. [36] which are recommended for use (see Sec. 3.3.6).

5.3.7 Placement of Concrete. Concerns have been expressed about the practicality of placement of high strength concrete in girder forms. This project demonstrated that high strength concrete could be placed without difficulty in girder forms with very tight clearances. This success was attributed to the use of super-plasticizers which produced flowing concrete that did not segregate. Therefore, the use of high strength concrete in the construction of bridge girders appears feasible.

CHAPTER 6

SUMMARY AND CONCLUSIONS

6.1 Summary

Recently, it has been demonstrated that high strength concrete can be produced using conventional materials and appropriate admixtures. For purposes of this study, high strength concrete is defined as concrete with a design compressive strength from 6,000 psi to 12,000 psi, which is the current range of strengths for readily attained field-produced concrete.

Therefore, this study was conceived for the purpose of investigating the use of high strength concrete in design of pretensioned girders with a normal strength composite deck. The scope of the study was limited to the consideration of simple span, non-skew pretensioned girder highway bridges where a composite deck is placed with the girder unshored.

Due to the lack of data for composite bridge construction with high strength concrete pretensioned girders, two test programs were developed and completed.

The first set of tests compared transfer characteristics of 0.5-in. diameter seven-wire strand in normal and high strength concrete. Two strengths of concrete were used to cast two sizes of specimens with square cross section which were pretensioned with a single concentric strand. The strands were pretensioned to levels common in practice. Concrete strains measured mechanically before and after release were used to determine transfer lengths. The data collected allowed evaluation of current code transfer length provisions with respect to use with high strength concrete.

Two scale-model high strength concrete pretensioned girders with normal strength composite decks, which were representative of possible long-span bridge designs, were tested in the second phase of the project. The specimens were one-third scale models of prototype modified Type IV girders spanning 146 ft and spaced 4 ft apart. The span-to-total depth ratio was 28.8. Specimen 2 contained close to the minimum number of strands permitted using current allowable stress and ultimate strength design criteria. Specimen 1 contained additional strands and still satisfied the allowable stress criteria but exceeded the maximum reinforcement limit.

High strength concrete was easily placed in the girders even where reinforcement was very congested. No problems in consolidation were encountered. Widespread shrinkage cracking occurred prior to release of Specimen 2. Although sweep was measured in both specimens at release, no difficulties were encountered handling the girders.

Prior to testing, however, both specimens were found to have significant sweep that necessitated lateral restraint of the specimens during testing to prevent further lateral movement.

The specimens were tested in flexure by applying equal loads at equal distances from midspan. Data were collected throughout the tests for strand strains, concrete strains, and deflections. A sudden and violent compression failure occurred for both specimens. At failure, the top portion of the girder was still in compression. It was not possible to determine conclusively whether crushing of the girder or deck concrete initiated failure.

6.2 Conclusions

In this section, major conclusions from the study are presented. Each conclusions or group of related conclusions is numbered and followed by a reference to the section from which the conclusion is taken. More complete and detailed conclusions were given as specific topics were considered in the body of the text.

1. On the basis of limited test data, the transfer length of strand in high strength concrete is slightly shorter than for normal strength concrete. (2.6)

2. The AASHTO expression for estimating transfer length is conservative for high strength concrete. (2.6)

3. Because of the modulus of elasticity can vary widely due to a number of factors, it is recommended that the modulus be determined experimentally when an accurate value is needed. (5.3.2)

4. Current code expressions for the modulus of elasticity are sufficiently accurate if data for a specific mix is not available (5.3.2)

5. In this study, the maximum usable concrete strain was found to be lower for high strength concrete than for normal strength concrete, which agrees with the trend of data reported by other investigators. (5.3.2)

6. In this study, compression failures occurred while measured compressive strains in both the deck and girder concrete were below the current code specified value of 0.003. (5.3.2)

7. Placement of high strength concrete in narrow, congested sections is possible through the use of high range water reducers (superplasticizers). (5.3.7)

A P P E N D I X A

MIX AND STRENGTH DATA FOR HIGH STRENGTH CONCRETE

This Appendix presents the mix and strength data for the high strength concrete used in the girders of Specimens 1 and 2. Data pertaining to materials and admixtures used in the concrete are given in Tables A.1 and A.2. Mix proportions and properties are given in Table A.3. Strength test data for compression and tension are given for the two specimens in Tables A.4 and A.5. Modulus data for both specimens appear in Table A.6. Values appearing in the tables are averages for the indicated number of tests performed. Plots of compressive and tensile strength data with age appear in Fig. A.1 and A.2 for the two specimens.

Concrete used in Specimen 1 was reported in Ref. [35] as mix number 22-110-34. The trial batch on which this mix design is based appeared in the same report as mix number 21-112-34.

Table A.1 Properties of Materials Used in Mix

MATERIAL	MATERIAL PROPERTIES
Cement	ASTM C150 Type I
Fly Ash	ASTM C618 Class C TSDHPT Type B BSG = 2.64 La Grange Type C Trinity Pozzolanic Admixture General Portland
Coarse Aggregate	Crushed dolomite ASTM C33 No. 8, 3/8-in. to #8 DRUW = 100 pcf BSG_{ssd} = 2.79 AC_{ssd} = 0.5%
Fine Aggregate	Natural river sand BSG_{ssd} = 2.62 AC_{ssd} = 1.0%

Table A.2 Properties of Chemical Admixtures Used in Mix

ADMIXTURE TYPE	ADMIXTURE PROPERTIES
Water reducing and retarding admixture (R-Plus - Gifford Hill)	ASTM C494 Type D Polymer-based S.G. = 1.24 % solids = 42% Dosage rates: 2-4 oz./cwt
High-range water reducing admixture (PSI Super- Gifford Hill)	ASTM C494 Type F Naphthalene-based S.G. = 1.21 % solids = 42% Dosage rates: Flowing concrete: 6-12 oz./cwt High-range water reduction: 12-16 oz./cwt

Table A.3 Final Mix Design and Properties

Design Strength	12,000 psi
Mix Design (Quantites in lbs. per cu. yard)	
Cement	698
Fly Ash	298
Coarse aggregate	1821
Fine aggregate	1039
Water	282
Water reducing and retarding admixture	20 oz.
High-range water reducing admixture	80 oz. at batch plant 100 oz. at laboratory
Quantity delivered (c.y.)	4
Cost per yard delivered	$65
Mix Properties	
Slump	1 in. at batch plant before adding HRWR
	10 in. at laboratory after second dose of HRWR
Unit weight	150 pcf
Air content	1.3 %
Water/Cement ratio	0.29
Cementitious content (sacks/cy)	10.5
% Cementitious as fly ash	30 %
% DRUW (Dry Rodded Unit Weight)	66 %

Table A.4 Results of Cylinder and Beam Tests - Specimen 1

	Age (Days)	Curing	Mold	Cap	No.	f'_c (ksi)
Compression Strength Tests						
6 x 12-in. cylinders	2	---	Plastic	S	2	7.58
	7	Air	Plastic	S	2	10.21
	14	Air	Plastic	S	2	10.84
	21	Air	Plastic	S	2	12.53
	28	Air	Steel	S	2	12.00
		Wet	Steel	S	2	12.42
	44	Air	Steel	S	2	13.02
		Wet	Steel	S	2	13.66
	66	Air	Steel	S	2	12.91
		Air	Plastic	S	3	12.49
	94	Air	Plastic	S	2	12.99
	114	Air	Plastic	S	2	13.16
		Air	Plastic	P	2	13.29
	135	Wet	Steel	P	2	14.69

Tensile Strength Tests

			No.	f'_t	$f'_t/\sqrt{f'_c}$
Beam Tests					
6 x 6 x 21-in.	28	Air	2	0.908	8.29
Third point loading		Wet	2	1.650	14.81
	44	Air	2	1.019	8.93
		Wet	2	1.715	14.67
Split Cylinder Tests - Plastic molds					
6 x 12-in. cylinders	114	Air	2	0.724	6.31

Notes:

Curing: Air - Curing compound applied after form removal. Cylinders and beams cured with girder
Wet - Cylinders and beams cured in lime bath

Cap type: S - High-strength sulfur capping compound
P - Pad caps

Table A.5 Results of Cylinder and Beam Tests - Specimen 2

	Age (Days)	Curing	Mold	Cap	No.	f'_c (ksi)
Compression Strength Tests						
6 x 12-in. cylinders	4	---	Plastic	S	2	8.62
	7	Air	Plastic	S	2	9.20
		Wet	Plastic	S	2	8.90
	14	Air	Plastic	S	2	10.10
	21	Air	Plastic	S	2	10.12
	28	Air	Plastic	S	3	10.75
		Wet	Plastic	S	3	10.66
	48	Air	Plastic	S	2	10.12
	55	Air	Plastic	S	3	10.78
		Wet	Plastic	S	3	11.14
	265	Air	Plastic	S	3	11.34
		Air	Steel	S	3	11.49
4 x 8-in. cylinders	28	Air	Steel	S	2	11.11
	55	Air	Steel	S	3	10.80
3 x 6-in. cylinders	29	Air	Steel	S	3	10.30
	55	Air	Steel	S	3	9.97

Tensile Strength Tests

			No.	f'_t	$f'_t/\sqrt{f'_c}$
Beam Tests					
6 x 6 x 21-in.	7	Air	2	0.879	9.16
Third point loading		Wet	2	1.598	16.94
	28	Air	2	0.965	9.31
		Wet	2	1.533	14.85
	55	Air	2	1.100	10.59
	265	Air	2	1.275	11.89
Split Cylinder Tests - Plastic molds					
6 x 12-in. cylinder	29	Air	2	0.722	6.96
		Wet	2	0.756	7.32

See Table A.4 for Notes

Table A.6 Modulus of Elasticity Data for Girder Concrete

Age (days)	Curing	Individual Cylinders Strength (ksi)	Individual Cylinders Modulus (ksi)	Average Strength (ksi)	Average Modulus (ksi)	$E_c/\sqrt{f'_c}$ ($\times 10^3$)
Specimen 1 - Steel molds						
44	Air	12.82	6410	13.02	6380	55.9
		13.22	6350			
66	Air	12.73	5900	12.91	5980	52.6
		13.09	6060			
66 *	Air	12.73	6360	12.91	6430	56.5
		13.09	6490			
Specimen 2 - Plastic molds						
7	Air	9.34	5260	9.20	5300	55.3
		9.06	5340			
21	Air	10.07	5550	10.12	5550	55.2
		10.17	5550			
28	Air	10.93	5850	10.75	5720	55.2
		10.62	5640			
		10.17	5680			
28	Wet	10.63	7760	10.66	7000	67.8
		10.79	6660			
		10.56	6690			
56	Air	10.78	5590	10.78	5675	54.7
		10.69	5710			
		10.87	5730			

Note: Unit weight of concrete is approximately 150 pcf

* Modulus determined using two electronic strain gages on each cylinder. All other data taken using a compressometer.

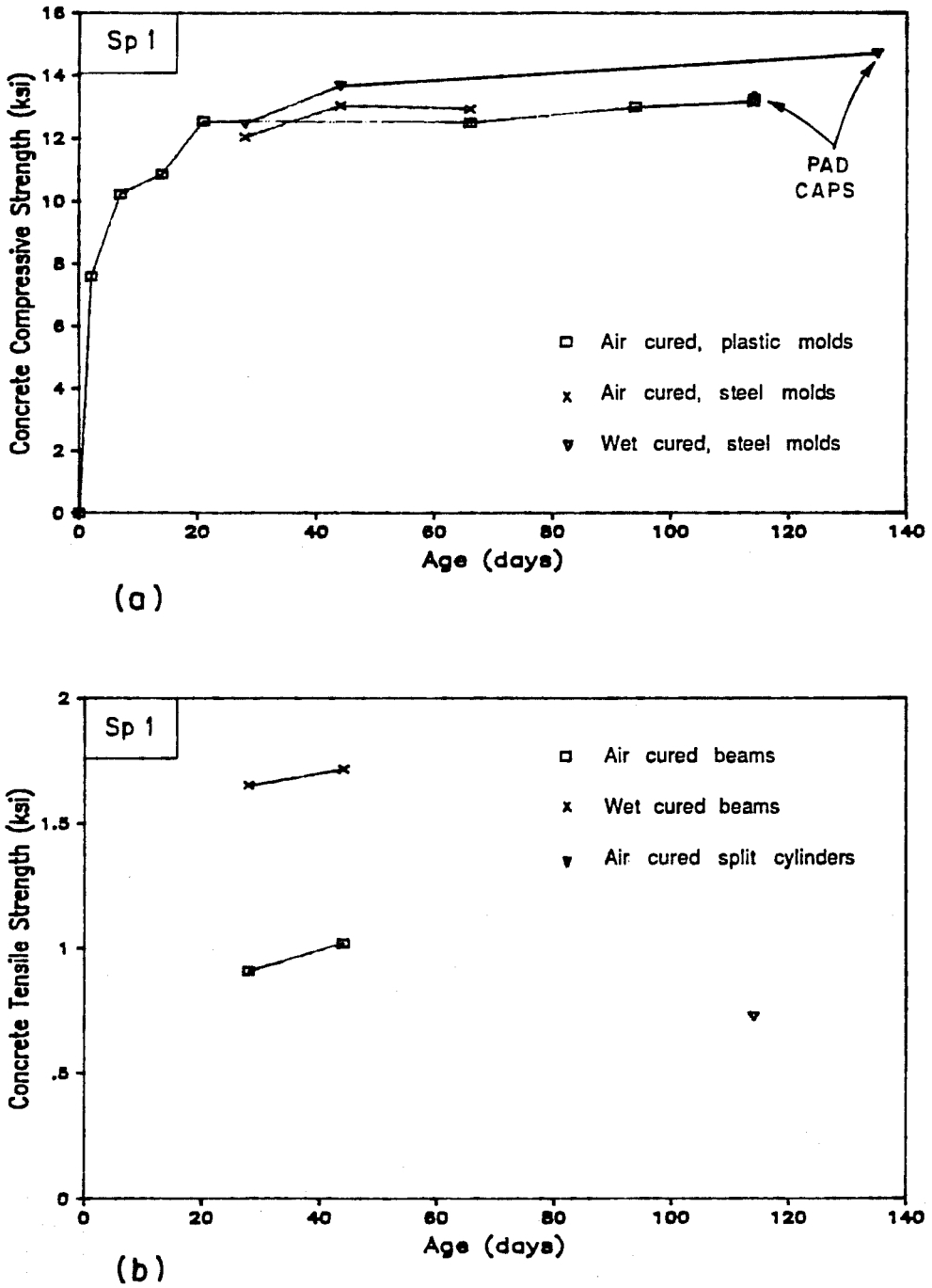

Fig. A.1 Strength gain with age for Specimen 1: a) compressive strength; b) tensile strength

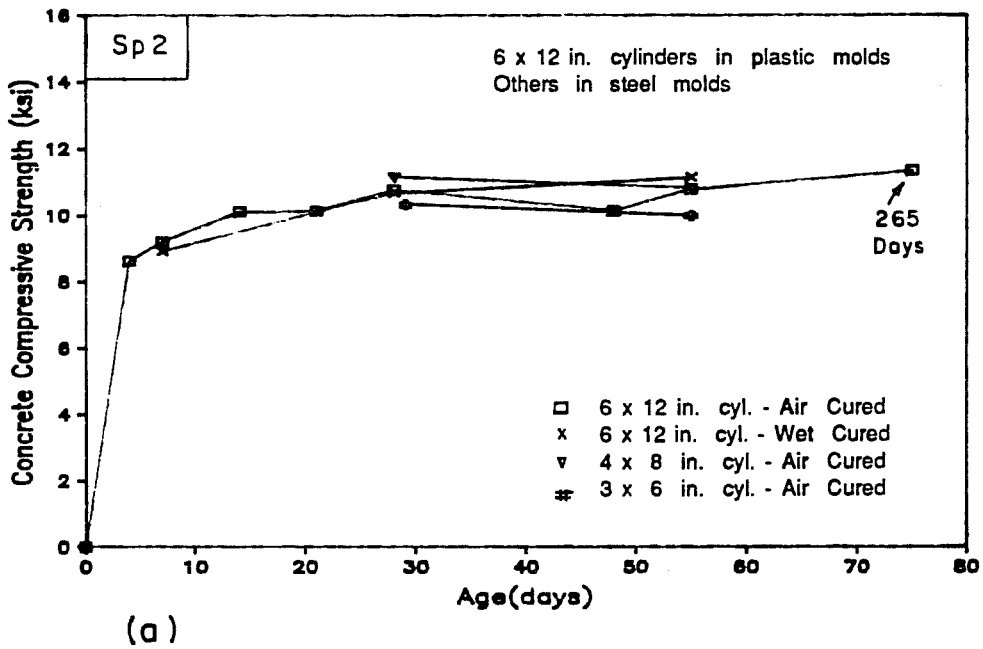

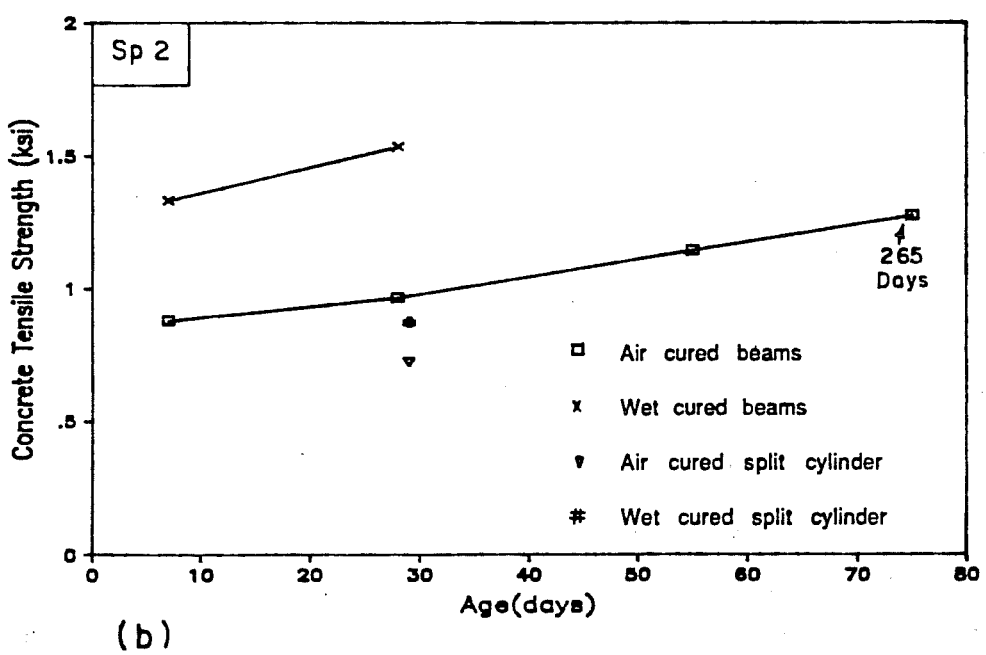

Fig. A.2 Strength gain with age for Specimen 2: a) compressive strength; b) tensile strength

A P P E N D I X B

HISTORY OF LONG-SPAN GIRDER SPECIMENS

B.1 Specimen 1 (13 strands)

Cast dates and significant changes in load are highlighted.

A detailed account of the ultimate flexure test is given because high strains were sustained for significant periods of time during the tests and such long-term load effects may have affected the response of the specimen. Only brief summaries are given for shear tests because long term effects were not as significant.

Date	Time	Net Time (hours)	Comments
1/ 8/86	16.5	-44.7	Connect 4 midspan strand gages to strain indicator
1/10/86	13.2	.0	ZERO HOUR FOR HISTORY - Zero readings for midspan strand gages
1/10/86	13.3	.1	Tension gaged strands to 17 kips each
1/10/86	13.4	.2	Tension gaged strands to 10 kips each
1/10/86	13.5	.3	Gaged strands seated
1/10/86	14.0	.8	All strands tensioned and seated
----------			STRANDS FULLY TENSIONED
1/16/86	13.3	144.1	Prior to fully tensioning all strands with large ram
1/16/86	16.4	147.2	All strands tensioned to approx 17 kips
1/21/86	10.1	260.9	Just prior to arrival of truck with girder concrete
1/21/86	12.4	263.3	Just prior to casting girder - truck arrived at 12:15
**********			CAST GIRDER
1/21/86	13.7	264.6	Finishing of concrete surface complete
1/21/86	15.3	266.1	Curing burlap and plastic in place
1/23/86	14.5	313.3	Remove girder forms
1/23/86	15.0	313.8	Apply curing compound by rag
1/27/86	17.0	411.8	Connect remaining strand, girder concrete and 4 stirrup ... ... gages to strain indicators; take initial readings.
1/28/86	14.4	433.3	Begin release procedure - hold downs released
1/28/86	14.6	433.4	NOTE: NO LOAD PLACED ON GIRDER DURING OR AFTER RELEASE
----------			RELEASE
1/28/86	15.0	433.8	Full release by detensioning with ram
1/28/86	16.3	435.1	Cut strands
1/29/86	10.5	453.3	Begin to move girder to pedestal
1/29/86	14.8	457.6	Girder in final location
----------			ADD 20 PLF DECK FORM LOAD
1/31/86	10.1	500.9	Slab forms placed; fully supported by girder
1/31/86	15.8	506.6	Just prior to placing dead load blocks
			Note: Dead load compensation blocks weigh approx. 470 lb. ea.
----------			ADD 156 PLF GIRDER DEAD LOAD COMPENSATION
1/31/86	17.0	507.8	16 dead load blocks placed to compensate for girder dead load
----------			ADD 78 PLF DECK DEAD LOAD COMPENSATION

2/ 4/86	8.3	595.2	24 blocks in pairs at 4 feet
----------			SUBTRACT 78 PLF DECK DEAD LOAD COMPENSATION
2/ 5/86	10.6	621.4	8 blocks removed since cast is delayed - 16 remain
----------			ADD 78 PLF DECK DEAD LOAD COMPENSATION
2/ 6/86	9.5	644.4	24 blocks again in place for full d.l. compensation
**********			CAST DECK
2/ 6/86	12.0	646.8	Deck concrete in place
2/ 6/86	13.3	648.1	Excess concrete removed
2/ 6/86	15.8	650.6	Curing burlap and plastic in place
2/11/86	11.5	766.3	Burlap and plastic removed
----------			SUBTRACT 20 PLF DECK FORM LOAD
2/11/86	15.2	770.1	Forms removed; 23 dead load blocks replaced on specimen ...
			... spaced at 2 feet with one at midspan
2/14/86	17.2	844.0	Connect deck concrete gages to strain indicators ...
			... take initial readings
2/18/86	8.3	931.1	1 block removed at each load point for loading head
2/18/86	14.3	937.2	Large cross head in place at each load point ...
			... no significant change in load
2/20/86	11.0	981.8	Rams and load cells in place
3/ 4/86	14.6	1273.5	Preliminary loading to to 2 kips to check setup
----------			FIRST ATTEMPT TO LOAD TO CRACKING
3/ 6/86	13.1	1319.9	Begin test
3/ 6/86	15.5	1322.3	7.14 kips - maximum load; increasing sweep halts test
3/ 6/86	16.8	1323.6	Unload
3/11/86	12.0	1438.8	Cross heads removed for modification
3/24/86	9.1	1747.9	New tied lower cross heads in place; dead load blocks ...
			... rearranged but load remains essentially unchanged
3/25/86	14.9	1777.7	Push and hold specimen to east to reduce sweep
----------			SECOND ATTEMPT TO LOAD TO CRACKING - SIDE SWAY PREVENTED
3/26/86	10.2	1797.0	-0.59 kips - No applied load
3/26/86	10.4	1797.2	0.00 kips - upper cross heads lifted by rams
3/26/86	10.6	1797.4	0.98 kips
3/26/86	10.8	1797.6	1.97 kips
3/26/86	10.8	1797.7	2.95 kips
3/26/86	11.0	1797.8	3.94 kips
3/26/86	11.0	1797.9	4.92 kips
3/26/86	11.2	1798.0	5.41 kips
3/26/86	11.3	1798.2	5.66 kips
3/26/86	11.4	1798.3	5.90 kips
3/26/86	11.6	1798.4	6.15 kips
3/26/86	12.0	1798.8	6.40 kips
3/26/86	12.3	1799.1	6.65 kips
3/26/86	12.4	1799.2	6.89 kips
3/26/86	12.6	1799.5	7.14 kips
3/26/86	12.8	1799.7	7.38 kips - Maximum load
3/26/86	13.2	1800.0	6.01 kips - load remaining after delay
3/26/86	13.3	1800.1	4.92 kips
3/26/86	13.5	1800.3	3.43 kips
3/26/86	13.6	1800.5	1.98 kips
3/26/86	13.8	1800.6	-0.73 kips - upper cross heads supported on nuts

----------			ULTIMATE FLEXURAL TEST
3/26/86	14.4	1801.3	-0.52 kips - No applied load
3/26/86	15.1	1802.0	1.97 kips
3/26/86	15.3	1802.1	4.03 kips
3/26/86	15.4	1802.3	5.41 kips
3/26/86	15.6	1802.4	5.90 kips
3/26/86	15.7	1802.5	6.40 kips
3/26/86	15.8	1802.7	6.89 kips
3/26/86	16.0	1802.8	7.38 kips
3/26/86	16.2	1803.0	7.87 kips
3/26/86	16.5	1803.3	8.37 kips
3/26/86	16.7	1803.5	8.86 kips
3/26/86	16.9	1803.8	9.35 kips - Reset load heads
3/26/86	17.6	1804.4	9.84 kips
3/26/86	17.8	1804.7	10.33 kips
3/26/86	18.0	1804.9	10.83 kips
3/26/86	18.2	1805.0	11.32 kips
3/26/86	18.3	1805.2	11.81 kips
3/26/86	18.5	1805.3	12.30 kips
3/26/86	18.8	1805.6	12.79 kips - Reset load heads
3/26/86	19.1	1806.0	13.29 kips - Failure occurred as load stage attained
----------			PREPARE SOUTH END FOR SHEAR TEST - STD STIRRUP DETAIL
			Note: No dead load blocks used during shear tests of south end
4/15/86	13.3	2280.2	Begin initial shear test
4/15/86	14.9	2281.8	Load system problems, stop test at approx. load of 24.34 kips
4/15/86	15.5	2282.3	Unload from initial test
4/23/86	14.1	2472.9	Begin preliminary loading to test load system
4/23/86	14.9	2473.7	Maximum load of preliminary loading - 24.34 kips
4/23/86	15.3	2474.1	Unload from preliminary test
----------			CRACKING SHEAR TEST - SOUTH END
4/24/86	9.1	2491.9	Begin test
4/24/86	10.8	2493.6	Maximum load - 34.83 kips
4/24/86	11.5	2494.4	Unload
----------			ULTIMATE SHEAR TEST - SOUTH END
4/24/86	13.3	2496.1	Begin test
4/24/86	16.2	2499.0	Failure occurred when shear of 63.24 kips achieved
4/24/86	17.1	2499.9	Partial unload
4/24/86	17.5	2500.4	Unload
----------			PREPARE NORTH END FOR SHEAR TEST - MODIFIED STIRRUP DETAIL
			Note: No dead load blocks used during shear tests of north end
5/ 8/86		2818.8	Place North end in testing frame
5/ 9/86		2842.8	Position specimen; set bearings and load head
----------			CRACKING SHEAR TEST - NORTH END
5/13/86	14.0	2952.8	Begin test
5/13/86	16.6	2955.4	Maximum load of 33.88 kips shear
5/13/86	17.3	2956.1	Unload
----------			ULTIMATE SHEAR TEST - NORTH END
5/14/86	13.5	2976.3	Begin test
5/14/86	16.6	2979.4	Failure occurred at shear of 65.22 kips
5/14/86	16.7	2979.6	Specimen supported a shear of 61.27 kips upon reloading

5/14/86 17.0 2979.8 Unload

B.2 Specimen 2 (9 strands)

Cast dates and significant changes in load are highlighted.

A detailed account of the ultimate flexure test is given because high strains were sustained for significant periods of time during the tests and such long-term load effects may have affected the response of the specimen. Only brief summaries are given for shear tests because long term effects were not as significant.

Date	Time	Net Time (hours)	Comments
6/27/86	14.3	.0	Connect strand gages to boxes; initial readings
6/30/86	9.1	66.8	Strands lying slack in bed
6/30/86	9.3	67.0	17 kips applied to strand 1 (center bottom row)
6/30/86	9.5	67.2	10 kips reapplied to strand 1
6/30/86	9.6	67.3	Strand 1 is seated
6/30/86	9.7	67.5	17 kips applied to strand 2 (draped strand row 3 at midspan)
6/30/86	9.8	67.6	10 kips reapplied to strand 2
6/30/86	12.3	70.0	All 9 strands are seated with approx 10 kips in each
7/ 1/86	11.2	92.9	Adjust height of north draped strand hold-up; tie stirrups
7/22/86	9.2	595.0	Begin tying end detail steel and preparing for casting
7/23/86	10.9	620.7	Just prior to full tensioning
----------			STRANDS FULLY TENSIONED
7/23/86	11.6	621.4	Full pretension force applied
7/23/86	18.3	628.1	Girder forms in place
7/24/86	12.6	646.3	Prior to casting
**********			CAST GIRDER
7/24/86	14.1	647.9	Concrete in place in girder forms
7/24/86	16.9	650.7	Curing burlap,towels and plastic sheeting in place
7/28/86	10.1	739.9	Forms removed; water and curing compound applied
7/31/86	14.7	816.4	8 dead load blocks in place near midspan
7/31/86	15.4	817.2	Zero readings taken on girder surface gages
7/31/86	15.8	817.6	Begin to pressurize ram for release
----------			RELEASE
			8 DEAD LOAD COMPENSATION BLOCKS PLACED IN PAIRS AT 3' AND 8.5' EACH SIDE OF MIDSPAN
			Note: Dead load blocks weigh approx. 470 lb. each
7/31/86	16.1	817.8	Release is complete; chucks are loose at both ends
8/ 1/86	9.2	834.9	Cut strands at each end
----------			ADD 8 DEAD LOAD BLOCKS; 16 TOTAL IN PAIRS AT 6 FT SPCG. FULL GIRDER DEAD LOAD COMPENSATION - 156 PLF
8/ 1/86	14.0	839.8	8 dead load blocks added; girder placed on bearing pads
9/ 9/86	11.7	1773.4	Girder moved from prestress bed and placed on pedestals
9/ 9/86	12.3	1774.0	Instrumentation boxes removed from girder - placed on table
			Central 8 blocks removed for placement of forms

			Center 3 form sections in place; place 8 blocks on these
			Remove 12 dead load blocks to place remaining forms
----------			ADD DECK FORM LOAD - 20 PLF - PLUS 8 DEAD LOAD BLOCKS
9/ 9/86	18.2	1780.0	All forms in place; 8 dead load blocks placed in pairs ...
			... at 4 ft spacing symm about midspan
9/10/86	7.4	1793.1	No change in loading
----------			ADD DEAD LOAD COMPENSATION FOR DECK - 235 PLF TOTAL
9/10/86	14.6	1800.3	All 24 blocks in place, spaced in prs at 4 ft
9/10/86	15.0	1800.8	Ready mix concrete truck arrives
**********			CAST DECK
9/10/86	15.6	1801.4	Concrete in place
9/10/86	17.0	1802.8	Deck finishing completed
9/10/86	17.7	1803.4	Burlap and plastic in place for curing
9/12/86	12.7	1846.5	Curing materials removed; curing cmpd applied to top surface
9/12/86	14.0	1847.8	Apply demecs and 3 gages ea location to deck at midspan
9/13/86	11.8	1869.6	Connect top deck gages to boxes; initial readings
9/15/86	8.0	1913.8	Ready to begin block removal and form stripping
----------			SUBTRACT DECK FORM LOAD - 20 PLF
9/15/86	13.8	1919.5	Deck forms removed; 18 dead load blocks and lower cross- ...
			... head in place for full dead load compensation
9/15/86	17.3	1923.1	Apply and connect remaining deck gages; initial readings
9/16/86	14.7	1944.4	Specimen pushed and held about .33 in. to west
9/16/86	17.0	1946.8	Deflection readings taken using optical level
9/17/86	8.0	1961.8	Initial readings taken for all instrumentation for test
----------			FLEXURE TEST
9/18/86	8.7	1986.5	Initial readings for flexure test
9/18/86	9.1	1986.9	0.00 kips - lift upper cross heads; rezero pressure
			transducers
9/18/86	9.4	1987.1	1.00 kip
9/18/86	9.6	1987.4	2.00 kips
9/18/86	9.8	1987.5	3.00 kips
9/18/86	9.9	1987.6	3.50 kips
9/18/86	10.0	1987.7	4.00 kips
9/18/86	10.3	1988.0	4.50 kips
9/18/86	10.3	1988.1	5.00 kips
9/18/86	10.6	1988.4	5.50 kips
9/18/86	10.7	1988.5	6.00 kips
9/18/86	11.1	1988.9	6.50 kips
9/18/86	11.2	1988.9	7.00 kips
9/18/86	11.4	1989.1	7.50 kips - lock deflection; retract rams; reset upper heads
9/18/86	11.6	1989.4	7.50 kips - reload
9/18/86	11.7	1989.4	8.00 kips
9/18/86	11.9	1989.7	8.25 kips
9/18/86	12.0	1989.7	8.50 kips
9/18/86	12.2	1990.0	8.75 kips
9/18/86	12.4	1990.2	9.00 kips
9/18/86	12.7	1990.4	9.25 kips - lock deflection; reset rams; reset upper heads
9/18/86	13.0	1990.7	9.25 kips - reload
9/18/86	13.1	1990.8	9.44 kips - lock deflection to replace leaking hose
9/18/86	13.5	1991.2	9.44 kips - reload

9/18/86	13.6	1991.4	9.67 kips - lock deflection; reset rams; reset upper heads
9/18/86	13.9	1991.7	9.59 kips - Failure during reload
9/18/86	17.0	1994.7	Unload
----------			PREPARE SOUTH END FOR SHEAR TEST - STD END DETAIL
			Note: No dead load blocks used during shear test of south end
4/14/87			Place specimen in 600 kip testing machine
----------			SHEAR TEST OF SOUTH END
4/15/87	10.5	7004.2	Begin shear test - no cracking test because girder previously cracked by shrinkage
4/15/87	13.9	7007.6	Maximum shear of 41 kips reached
4/15/87	14.1	7007.8	Specimen fails while reloading at 40.9 kips due to loss of strand bond. Application of additional displacement causes slow reduction of capacity.
4/15/87			Remove specimen from testing machine
----------			PREPARE NORTH END FOR SHEAR TEST - 6 INCH EXTENSION OF GIRDER BEYOND BEARING
			Note: No dead load blocks used during shear test of north end
4/15/87			Place specimen in 600 kip testing machine
----------			SHEAR TEST OF NORTH END
4/16/87	11.0	7028.7	Begin shear test - no cracking test because girder previously cracked by shrinkage
4/16/87	14.8	7032.5	Web crushing begins - load drops as deformation added
4/16/87	15.1	7032.8	Shear increases again when additional deformation applied
4/16/87	15.2	7032.9	Maximum shear of 48.8 kips reached
4/16/87	15.9	7033.6	Final load stage - web crushing is extensive and load is dropping with additional deformation

REFERENCES

1. Ahmad, S.H., and Shah, S.P., "Stress-Strain Curves of Concrete Confined by Spiral Reinforcement," ACI Journal, Proceedings Vol. 79, No. 6, Nov.-Dec. 1982, pp. 484-490.

2. Ahmad, S.H., and Shah, S.P., "Structural Properties of High Strength Concrete and Its Implications for Precast Prestressed Concrete" PCI Journal, Vol. 30, No. 6, Nov.-Dec. 1985, pp. 92-119.

3. Ahmad, S.H., Khalo, A.R., and Poveda, A., "Shear Capacity of Reinforced High-Strength Concrete Beams," ACI Journal, Proceedings Vol. 83, No. 2, Mar.-Apr. 1986, pp. 297-305.

4. Aitcin, Pierre-Claude, Laplante, Pierre, and Bedard, Claude, "Development and Experimental Use of a 90 MPa (13,000 psi) Field Concrete", High Strength Concrete, SP-87, American Concrete Institute, Detroit, 1985, pp. 51-70.

5. Ali, I. Discussion of "Researches Toward a General Flexural Theory for Structural Concrete," by Hubert Rusch, ACI Journal, Proceedings Vol. 32, No. 9, Mar. 1961, pp. 1147-1149.

6. Anderson, Arthur R., "Lateral Stability of Long Prestressed Concrete Beams", PCI Journal Vol. 16, No. 3, May-June 1971, pp. 7-9.

7. Anderson, Arthur R., Author's closure to discussion of "Lateral stability of Long Prestressed Concrete Beams," PCI Journal, Vol. 16, No. 6, Nov.-Dec. 1971, pp. 86-87.

8. American Association of State Highway Officials, Standard Specification for Highway Bridges, Seventh Edition, Washington, D.C., 1957.

9. American Association of State Highway Officials, Standard Specification for Highway Bridges, Eighth Edition, Washington, D.C., 1961.

10. American Association of State Highway and Transportation Officials, Standard Specification for Highway Bridges, Thirteenth Edition, Washington, D.C., 1983.

11. American Concrete Institute, "Building Code Requirements for Reinforced Concrete (ACI 318-56)", ACI Journal, Proceedings, Vol. 52, No. 9, May 1956, pp. 913-986.

12. American Concrete Institute, Building Code Requirements for Reinforced Concrete (ACI318-63), Detroit, 144 pp.

13. American Concrete Institute, Building Code Requirements for Reinforced Concrete (ACI 318-71), Detroit, 78 pp.

14. American Concrete Institute, Building Code Requirements for Reinforced Concrete (ACI 318-77), Detroit, 102 pp.

15. American Concrete Institute, Building Code Requirements for Reinforced Concrete (ACI 318-83), Detroit, 111 pp.

16. American Concrete Institute, Commentary on Building Code Requirements for Reinforced Concrete (ACI 318-63), SP-10, American Concrete Institute, Detroit, 1965.

17. American Concrete Institute, Commentary on Building Code Requirements for Reinforced Concrete (ACI 318-83), Detroit, 1983.

18. American Concrete Institute, 318 Change Submittal, No. CE11, "Shear Strength of High Strength Concrete", Nov. 19, 1986.

19. American Concrete Institute - American Society of Civil Engineers, Committee 323, "Tentative Recommendations for Prestressed Concrete," ACI Journal, Proceedings Vol. 54, No. 7, Jan. 1958, pp. 545-578.

20. American Concrete Institute - American Society of Civil Engineers, Committee 327, Ultimate Load Design, "Ultimate Strength Design", ACI Journal, Proceedings Vol. 52, No. 5, Jan. 1956, pp. 505-524. Also, "Report of ASCE-ACI Joint Committee on Ultimate Strength Design," Proceedings, ASCE, Vol. 81, Oct. 1955, 68 pp.

21. American Concrete Institute Committee 343, "Analysis and Design of Reinforced Concrete Bridge Structures," ACI Manual of Concrete Practice, Part 4, American Concrete Institute, Detroit, 1981, 118 pp.

22. American Concrete Institute Committee 363, "State-of-the Art Report on High-Strength Concrete," ACI Journal, Proceedings Vol. 81, No. 4, July-Aug. 1984, pp. 363-411.

23. American Concrete Institute Committee 435, "Deflections of Prestressed Concrete Members," (ACI 435.1R-63)(Reaffirmed 1979), ACI Journal, Proceedings Vol. 60, No. 12, Dec. 1963, pp. 1697-1728. Also, ACI Manual of Concrete Practice, Part 4, American Concrete Institute, Detroit, 1981.

24. American Concrete Institute Committee 435, Subcommittee 5, "Deflections of Prestressed Concrete Members," ACI Journal, Proceedings Vol. 60, No. 12, Dec. 1963, pp. 1697-1728.

25. ASTM Standards in ACI 301, 318 and 349, SP-71, American Concrete Institute, Detroit.

26. Aswad, A. and Hester, W.T. "Impact of High-Strength Concrete on Design and Service Behavior of Prestressed Precast Concrete Members," High Strength concrete, SP-87, American Concrete Institute, Detroit, 1985, pp. 9-20.

27. Base, G.D., "An Investigation of Transmission Length in Pre-Tensioned Concrete," Session III, Paper No. 9, Third Congress of the Federation Internationale de la Preconstrainte, Berlin, 1958, Papers, pp. 603-623.

28. Base, G.D., "An Investigation of Transmission Length in Pretensioned Concrete," Research Report No. 5, Aug., 1958, Cement and Concrete Association, London, 24 pp.

29. Base, G.D., "An Investigation of the Use of Strand in Pretensioned Prestressed Concrete Beams," Research Report No. 11, Jan. 1961, Cement and Concrete Association, London, 12 pp.

30. Billet, D.F., and Appleton, J.H., "Flexural Strength of Prestressed Concrete Beams", ACI Journal, Proceedings, Vol. 50, No. 10, June 1954, pp. 837-854.

31. Blume, J.A., Newmark N.M., and Corning, L.H., "Design of Multistory Reinforced Concrete Buildings for Earthquake Motions," Portland Cement Association, Chicago, 1961, 318 pp.

32. Bradberry, T.E., "Time Dependent Deformation of Long Span Prestressed Concrete Beams Having Low Relaxation Strands," Unpublished M.S. Report, The University of Texas at Austin, May 1986.

33. Bureau of Public Roads, Strength and Serviceability Criteria-Reinforced Concrete Bridge Members - Ultimate Design, U.S. Department of Commerce, U.S. Government Printing Office, Washington, D.C., Aug. 1966, 81 pp.

34. Burns, Ned H., "Moment Curvature Relationships for Partially Prestressed Concrete Beams," PCI Journal, Vol. 9, No. 1, Feb. 1964, pp. 52-63.

35. Carrasquillo, P.M. and Carrasquillo, R.L., "Guidelines for Use of High Strength Concrete in Texas Highways," Research Report 367-1F, Center for Transportation Research, The University of Texas at Austin, Aug. 1986, 227 pp.

36. Carrasquillo, R.L., Nilson, A.H., and Slate, F.O., "Properties of High Strength Concrete Subject to Short-Term Loads", ACI Journal, Proceedings Vol. 78, No. 3, May-June 1981, pp. 171-178.

37. Carreira, Domingo J., and Chu, Kuang-Han, "Stress-Strain Relationship for Plain Concrete in Compression," ACI Journal, Proceedings, Vol. 82, No. 6, Nov.-Dec. 1985, pp. 797-804.

38. Castrodale, R.W., "The Shear Design of Prestressed Concrete Members Using the Truss Model," Unpublished M.S. Thesis, University of Texas at Austin, Dec. 1983, 348 pp.

39. Colaco, J.P., "75-Story Texas Commerce Plaza, Houston - The Use of High-Strength Concrete," High Strength Concrete, SP-87, American Concrete Institute, Detroit, 1985, pp. 1-8.

40. Collins, M.P., and Mitchell, D., "Shear and Torsion Design of Prestressed and Non-Prestressed Concrete Beams," PCI Journal, Vol. 25, No. 5, Sept. - Oct. 1980, pp. 32-100.

41. Comite Euro-International du Beton, Recommendations for an International Code of Practice for Reinforced Concrete, Translation by American Concrete Institute and Cement and Concrete Association, 156 pp.

42. Csagoly, P., "Bridge Girder Test," Engineering News-Record, Mar. 13, 1986, p. 9.

43. Drake, Kingsley D., "High-Strength Concrete in Seattle," High Strength Concrete, SP-87, American Concrete Institute, Detroit, MI, 1985, pp. 21-34.

44. Elzanaty, A.H., Nilson, A.H. and Slate, F.O., "Shear-Critical High-Strength Concrete Beams," Research Report No. 85-1, Department of Structural Engineering, Cornell University, Feb. 1985, 216 pp.

45. Elzanaty, A.H., Nilson, A.H., and Slate, F.O., "Shear Capacity of Reinforced Concrete Beams Using High-Strength Concrete," ACI Journal, Proceedings Vol. 83, No. 2, Mar.-Apr. 1986, pp. 290-296.

46. Elzanaty, A.H., Nilson, A.H., and Slate, F.O., "Shear Capacity of Prestressed Concrete Beams Using High-Strength Concrete," ACI Journal, Proceedings Vol. 83, No. 3, May-June 1986, pp. 359-368.

47. Fafitis, A., and Shah, S.P., "Lateral Reinforcement for High-strength Concrete Columns," High Strength Concrete, SP-87, American Concrete Institute, Detroit, 1985, pp. 213-232.

48. Furlong, R.W., "Design of Concrete Frames by Assigned Limit Moments," ACI Journal, Proceedings Vol. 67, No. 4, Apr. 1970, pp. 341-353.

49. Ghosh, S.K., and Chandrasekhar, C.S., Discussion of "Flexural Behavior of High-Strength Concrete Beams" by Leslie, Rajagopalan and Everard, ACI Journal, Proceedings Vol. 74, No. 3, Mar. 1977, pp. 140-142.

50. Grossfield, B., and Birnstiel C., "Tests of T-Beams with Precast Webs and Cast-in-Place Flanges," ACI Journal, Proceedings Vol. 59, No. 6, June 1962, pp. 843-851.

51. Hansen, T.C., and Mattock, A.H., "Influence of Size and Shape of Member on the Shrinkage and Creep of Concrete," ACI Journal, Proceedings Vol. 63, Feb. 1966, pp. 267-290. Also PCA Bulletin D103 which contains an added appendix.

52. Hanson, Norman W., "Precast-Prestressed Concrete Bridges - 2. Horizontal Shear Connections," Journal of the PCA Research and Development Laboratories, Vol. 2, No. 2, 1960, pp. 38-58.

53. Hanson, Norman W., "Influence of Surface Roughness of Prestressing Strand on Bond Performance," PCI Journal, Vol. 14, No. 1, Feb. 1969, pp. 32-45.

54. Hanson, N.W., and Kaar, P.H., "Flexural Bond Tests of Pre-Tensioned Prestressed Beams," ACI Journal, Proceedings Vol. 55, Jan. 1959, pp. 783-802.

55. Harajli, M.H., and Naaman, A.E., "Deformation and Cracking of Partially Prestressed Concrete Beams under Static and Cyclic Fatigue Loading," Research Report No. UMEE 84R1, Department of Civil Engineering, The University of Michigan, Ann Arbor, Aug. 1984, 179 pp.

56. Harajli, M.H., and Naaman, A.E., "Static and Fatigue Tests on Partially Prestressed Beams," Proceedings, ASCE, Vol. 111, ST7, July 1985, pp. 1602-1618.

57. Harajli, M.H., Naaman, A.E., and Wight, J.K., "Analysis of Ductility in Partially Prestressed Concrete Flexural Members", PCI Journal, V. 32, No. 3, May-June 1986, pp. 64-87.

58. Hognestad, Eivind, "A Study of Combined Bending and Axial Load in Reinforced Concrete Members," Bulletin No. 399, University of Illinois Engineering Experiment Station, Nov. 1951, 128 pp.

59. Hognestad, Eivind, "Confirmation of Inelastic Stress Distribution in Concrete," Proceedings, ASCE, Vol. 83, ST2, Mar. 1957, pp. 1-17. Also PCA Bulletin D31.

60. Hognestad, E., Hanson, N.W., and McHenry, D., "Concrete Stress Distribution in Ultimate Strength Design," ACI Journal, Proceedings Vol. 52, Dec. 1955, pp. 455-479. Also PCA Bulletin D6.

61. Hognestad, E., Hanson, N.W., and McHenry, D., Authors' closure to discuss of "Concrete Stress Distribution in Ultimate Strength Design," ACI Journal, Proceedings Vol. 52, Part 2, Dec. 1956, pp. 1305-1330. Also, PCA Bulletin D6A.

62. Horn, D.G., and Preston, H.K., "Use of Debonded Strands in Pretensioned Bridge Members", PCI Journal, Vol. 26, No. 4, July-Aug. 1981, pp. 42-58.

63. Huang, T., "Loss Estimation for Multistage Prestressed Concrete Members," Advances in Structural Concrete Design, Proceedings of NJIT-ASCE-ACI Structural Concrete Design Conference, Newark, 1983, pp. 187-203.

64. Hunt, F.F., and Preston, H.K., "Performance of a New Corrosion Resistant Prestressing Strand", Presentation at "Advances in Prestressed Concrete" Session at ASCE Fall Convention and Structures Congress, Houston, Texas, Oct. 17-21, 1983.

65. Janney, Jack R., "Nature of Bond in Pretensioned Prestressed Concrete," ACI Journal, Proceedings, Vol. 50, May 1954, pp. 717-736. Also, PCA Bulletin D2.

66. Janney, J.R., Hognestad, E., and McHenry D., "Ultimate Flexural Strength of Prestressed and Conventionally Reinforced Concrete Beams", ACI Journal, Proceedings Vol. 52, Feb. 1956, pp. 602-620. Also, PCA Bulletin D7.

67. Janney, Jack R., "Report of Stress Transfer Length Studies on 270k Prestressing Strand", PCI Journal, Vol. 8, No. 1, Feb. 1963, pp. 41-45.

68. Jensen, V.P., "The Plasticity Ratio of Concrete and Its Effect on the Ultimate Strength of Beams," ACI Journal, Journal Vol. 39, No. 6, June 1943, pp. 565-582.

69. Jobse, H.J., "Applications of High Strength Concrete for Highway Bridges,", Report No. FHWA/RD-82/097, Oct. 1981, Federal Highway Administration, 228 pp.

70. Karr, P.H., LaFraugh, R.W., and Mass, M.A. "Influence of Concrete Strength on Strand Transfer Length," PCI Journal Vol. 8, No. 5, Oct. 1963, pp. 47-67. Also, PCA Bulletin D71.

71. Kaar, P.H., Hanson, N.W., and Capell, H.T., "Stress-Strain Characteristics of High-Strength Concrete," Douglas McHenry International Symposium on Concrete and Concrete Structures, SP-55, American Concrete Institute, Detroit, 1978, pp. 161-185.

72. Kelly, D.J., "Time Dependent Deflections of Pretensioned Beams," Unpublished M.S. Thesis, The University of Texas at Austin, Aug. 1986, 307 pp.

73. Kent, D.C., and Park R., "Flexural Members with Confined Concrete," Proceedings, ASCE, Vol. 97, ST7, July 1971, pp. 1969-1990.

74. Khachaturian, Marbey, and Gurfinkel, German, Prestressed Concrete, McGraw-Hill, New York, 1969, 460 pp.

75. Kriz, L.B. and Lee, S.L., "Ultimate Strength of Over-Reinforced Beams," Proceedings, ASCE, Vol. 86, EM3, June 1960. Also, PCA Bulletin D36.

76. Leslie, Keith E., Rajagopalan, K.S., and Everard, Noel J., "Flexural Behavior of High-Strength Concrete Beams," ACI Journal, Proceedings Vol. 73, No. 9, Sept. 1976, pp. 517-521.

77. MacGregor, J.G., "Ductility of Structural Elements," Handbook of Concrete Engineering, 1st Ed., M. Fintel (Editor), Prentice Hall, 1974, pp. 229-248.

78. Malhotra, V.M., "Are 4 X 8 Inch Concrete Cylinders as Good as 6 X 12 Inch Cylinders for Quality Control of Concrete?", ACI Journal, Proceedings Vol. 73, No. 1, Jan. 1976, pp. 33-36.

79. Martin, L.D. and Scott, N.L., "Development of Prestressing Strand in Pretenioned Members," ACI Journal, Proceedings Vol. 73, No. 8, Aug. 1976, pp. 453-456.

80. Martin, L.D., "A Rational Method for Estimating Camber and Deflection of Precast Prestressed Members," PCI Journal, Vol. 22, No. 1, Jan.-Feb. 1977, pp. 100-108.

81. Martinez, S., Nilson, A.H., and Slate, F.O., "Short-Term Mechanical Properties of High-Strength Light-Weight Concrete," Research Report No. 82-9, Dept. of Structural Engineering, Cornell University, Aug. 1982, 98 pp.

82. Martinez, S., Nilson, A.H., and Slate, F.O., "Spirally Reinforced High-Strength Concrete Columns," ACI Journal, Proceedings Vol. 81, No. 5, Sept.-Oct. 1984, pp. 431-442.

83. Mast, R.F., "Auxiliary Reinforcement in Concrete Connections," Proceedings, ASCE, Vol. 94, ST6, June 1968, pp. 1485-1504.

84. Mattock, Alan, H., "Modification of ACI Code Equation for Stress in Bonded Prestressed Reinforcement at Flexural Ultimate," ACI Journal, Proceedings Vol. 81, No. 4, July-

85. Mattock, A.H., Kaar, P.H., "Precast-Prestressed Concrete Bridges - 4. Shear Tests of Continuous Girders," Journal of the PCA Research and Development Laboratories, Vol. 3, No. 1, Jan. 1961, pp. 19-46.

86. Mattock, Alan, H., and Kriz, Ladislav, B., "Ultimate Strength of Nonrectangular Concrete Members," ACI Journal, Proceedings Vol. 57, No. 7, Jan. 1961, pp. 737-766.

87. Mattock, Alan H., Kriz, Ladislav, B., and Hognestad, Eivind, "Rectangular Concrete Stress Distribution in Ultimate Strength Design", ACI Journal, Proceedings Vol. 57, Feb. 1961, pp. 875-928. Also PCA Bulletin D49.

88. Mattock, A.H., and Hawkins, N.M., "Shear Transfer in Reinforced Concrete - Recent Research," PCI Journal, Vol. 17, No. 2, Mar.-Apr. 1972, pp. 55-75.

89. Mayfield, B., Davies, G., and Kong, F.K., "Some tests on the transmission length and ultimate strength of pretensioned concrete beams incorporating Dyform strand:", Magazine of Concrete Research, Vol. 22, No. 73, Dec. 1970, pp. 219-226.

90. Mphonde, Andrew G., and Frantz, Gregory C., "Shear Tests of High- and Low-Strength Concrete Beams Without Stirrups," ACI Journal, Proceedings Vol. 81, No. 4, July-Aug. 1984, pp. 350-357.

91. Mphonde, A.G., and Frantz, G.C., "Shear Tests of High- and Low-Strength Concrete Beams with Stirrups," High Strength Concrete, SP-87, American Concrete Institute, Detroit, 1985, pp. 179-196.

92. Muller, Jean, "Lateral Stability of Precast Members During Handling and Placing," PCI Journal, Vol. 7, No. 1, Feb. 1962, pp. 20-31.

93. Naaman, A.E., "Ultimate Analysis of Prestressed and Partially Prestressed Sections by Strain Compatibility," PCI Journal, Vol. 22, No. 1, Jan.-Feb. 1977, pp. 32-51.

94. Naaman, A.E., "A Proposal to Extend Some Code Provisions on Reinforcement to Partial Prestressing," PCI Journal, Vol. 26, No. 2, Mar.-Apr. 1981, pp. 74-91.

95. Naaman, A.E., "Partially Prestressed Concrete: Review and Recommendations," PCI Journal, Vol. 30, No. 6, Nov.-Dec. 1985, pp. 30-71.

96. Naaman, A.E., Harajli, M.H., and Wight, J.K., "Analysis of Ductility in Partially Prestressed Flexural Members," PCI Journal, Vol. 31, No. 3, May-June 1986, pp. 64-87.

97. Naaman, A.E., Harajli, M.H., and Wight, J.K., Authors' Closure to discussion of "Analysis of Ductility in Partially Prestressed Flexural Members," PCI Journal, Vol. 32, No. 1, Jan.-Feb., 1987, pp. 142-145.

98. Ngab, Ali S., Nilson, Arthur H., and Slate, Floyd O., "Shrinkage and Creep of High Strength Concrete," ACI Journal, Proceedings Vol. 78, No. 4, July-Aug. 1981, pp. 255-261.

99. Nilson, Arthur H., "Design Implications of Current Research of High-Strength Concrete," High Strength Concrete, SP-87, American Concrete Institute, Detroit, 1985, p. 85-118.

100. Over, R.S., and Au, Tung, "Prestress Transfer Bond of Pretensioned Strands in Concrete," ACI Journal, Proceedings Vol. 62, No. 11, Nov. 1965, pp. 1451-1460.

101. Overman, T.R., Breen, J.E., and Frank, K.H., "Fatigue Behavior of Pretensioned Concrete Girders," Research Report 300-2F, Center for Transportation Research, The University of Texas at Austin, Nov. 1984, 354 pp.

102. Park, R., and Paulay, T. Reinforced Concrete Structures, John Wiley and Sons, New York, 1975, 769 pp.

103. Pastor, J.A., Nilson, A.H., and Slate, F.O., "Behavior of High-Strength Concrete Beams," Research Report No. 84-3, Department of Structural Engineering, Cornell University, Feb. 1984, 311 pp.

104. Peterman, M.B. and Carrasquillo, R.L., "Production of High Strength Concrete," Research Report 315-1F, Center for Transportation Research, The University of Texas at Austin, Oct. 1983, 286 pp.

105. PCI Committee on Allowable Stresses in Prestressed Concrete Design, "Allowable Tensile Stresses for Prestressed Concrete," PCI Journal, Vol. 15, No. 1, Feb. 1970, pp. 37-42.

106. PCI Committee on Prestress Losses, "Recommendations for Estimating Prestress Losses", PCI Journal, Vol. 20, No. 40, July-Aug. 1975, pp. 43-75.

107. Preston, H.K., "Testing 7-Wire Strand for Prestressed Concrete-The State of the Art", PCI Journal, Vol. 30, No. 3, May-June 1985.

108. Rabbat, B.G., and Russell, H.G., "Optimized Sections for Precast, Prestressed bridge Girders," (RD080.01E), Portland Cement Association, 1982.

109. Rabbat, B.G., Takayanagi, T., Russell, H.G., "Optimized Sections for Major Prestressed Concrete Bridge Girders," Report No. FHWA/RD-82/005, Feb. 1982, Federal Highway Administration, 172 pp.

110. Ramirez, J.A., and Breen, J.E., "Proposed Design Procedures for Shear and Torsion in Reinforced and Prestressed Concrete," Research Report 248-4F, Center for Transportation Research, The University of Texas at Austin, Nov. 1983, 254 pp.

111. Ramirez, J.A., and Breen, J.E., "Review of Design Procedures for Shear and Torsion in Reinforced and Prestressed Concrete," Research Report 248-2, Center for Transportation Research, The University of Texas at Austin, Nov. 1983, 186 pp.

112. RILEM, Final REcommendations, Reinforcements for Reinforced and Prestressed Concrete: II. Recommendations for Prestressing Steels. Materials and Structures, Research and Testing (RILEM, Paris), Vol. 12, No. 68, Mar.-Apr. 1979, pp. 75-127.

113. Rowe, R.E., "Trends and Needs in Concrete Bridge Design," Seventh Annual Henry M. Shaw Lecture Series in Civil Engineering, Department of Civil Engineering, North Carolina State University, Raleigh, Mar. 1972, 36 pp.

114. Rusch, Hubert, "Researches Toward a General Flexural Theory for Structural Concrete," ACI Journal, Proceedings Vol. 57, No. 1, July 1960, pp. 1-28.

115. Saemann, J.C., and Washa, G.W., "Horizontal Shear Connections Between Precast Beams and Cast-in-Place Slabs," ACI Journal, Proceedings, Vol. 61, No. 11, Nov. 1964, pp. 1383-1409.

116. Shaikh, A.F., and Branson, D.E., "Non-Tensioned Steel in Prestressed Concrete Beams," PCI Journal, Vol. 15, No. 1, Feb. 1970, p. 14-36.

117. Smadi, M.M., Slate, F.O., and Nilson, A.H., "High-, Medium-, and Low-Strength Concretes Subject to Sustained Overloads - Strains, Strengths, and Failure Mechanisms," ACI Journal, Proceedings Vol. 82, No. 5, Sept.-Oct. 1985, pp. 657-664.

118. Smith, R.G., Discussion of "Researches Toward a General Flexural Theory for Structural Concrete," by Hubert Rusch Reference, ACI Journal, Proceedings Vol. 32, No. 9, Mar. 1961, pp. 1160-1163.

119. Suttikan, C., "A Generalized Solution for Time Dependent Response and Strength of Non-Composite and Composite Prestressed Concrete Beams," Unpublished Ph.D. Dissertation, The University of Texas at Austin, Aug. 1978.

120. Swamy, R.N., "High-Strength Concrete - Material Properties and Structural Behavior," High Strength Concrete, SP-87, American Concrete Institute, Detroit, 1985, pp. 119-146.

121. Swamy, R.N., and Anand, K.L., "Transmission Length and Prestress Losses in High Strength Concrete," Paper presented at the Seventh International Congress of the Federation Internationale de la Preconstrainte, New York, May 26 - June, 1974.

122. Swann, R.A., Discussion of "Lateral Stability of Long Prestressed Concrete Beams," by Arthur R. Anderson, PCI Journal, Vol. 16, No. 6, Nov.-Dec. 1971, p. 85-86.

123. Swann, R.A., and Godden, W.G., "The Lateral Buckling of Concrete Beams Lifted by Calbes," The Structural Engineer, Vol. 44, No. 1, Jan. 1966, London, pp. 21-23.

124. Swartz, S.E., Nikaeen, A., Harayan Babu, H.D., Periyakaruppan, N., and Refai, T.M.E. "Structural Bending Properties of Higher Strength Concrete," High Strength Concrete, SP-87, American Concrete Institute, Detroit, 1985, pp. 147-178.

125. Tadros, M.K., and Peterson, D.N., "Code Consideration of Flexural Design with Partial Prestressing," Vol. 3, Hyperstatic Structures: Nonlinear Design, Codes and Practice, International Symposium - Nonlinearity and Continuity in Prestressed Concrete, University of Waterloo, 1983, pp. 125-156.

126. Thoman, William, H., and Raeder, Warren, "Ultimate Strength and Modulus of Elasticity of High Strength Portland Cement Concrete," ACI Journal, Proceedings Vol. 30, No. 3, Jan. - Feb., 1934, pp. 231-=238.

127. Thompson, K.J., and Park R., "Ductility of Prestressed and Partially Prestressed Concrete Beam Sections," PCI Journal, Vol. 25, No. 2, Mar.-Apr. 1980, pp. 46-70.

128. Tognon, G., Ursella, P., and Copetti, G., "Design and Properties of Concretes with Strength over 1500 kgf/cm^2," ACI Journal, Proceedings Vol. 77, No. 3, May-June 1980, pp. 171-178.

129. Towles, Thomas T., "Advantages in the Use of High Strength Concretes," ACI Journal, Proceedings, Vol. 28, No. 9, May 1932, pp. 607-612.

130. Wang, F., Shah, S.P., and Naaman, A.E., Discussion of "Flexural Behavior of High-Strength Concrete Beams," ACI Journal, Proceedings Vol. 74, No. 3, Mar, 1977, pp. 143, 144.

131. Wang, Pao-Tsan, Shah, Surendra P., and Naaman, Antoine E., "High-Strength Concrete in Ultimate Strength Design", Proceedings, ASCE, Vol. 104, ST11, Nov. 1978, pp. 1761-1773.

132. Wang, P.T., Shah, S.P., and Naaman, A.E., "Stress-Strain Curves of Normal and Lightweight Concrete in Compression," ACI Journal, Proceedings, Vol. 75, No. 11, Nov. 1978, pp. 603-611.

133. Warwaruk, J., Sozen, M.A., and Siess, C.P., "Investigation of Prestressed Reinforced Concrete for Highway Bridges, Part III-Strength and Behavior in Flexure of Prestressed Concrete Beams," Bulletin No. 464, Engineering Experiment Station, University of Illinois, Urbana, 1962, 105 pp.

134. Whitney, Charles S., "Plastic Theory of Reinforced Concrete Design," Proceedings ASCE, Dec. 1940; Transactions ASCE, Vol. 107, 1942, pp. 251-326.

135. Zia, Paul, "Review of ACI Code for Design with High Strength Concrete," Concrete International: Design and Construction, Vol. 5, No. 8, Aug. 1983, pp. 16-20.

136. Zia, P., and Mostafa, T., "Development Length of Prestressing Strands," PCI Journal, Vol. 22, No. 5, Sept. - Oct. 1977, pp. 54-65.

137. Zia, P., Preston, H.K., Scott, N.L., and Workman, E.B., Estimating Prestress Losses," Concrete International: Design and Construction, Vol. 1, No. 6, June 1979, pp. 32-38.

138. Hartmann, David L., Breen, J.E., and Kreger, M.E., "Shear Capacity of High-Strength Prestressed Concrete Girders," Research Report 381-2, Center for Transportation Research, The University of Texas at Austin, January 1988, 268 pp.

139. Castrodale, Reid W., Kreger, M.E., and Burns, N.H., "A Study of Pretensioned High-Strength Girders in Composite Highway Bridges-Design Considerations," Research Report 381-4F, Center for Transportation Research, The University of Texas at Austin, January 1988, 306 pp.

140. Castrodale, Reid W., "A Study on Pretensioned High-Strength Concrete Girders in Composite Highway Bridges," Ph.D. Dissertation, The University of Texas at Austin, May 1988, 662 pp.

141. Cousins, T.E., Johnston, D.W., and Zia, P., "Bond of Epoxy Coated Prestressing Strand," Report No. FHWA/NC/87-005, Center for Transportatin Engineering Studies, North Carolina State University, Raleigh, December 1986, 191 pp.